



**FORTH**

INSTITUTE OF MOLECULAR BIOLOGY & BIOTECHNOLOGY

ΠΑΝΕΠΙΣΤΗΜΙΟ ΚΡΗΤΗΣ ΤΜΗΜΑ ΙΑΤΡΙΚΗΣ  
UNIVERSITY OF CRETE MEDICAL SCHOOL

***Διδακτορική Διατριβή***

***Η επίδραση των νευροστεροϊδών στο κεντρικό νευρικό σύστημα και το αντίκτυπο στην απομυελίνωση***

***Ph.D. Thesis***

***The effect of neurosteroids in the central nervous system and impact on demyelination***

***Ηλίας Καλαφατάκης***  
***Ilias Kalafatakis***

***Ηράκλειο, Ιούνιος 2020***  
***Herakleion, June 2020***

***«This research is co-financed by Greece and the European Union (European Social Fund- ESF) through the Operational Programme «Human Resources Development, Education and Lifelong Learning» in the context of the project “Strengthening Human Resources Research Potential via Doctorate Research” (MIS-5000432), implemented by the State Scholarships Foundation (IKY)»***



Ευρωπαϊκή Ένωση  
European Social Fund

Operational Programme  
**Human Resources Development,  
Education and Lifelong Learning**

Co-financed by Greece and the European Union



## **ΕΥΧΑΡΙΣΤΙΕΣ**

*Φτάνοντας στο τέλος ενός πολύ όμορφου ερευνητικού ταξιδιού, ήρθε η στιγμή να ευχαριστήσω όλους εκείνους που στάθηκαν δίπλα μου και με στήριξαν σε όλη αυτή την πορεία, ελπίζοντας ειλικρινά να μην ξεχάσω κάποιον.*

*Δε θα μπορούσα να μην ξεκινήσω ευχαριστώντας την καθηγήτρια μου, Δόμνα Καραγωγέως. Ένα ευχαριστώ είναι λίγο για τον άνθρωπο που με πίστεψε από την πρώτη στιγμή και με εμπιστεύτηκε. Σας ευχαριστώ που όλα αυτά τα χρόνια μου δώσατε την ευκαιρία να είμαι μέλος της ομάδας σας, με εξελίξατε ερευνητικά, μου μάθατε να έχω αυτόνομη σκέψη και ταυτόχρονα με αφήσατε να παίρνω τις πρωτοβουλίες που ήθελα. Επιπλέον σας ευχαριστώ που όλα αυτά τα χρόνια μου δώσατε την ευκαιρία να πάρω μέρος σε πολλά σημαντικά συνέδρια, αποκτώντας πολύτιμες εμπειρίες και γνωρίζοντας αξιοθαύμαστους ανθρώπους.*

*Ο δεύτερος άνθρωπος που θέλω να ευχαριστήσω είναι το δεύτερο μέλος της τριμελούς επιτροπής μου, ο κύριος Ιωάννης Χαραλαμπόπουλος. Οι συμβουλές σας και οι συζητήσεις που κάναμε όλα αυτά τα χρόνια ήταν καθοριστικές και πραγματικά ήταν χαρά και τιμή μου να σας έχω στην επιτροπή μου.*

*Σε αυτό το σημείο να ευχαριστήσω και το τρίτο μέλος της επιτροπής μου, την κυρία Μαρία Βενυχάκη Σας ευχαριστώ τόσο για την άψογη συνεργασία μας όσο και για το γεγονός πώς πάντα η πόρτα του γραφείου σας ήταν ανοιχτή για εμένα.*

*Επιπλέον ένα μεγάλο ευχαριστώ στα μέλη της επταμελούς επιτροπής μου, στον κύριο Αχιλλέα Γραβάνη, στον κύριο Γιώργο Μαυροθαλασσίτη, στον κύριο Νικόλαο Γρηγοριάδη και στην Μαρίνα Βιδάκη, που δέχτηκαν με χαρά και ενδιαφέρον να αξιολογήσουν την δουλειά μου.*

*Το επόμενο ευχαριστώ το οφείλω στον κύριο Κωνσταντίνο Θεοδωράκη. Σας ευχαριστώ πρώτα από όλα για την εμπιστοσύνη και την εκτίμηση που μου δείξατε, για το ότι ήσασταν πάντα πρόθυμος να με βοηθήσετε και να με ακούσετε σε οτιδήποτε επιστημονικό ή μη και για την εξαιρετική συνεργασία μας όλα αυτά τα χρόνια.*

*Τι να πω για την Μαρία Σαββάκη... Μαρία μου σε ευχαριστώ γιατί ήσουν και είσαι πάντα δίπλα μου όταν σε χρειάζομαι, καθώς και για τις άπειρες συμβουλές σου όλα αυτά τα χρόνια. Ήσουν ο άνθρωπος που ουσιαστικά με εκπαίδευσε δίνοντας μου όλες τις απαραίτητες γνώσεις έτσι ώστε να μπορώ να δρω ανεξάρτητα. Είμαι χαρούμενος και περήφανος που εκτός από*

*συνεργάτες, είμαστε πολύ καλοί φίλοι και είχα την χαρά να είμαι παρόν σε όλες τις ευτοχισμένες προσωπικές σου στιγμές όλα αυτά τα χρόνια.*

*Δεν μπορώ να μην αναφερθώ και στην αγαπημένη μου Λήδα Ζούπη. Μπορεί να τελευταία 5 χρόνια να ανήκεις σε άλλη ερευνητική ομάδα, αλλά ποτέ δεν θα ξεχάσω τις συμβουλές σου και όλα όσα μου έμαθες για να μπορώ να ανταποκριθώ στα καθήκοντα που είχα έως σήμερα.*

*Το επόμενο ευχαριστώ θα πάει στον γιατρό του εργαστηρίου μας που δεν είναι άλλος από τον Γιώργο Μπαστάκη, ένα από τα πιο συγκροτημένα και αξιοσέβαστα άτομα που έχω γνωρίσει. Γιώργο, σε ευχαριστώ για όλες τις συζητήσεις που έχουμε κάνει αυτά τα χρόνια. Είσαι πρότυπο γιατρού, ερευνητή και οικογενειάρχη ταυτόχρονα.*

*Νικάκι μου (Νίκη Κτενά)... Ότι και να πω για σένα είναι λίγο... Θα μπορούσα να γράψω πολλά αλλά νομίζω θα γίνω γραφικός... Έχεις όλες τις προδιαγραφές να γίνεις μία σπουδαία ερευνήτρια, καθώς δουλεύεις με μεγάλη ωριμότητα, υπομονή και επιμονή. Αλλά αυτά έρχονται σε δεύτερη μοίρα όταν χρειάζεται να μιλήσω για εσένα... Σε ευχαριστώ που όλο αυτό το ταξίδι το περάσαμε μαζί, σε ευχαριστώ που πάντα με στηρίζεις και που κάνεις την κάθε μέρα στο εργαστήριο πολύ πολύ πιο ευχάριστη... Ήσουν και είσαι το άτομο που μοιράζομαι τα πάντα και πραγματικά είμαι χαρούμενος που μέσα από όλο αυτό ήρθαμε τόσο κοντά και πια μπορώ να πω πως έχω μία σπουδαία φίλη, την οποία εμπιστεύομαι και θαυμάζω για τον χαρακτήρα και το ήθος της.*

*Το επόμενο ευχαριστώ πάει στην Κατερίνα Καλεμάκη.. Άλλο ένα άτομο που θεωρώ πρώτα από όλα φίλη μου και μετά συνεργάτη όλα αυτά τα χρόνια. Είμαι περήφανος που μέσα από την διαδικασία του διδακτορικού ήρθαμε κοντά, με εμπιστευτήκες και σε εμπιστεύτηκα, πήρες και πήρα πράγματα από τις συζητήσεις και τις απόψεις που ανταλλάσσαμε. Είσαι ένα άτομο που ό,τι βάλει ως στόχο πάντα το καταφέρνει, που ποτέ δεν διαλέγει την εύκολη λύση, αλλά πάντα πάει με βάση τα όνειρα, το ήθος και τα πιστεύω του. Είμαι πάρα πολύ περήφανος για εσένα και το ξέρεις. Συνέχισε να κάνεις τα όνειρα σου πραγματικότητα και εγώ θα είμαι κάπου εκεί δίπλα να σε θαυμάζω.*

*Ζουζανάκη (Ζουζάνα Κούνουπα)... Σε ευχαριστώ για όλα. Είσαι από τα πιο καλόψυχα άτομα που έχω γνωρίσει και από τα πιο εργατικά. Πάντα εκεί δίπλα μου όταν χρειάζομαι συμβουλές, πάντα με μία καλή και ειλικρινή κουβέντα στο στόμα. Ποτέ δεν παρέκκλινες από τα πιστεύω σου και πάντα δούλευες με σωστές αρχές και ήθος, κάτι για το οποίο θα πρέπει να είσαι πολύ περήφανη. Δεν έχω την παραμικρή αμφιβολία για τις επαγγελματικές και προσωπικές*

*επιτυχίες σου. Σε ευχαριστώ που όλα αυτά τα χρόνια ένιωθα πως μπορώ να σου πω τα πάντα και ελπίζω να ένιωθες και εσύ το ίδιο.*

*Στην συνέχεια θα ήθελα να ευχαριστήσω ακόμα μερικά άτομα με τα οποία συνεργάστηκα. Ευχαριστώ λοιπόν την Αγγελική Βέλλη, την Μαρία Κόκκαλη, την Μαριλένα Καστρίτη, την Θεοδώρα Βελόνα, την Giulia Bonetto, τον Αλέξανδρο Τσιμπόλη, τον Αλέξανδρο Πατέλλη, τον Δημήτρη Μαριάτο και τον Στέφανο Καπλάνη.*

*Δεν θα μπορούσα να μην ευχαριστήσω και την παρέα μου όλα αυτά τα χρόνια, με την οποία ουσιαστικά έχουμε μεγαλώσει μαζί και που πάντα μοιραζόμασταν την κάθε ξεχωριστή στιγμή. Ένα τεράστιο ευχαριστώ στην Αργυρώ Γιαννακοπούλου, στην Βάσω Γεωργοπούλου, στον Νίκο Χαρμπίλα, στον Μάνο Στρατάκη, καθώς και στον Μανόλη Αθανασόπουλο, που πάντα ήταν και είναι δίπλα μου.*

*Και έφτασε η στιγμή να ευχαριστήσω το Ειρηνάκι μου...Τον άνθρωπο που κυριολεκτικά είναι δίπλα μου όλα αυτά τα χρόνια, με στηρίζει, με ακούει και μου δίνει δύναμη. Μαζί μεγαλώσαμε και μαζί πετυχαίναμε τους στόχους μας έναν προς έναν...Είμαι πάρα πολύ περήφανος για εσένα, για όλα όσα έχεις καταφέρει και για όλα όσα θα καταφέρεις στο μέλλον...Ένα ευχαριστώ είναι πολύ λίγο...*

*Τέλος, το μεγαλύτερο ευχαριστώ από όλους το οφείλω στην οικογένεια μου. Στον Κωνσταντίνο, τον αγαπημένο μου αδερφό, που πάντα με στηρίζει και που από μικρό παιδί έχω σαν πρότυπο για την συνέπεια και την σοβαρότητα που επιδεικνύει έτσι ώστε να εκπληρώνει τους στόχους του. Και φυσικά στους γονείς μου...Γιώργο και Ρένα...Σας ευχαριστώ που κυριολεκτικά μία ολόκληρη ζωή είστε δίπλα μου, δίνοντας μου απέραντη αγάπη, κουράγιο και δύναμη να κάνω τα όνειρα μου πραγματικότητα. Σας ευχαριστώ που με στηρίζετε σε όλες μου τις αποφάσεις, μα κυρίως σας ευχαριστώ για τις αρχές και το ήθος που μου μάθατε να έχω....Ό,τι και αν πετυχαίνω σε αυτή την ζωή το αφιερώνω σε εσάς...*

*To my parents, George and Rena and my brother,  
Konstantinos...*

## TABLE OF CONTENTS

<b>ABSTRACT I</b> .....	<b>8</b>
<b>ABSTRACT II</b> .....	<b>9</b>
<b>ΠΕΡΙΛΗΨΗ I</b> .....	<b>10</b>
<b>ΠΕΡΙΛΗΨΗ II</b> .....	<b>11</b>
<b>A. INTRODUCTION I</b> .....	<b>12</b>
A.1 The importance of myelination	
A.2 Myelin origin	
A.3 Oligodendrocytes and CNS myelination during development	
A.4 Myelination and demyelination during adulthood in the CNS	
A.5 The role of glial cells in myelin development, damage and repair	
A.6 Multiple Sclerosis	
A.7 Experimental models of MS	
A.8 Neurotrophins and their receptors	
A.9 Neurotrophins and demyelination	
A.10 Neurosteroids	
A.11 Dehydroepiandrosterone	
A.12 Microneurotrophins (BNNs)	
A.13 BNN27 Microneurotrophin	
A.14 BNN20 Microneurotrophin	
<b>B. INTRODUCTION II</b> .....	<b>38</b>
<b>C. AIM OF THE STUDY I</b> .....	<b>39</b>
<b>D. AIM OF THE STUDY II</b> .....	<b>40</b>
<b>E. MATERIAL AND METHODS I</b> .....	<b>41</b>
E.1 Animals	
E.2 LPC demyelination mouse model	
E.3 Tissue fixation, dissection and isolation	
E.4 Embedding, freezing and cryosectioning	
E.5 Immunohistochemistry on cryosections derived from adult mice	
E.6 Quantification of demyelination	
E.7 Quantification of astrocytes and microglia/macrophages	
E.8 Quantification of OLs and OPCs	
E.9 OLs and microglia primary cultures	
E.10 <i>In vitro</i> studies regarding OPCs and OLs	
E.11 <i>In vitro</i> studies regarding microglia	
E.12 Immunocytochemistry	
E.13 Propidium iodide staining	
E.14 Quantification of OPCs and OLs	
E.15 Analysis of microglia morphology	
E.16 Western Blot	
E.17 Western Blot analysis	
E.18 Statistical analysis	
<b>F. MATERIAL AND METHODS II</b> .....	<b>49</b>
F.1 Pipeline of the methodology implemented in this work	
F.2 Technical aspects of the Allen Institute ISH experiments	
F.3 Gene identification	
F.4 Brain segmentation and data collection	
F.5 Whole-brain relative gene expression data visualization	
F.6 Cntn2 genomic spatial correlation analysis	

F.7 Data collection regarding the expression of genes of interest among different brain cell populations	
<b>G. RESULTS I.....</b>	<b>56</b>
G.1 BNN20 reduces myelin loss in the lesion area of the LPC-induced demyelination mouse model	
G.2 BNN20 increases the number of mature OLs in the lesion area of LPC-induced demyelination mouse model	
G.3 BNN20 reduces accumulation of astrocytes in the lesion area of LPC-induced demyelination mouse model with no effect on accumulation of microglia/macrophages.	
G.4 BNN20 reduces microglia activation and transition to their pro-inflammatory state upon LPS stimulation <i>in vitro</i>	
G.5 BNN20 increases the number of mature OLs even after LPC treatment, while it does not affect the proliferation of OPCs <i>in vitro</i>	
G.6 BNN20 increases the number of mature OLs after LPC treatment <i>in vitro</i> in a TrkA-dependent manner	
<b>H. RESULTS II.....</b>	<b>79</b>
H.1 Cntn2 gene expression across the brain	
H.2 Gene identification encoding proteins related to Contactin-2 based on current knowledge	
H.3 Cntn2 genomic spatial correlation analysis with the 23 genes, whose products interact functionally or structurally with Contactin-2	
H.4 Cntn2 genomic spatial correlation analysis with markers of oligodendrocytes	
H.5 Expression of genes spatially correlated or anti-correlated with Cntn2 among different brain cell populations	
<b>I. DISCUSSION I.....</b>	<b>88</b>
<b>J. DISCUSSION II.....</b>	<b>92</b>
<b>REFERENCES I.....</b>	<b>95</b>
<b>REFERENCES II.....</b>	<b>115</b>
<b>APENDIX.....</b>	<b>121</b>
Table 1: Primary antibodies used in this study	
Table 2: Secondary antibodies and fluorescent-conjugated probes used in the study	
<b>PRINTED VERSIONS OF PUBLICATIONS.....</b>	<b>123</b>

## ABSTRACT I

In the first part of this doctoral thesis, we focused on BNN20 which is a C17-spiroepoxy derivative of the neurosteroid DHEA and has been shown to have strong neuroprotective properties. The aim of this study was to investigate the effect of BNN20 on glial populations by using *in vitro* and *in vivo* approaches, taking advantage of the well-established lysophosphatidylcholine-induced focal demyelination mouse model. Our *in vivo* studies, using this model and performed in male mice, showed that treatment with BNN20 leads to decreased myelin loss and increased number of mature oligodendrocytes. BNN20 reduces astrocytic accumulation during demyelination phase leading to a faster remyelination process, while it does not affect oligodendrocyte precursor cell recruitment or microglia/macrophage accumulation. In addition, our *in vitro* studies showed that BNN20 acts directly to oligodendrocytes by enhancing their maturation and increasing the number of mature myelinating oligodendrocytes, even after treatment with lysophosphatidylcholine. This beneficial effect of BNN20 is mediated, primarily, through the neurotrophin receptor TrkA. Lastly, BNN20 reduces microglia activation and their transition to their pro-inflammatory state upon LPS stimulation *in vitro*. According to the data presented in this work, we propose that BNN20 could serve as an important molecule to develop BBB-permeable synthetic agonists of neurotrophin receptors that could reduce inflammation and increase the number of functional oligodendrocytes by promoting their differentiation/maturation.



## ΠΕΡΙΛΗΨΗ I

Στο πρώτο κομμάτι της διδακτορικής διατριβής το ενδιαφέρον μας επικεντρώθηκε στο μόριο BNN20, το οποίο είναι ένα συνθετικό ανάλογο του νευροστεροειδούς DHEA με ισχυρή νευροπροστατευτική δράση. Στόχος μας ήταν να διευκρινιστεί εάν το BNN20 έχει κάποια δράση σε γλοιακούς πληθυσμούς σε καταστάσεις απομυελίνωσης και επαναμυελίνωσης. Για το σκοπό αυτό χρησιμοποιήσαμε *in vivo* και *in vitro* προσεγγίσεις. Σχετικά με το *in vivo* κομμάτι χρησιμοποιήσαμε το LPC μοντέλο απομυελίνωσης σε αρσενικούς μύες. Χορήγηση του BNN20 είχε σαν αποτέλεσμα την μείωση της καταστροφής της μυελίνης, την αύξηση του αριθμού των ώριμων ολιγοδενδροκυττάρων, καθώς και την μείωση της συσσώρευσης των αστροκυττάρων στην περιοχή της βλάβης, οδηγώντας σε ταχύτερη επαναμυελίνωση. Το BNN20 δεν φαίνεται να έχει κάποια δράση στους πληθυσμούς των πρώιμων ολιγοδενδροκυττάρων και των μακροφάγων/μικρογλοιακών που συσσωρεύονται στην περιοχή της βλάβης. Σχετικά με το *in vitro* κομμάτι απομονώσαμε πρωτοταγείς καλλιέργειες ολιγοδενδροκυττάρων και μικρογλοιακών. Σχετικά με τα ολιγοδενδροκύτταρα διαπιστώσαμε πως η χορήγηση του BNN20 αυξάνει την διαδικασία της ωρίμανσης αυτών, αυξάνοντας έτσι τον συνολικό αριθμό των ώριμων ολιγοδενδροκυττάρων στην καλλιέργεια, ακόμα και μετά από χρήση του LPC *in vitro*. Επιπλέον δείξαμε πως το BNN20 δρα στα ολιγοδενδροκύτταρα μέσω του υποδοχέα TrkA. Τέλος, σχετικά με τα μικρογλοιακά δείξαμε πως η χορήγηση του BNN20 μειώνει την επαγόμενη από LPS ενεργοποίηση των μικρογλοιακών και την μετάβασή τους στην προ-φλεγμονώδη κατάσταση. Με βάση τα αποτελέσματα της συγκεκριμένης μελέτης πιστεύουμε πως το συγκεκριμένο συνθετικό ανάλογο θα μπορεί να χρησιμοποιηθεί σαν πρότυπο για την παραγωγή ουσιών που θα μπορούν διαπερνώντας τον αιματοεγκεφαλικό φραγμό και δρώντας μέσω των υποδοχέων νευροτροφινών, να μειώνουν την φλεγμονή και να αυξάνουν την διαφοροποίηση των ολιγοδενδροκυττάρων κάτι που θα οδηγούσε τελικά σε μεγαλύτερο αριθμό λειτουργικών ώριμων ολιγοδενδροκυττάρων.

## ABSTRACT II

In the second part of this doctoral thesis, we used the data of the Allen gene expression atlas in combination with Tabula Muris, which is a compendium of single cell transcriptome data collected from mice, enabling direct and controlled comparison of gene expression among cell types to provide further insights into the physiology of TAG-1/Contactin-2 and its interactions, by presenting the expression of the corresponding gene across the adult mouse brain under baseline conditions and to investigate any spatial genomic correlations between TAG-1/Contactin-2 and its interacting proteins and markers of mature and immature oligodendrocytes, based on preexisting experimental, bibliographical or computational evidence. The across-brain correlation analysis on the gene expression intensities showed a positive spatial correlation of TAG-1/Contactin-2 with the gene expression of *Plp1*, *Myrf*, *Mbp*, *Mog*, *Cldn11*, *Bace1*, *Kcna1*, *Kcna2*, *App* and *Nfasc*, and a negative spatial correlation with the gene expression of *Cspg4*, *Pdgfra*, *L1cam*, *Ncam1*, *Ncam2* and *Ptprz1*. Spatially correlated genes are mainly expressed by mature oligodendrocytes (like *Cntn2*), while spatially anticorrelated genes are mainly expressed by oligodendrocyte precursor cells. According to the data presented in this work, we suggest that even though Contactin-2 expression during development correlates with high plasticity events such as neuritogenesis, in adulthood it correlates with pathways characterized by low plasticity.

## ΠΕΡΙΛΗΨΗ II

Στο δεύτερο μέρος της διδακτορικής διατριβής αντλήσαμε δεδομένα από τον άτλαντα γονιδιακής έκφρασης Allen, καθώς και από την πλατφόρμα Tabula Muris, έτσι ώστε να παρέχουμε νέες πληροφορίες σχετικά με την φυσιολογία του μορίου κυτταρικής συνάφειας TAG-1/Contactin-2, καθώς και σχετικά με τις αλληλεπιδράσεις αυτού με άλλα μόρια. Στη μελέτη αυτή παρουσιάσαμε την έκφραση του γονιδίου της Contactin-2 (Cntn2) στις διαφορετικές περιοχές του εγκεφάλου ενήλικων μυών υπό φυσιολογικές συνθήκες, καθώς και η χωρική συσχέτιση του γονιδίου αυτού με άλλα γονίδια, των οποίων τα προϊόντα με βάση παλαιότερες πειραματικές ή υπολογιστικές μελέτες (πιθανόν) αλληλεπιδρούν με την Contactin-2. Τα αποτελέσματα της ανάλυσης αυτής έδειξαν πως υπάρχει μία θετική χωρική συσχέτιση της γονιδιακής έκφρασης του γονιδίου Cntn2 με τα γονίδια P1p1, Myrf, Mbp, Mog, Cldn11, Bace1, Kcna1, Kcna2, App και Nfasc και μία αρνητική χωρική συσχέτιση με τα γονίδια Cspg4, Pdgfra, L1cam, Ncam1, Ncam2 και Ptpnz1. Τα γονίδια με την θετική χωρική συσχέτιση εκφράζονται κυρίως από ώριμα ολιγοδενδροκύτταρα (όπως και το γονίδιο Cntn2), ενώ τα γονίδια με την αρνητική χωρική συσχέτιση εκφράζονται κυρίως από πρώιμα ολιγοδενδροκύτταρα. Με βάση τα αποτελέσματα που παρουσιάζουμε στην συγκεκριμένη μελέτη προτείνουμε πως παρόλο που η έκφραση του μορίου κυτταρικής συνάφειας Contactin-2 κατά την διάρκεια της ανάπτυξης σχετίζεται με διεργασίες υψηλής πλαστικότητας όπως για παράδειγμα η νευριτογέννεση, κατά την ενήλικη φάση σχετίζεται κυρίως με διεργασίες χαμηλής πλαστικότητας.

## A. INTRODUCTION I

### A.1. The importance of myelination

One of the consequences of vertebrate evolution was the increase in body size, a fact that created the need of action potential propagation along bigger distances. This signal propagation could be promoted by a decrease in axonal capacitance and an increase in axial resistance by means of physical insulation. This physical insulation was accomplished by axonal ensheathment by the membrane of specialized cells, called glial cells, in a process called myelination. Myelination improved signal conduction in larger and more complex species. As an example, the velocity of action potential propagation along a non-myelinated fiber with a diameter of 10  $\mu\text{m}$  is less or equal to 1 m/sec, while in a myelinated axon of the same caliber it increases to 50-100 m/sec (Zalc et al., 2008).

In addition to the increased signal propagation, myelin has also two additional important functions. Firstly, it protects the axons mechanically by creating an additional layer around them isolating the electrical signal from the surrounding tissue. Secondly, it supports the axons by providing energy metabolites (Funfschilling et al., 2012; Lee et al., 2012a; Lee et al., 2012b; Morrison et al., 2013). There are two mechanisms of transport from the soma to the axons: the active transport via motor proteins, such as in the case of vesicles and the passive transport via diffusion of soluble molecules.

In conclusion, the importance of myelination favored the evolutionary success of vertebrates that possess myelinated axons by allowing increased brain, body size and the evolution of complex and sophisticated behavioral traits.

### A.2. Myelin origin

Myelin is formed by glial cells, which expand their plasma membrane around the axon and wrap around it several times. In the central nervous system (CNS) myelin is formed by oligodendrocytes (OLs), while in the peripheral nervous system (PNS) by Schwann cells. Myelin is composed of 70-80% lipids and 15-30% of myelin-specific proteins. The increased composition of myelin in lipids is different from other biological membranes, which have a higher protein-to-lipid ratio (Barateiro and Fernandes, 2014). The distinct composition of the cell membrane of the two glial types results in unique myelin proteins in the CNS and the PNS. CNS myelin is composed of the myelin basic protein (MBP), proteolipid protein (PLP), 2':3'-Cyclic nucleotide-3'-phosphodiesterase (CNP) and myelin-associated glycoprotein (MAG). In the PNS, myelin shares some common proteins with the CNS, such as MBP and MAG, while it is also composed by others, which are unique for PNS such as P<sub>0</sub> and peripheral myelin protein-22 (PMP-22).

OLs and Schwann cells have a different origin but in both CNS and PNS, myelination is a dynamic procedure throughout development and adult life and depends on continuous cell-cell interactions between axons and glial cells. However, a striking difference between the two is the constant need of the Schwann cell to receive contact-dependent signaling from the axons (Mirsky et al., 1980). Even to be cultured in vitro, Schwann cells require cAMP, which mimics

the presence of neurons (Morgan et al., 1991; Bacallao and Monje, 2015). On the other hand, OLs are able to myelinate even when a simulation of an axon is present, like a fixed axon or a nanofiber with a diameter within the range of that of axons (Rosenberg et al., 2008; Lee et al., 2012; Lee et al., 2013). Furthermore, while one OL myelinates up to 40 axonal segments (Pfeiffer et al., 1993), each Schwann cell wraps only around a single axon (Figure 1). In conclusion, the differences in cell biology and origin of the two types of glial cells may account for the functional differences as well. In this study we will focus on the CNS.

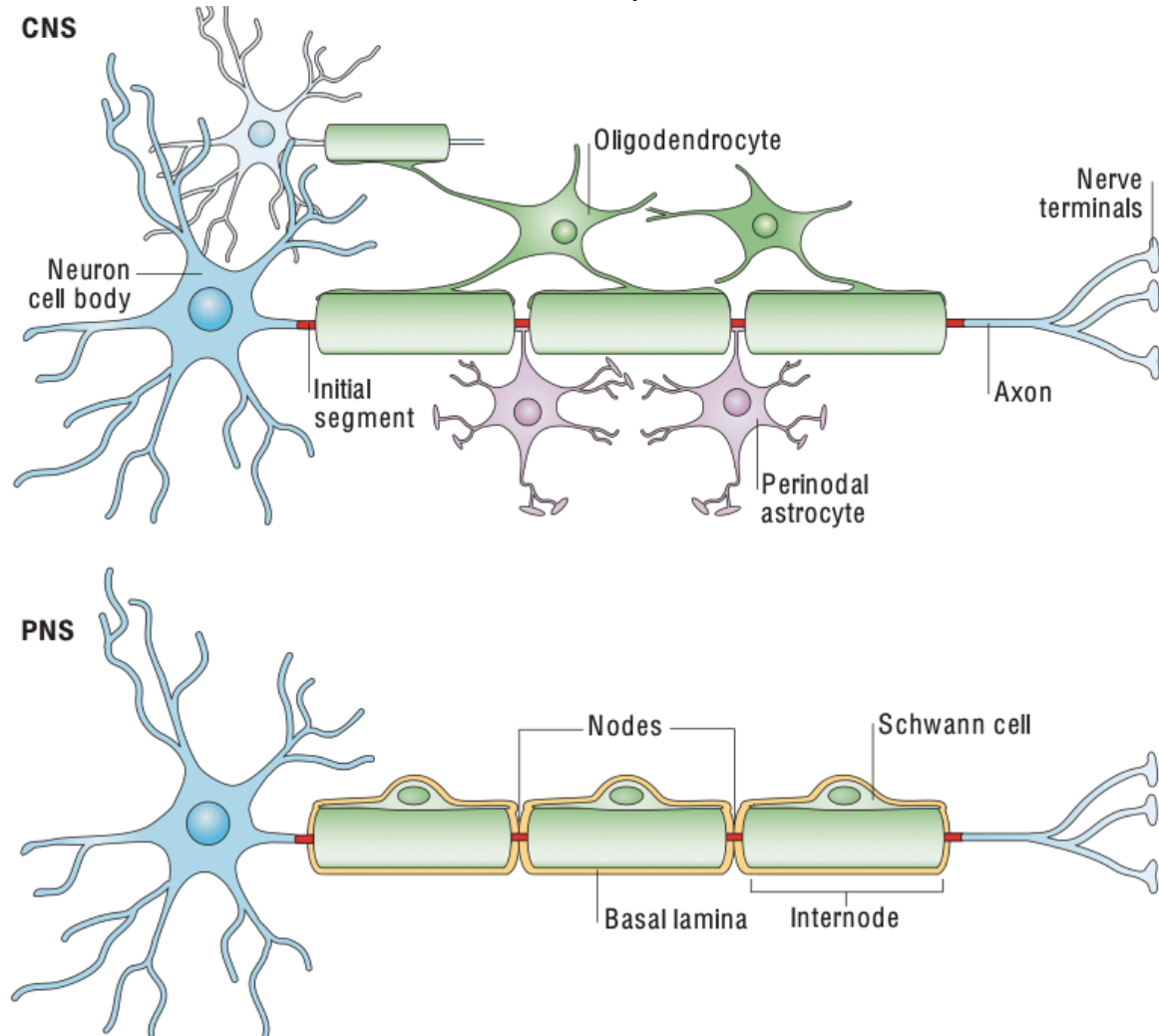


Figure 1: Structure of myelinated axons in CNS and PNS: OLs in the CNS and Schwann cells in the PNS, form the myelin sheath by enwrapping their membrane several times around the axon. Myelin enwrapps the axon at internodes, leaving gaps called nodes of Ranvier. OLs can myelinate different axons and several internodes per axon, whereas Schwann cells myelinate a single internode in a single axon (Poliak and Peles, 2003).

### A.3. Oligodendrocytes and CNS myelination during development

Mouse oligodendrocyte precursor cells (OPCs) are generated in discrete waves during embryogenesis from neuroepithelial precursors situated in or adjacent to the ventricular zone

(VZ) and are characterized by the expression of the proteoglycan NG2, the platelet-derived growth factor receptor alpha (Pdgfra) and the oligodendrocyte lineage transcription factor Olig2 (Rowitch, 2004; Richardson et al., 2006, Tomassy and Fossati, 2014).

Three sequential waves of OPCs are generated from different regions of the forebrain VZ (Figure 2a). The first wave (OPC1) arises from *Nkx2.1*-expressing precursors in the medial ganglionic eminence (MGE), starting at E12.5. The second wave (OPC2) arises from precursors expressing the homeobox gene *Gsx2* in the lateral and medial ganglionic eminences, starting at E15.5, while and the third and last wave (OPC3) arises from precursors expressing the homeobox gene *Emx1* in the cortex, starting at birth (Rowitch and Kriegstein, 2010).

Two distinct waves of OPCs arise from the ventral region and the dorsal region of the spinal cord in the embryo and fetus, respectively, while a third wave arises after birth (Figure 2b). In the first wave (OPC1), ventral OPCs arise from *Olig2*-expressing progenitor cells in the pMN domain at E12.5 and subsequently migrate to populate the entire neural tube. The development of these cells is mediated by Sonic Hedgehog (Shh) signaling, while is inhibited by dorsally derived BMPs and WNT proteins (Warf et al., 1991; Pringle and Richardson, 1993; Sun et al., 1998; Orentas et al., 1999; Richardson et al., 2000; Rowitch, 2004). In the second wave (OPC2), dorsal OPCs develop from *Olig2*-expressing cells of the dP3, dP4, dP5 and dP6 domains at day E15.5 in a Shh-independent manner. The origins of the third wave (OPC3), that occurs after birth, remain unclear. These OPCs could either arise from progenitor cells, which remain around the central canal, or from proliferative *Ng2*-expressing precursor cells throughout the parenchyma (Rowitch and Kriegstein, 2010).

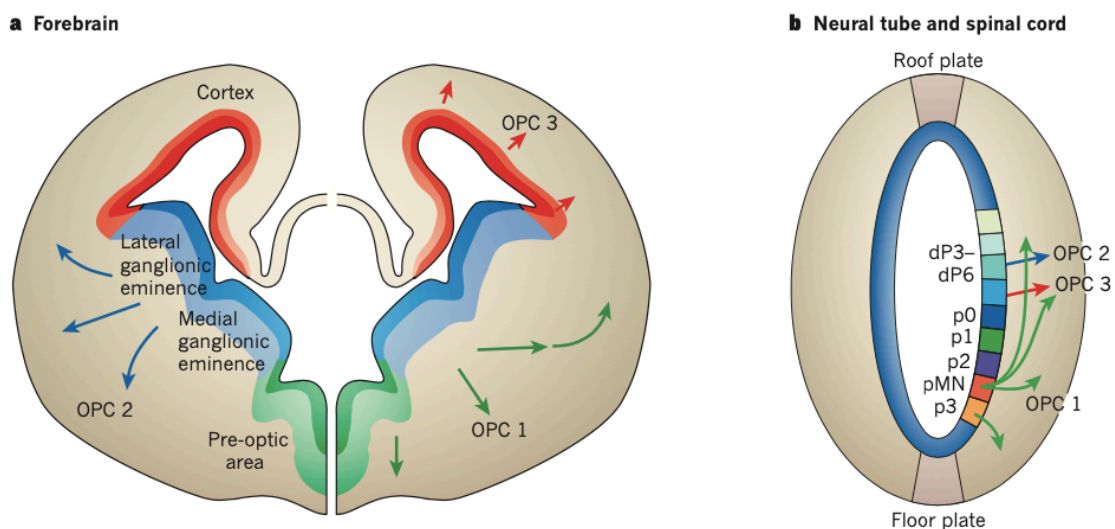


Figure 2: Different waves of oligodendrocyte generation in the mammalian CNS. (a) Three different waves of oligodendrocyte production observed in the forebrain ventricular zone. The first one (OPC1) arises at E12.5, the second one (OPC2) at E15.5, while the third one starts at birth. (b) Three different waves of oligodendrocyte production observed in neural tube and the ventral and dorsal region of the spinal cord. The first one (OPC1) arises at E12.5, the second one (OPC2) at E15.5, while the third one starts after birth (Rowitch and Kriegstein, 2010).

After their specification, OPCs migrate while still proliferating to populate the spinal cord and forebrain. Their migration is controlled by various morphogens and extracellular matrix (ECM) proteins as well as the corresponding receptors (de Castro and Bribian, 2005; Colognato and Tzvetanova, 2011; Mitew et al., 2014; Ackerman et al., 2015). When reaching their destination, OPCs become post-mitotic and acquire a pre-myelinating identity as Nkx2.2<sup>+</sup> cells, mainly in white matter regions. Pre-myelinating OPCs are able to wrap around axons with their plasma membrane but do not form mature myelin (Kirby et al., 2006; Kucenas et al., 2008; Mitew et al., 2014; Snaidero et al., 2014; Zhu et al., 2014). In mice, this state is highly transient and the cells either progress to become myelinating OLs or proceed to apoptosis (Barres et al., 1992; Trapp et al., 1997).

There is a variety of mechanisms that are responsible for the development and differentiation of oligodendrocytes. PDGFR $\alpha$  and NG2 are markers of OPCs, while OLs express *adenomatous polyposis coli* (APC/CC1) and proteolipid protein (PLP). Myelinating OLs express myelin basic protein (MBP) and myelin oligodendrocyte glycoprotein (MOG). During embryogenesis, Shh signaling is required until the time of OPC migration from the ventricular zone, as mentioned above. It is also shown that *Gli2*, Nkx6.1, Nkx6.2, as well as temporal-dependent cell fate specification mechanisms play an essential role during this procedure (Briscoe and Novitch, 2008). Later phases of OPC maturation are Shh-independent requiring Sox10, Nkx2.2, and Olig1 function. According to the literature, there are several key regulators of developmental myelination, including transcription factors YY1, MRF, ZFP191, and Tcf4, intracellular signaling pathways such as Wnt (mediated by  $\beta$ -catenin/Tcf4), and also posttranscriptional control via miRNAs (Figure 3) (Fancy et al., 2011).

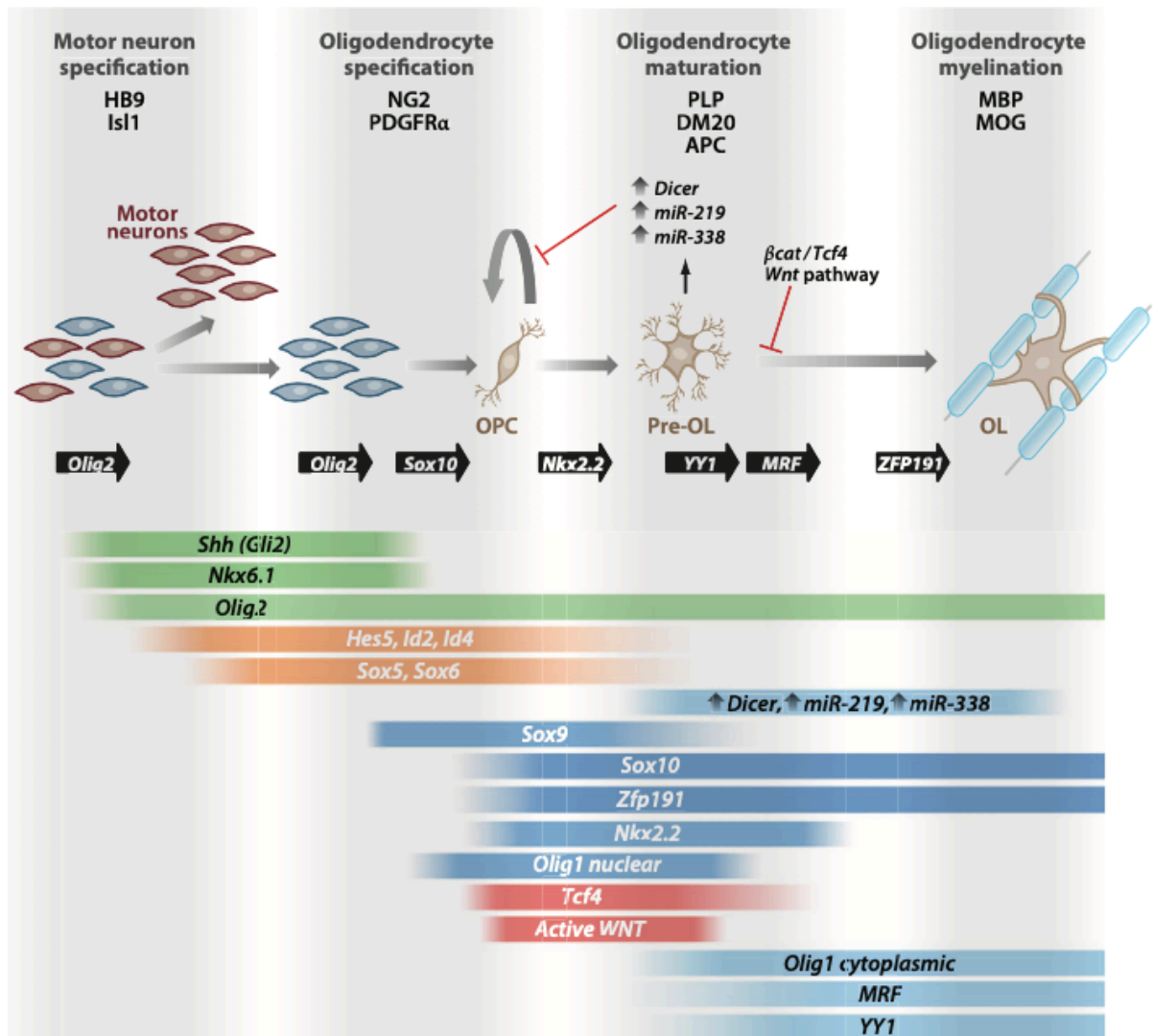


Figure 3: Schematic representation of different mechanisms influencing oligodendrocyte development and differentiation during various developmental stages (Fancy et al., 2011).

#### A.4. Myelination and demyelination during adulthood in the CNS

Although most OPCs differentiate during the first weeks of postnatal life, there is a 5-8% of glial cells of the CNS that remains undifferentiated. Myelin keeps being generated in the healthy adult nervous system as a result of neuronal activity, both in mice and humans (Giedd, 2004; Miller et al., 2012). In humans this process is performed by OLs that have already differentiated during development, while in mice new myelin is formed by newly differentiated OLs (Young et al., 2013; Yeung et al., 2014).

Demyelination is defined as the loss of myelin around axons (Figure 4). It can either be due to a congenital condition affecting glial cells or an acquired inflammatory pathology, such as multiple sclerosis (MS). Following damage, remyelination occurs due to adult OPCs and neural stem cells (NSCs). Adult OPCs express NG2 and Pdgfra and can be found not only in healthy brain parenchyma but also in and around demyelinating MS lesions (Scolding et al., 1998). These cells are not capable of migrating along long distances but they differentiate locally



(Gensert and Goldman, 1997; Zawadzka et al., 2010). NSCs express glial fibrillary acidic protein (GFAP) and Nestin and are located in the subventricular zone (SVZ) of the brain. Under normal circumstances NSCs are quiescent but after a demyelinating incidence they can give rise to OLs as a response to local increase to Shh and induction of the effector molecule Gli1 (Menn et al., 2006; Samanta et al., 2015).

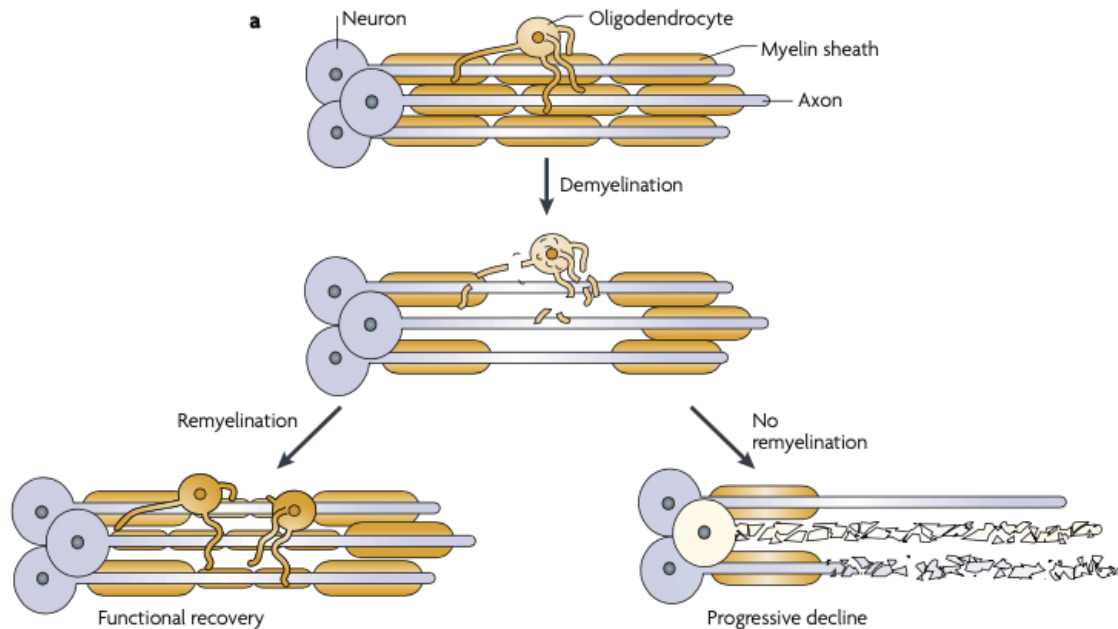


*Figure 4: Demyelination in the CNS. Following demyelination in the CNS there are two possibilities. Either there is a successful remyelination process, which occurs from newly differentiated OLs, resulting in the formation of thinner, but still sufficient myelin sheaths and functional recovery of the axons or remyelination is not successful and axons eventually degenerate due to loss of trophic support. (Franklin and Ffrench-Constant, 2008).*

Unfortunately, in the adult CNS, axons do not always become properly remyelinated following an insult (Mason et al., 2001). It is believed that this happens due to the formation of a glial scar (accumulation of astrocytes and microglia) that surrounds the damaged area and/or due to faulty re-ensheathment of axons by the OLs (Huebner and Strittmatter, 2009). This failure is observed not only in mice, but also in human inflammatory demyelinating pathologies such as MS, especially during later stages of the disease (Prineas and Connell, 1979; Franklin and Ffrench-Constant, 2008; Franklin and Goldman, 2015). During early disease progression remyelination proceeds successfully and is correlated with increased OPC proliferation, while later on remyelination attempts are unsuccessful leading to degeneration of the denuded axons (Raine et al., 1981; Franklin and Ffrench-Constant, 2008). Although the reason why this happens remains unclear, it is believed that either insufficient OPCs are recruited in the damaged area or the increased numbers of NG2<sup>+</sup> OPCs that are found in and around MS lesions during early and chronic disease stages do not have the capacity to differentiate fully to OLs (Wolswijk, 1998; Kuhlmann et al., 2008; Fancy et al., 2011) (Figure 5).

While current dogma suggests that surviving mature oligodendrocytes do not participate in remyelination, there is very recent evidence from a variety of animal models of demyelinating

injury suggesting that surviving myelinating oligodendrocytes are able to make new myelin sheaths. More specifically, recent studies showed that motor learning can improve remyelination by both promoting OPC differentiation (thus oligodendrogenesis) and myelin sheath formation by surviving oligodendrocytes (Bacmeister et al., 2020).

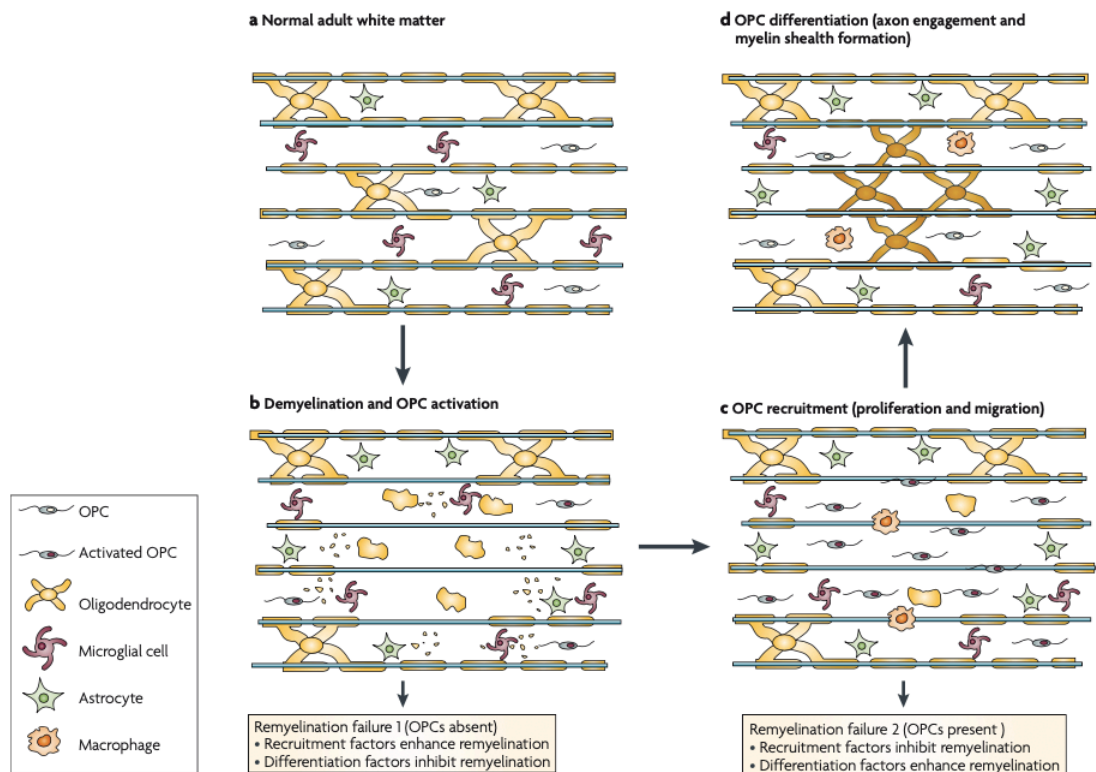


Figure 5: The phases of remyelination. (a) Normal adult white matter contains OLs, OPCs, astrocytes and microglia. (b) Following demyelination microglia and astrocytes become activated, leading to the activation of any OPCs in the vicinity. (c) Activated OPCs respond to mitogens and pro-migratory factors generated by reactive astrocytes and inflammatory cells leading to proliferation and migration of the OPCs in the demyelinated area. Macrophages also start removing the myelin debris. (d) The recruited OPCs differentiate into remyelinating oligodendrocytes. Remyelination can be unsuccessful either due to failure of OPC recruitment or due to failure of differentiation. (Franklin and Ffrench-Constant, 2008).

### A.5. The role of glial cells in myelin development, damage and repair

Astrocytes, OLs and microglia represent glial cells in the adult mammalian CNS. The role of glial cells under normal and pathological conditions have been partially ignored because many basic properties of their physiology and pathophysiology are still not completely understood. However, it is becoming obvious that glial cell crosstalk plays a very important role in brain function during development and disease, including the modulation of homeostatic and synaptic functions, myelination, nerve signal propagation and responses to neural injury (Herculano-Houzel, 2014).

Astrocytes have star-shape morphology being the most abundant CNS glial cell type. They have an important role in blood brain barrier (BBB) maintenance, neuronal survival and in synapse formation, strength and turnover (Barres, 2008). Both OLs and astrocytes originate from a common lineage of neural progenitor cells within the neuroectoderm, while microglia, which are the main innate immune cells of the CNS, arise from hematopoietic stem cells in the yolk sac during early embryogenesis. Being ontogenetically different from other tissue-macrophages they have longevity and capacity for self-renewal (Prinz and Priller, 2014).

Astrocytes originate from neural embryonic progenitor cells that line the lumen of the embryonic neural tube. However, they can be formed indirectly via radial glia cells, which in addition to functioning as scaffolding for newborn neuron migration, can serve as progenitor cells giving rise to astrocytes (Kessaris et al., 2008). In mammals, astrocytes arise from radial glial cells in the ventricular zone. In mice, this differentiation starts at approximately embryonic day 12.5 in the spinal cord and embryonic day 16 in the brain in which migration and asymmetric proliferation produce immature astrocytes (Akdemir et al., 2020; Rawji et al., 2020).

Protoplasmic astrocytes are localized in the gray matter and are responsible for the ensheathment of synapses and blood vessels promoting synapse and BBB functions, respectively. Fibrous astrocytes are localized in the white matter and their role is to contact the nodes of Ranvier and the blood vessels (Sofroniew and Vinters, 2010). Astrocytes can acquire different states ranging from inactive or quiescent, to active and reactive. Quiescent astrocytes exist in the normal resting CNS tissue. Upon injury or insult, astrocytes become activated by various mechanisms resulting in mild astrogliosis. Reactive astrocytes are found near the injury site and are responsible for glial scar formation (Nash et al., 2011).

Astrocytes and OLs crosstalk and this has an impact on myelination. For example, protoplasmic astrocytes were found to expand O-2A progenitors from neonatal rat optic nerve. Such expansion was mediated by unidentified soluble growth factors (Noble and Murray, 1984), later identified as platelet-derived growth factor (PDGF) (Noble et al., 1988) and basic fibroblast growth factor (FGF2) (Bogler et al., 1990). PDGF and FGF2 are both potent mitogens for OPCs while at the same time inhibit premature oligodendrocyte differentiation. There are also other soluble factors secreted by astrocytes implicated in enhancing myelination, such as the leukemia inhibitory factor-like protein (LIF), which is responsible for OL survival and OL maintenance in a mature myelinogenic state (Gard et al., 1995). Other examples are neuregulin-1 (Taveggia et al., 2008), gamma-secretase (Watkins et al., 2008), ciliary neurotrophic factor (CNTF) (Stankoff et al., 2002), insulin-like growth factor 1 (IGF-1) (Zeger et al., 2007), and neurotrophin-3 (NT3) (Kumar et al., 2007). Physical contact with astrocytes can also accelerate the maturation of oligodendrocytes (Sakurai et al., 1998). Astrocytes promote adult mouse OL survival through a cell-contact dependent mechanism involving the interaction of  $\alpha 6 \beta 1$  integrin on OLs with laminin on astrocytes (Corley et al., 2001). In addition to promoting OL survival and differentiation, astrocytes are also able to affect other aspects of OL biology, such as process extension through FGF2 in combination with the ECM proteins fibronectin and laminin (Oh and Yong, 1996).

According to previous studies and by taking advantage of remyelinating models, it was shown that *in vivo* transplantation of protoplasmic astrocytes resulted in OL remyelination and increased the thickness of myelin sheaths (Franklin et al., 1991). The expression of TNFR2 in

astrocytes resulted in the autocrine expression of CXCL12, which acted via its receptor CXCR4 on OPCs and induced their proliferation and differentiation, thus enabling remyelination (Patel et al., 2012). Moreover, previous studies showed that ablation of astrocytes during cuprizone-induced demyelination did not prevent myelin damage, while it inhibited the removal of myelin debris and delayed remyelination (Skripuletz et al., 2013). All these results suggest that the astrocyte free regions of the lesion either contained inhibitory signals preventing terminal differentiation of OPCs or lack appropriate signals necessary for OPCs to undergo terminal differentiation.

There are also studies suggesting that astrocytes have detrimental effects on oligodendrocyte differentiation and more specifically those within the glial scar, inhibiting regeneration and having a negative impact on remyelination (Silver and Miller, 2004). *In vitro* studies showed that protoplasmic astrocytes inhibited myelination of dorsal root ganglion axons by OLs (Rosen et al., 1989). Astrocytes secrete factors that are implicated in the inhibition of myelination and remyelination. Besides the above mentioned PDGF and FGF2 (Bogler et al., 1990), which promote OPC proliferation and inhibit their differentiation, others such as tenascin C (Nash et al., 2011), BMP 2/4 (Wang et al., 2011), and hyaluronan (Sloane et al., 2010) have also been described. After injury to the CNS, a variety of different cell populations including reactive astrocytes, microglia/macrophages, and pericytes, secrete extracellular matrix components [56], including the chondroitin sulphate proteoglycans (CSPGs), hyaluronan, tenascin-C, and fibronectin. All these components inhibit remyelination, while they are found to be present in lesions from MS patients (Lau et al., 2013). In addition to the extracellular matrix components, astrocytes express endothelin-1 (ET-1), a molecule that has been shown to be inhibitory to remyelination through notch activation in mice. Astrocytes, that respond to ET-1, upregulate the Notch1 receptor ligand, jagged-1, leading to an inhibitory interaction between astrocytes and OPCs (Hammond et al., 2014; Hammond et al., 2015; Rawji et al., 2020).

Overall, these studies suggest that the outcome of glial interactions in myelination depends on the surrounding microenvironment, meaning that the activation state of astrocytes likely determines their permissive or inhibitory influence on oligodendrocyte development. In addition to the different astrocyte phenotypes, the distance of these populations to the lesion site should also be considered, as relatively small changes in the responsive milieu may have different impacts on oligodendrocyte behavior. It is suggested that while astrocytes more distal to the lesion are activated cells contributing to a greater extent to regeneration through the secretion of growth factors and cytokines, astrocytes that are very close to injury are more reactive and may negatively affect the remyelination process (Nash et al., 2011).

Microglia comprise the myeloid resident population of the CNS, representing around 10% of the total glial cells within the nervous tissue (Soulet and Rivest, 2008). They are the resident macrophages of the CNS, representing the first line of defense against injury and infections. Microglia originate from yolk-sac macrophages (YSM) and enter the brain after the first generation of neurons (around embryonic day 9.5 in mice) (Prinz et al., 2017). They expand and self-renew during adulthood (Thion and Garel, 2017). Except their immune roles, recent studies have shown that both fetal and adult microglia contribute to different important processes including brain development, homeostasis, and function, while they also regulate synaptic transmission, synaptic pruning and formation, cell death and survival, as well as embryonic wiring (Hong et al., 2016; Thion and Garel, 2017).

Recent studies have shown that there is a strong neuroimmune interplay in adults determining how the brain modulates tissue immunity, normal processes of aging, as well as inflammation and neurological disorders including Alzheimer's disease, Parkinson's disease, multiple sclerosis, and various autoimmune pathologies. Additionally, activation of the immune system during pregnancy or early life exerts long-term effects on the wiring of neural circuits and may contribute to the etiology of neurodevelopmental disorders (Li and Barres, 2018).

Further studies have also shown that microglia undergo distinct phases of differentiation relying on signals derived from the maturing CNS (Thion et al., 2018). These signals include colony-stimulating factor 1 (CSF1), IL-34, and transforming growth factor- $\beta$  (TGF- $\beta$ ) (Li and Barres, 2018). At the molecular level, transition between a brain macrophage and a microglial profile can be identified by the expression of core genes, including genes encoding the transcription factor SALL1 and the receptor P2Y12 (Li and Barres, 2018; Holtman et al., 2017). Additionally, the fact that the adult CNS environment is not sufficient to induce full microglial differentiation, indicates that both their early origin and interactions with the CNS are critical for the acquisition of a microglial identity (Bennett, 2018; Thion et al., 2018).

Moreover, local neural signals possibly regulate the brain colonization pattern and heterogeneity of microglial populations in time and space. Microglia enter the CNS in sequential waves and transiently adopt a stereotypical and heterogeneous pattern of localization (Swinnen et al., 2013; Cunningham et al., 2013). For example, microglia undergo timely invasion into the deep layers of the neocortex, while they also associate with distinct axonal tracts, including the corpus callosum and dopaminergic midbrain axons, and populate specific niches known to contain neurogenic progenitors (Cunningham et al., 2013). This pattern is possibly regulated by transient CNS cell expression of IL-34, CSF1, CXCL12, and CX3CL1. Furthermore, recent studies have shown that developmental programmed cell death in the CNS regulates microglial colonization. Following early colonization adult microglia display some heterogeneity across brain regions, particularly in the corpus callosum, prefrontal cortex, cerebellum, or basal ganglia (Li and Barres, 2018; Hagemeyer et al., 2017; Thion et al., 2018). According to literature, the developmental trajectory of microglia is influenced by sexual identity and systemic signals such as those derived from the microbiota or inflammation at pre- and postnatal stages (Thion et al., 2018; Hanamsagar et al., 2017; ). There are several studies showing a distinct transcriptomic signature of microglia in males versus female animals that begins postnatally and is maintained in adults (Hanamsagar et al., 2017; Villa et al., 2018). It is believed that this sexual dimorphism is conserved after grafting and may occur independently of circulating sex hormones, suggesting long-lasting programming by early life hormones or genetic factors (Villa et al., 2018; Thion et al., 2018).

Microglia are critically involved in the scavenging of dying cells, pathogens and molecules that engage pattern recognition receptors. Under normal conditions, microglia are characterized by a ramified morphology and their role is to "scan" CNS for any potential threats. During CNS injury, these cells are activated and change from a ramified to an amoeboid morphology (Figure 6). The activated microglia can be either pro-inflammatory secreting factors like IL-1, IL-12, IL-23, TNF $\alpha$  and iNOS, when promoting inflammation and cytotoxicity or anti-inflammatory secreting factors like IL-4, IL-10, IL-13, TGF $\beta$  and Arg1, when reducing inflammation and promoting a neuroprotective response (Gordon and Taylor, 2005; Colton,

2009). In general, microglia are able to shift functions in order to retain tissue homeostasis influenced by the environment (Orihuela et al., 2016).

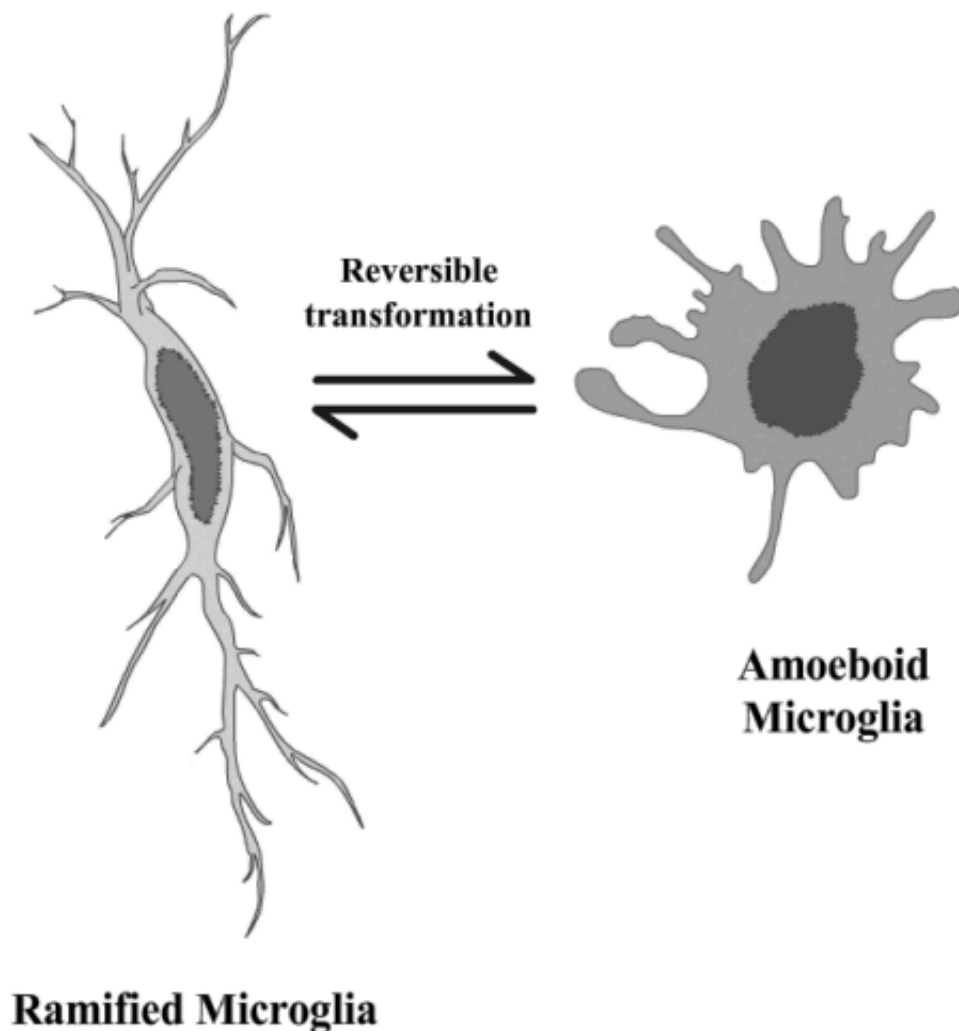


*Figure 6: Two different microglia morphologies. During their resting state microglia are characterized by a ramified morphology, while during their activated state there are characterized by an amoeboid morphology. (Ghosh, 2010)*

Microglial activation has been described extensively in autoimmune diseases such as MS in humans and in the EAE mouse MS model. In these pathological conditions, microglia are able to produce and release neurotoxic or neurotrophic molecules, pro and anti-inflammatory cytokines or chemokines as mentioned above, and present self-antigens to immune cells. Pathological evidence suggests that the remyelination onset in fresh lesions of brain and spinal cord of patients with MS occurs in acute, active lesions, which are characterized by a robust inflammatory response (Prineas et al., 1989). Following injury, different inflammatory molecules such as cytokines and chemokines are secreted and released by microglia in the surrounding milieu. In this scenario, microglia become activated, expand, migrate and

accumulate within the damaged area of the neuronal parenchyma, playing both beneficial and detrimental roles during myelin damage and repair.

Previous studies using microglia and oligodendrocyte co-cultures showed that microglia increase the expression of the myelin-specific proteins MBP and PLP in OLS, suggesting a positive role for microglia in myelination (Hamilton and Rome, 1994). In agreement with this, conditioned medium derived from non-activated microglia enhanced OPC survival and maturation through the increase of PDGF $\alpha$  receptor-signaling pathway and modulation of NF- $\kappa$ B activation (Nicholas et al., 2001). The iron status of microglia is also important for OL survival. Increasing the iron load promotes the release of H-ferritin by microglia and incubation of OL cultures with conditioned medium of iron-loaded microglia is associated with increased survival of these cultures (Poliani et al., 2015).

Conditioned medium of non-activated microglia cultures was compared with that of astrocytes in order to evaluate their effect in OPC proliferation and differentiation. The results showed that astrocyte-conditioned medium was more efficient in promoting OPC proliferation, while microglia-conditioned medium accelerated oligodendrocyte differentiation more efficiently than that of astrocytes. Analysis of the media composition revealed that astrocyte-conditioned medium had increased levels of PDGF $\alpha$ , FGF2, FGF2 binding protein, CNTF, growth hormone, TIMP-1 and thrombospondin. In contrast, levels of IGF-1, E-selectin, fractalkine (CX3CL1), neuropilin-2, IL-2, IL-5 and vascular endothelial growth factor (VEGF) were significantly higher in microglia-conditioned medium. This distinct pattern of cytokines and growth factors in the conditioned medium of astrocytes and of microglia correlates with differentially activated intracellular signaling pathways in OPC exposed to the two different media (Pang et al., 2013).

In polarization conditions, such as *in vitro* stimulation with lipopolysaccharide (LPS), the release of cytotoxic effectors by both astrocytes and microglia, produces the opposite effects on OPC (Pang et al., 2000). LPS-activated microglia hinders OPC differentiation by nitric oxide (NO)-dependent oxidative damage in an early phase and TNF in a later phase (Pang et al., 2010). In the presence of astrocytes, LPS-polarized microglia is toxic to differentiating oligodendrocytes via TNF signaling but not via NO-dependent oxidative damage (Li et al., 2008).

During remyelination, it is shown that microglia can play dual roles too. Microglia that express the CCR5 receptor were identified within early remyelinating lesions in patients at early stages of MS, suggesting a possible role for these cells in initiation of remyelination (Trebst et al., 2008). The phenotype of activated microglia was also shown to affect its beneficial role in efficient remyelination. This process depends on microglia changing from a pro-inflammatory to an anti-inflammatory dominant response in the lysolecithin-induced demyelination model. Oligodendrocyte differentiation was enhanced with anti-inflammatory microglia-conditioned medium *in vitro* and impaired *in vivo* following intralésional depletion of anti-inflammatory microglia (Miron et al., 2013).

Another important aspect of microglia during remyelination concerns its role in the clearance of myelin debris. In fact, in order to have an effective remyelination process, myelin debris has to be cleared from the injury site (Kotter et al., 2006). Myelin clearance by microglia after cuprizone-induced demyelination was found to depend on the expression of microglial triggering receptor expressed on myeloid cells 2 (TREM2), which is a surface receptor that

binds polyanions, such as dextran sulfate and bacterial LPS, and activates downstream signaling cascades through the adapter DAP12 (Poliani et al., 2015). In the cuprizone model, astrocytes are thought to recruit microglia to the lesion site to phagocyte and clear damaged myelin, a process which is regulated by the chemokine CXCL10. In the absence of astrocytes and, consequently, microglia recruitment, removal of myelin debris is significantly delayed, resulting in the inhibition of OPC proliferation and remyelination (Skripuletz et al., 2013). In conclusion, homeostasis of the CNS myelination depends on the crosstalk between oligodendrocytes, astrocytes and microglia (Figure 7). Therefore, it is very important to understand the nature and complex dynamics of such interactions, which have both beneficial and detrimental roles during damage and repair, in order to increase our knowledge of demyelinating diseases, and help us to devise novel and more holistic ways to manipulate and improve remyelination.

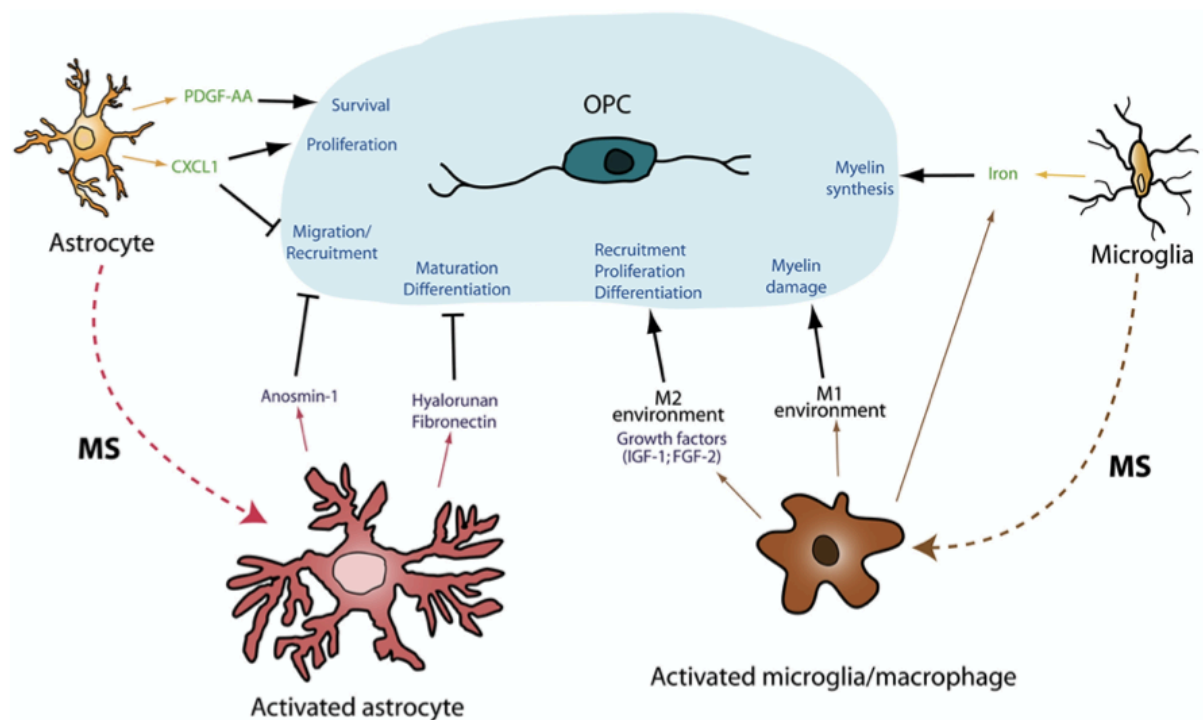


Figure 7: Representation of glia-glia interactions during development and pathology. Myelination is the result of a variety of processes affecting OPCs. During development, astrocytes and microglia release several molecules controlling a variety of aspects of oligodendrogligenesis. Both astrocytes and microglia have the ability to turn into an activated state in pathological conditions, such as MS. These activated cells produce molecular factors, affecting adult OPCs, enhancing or impairing all the processes implicated in myelin synthesis and repair. (Clemente et al., 2013)

## A.6. Multiple Sclerosis

MS is a demyelinating disease in which myelin is damaged. This damage leads to the disruption of the ability of axons of CNS to transmit signals, resulting in a range of signs and symptoms, including mainly physical and mental problems. MS is an inflammatory disease of the CNS that causes focal destruction of the myelin sheath and the



formation of the so-called glial scar (Lucchinetti et al., 1996; Lassmann, 1998). The pathological hallmark of MS is the white matter "plaque" that is widely scattered throughout the CNS, with most common cases being found in the optic nerves, brainstem, spinal cord and periventricular white matter. There are 3 main different categories of MS: the relapsing-remitting MS (RRMS), the primary progressive MS (PPMS) and the secondary progressive MS (SPMS).

Relapsing-remitting MS is characterized by unpredictable relapses followed by periods of months to years of relative remission with no new signs of disease activity. Deficits occurring during attacks can be either resolved or result in permanent disabilities. The relapsing-remitting subtype usually starts with a clinically isolated syndrome (CIS). In CIS, a person has an attack suggestive of demyelination, but does not fulfill the criteria for MS. 30 to 70% of persons who experience CIS, later develop MS. Primary progressive MS occurs in approximately 10–20% of individuals, with no remission after the initial symptoms, characterized by progression of disability from onset. The most common age of onset for the primary progressive subtype is later than the one of the relapsing-remitting subtype. Secondary progressive MS occurs in around 65% of those with initial relapsing-remitting MS, who eventually have progressive neurologic decline between acute attacks without any definite periods of remission. Occasional relapses and minor remissions may appear. The most common length of time between disease onset and conversion from relapsing-remitting to secondary progressive MS is approximately 20 years (Compston and Coles, 2008).

The pathogenesis of MS is characterised by a cascade of pathobiological events, that range from focal lymphocytic infiltration and microglia activation to demyelination and axonal degeneration (Ciccarelli et al., 2014). The hypothesis in MS, referred as "immune initiated disease", implicates that autoreactive T cells that are generated in the systemic compartment, access the CNS and induce an inflammatory cascade resulting in the injury of previously normal neural tissues (Kawakami et al., 2004; Trapp, 2004). A second hypothesis, the so-called "neural initiated disease", suggests that events within the CNS initiate the MS disease process. A frequent speculation is that an acquired acute or persistent infection of neural cells results in release of tissue antigens that, in turn, would provoke an autoimmune response (Antony et al., 2004; Rotola et al., 2004) (Figure 8).

Remyelination acts as a repair process and involves the recruitment of OPCs at the lesion site and their differentiation to mature myelinating OLs. However, remyelination is insufficient in most cases, since either not enough OPCs are present in the lesion area or the OPCs that are recruited do not differentiate in mature myelinating OLs to a sufficient level.

The licensed MS therapies have shown ability in the management of RRMS forms, but they have not shown efficacy for PMS (D'Amico et al., 2016). More specifically, the already existing therapeutic options mainly aim on stabilizing the disease progression without having any established effect on remyelination or on reversing the pathogenetic mechanisms.

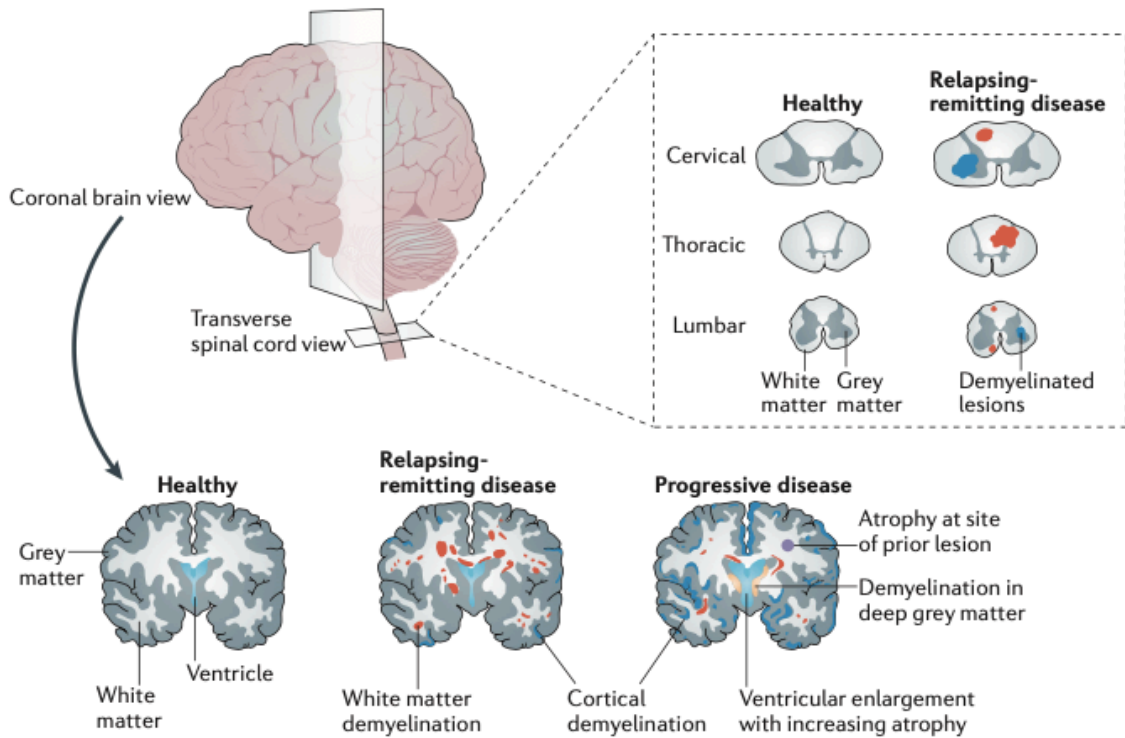


Figure 8: MS pathology is characterized by demyelinated areas in the white and grey matter of the brain and spinal cord which are called plaques or lesions indicating a loss of myelin and oligodendrocytes. Although axons and neurons are mostly preserved in early MS, progression of the disease leads to gradual neuroaxonal loss resulting in brain atrophy and patient disability. Astrocytes form glial scars in white matter lesions. Demyelinated areas of the white matter can be partially repaired by remyelination. Demyelination can also be found in the grey matter of the cortex, nuclei and spinal cord. Inflammation is present at all stages of MS, but it is more obvious in acute phases than in chronic phases. Early lesions show invading peripheral immune cells and leakage of the BBB. Macrophages dominate the infiltration, followed by CD8+, CD4+ T cells, B cells and plasma cells. As the disease continues, activation of astrocytes and microglia is observed followed by myelin reduction and axonal injury. Although T cell composition of infiltrates does not differ as the disease develops, the proportion of B cells and plasma cells increases, while microglia and macrophages remain in a chronic state of activation throughout the disease. (Dendrou et al., 2015; Kastriti et al., 2015)

### A.7. Experimental models of MS

As mentioned above, it is widely accepted that MS is an inflammatory disease, controlled by T cell mediated autoimmune reaction against the myelin sheath which predominantly affects the white matter. However, this scheme is not able to explain the entire spectrum of lesion formation in MS (Barnett and Prineas, 2004). Therefore, several animal models have been developed in order to facilitate research into the nature and treatment of MS as well as other myelin disorders. There are three main types of de- /remyelination models: the autoimmune,

virus-induced and toxin-induced (Miller et al., 1996). The most common autoimmune model is the experimental autoimmune encephalomyelitis (EAE). While there are others, the most frequently used virus-induced model is the Theiler's murine encephalomyelitis virus (TMEV). Toxins commonly used to study myelin disorders are ethidium bromide, lysolecithin and cuprizone (Miller et al., 1996).

EAE is one of the most frequently used models that mimics MS pathology allowing a detailed insight into the immunological aspects of this disease. Chronic models of EAE provide both histological and behavioural outcomes that mirror some aspects of progressive disease (Amor et al., 2005; Papadopoulos et al., 2006). EAE is a T-helper cell-mediated autoimmune disease characterized by T-cell and monocyte infiltration in the CNS, associated with local inflammation. The result of this infiltration is primary demyelination of axonal tracks, impaired axonal conduction in the CNS and progressive hind-limb paralysis. There are currently many different forms of EAE with varying patterns of clinical presentation depending on the animal species and strain, priming protein/peptide, and route of immunization employed, used to study disease development and specific histopathologic characteristics with relevance to MS, and to dissect mechanisms of potential therapeutic interventions (Robinson et al., 2014).

The TMEV model is based on virus-induced demyelination. In this model, intracranial infection of susceptible mouse strains with TMEV leads to biphasic disease of the CNS, that consists of early acute and late chronic demyelinating phase. The late chronic stage of demyelination in the TMEV infection makes this experimental model highly suitable for studying different aspects of the pathophysiology and mechanism of MS (Oleszak et al., 2004).

The common feature of the so-called toxin induced demyelination models is that neurotoxic agents are used to induce the loss of myelin sheath in certain areas in the CNS. Experimental models of demyelination based on the use of toxins have provided a remarkable tool for studying the biology of remyelination with the most frequently used demyelinating agents being lysolecithin, ethidium bromide and the copper chelator cuprizone (Blakemore and Franklin, 2008).

The administration of the copper chelator cuprizone (bis-cyclohexanone oxaldihydrazone) to mice induces spatially and temporally well-defined histopathological alterations in the CNS, including copper deficiency and demyelination (Matsushima and Morell, 2001). It is generally suggested that cuprizone induces metabolic disturbances in OLs, leading to apoptosis involving a mitochondrial mechanism. The massive OL apoptosis is followed by extensive demyelination, while complete demyelination of the corpus callosum (CC) is usually observed after six weeks of treatment. Another prominent pathological feature that is associated with OL apoptosis is the invasion of demyelinated areas by activated microglia and astrocytes. Remyelination occurs later on, mostly 3 weeks after mice stop being treated with the toxin. This aspect is important and can be studied in this and the following model but not in EAE.

Injection of lysolecithin (LPC) very quickly achieves local demyelination, acting 30 minutes post-injection. The myelin sheath is directly destroyed by this agent, attracting an inflammatory microglia and astrocyte response. LPC induces myelin phagocytosis with the exact mechanism being still unknown. This myelin disruption leads to oligodendrocytes loss. Remyelination is spontaneous and begins when the myelin debris are cleared and finishes in a matter of weeks. Mainly, remyelination starts after the second or third week post injection. (Hall, 1972). Like lysolecithin, local injection of ethidium bromide causes short-lived demyelination followed by spontaneous remyelination (Yajima and Suzuki, 1979). Because demyelination is not mediated by the immune system in these models, toxins are used to study the glial aspects of demyelination and remyelination without the complicating factors of lymphocytes and a breached BBB (Crang et al., 1991).

### **A.8. Neurotrophins and their receptors**

Neurotrophins are a family of secreted proteins, which play an important role in neuronal development, growth and survival. There are 4 different neurotrophins expressed in mammals, the nerve growth factor (NGF), the brain-derived neurotrophic factor (BDNF), the neurotrophin-3 (NT-3) and neurotrophin-4 (NT-4). NGF was discovered during a search for survival factors which could explain the deleterious effects of target tissues on the subsequent survival of motor and sensory neurons (Levi-Montalcini, 1987; Shooter, 2001). This discovery validated the central model of neurotrophic factor action, which is that targets of neuronal innervation secrete limiting amounts of survival factors, which role is to balance the size of a target tissue with the number of innervating neurons. The second neurotrophin that was characterized was BDNF. BDNF was purified from the pig brain as a survival factor for several neuronal populations that were not responsive to NGF (Barde et al., 1982).

Neurotrophins and their genes share homologies in sequence and structure, while the organization of the genomic segments next to these genes is also similar. These observations suggest that the neurotrophin genes have been developed through successive duplications of a portion of the genome derived from an ancestral chordate. The protein product of each gene consists of a signal sequence and a prodomain, that is followed by the mature neurotrophin sequence. Thus, each gene product should be processed by proteolysis to form a mature protein (Hallbook, 1999).

The neurotrophins interact with two different classes of receptors, the p75 neurotrophin receptor (p75<sup>NTR</sup>) and the tropomyosin receptor kinases (Figure 9). p75<sup>NTR</sup> was identified as a low-affinity receptor for NGF, but it was subsequently shown to bind each of the neurotrophins with a similar affinity (Rodriguez-Tebar et al., 1990; Frade and Barde, 1999). It is a member of the tumour necrosis receptor superfamily having an extracellular domain that consists of four cysteine-rich motifs, a single transmembrane domain and a cytoplasmic domain including a 'death' domain similar to those present in other members of this family. Although this receptor lacks of a catalytic motif, it interacts with several proteins that have the ability to transmit signals important for the regulation of neuronal survival and differentiation as well as synaptic plasticity. The three-dimensional structure of the extracellular domain of p75<sup>NTR</sup> in

association with an NGF dimer has demonstrated that each of the four cysteine-rich repeats is participating in binding to NGF (He and Garcia, 2004). More specific, p75<sup>NTR</sup> binds NGF along the interface between the two NGF monomers and this binding leads to a conformational change of NGF altering the monomeric interface on the opposite side of the NGF dimer, eliminating the possibility of the binding of one NGF dimer to two p75<sup>NTR</sup> monomers. After the binding, p75<sup>NTR</sup> undergoes oligomerization with other p75<sup>NTR</sup> or homologous receptors. This process is crucial for the association of the receptor with its signaling molecules, such as Jun kinase, small GTPases, as well as the transcription factor NF- $\kappa$ B (Anastasia et al., 2015). Oligomerized p75<sup>NTR</sup> receptors are cleaved by  $\alpha$ - and  $\gamma$ -secretases, leading to the release to the cytoplasm of the peptide p75- intracellular domain (p75-ICD). After being transferred to the nucleus, p75-ICD regulates the transcription of various genes. Moreover, p75<sup>NTR</sup> can be cleaved also by surface metalloproteinases leading to the formation of p75-extracellular domain (p75-ECD) (Le Moan et al., 2011).

According to previous studies in both normal and pathological cells, p75<sup>NTR</sup> plays an important role in the inhibition of cellular functions. More specific, *in vitro* studies in primary cultures of mice neurons, in the rat neural cell line PC12 and *in vivo* studies in mice, have shown that p75<sup>NTR</sup> inhibits processes such as Na<sup>+</sup> currents, cytosolic Ca<sup>2+</sup> responses, excitability, persistent firing and neurite outgrowth (Gibon et al., 2015, Trigos et al., 2015). Additional effects in mouse hippocampal neurons, induced by p75<sup>NTR</sup> are associated with inhibition and even neuronal death (Yang et al., 2014).

The second class of neurotrophin receptors are the Trk receptors, including 3 different members, TrkA, TrkB and TrkC. The activation of these receptors is stimulated by neurotrophin-mediated dimerisation and transphosphorylation of loop kinases (Huang and Reichardt, 2003). Trk receptors are activated specifically by mature and not pro-forms of the neurotrophin gene products (Lee et al., 2001). Thus, the proteases controlling the processing of proneurotrophins control Trk receptor responsiveness. The cytoplasmic domains of Trk receptors contain several additional tyrosines being also substrates for phosphorylation by each receptor's tyrosine kinase. Upon phosphorylation, these residues form the cores of binding sites that serve as a scaffolding for the recruitment of a variety of adaptor proteins and enzymes that propagate the neurotrophin signal (Longo and Massa, 2013).

Regarding the extracellular domain of each of the Trk receptors, it consists of a cysteine-rich cluster followed by three leucine-rich repeats, another cysteine-rich cluster and two Ig-like domains. Each receptor spans the membrane once and is terminated with a cytoplasmic domain consisting of a tyrosine kinase domain surrounded by several tyrosines, which serve as phosphorylation-dependent docking sites for cytoplasmic adaptors and enzymes. Within the activated Trk molecule the phosphotyrosines and their surrounding amino acid residues create binding sites for proteins containing phosphotyrosine-binding (PTB) or Src homology 2 (SH2) domains. Additionally, endocytosis and transfer of Trk receptors to different membrane compartments control the efficiency and duration of Trk-mediated signalling, because of the localization of adaptor proteins to specific membrane compartments (Longo and Massa, 2013).

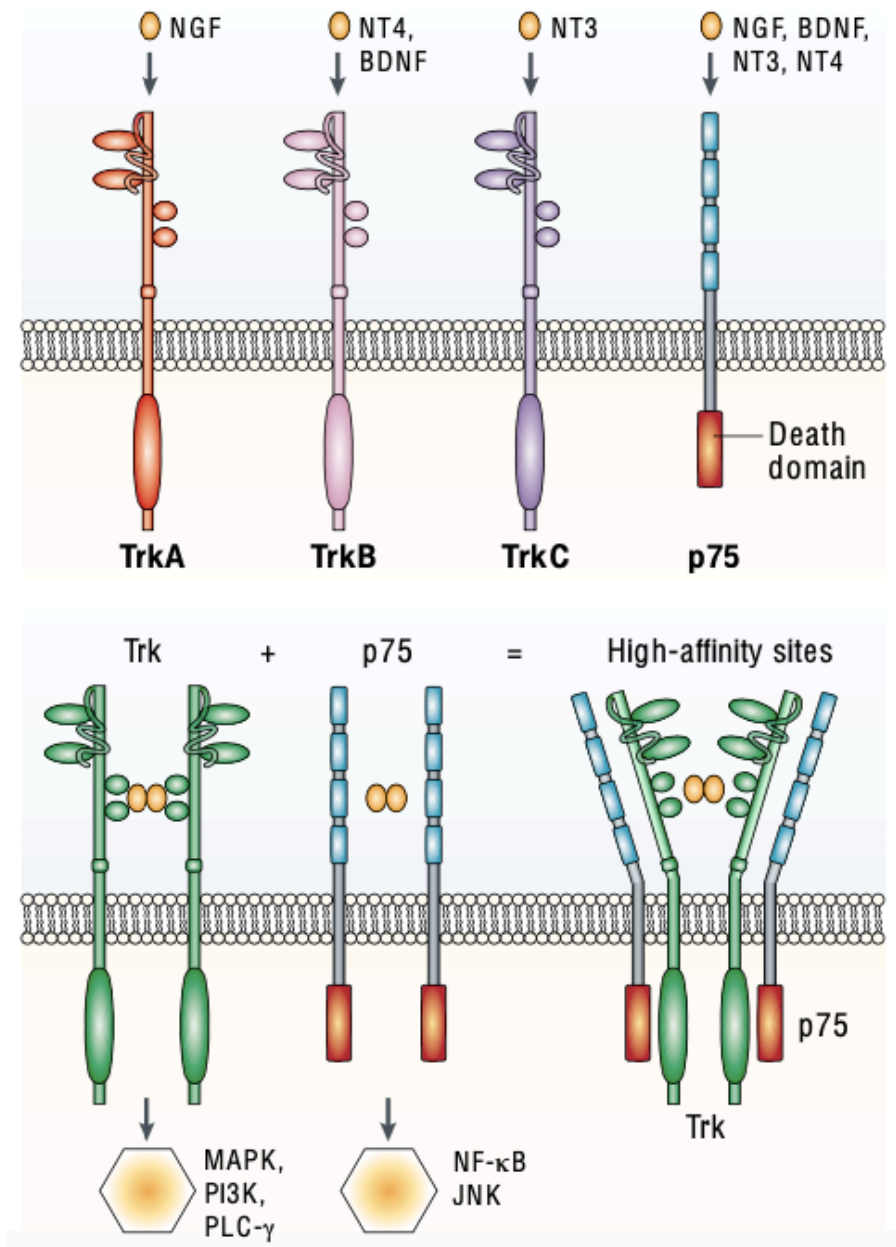


Figure 9: Neurotrophins and their receptors. Binding of neurotrophins to their receptors leads to dimerization of each receptor. Different neurotrophins bind to different Trk receptors, while all neurotrophins bind to  $p75^{NTR}$ . Trk receptors consist of extracellular immunoglobulin G (IgG) domains which are responsible for ligand binding and of a catalytic tyrosine kinase sequence in the intracellular domain. Each receptor has the ability to activate several signal transduction pathways. The extracellular portion of  $p75^{NTR}$  consists of 4 cysteine-rich repeats, while the intracellular part consists of a death domain. Interactions between Trk and p75 receptors can result in changes of the binding affinity for neurotrophins. (Chao, 2003)

In contrast to interactions with  $p75^{NTR}$ , neurotrophins dimerize Trk receptors leading to activation through trans-phosphorylation of kinases present in their cytoplasmic domains. The

four neurotrophins are specified in their interactions with the three members of this receptor family with NGF activating TrkA, BDNF and NT-4 activating TrkB, and NT-3 activating TrkC. In addition, NT-3 can activate the other Trk receptors too, but with lower efficiency. Neurotrophins interact with these receptors through the membrane-proximal Ig-like domain. Expression of a specific Trk receptor presents responsiveness to the neurotrophins to which it binds. However, splicing introduces some limitations to this generalization. More specifically, differential splicing affects ligand interactions of each of the Trk receptors through insertions of short amino acid sequences into the juxtamembrane regions of the extracellular domains of TrkA, TrkB and TrkC (Strohmaier et al., 1996). These insertions result in the binding of the receptor to non-preferred ligands. Differential splicing of exons encoding portions of the intracellular domains of Trk receptors are also responsible for the regulation of the signaling initiated by neurotrophin binding. However, differential splicing of the Trk receptor mRNAs is not the only factor that modulates neurotrophin binding and action. In some CNS neurons, many Trk receptors are localized in intracellular vesicles. Second signals, such as cAMP or Ca<sup>2+</sup>, have the ability to promote insertion of the receptors into the surface membrane, where they are accessible to neurotrophins (Du et al., 2000). In these cells, responsiveness to neurotrophins may require incorporation of neurons into signaling networks resulting in the production of these second messengers.

Upon binding their specific neurotrophins, Trks dimerize and undertake auto-phosphorylation (Colombo et al., 2014). The effects of their activation include neuronal survival, proliferation and differentiation (Chao et al., 2006) being potentiated when the receptors are internalized and undergo intracellular trafficking (Chao et al., 2006; Philippidou et al., 2011). Signaling of all Trks include activation of ERK, AKT and PLC $\gamma$  signaling cascades (Chen et al., 2012) which trigger differential effects in various neurons (Figure 10). For example, in mice Purkinje neurons, neurite outgrowth and spine density primarily TrkC dependent (Joo et al., 2014), while in pyramidal CA1 hippocampal neurons are TrkB dependent (Wang et al., 2015). In hippocampal and other neuron synapses, TrkB is also responsible for the prolonged reinforcement of synaptic activity (long-term potentiation, LTP) (Guo et al., 2014). However, at layer 2/3 cortical synapses, the activation of TrkB does not lead to synaptic reinforcement but rather to prolonged weakening (long-term depression, LTD) (Zhao et al., 2015).

In conclusion, the two types of NT receptors have different and often opposite roles in a variety of brain functions playing defined, but not unique roles. Due to their multiple functions, the two types of NT receptors are associated with several diseases.

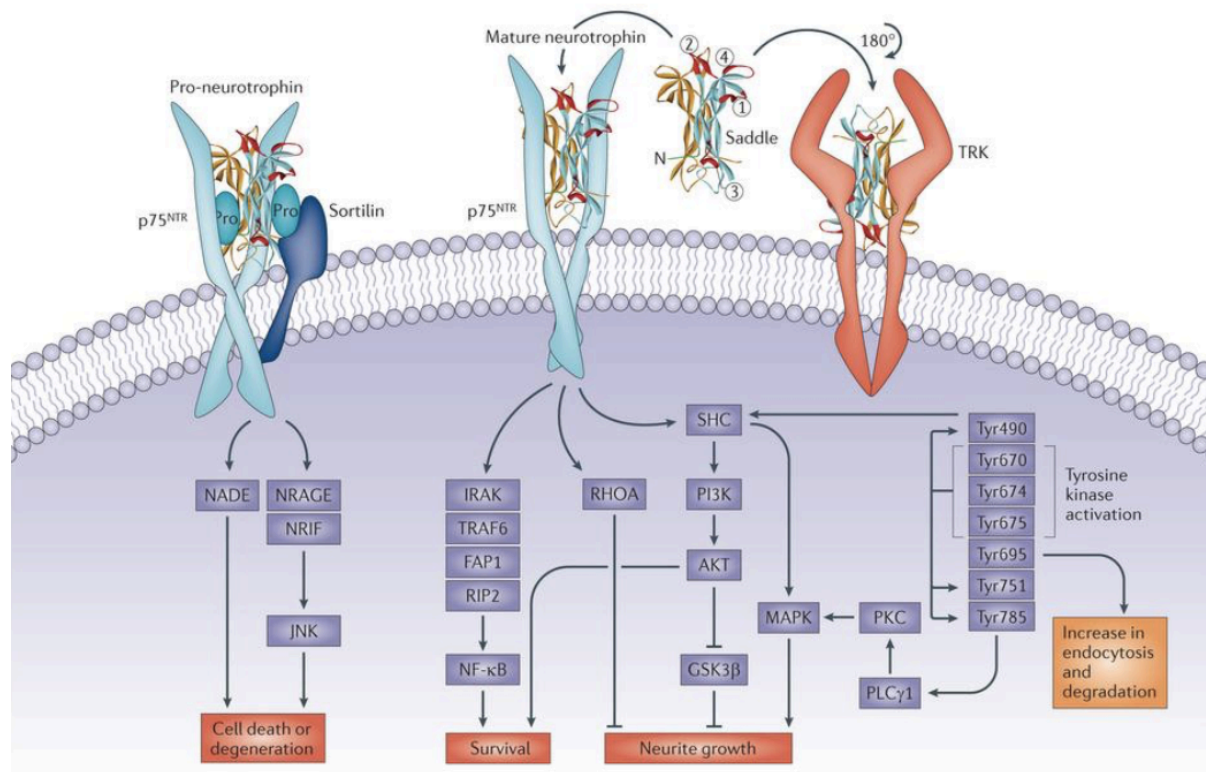


Figure 10: Neurotrophins receptor signaling. In Trk complexes, the neurotrophin apical region is near the membrane, whereas in the  $p75^{NTR}$  complex it looks away from the membrane. Pro-neurotrophins are proteolytically processed intra- or extracellularly to remove the pro-region, which is the principal site of interaction with the co-receptor sortilin. Neurotrophin signaling proceeds through preformed or induced receptor dimers. Binding of mature neurotrophins to the Trk ligand leads to phosphorylation of an array of intracellular domain tyrosine residues that activate kinase activity, leading to further receptor autophosphorylation. Phosphorylation at Tyr490, Tyr785 and possibly Tyr751 forms adaptor binding sites that couple the receptor to mitogen-activated protein kinases (MAPKs), phosphoinositide 3-kinase (PI3K) and phospholipase C $\gamma$ 1 (PLC $\gamma$ 1) pathways, which act locally and/or via signaling endosomes that are transported to the nucleus, to ultimately promote neurite outgrowth, differentiation and cell survival. Binding of mature neurotrophins to  $p75^{NTR}$  may increase neurotrophin binding to Trk receptors, boost Trk signaling through AKT and MAPKs, and further increase survival through the nuclear factor- $\kappa$ B (NF- $\kappa$ B) pathway, or antagonize the actions of Trk through the activation of JUN N-terminal kinase (JNK) and RHOA pathways. Pro-neurotrophin binding in complex with sortilin selectively activates cell-death-related pathways. (Longo and Massa 2013)

### A.9. Neurotrophins and demyelination

Current MS treatments reduce severity and slow disease progression, however they do not repair damaged myelin and degenerated axons. For this reason, MS research is recognizing the importance of neurotrophins as a potential novel therapeutic strategy to facilitate remyelination.



In the CNS, the role of neurotrophins is associated with neuronal differentiation, survival and death, axonal outgrowth, synapse formation and plasticity (Longo and Massa, 2013). For example, NGF possesses neuroprotective (Martinez-Serrano and Bjorklund, 1996), immunosuppressive and immunomodulatory functions (Villoslada et al., 2000). The results of various studies using the EAE model have shown that exogenous administration of NGF delayed the onset of clinical EAE and, pathologically, prevented the full development of EAE lesions (Villoslada et al., 2000; Kuno et al., 2006), while administration of NGF antibodies exacerbated neuropathological signs of EAE (Micera et al., 2000). Human MS studies also support the beneficial role of NGF. For example, cerebral spinal fluid of MS patients show increased NGF levels during acute attacks that significantly decrease during remission (Laudiero et al., 1992), suggesting that NGF levels increase in response to the immune system that insults myelin facilitating neurological recovery. Once myelin is repaired, NGF levels subside back to baseline values required for normal myelin maintenance.

The beneficial effects of NGF are thought to occur through its ability to enhance axonal regeneration (Oudega and Hagg, 1996) and remyelinate axons through its protective and survival effects on OPCs and OLs (Takano et al., 2000). In addition, the immunomodulatory effects of NGF become evident by the fact that a variety of different cell types like for example neurons, microglia, astrocytes, OLs, immune cells, such as T cells, B cells, and mast cells have all been identified as cellular sources and targets of NGF (Ehrhard et al., 1993; Leon et al., 1994; Santambrogio et al., 1994; Micera et al., 1995; Frade and Barde, 1998).

BDNF is also suggested as a possible therapeutic target. Although it is well known for its actions on neurons (Huang and Reichardt, 2001; Thoenen, 2000), it is recently associated with beneficial effects on oligodendrocytes, particularly, after demyelination. For example, *in vitro* studies showed that BDNF enhances numbers of oligodendrocytes of the basal forebrain (Du et al., 2003). *In vivo* studies showed that BDNF deficient mice are associated with decreased myelin proteins in oligodendrocytes of the spinal cord and optic nerve during development. These myelin deficits recover as the animal ages (Xiao et al., 2010), however in the basal forebrain the deficits remain throughout life (Vondran et al., 2010). Additionally, BDNF deficiency results in abnormalities in oligodendrocyte proliferation and differentiation after demyelination (VonDran et al., 2011). In EAE, administration of BDNF into the brain through transformed MSCs is associated with reduction of the clinical score, decrease of inflammation and apoptosis, as well as demyelination (Makar et al., 2009; Makar et al., 2008). Moreover, BDNF seems to play an important role under demyelinating conditions, since it positively affects myelin protein synthesis (Fulmer et al., 2014), oligodendrocyte progenitor proliferation, maturation and OL myelination (Tsiperson et al., 2015; VonDran et al., 2011; Wong et al., 2014).

NT-3 is another neurotrophin with beneficial effects during demyelination. More specifically, NT-3 is associated with an increase in the neuronal survival in EAE-induced demyelination (Yan et al., 1992). Moreover, administration of NT-3 decreases demyelination volume and

increases the number of mature OLs in the L- $\alpha$ -lysophosphatidylcholine (LPC)-induced demyelination model (Jean et al., 2003).

All these beneficial biological effects of neurotrophins suggest that they can be used as key mediators regulating myelin formation and repairing demyelinating lesions. Unfortunately, the polypeptidic nature of neurotrophins limits their therapeutic potential, since they cannot cross the blood brain barrier (BBB), they have poor pharmacokinetic stability *in vivo* and they can cause dose-dependent hyperalgesia (Yi et al., 2014).

## **A.10 Neurosteroids**

The term neurosteroids was first introduced in 1981 by the French endocrinologist Étienne-Émile Baulieu in order to describe steroids that are produced *de novo* in the brain from cholesterol (Corpechot et al., 1981). Later on, it also included those derived from the local metabolism of peripherally derived steroid precursors such as progesterone and corticosterone (Baulieu and Robel, 1990). They are able to modulate aminobutyric acid type A receptors (GABAAR) and induce analgesic, anxiolytic, sedative, anesthetic and anticonvulsant effects (Belelli et al., 2009).

There are three main categories of neurosteroids (Figure 11): the pregnane (e.g., allopregnanolone), the sulfated (e.g., dehydroepiandrosterone sulfate, or DHEAS) and the androstane (e.g., androstanediol), which are classified according to their structural homology (Reddy, 2010). Allopregnanolone and THDOC can be synthesized from cholesterol by a series of steroidogenic enzymes (Belelli and Lambert, 2005). More specific, the cholesterol is transported into the inner mitochondrial membrane via the steroidogenic acute regulatory protein (StAR) and translocator protein 18 kDa (TSPO) (Papadopoulos et al., 2006). The mitochondrial cholesterol side-chain cleavage enzyme (cytochrome P450<sub>scc</sub>) catalyzes a side chain cleavage converting cholesterol into pregnenolone, an important rate-limiting step for the production of allopregnanolone and THDOC. Pregnenolone is then converted by 3 $\beta$ -hydroxysteroid dehydrogenase (3 $\beta$ -HSD) into progesterone, with further metabolism of progesterone by 21 hydroxylase (p450<sub>c21</sub>), yielding deoxycorticosterone. Finally, progesterone and deoxycorticosterone are metabolized by 5 $\alpha$ - reductase followed by 3 $\alpha$ -hydroxysteroid dehydrogenase (3 $\alpha$ -HSD), to yield allopregnanolone and THDOC, respectively.

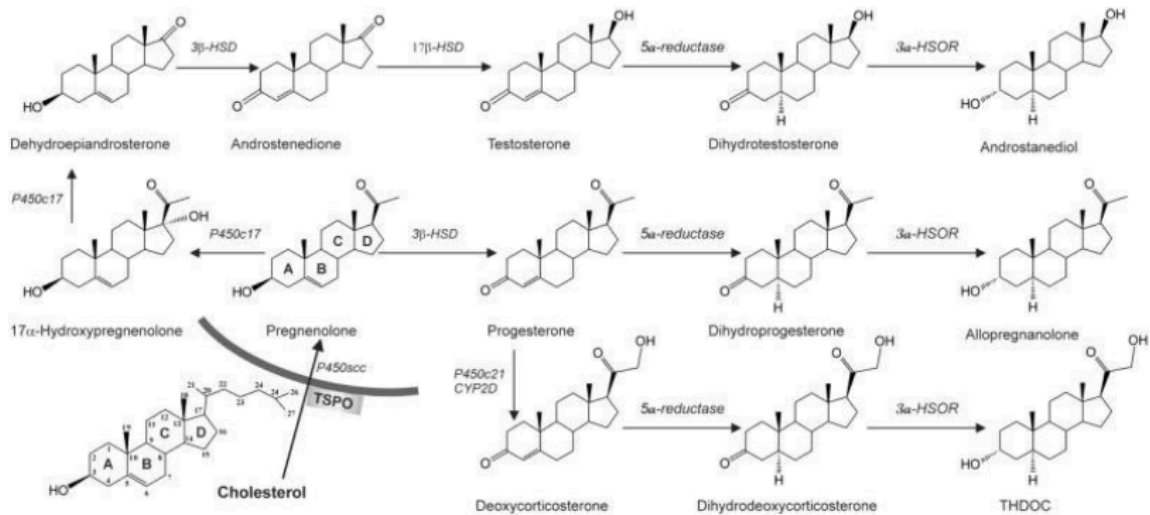


Figure 11: Neurosteroids biosynthesis. Cholesterol is converted to pregnenolone by P450scC in the inner mitochondrial membrane. Pregnenolone is the precursor for progesterone and other neurosteroids. Progesterone, deoxycorticosterone and testosterone undergo two sequential A-ring reduction steps catalyzed by 5 $\alpha$ -reductase and 3 $\alpha$ -HSOR to form the 5 $\alpha$ , 3 $\alpha$ -reduced neurosteroids. The conversion of progesterone, deoxycorticosterone or testosterone into neurosteroids occurs in several regions within the brain (Papadopoulos et al., 2006).

### A.11 Dehydroepiandrosterone

The neurosteroid dehydroepiandrosterone (DHEA), which is a C19 adrenal steroid produced by neurons and glia (astrocytes and oligodendrocytes), was first isolated in 1934 from male urine and in 1954 from human plasma (Orentreich et al., 1992; Baulieu and Robel, 1998; Zwain and Yen, 1999). Dehydroepiandrosterone sulfate (DHEAS), which is a sulfated form of DHEA, was obtained in 1944 (Lieberman, 1995). DHEA and its sulfate ester DHEAS, together represent the most abundant steroid hormones in the human body (Maninger et al., 2009).

During human gestation, high concentrations of DHEA(S) are secreted by the fetal zone of the adrenal gland (Mesiano and Jaffe, 1997). After birth, DHEA(S) concentrations decline over the first six months and remain low until adrenarche starts at six to eight years in both sexes, at which point DHEA(S) is synthesized and secreted from the zona reticularis layer of the adrenal cortex and circulating concentrations begin to rise. Adult humans secrete both DHEA and DHEAS from the zona reticularis of the adrenal cortex and also DHEA from the ovary and testis (Havelock et al., 2004). Circulating concentrations (in both plasma and cerebrospinal fluid) peak in the mid-20's and then progressively decline with age in both sexes. The reduced concentration of DHEA during aging is associated with different age-related diseases (Schumacher et al., 2003; Weill-Engerer et al., 2003, 2002).

DHEA binds with high affinity to all neurotrophin receptors (TrkA, TrkB, TrkC and p75<sup>NTR</sup>) (Lazaridis et al., 2011; Padiaditakis et al., 2015). It has strong neuroprotective effects, inducing

pro-survival signaling by enhancing ERK1/2 and Akt activity, increasing the expression of anti-apoptotic Bcl-2 proteins and activating NFkB and CREB transcriptional machinery (Charalampopoulos et al., 2004; Charalampopoulos et al., 2008; Compagnone and Mellon, 2000; Mellon and Griffin, 2002). Moreover, DHEA and some of its steroid derivatives seem to inhibit relapsing-remitting EAE in mice by restricting the production of autoimmune T cells or by suppressing T17 cells via ERβ signaling (Du et al., 2001; Offner et al., 2002; Saijo et al., 2011; Aggelakopoulou et al., 2016). Furthermore, DHEA has been shown to inhibit acute microglia-mediated inflammation through activation of the TrkA-Akt1/2-CREB-Jmjd3 pathway (Alexaki et al., 2018).

However, neurosteroids like DHEA are metabolized into estrogens, androgens, or progestins and their long-term administration could exert important endocrine side effects, like hormone-dependent tumours (Compagnone and Mellon, 2000). Unfortunately, these pharmacological properties limit their clinical application.

### **A.12 Microneurotrophins (BNNs)**

To overcome the limitations of DHEA mentioned above, our collaborators, Theodora Calogeropoulou, Ioannis Charalampopoulos and Achille Gravanis, have synthesized different analogues of the endogenous DHEA, called microneurotrophins due to their small size and agonistic effects through Trks and p75<sup>NTR</sup> receptors. These molecules are modified at C17 blocking their metabolism to estrogens or androgens, while being able to cross the BBB. These modifications abolish the endocrine side effects of DHEA through the classical steroid receptors and simultaneously they maintain the strong neuroprotective activity and the anti-apoptotic effects *in vitro* by binding with high affinity to TrkA, TrkB and p75 receptors. Two of the most potent compounds are BNN20 and BNN27 (Calogeropoulou et al., 2009).

### **A.13 BNN27 Microneurotrophin**

BNN27 does not interact with the classical steroid receptors neither TrkB nor TrkC (Pediaditakis et al., 2016a). According to previous studies BNN27 specifically activates the NGF receptors, TrkA and p75 downstream neuron survival signaling. Moreover, in these studies, it was shown that BNN27 is able to rescue from apoptosis TrkA-NTR expressing sympathetic sensory neurons and p75<sup>NTR</sup> expressing cerebellar granule neurons, while being deprived of the hyperalgesic properties described for NGF (Pediaditakis et al. 2016a; Pediaditakis et al., 2016b). Additionally to its effect on neuronal cells, BNN27 induces TrkA phosphorylation (at Y490) of TrkA-expressing BV2 mouse glial cells in culture (Blasi et al., 1990; Henn et al., 2009), decreasing the levels of interleukin (IL) 6 mRNA (Pediaditakis et al., 2016a). BNN27 has shown beneficial and neuroprotective effects in animal models of ALS (Glajch et al., 2016), retinal detachment (Tsoka et al., 2018), ketamine-induced psychosis (Zoupa et al., 2019), scopolamine-induced cognitive deficits (Pitsikas and Gravanis, 2017) and a model of retina degeneration in the streptozotocin-induced diabetic rats (Iban-Arias et al., 2018), while recent studies also showed that this microneurotrophin is able to affect locomotion, progesterone, and testosterone levels, as well as the glutamatergic and GABAergic

systems of the hippocampus and prefrontal cortex in a sex-dependent way (Kokras et al., 2020). Findings of our group showed that BNN27 can be also effective in a demyelination mouse model. More specific, BNN27 protects mature oligodendrocytes against cuprizone-induced cell death in TrkA-dependent matter, while reducing activation of astrocytes and microglia (Bonetto et al., 2017).

#### **A.14 BNN20 Microneurotrophin**

BNN20 is another DHEA derivative that binds and activates not only TrkA and p75<sup>NTR</sup> like BNN27, but also TrkB. According to studies, it was demonstrated that this compound protects dopaminergic neurons, possibly, through TrkB in the weaver mouse mutant, a mouse model for Parkinson's disease (Botsakis et al., 2017). Moreover, recent studies showed that this compound exerts strong anti-inflammatory activity, while being able to restore BDNF levels in this specific mouse model (Panagiotakopoulou et al., 2020).

## B. INTRODUCTION II

TAG-1/Contactin-2 (herein called Contactin-2) is a GPI-anchor glycoprotein belonging to the immunoglobulin superfamily (IgSF). This group of proteins consists of multiple extracellular immunoglobulin-like and fibronectin III-like domains and is mainly found in the nervous system (Dodd et al., 1988; Furley et al., 1990; Gennarini and Furley, 2017; Karageos, 2003; Yamamoto et al., 1986). Although Contactin-2 acts as a cell adhesion molecule and is normally found on the membrane surface during development, it can also be found in a soluble form through the brain due to its cleavable GPI linkage (Furley et al., 1990; Karageos et al., 1991; Zhou et al., 2012). It has a variety of different functions in both the developing and the adult nervous system.

Regarding the embryonic nervous system, Contactin-2 plays an important role in a lot of different developmental processes (Denaxa et al., 2003; Karageos, 2003). According to previous studies, it is highly expressed on the surface of axons of commissural neurons, while they approach the floor plate. Upon crossing it, Contactin-2 expression is highly reduced and L1 is expressed instead (Dodd et al., 1988). Additionally, Contactin-2 is found on the surface of dorsal root ganglion (DRG) axons playing a significant role in their elongation, fasciculation and guidance (Karageos et al., 1991; Masuda et al., 2000; Stoeckli et al., 1991). Contactin-2 is also involved in the interactions between mature axons and immature neurons of the cerebral cortex, while it also plays an important role in the axonal formation of the latter (Namba et al., 2014). Moreover, Contactin-2 is essential for the migration of a variety of neurons in the cerebral cortex and the medulla (Denaxa et al., 2001; Denaxa et al., 2005; Kyriakopoulou et al., 2002; Okamoto et al., 2013), while in cerebellum it is expressed on the surface of granule precursor cells preventing their premature differentiation (Bailly et al., 1996; Buttiglione et al., 1998; Xenaki et al., 2011; Wang et al., 2011).

Regarding the adult nervous system, Contactin-2 is expressed in both axons and glial cells (Traka et al., 2002). Previous studies have shown that this molecule is essential for the clustering of potassium channels and Caspr2 at the juxtaparanodes of myelinated fibers (Savvaki et al., 2008; Traka et al., 2003), while absence of this protein is correlated with hypomyelination, abnormalities in the caliber distribution and cytoskeletal defects of axons (Chatzopoulou et al., 2008). Additionally, absence of Contactin-2 leads to significant impairments in motor coordination as well as learning and memory (Savvaki et al., 2008). Moreover, it was also shown that this molecule can transiently affect the expression of myelin genes and myelin-regulating genes and the morphology of myelinating oligodendrocytes, the extent of myelination and the axonal conduction properties of white matter tracts (Zoupi et al., 2018). Lastly, it is important to be mentioned that Contactin-2 is recognized as an autoantigen in multiple sclerosis patients, contributing to the development of gray matter pathology (Derfuss et al., 2009), while there are some indications that this molecule is also implicated with other pathologies such as gliomas, Alzheimer disease, epilepsy and chronic inflammatory demyelinating polyneuropathy (Iijima et al., 2009; Stogmann et al., 2013; Tachi et al., 2010; Yan and Jiang, 2016).

### **C. AIM OF THE STUDY I**

The aim of this study was to elucidate the exact role of microneurotrophin BNN20 in de- and remyelination, taking advantage of LPC-induced demyelination mouse model, in which these processes can be studied without the direct involvement of the adaptive immune system. We focused on the effects of BNN20 in glial population and myelin. More specifically, we investigated if BNN20 has a beneficial role regarding myelin, OLs, OPCs, astrocytes and microglia using *in vivo* and *in vitro* approaches. It is important to mention that all the available treatments for MS can only reduce or prevent specific aspects of the disease while failing to promote myelin restoration and neuroprotection. For this reason, developing therapeutic agents that could improve remyelination is a very challenging project.

## D. AIM OF THE STUDY II

Previous studies on Contactin-2 have revealed a variety of functional or structural interactions between this glycoprotein and other molecules. These interactions have been revealed either by experimentation in biological systems or *in silico*, by modern computational tools. In this study, we have hypothesized that if the co-involvement of Contactin-2 and these other molecules was crucial for normal neuronal and/ or glial function, the cells would ensure their co-presence by regulating their co-expression at a genomic level.

To establish any spatial genomic correlations between Contactin-2 with its functionally or structurally interacting molecules in the adult mouse brain, we used the corresponding data from two sources: firstly from the anatomic gene expression atlas (AGEA) of the adult mouse brain of the Allen Institute for Brain Science, which is an online transcriptome-based atlas of the adult C57Bl/6J mouse brain, showing the spatial registration of the expression intensity of 4376 genes into 51533, 200  $\mu\text{m}$ -diameter cubic voxels. All information presented in the AGEA are based on extensive *in situ* hybridization (ISH) experiments of the Institute (Ng et al., 2009). And secondly from Tabula Muris, a compendium of single cell transcriptome data collected from mice, which contains nearly 100,000 cells from 20 organs and tissues. These data provide the option of direct and controlled comparison of gene expression among cell types of different tissues (Tabula Muris Consortium et al., 2018). The main goal of this study was to gain further insight into the physiological role of Contactin-2 and provide insights for more targeted hypotheses for future experimentation on the field.



## **E. MATERIAL AND METHODS I**

### **E.1 Animals**

All animals used in this study were C57BL/6 and were kept at the animal facility of the Institute of Molecular Biology and Biotechnology, in a temperature-controlled facility on a 12 hr light/dark cycle, fed by standard chow diet and water ad libitum. The animal facility of the Institute of Molecular Biology and Biotechnology (IMBB) - Foundation for Research and Technology Hellas (FORTH) (license nos. EL91-BIObr-01 and EL91-BIOexp-02) complies with all regulations and standards outlined in the Presidential Decree 56/30.04.2013 (Greek Law). The particular experimental protocol has been approved with license number 93164 (ΑΔΑ: 73XB7ΛΚ-ΦΙΣ). These regulations follow and are in accordance with the EU directives and regulations (2010/63/EU and L 276/33/20.10.2010) that are equivalent to NIH standards established by the Animal Welfare Acts and the documents entitled "Principles for Use of Animals" and "Guide for the Care and Use of Laboratory Animals" from the Office of Laboratory Animal Welfare. Regarding the number of animals used in our study, we followed the 3R principle for animal research to decrease animal experimentation, while achieving reproducibility of our data.

### **E.2 LPC demyelination mouse model**

In this study we used the LPC demyelinating mouse model to study demyelination and remyelination. In order to induce focal demyelination with LPC injection the protocol was standardized by small modifications on that published by Ferent et al. 2013. C57BL/6 male mice were used at 8-10 weeks of age. Mice were weighted prior to the experimental procedure and received anesthesia by intra-peritoneal injection of ketamine/xylazine (per g of body weight: 100 µg of ketamine and 15 µg of xylazine). Responsiveness to painful stimuli was checked by pinching the tail or hind limb. Each mouse was fixed on a small animal stereotactic frame by means of a mouse nose clamp adaptor and ear bars which are incorporated on the frame. The head was positioned so as to assure that the height of the bregma and lambda was identical, as well as that of the right and left hemisphere. The skull was exposed and a drill was used to create a small opening. 1 µL of either the vehicle solution (1x sterile PBS) or the LPC (Sigma-Aldrich) solution (1% w/v LPC in 1x sterile PBS) was injected in the corpus callosum at a flow of 0.1 µL/1.5 min (anteroposterior axis (AP): +1 mm from the bregma, mediolateral axis (ML): +1 mm from the bregma, dorsoventral axis (DV): -2.2 mm from the dura). Next, animals were carefully removed from the frame, sutured and left to recover in a clean cage with excess of food and water. Animals that received the vehicle or the toxin were sacrificed at 5, 10 and 15 days post injection (dpi). One more group was added to the study, in which BNN20 was administered to LPC injected animals daily with intraperitoneal injections till the day the animals were sacrificed (10mg/kg BNN20 diluted in 5% DMSO) starting at day 1 post intracerebral injection. The dose concentration was selected according to previous studies regarding BNN27, which is another DHEA analogue with high chemical similarity with BNN20 (Iban-Arias et al., 2017). At 5 and 10dpi demyelination is expected to be observed, while at 15dpi there is the onset of remyelination (Figure 12). Lesions were identified either

due to the loss of myelin observed after PLP/MBP staining or due to the accumulation of astrocytes or microglia/macrophages detected after GFAP or IBA staining. Following groups were used for this *in vivo* study: Control 5dpi (n=4), control 10dpi (n=4), control 15dpi (n=4), LPC 5dpi (n=5), LPC 10dpi (n=6), LPC 15dpi (n=3), LPC/BNN20 5dpi (n=8), LPC/BNN20 10dpi (n=4), LPC/BNN20 15dpi (n=3). Following fixation, the forebrain was collected and further processed. [SEP]

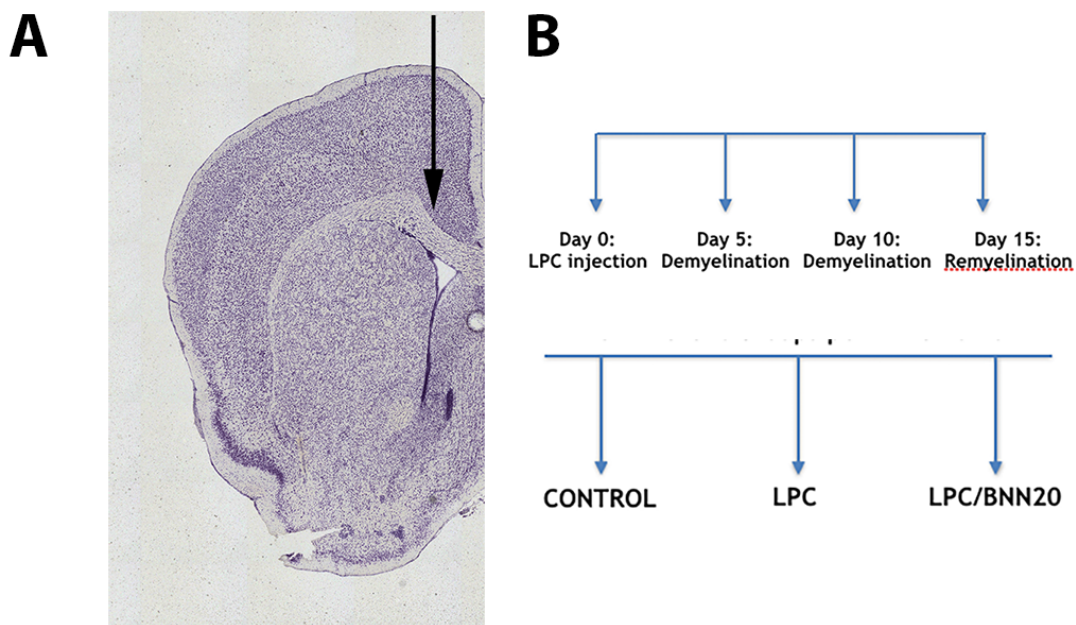


Figure 12: (A) Coronal section of the adult brain at bregma 0.98mm showing the region where the lesion is generated in the corpus callosum (arrow). In LPC-induced demyelination mouse model, lyssolecithin is injected at the site of interest and very quickly causes local demyelination. The myelin sheath is directly destroyed, attracting an inflammatory microglia/macrophages and astrocyte response, leading to OL loss. Total remyelination occurs later on, typically after the 2nd-3rd week post-injection. (B) Timeline of the LPC model showing the time points when defects are observed (top) and the experimental groups (bottom).

### **E.3 Tissue fixation, dissection and isolation**

Adult mice received an intraperitoneal injection of euthanasia (per g of body weight: 200 µg of ketamine and 30 µg of xylazine), while transcardially perfused with PBS followed by cold 4% PFA in 1x PBS. Forebrains were carefully dissected and post-fixed in 4% PFA in 1xPBS on ice, for 20-30 min.

### **E.4 Embedding, freezing and cryosectioning**

After post-fixation, samples were washed 3 times with 1xPBS and incubated in 30% sucrose, 0.1% NaN<sub>3</sub> in 1xPBS. Samples were kept at 4°C until the sucrose completely replaces the intracellular water (usually 1-2 days). After cryoprotection with sucrose, samples were embedded in a gel containing 15% w/v sucrose, 7.5% gelatin from porcine skin (Cat. No. G-2500, Sigma) in 1xPBS. To ensure uniform freezing, samples were submerged in methylbutane and frozen at -35 to -40°C. Tissue blocks were then stored at -80°C before proceeding to cryosectioning (Leica). 15-µm-thick sections were collected on superfrost plus glass slides (Thermo scientific) and stored in cryoboxes at -20°C until further processing.

### **E.5 Immunohistochemistry on cryosections derived from adult mice**

- Cryosections were encircled in Dako Pen (Cat. No. S200230, Dako, Agilent Technologies).
- Cryosections were post-fixed in ice-cold acetone at -20°C for 10 min.
- Cryosections were washed 3 times with 1x PBS (5 minutes each).
- Cryosections were incubated in blocking solution of 5% bovine serum albumin (fraction V, BSA) in 0.5% Triton X-100 in 1x PBS for 1 hour at room temperature.
- Blocking solution was removed and slides were incubated with the appropriate primary antibodies diluted in blocking solution at 4°C, overnight.
- Cryosections were washed 3 times with 1x PBS.
- Cryosections were incubated with the appropriate secondary fluorescently labeled antibodies (1:800, Molecular Probes) in blocking solution for 2 hours at room temperature.
- Cryosections were washed 3 times with 1x PBS.
- Cryosections were counterstained with Topro-3 iodide (500 nM in 1x PBS, Molecular Probes, Thermo Fisher Scientific) for 3 min at room temperature.
- Cryosections were washed 3 times with 1x PBS.
- Cryosections were mounted with Mowiol® 4-88 Reagent (Cat. No. 475904, Calbiochem, EMD Chemicals, Merck KGaA).

Slides were kept at 4°C until imaging took place or at -20°C for long term storage. Images were obtained using a Leica SP2 confocal microscope (Leica Microsystems, Germany) with 10x and 40x lenses.

For our experiments we used following primary antibodies: anti-PLP (1:1000, rabbit, Abcam Cat# ab28486), anti-MBP (1:200, rat, Serotec), anti-APC/CC-1 (1:100, mouse, Millipore Cat#

OP80), anti-PDGFRa (1:100, rat, Millipore Cat# CBL1366), anti-Olig2 (1:500, rabbit, Abcam Cat# ab42453), anti-IBA-1 (1:500, rabbit, Wako Cat# 019-19741), anti-GFAP (1:2000, mouse, Sigma-Aldrich Cat# G3893).

### **E.6 Quantification of demyelination**

For quantification of the extent of demyelination we immunostained for PLP and Topro-3. Lesion was recognized by both, PLP staining and accumulation of Topro-3+ nuclei, which represents the accumulation of astrocytes and microglia. The lesion was marked and densitometric analysis of the myelin marker PLP was performed using Fiji Image J software.

### **E.7 Quantification of astrocytes and microglia/macrophages**

The density of astrocytes and microglia in the lesion area was quantified by densitometric analysis of the astrocytic marker GFAP and the microglia/macrophages marker IBA-1 using Fiji Image J software

### **E.8 Quantification of OLs and OPCs**

The density of OLs, mature OLs and OPCs in the lesion area was quantified by manually counting the number of cells stained for Olig2 (general marker of oligodendrocytes), CC-1 (marker of mature oligodendrocytes) and PDGFRa (marker of oligodendrocyte precursor cells). Values were expressed as number of positive cells per  $100.000\mu\text{m}^2$ .

### **E.9 OLs and microglia primary cultures**

Primary mixed glial cell cultures were prepared from the cortices of mouse pups 2 days old, as previously described (McCarthy and de Vellis, 1980), with minor modifications (Tamashiro et al., 2012). In the beginning, the meninges were removed, then the cortices were chopped into small pieces and mechanically dissociated. Cells were plated into poly-L-lysine (PLL, Sigma-Aldrich, 100 mg/ml)-coated  $75\text{ cm}^2$  culture flasks and cultured in DMEM (Glutamax<sup>TM</sup>, 14,5 g/L D-Glucose, -Pyruvate), supplemented with 10% FBS (Gibco) and 2% penicillin/streptomycin (P/S), until a clear layer of glial cells was formed. The culture medium was replenished twice a week. Once the mixed glial cell cultures achieved 90% confluence (after 10–14 days), microglia cells were isolated using an orbital shaker at 200 rpm for 1 hr at 37°C. Medium was removed and microglia were pelleted via centrifugation (300 g for 10 min). After resuspension they were maintained in DMEM supplemented with 10% FBS and 2% P/S, at a concentration of  $2 \times 10^5$  cells per coverslip (13 mm diameter) in PLL-coated 24-well culture plates. Non-adherent cells were removed after 60 min and then adherent microglia were incubated for 24 hr in culture medium before being serum- starved for 4 hr prior to the experiments. Culture purity was verified by immunostaining using cell type-specific antibodies against ionized calcium-binding adapter molecule 1 (IBA-1; microglia), glial fibrillary acidic protein (GFAP; astrocytes) and neuronal nuclear antigen (NeuN; neurons) and revealed a high purity of microglia.

After microglia detaching, OPC population was separated from the underlying astrocytic cell

layer by vigorous shaking (16 hr at 240 rpm, 37°C) and plated into PLL-coated coverslips (13 mm diameter in 24-well plates) at  $5 \times 10^4$  cells per coverslip. The cells were cultured in DMEM (Glutamax™, 14,5 g/L D-Glucose, -Pyruvate) supplemented with 1% N2, 1 mM biotin, 0.1% BSA-FFa (Sigma-Aldrich), 60 mg/ml cysteine (Sigma-Aldrich), 1% P/S, 10 ng/ml FGF-2 (Peprotech), and 10 ng/ml PDGF-AA (Peprotech), the last two being essential growth factors for OPC proliferation (from now on referred as proliferation medium). For differentiation, the cells were cultured for at least 2 more days in the same medium as before, without FGF-2 and PDGF-AA, but with triiodothyronine (T3, Sigma-Aldrich, 40 ng/ml), an agent inducing OPC differentiation (from now on referred as differentiation medium). The medium was changed every other day. The cultures were named d1 to d6 with respect to the number of days cultured under proliferating or differentiating conditions. More than 90% of total cell number stained for oligodendroglial marker Olig2, indicating a high purity of the cultures.

### **E.10 *In vitro* studies regarding OPCs and OLs**

To study the role of BNN20 regarding OPC proliferation, OPCs were cultured in proliferation medium at d1, while at d2 BNN20 (100nM) was added to the medium (BNN20 was diluted in 100% Ethanol). After 24 hours cells were fixed. In order to study the role of BNN20 in oligodendrocytes maturation, at d3 the medium was changed from proliferation medium to differentiation medium, while at d4 BNN20 (100nM) was added. After 24 hours cells were fixed. In order to study the role of BNN20 in mature OLs after LPC treatment, the medium was changed at d3 from proliferation to differentiation. At d4 OLs were treated for 24 hr with LPC ( $2 \times 10^{-5}$ M) alone or in combination with BNN20 (100nM), while control cultures were kept in culture medium (LPC was diluted directly into the medium). The concentrations used for LPC and BNN20 were selected according to previous studies (Bonetto et al., 2017; Botsakis et al., 2017; Fressinaud, 2005). After 24 hours (d5) LPC was removed and replaced with differentiation culture medium for another 24 hours as previously described (Fressinaud and Eyer, 2013) with minor modifications. Then, at d6 the cells were fixed before immunohistochemistry. At d6 of control cultures, 8% of the cells were mature myelinating OLs. To block the action of BNN20 on the TrkA and TrkB receptor, a specific TrkA inhibitor (1μM, GW441756, CAS No 504433-23-2, Alomone Labs) and a specific TrkB inhibitor (1μM, ANA-12, CAS No 219766-25-3, Alomone Labs) was applied for 1 hr to d4 OL cultures prior to the addition of LPC and BNN20 and then maintained for 24 hr (Trk inhibitors were diluted in 100% DMSO). The concentrations used for TrkA inhibitor (GW441756) and TrkB inhibitor (ANA-12) were selected according to previous studies (Hannan et al., 2019; Mishchenko et al., 2019). In order to verify that the selected concentrations block the activity of TrkA and TrkB receptors, we added NGF (100ng/ml, Millipore) and BDNF (100ng/ml, Alomone Labs) in our cultures instead of BNN20, which are known for their protective role on OLs and which activate TrkA and TrkB receptors respectively (NGF and BDNF were diluted in 100% DMSO). Both inhibitors blocked the beneficial function of both NGF and BDNF, respectively. The concentrations used for NGF and BDNF were selected according to previous studies (Lazaridis et al., 2011; Pediaditakis et al., 2015).

### **E.11 *In vitro* studies regarding microglia**

Microglia were cultured for 24 or 48 hours, the medium was then removed, the cells washed in phosphate-buffered saline (PBS) and incubated with 100 ng/ml of LPS (Sigma-Aldrich) in the culture medium for 24 or 48 hr. In all experiments, cells were serum starved for 4 hr prior the addition of LPS or BNN20 (100 nM). LPS and BNN20 concentrations were selected according to previous studies (Bonetto et al., 2017; Botsakis et al., 2017).

### **E.12 Immunocytochemistry**

- Cells were fixed in 4% paraformaldehyde (PFA) for 10 min
- Cells were washed 3 times with 1 x PBS.
- Cells were permeabilized with 0.1% Triton X-100 for 10 min.
- Cells were immunolabelled with the appropriate primary antibodies for 1 hr.
- Cells were washed 3 times again with 1 x PBS.
- Cells were incubated with the appropriate fluorochrome-labeled secondary antibody for 30 min (1:800, Molecular Probes).
- Cells were washed again 3 times with 1 x PBS
- Cells were incubated for 2 minutes with Topro-3 iodide (500 nM in 1x PBS, Molecular Probes, Thermo Fisher Scientific) for nuclear staining.
- Coverslips were covered with Mowiol® 4-88 Reagent (Cat. No. 475904, Calbiochem, EMD Chemicals, Merck KGaA) and placed in slides.

Slides were kept at 4°C until imaging took place or at -20°C for long term storage, while imaging was performed using a Leica SP2 confocal microscope (Leica Microsystems, Germany) with 20x or 40x lens.

In our experiments we used the following primary antibodies: anti-MBP (1:200, rat, Serotec), anti-PLP (1:1000, rabbit, Abcam Cat# ab28486), anti-PDGFRa (1:100, rat, Millipore Cat# CBL1366), anti-IBA (1:500, rabbit, Wako Cat# 019-19741), anti-GFAP (1:2000, mouse, Sigma-Aldrich Cat# G3893) , anti-Ki-67 (1:200, rabbit, Thermo Fisher Scientific Cat# PA1-21520).

### **E.13 Propidium iodide staining**

- Medium was removed and cells were washed with 1x PBS.
- 0.02mg/ml PI diluted in 1x PBS was used for 10 minutes at 37°C.
- Cells were fixed in 4% PFA for 10 minutes at RT and stained with Hoechst.

As a positive control a well was used in which 0.2% Triton in 1xPBS was added for 10 min before adding PI staining. The number of PI+ cells over the total number of cells were calculated with the help of Operetta High Content Imaging. Each experimental group was in triplicates, for each experiment. PI experiments were performed three independent times.

### **E.14 Quantification of OPCs and OLs**

For the quantification of the percentage of proliferating OPCs, OPCs were immunostained with antibodies against Ki-67, PDGFR- $\alpha$  and Topro-3. For the quantification of the percentage of OLs, OLs were immunostained with antibodies against MBP or PLP and Topro-3. The number of Ki67+PDGFR $\alpha$ + cells over the total number of cells or the number of MBP+ or PLP+ cells over the total number of cells were calculated within 10 random fields taken with 20x magnification in SP2 confocal microscope for each experimental group, in triplicates, for each experiment. These experiments were performed three independent times.

### **E.15 Analysis of microglia morphology**

To verify the presence of morphological changes, cells were immunostained with antibodies against IBA1. They were categorized into ramified and amoeboid groups. Ramified microglia (resting microglia) were defined as having a small circular body with ramified processes. In response to LPS administration, ramified microglia transformed into activated cells, characterized by the swelling of the cell body, a thickening of the proximal processes, and an amoeboid shape (activated/pro-inflammatory microglia). The percentage of each cell type, over the total number of microglia, was calculated within ten random fields taken with 40x magnification in SP2 confocal microscope for each experimental group, in triplicates, for each experiment. The experiment was performed three independent times.

### **E.16 Western Blot**

- Cultured microglia were incubated in ice-cold RIPA buffer (10 mM sodium phosphate pH 7.0, 150 mM NaCl, 2 mM EDTA, 50 mM sodium fluoride, 1% NP-40, 1% sodium deoxycholate, and 0.1% SDS) with an addition of protease inhibitor cocktail (Roche), followed by a brief sonication on ice.
- The total protein concentration in each sample was quantified with the Bradford assay (Bio-Rad Laboratories).
- Samples (equal amount of total protein/lane) were resolved on a SDS–polyacrylamide gel of 12% acrylamide.
- Samples were transferred to a 0.45- $\mu$ M Protran nitrocellulose transfer membrane (Schleicher & Schuell, Bioscience) over 1 hr, using a wet transfer unit (Bio-Rad Laboratories).
- Blocking (5% powdered skim milk and 0.1% Tween-20 in PBS) for 1 hr.
- The membrane was incubated overnight at 4°C with the appropriate primary antibodies.
- 3 washes in 0.1% Tween-20 in PBS (10 minutes each).
- Samples were incubated for 1 hr at room temperature with horseradish peroxidase-coupled secondary anti-rabbit antibody (1:5000, Jackson ImmunoResearch Laboratories).
- 3 washes in 0.1% Tween-20 in PBS (10 minutes each).

In our experiments we used the following primary antibodies: iNOS (1:2000, rabbit, Millipore Cat# ABN26) and  $\alpha$ -Gapdh (1:2000, rabbit, Millipore Cat#ABS16).

### **E.17 Western Blot analysis**

Proteins were visualized by enhanced chemiluminescence (ECL Plus, GE Healthcare Bio-Sciences), while the intensity of the bands was measured with Fiji Image J software (RRID:SCR\_003070) and normalized using Gapdh as loading control. Expression values are shown as percentage considering control animal values as 100%. Three independent experiments were performed.

### **E.18 Statistical analysis**

Image processing, analysis and measurements were performed using Photoshop 9.0-CS2 and Fiji Image J software. Statistical analyses were performed using GraphPad Prism version 8. Data are depicted as means +/- standard error of the mean. All data values are shown as percentage considering control group values as 100%. For all the quantifications, unpaired t-test or one-way analysis of variance (ANOVA), followed by Tukey post-hoc test for multiple comparison procedures, was performed. Differences were considered significant at values of  $p < 0.05$  or lower.



## F. MATERIAL AND METHODS II

### F.1 Pipeline of the methodology implemented in this work

Genes of interest (genes that their corresponding proteins have been found to interact structurally or functionally with Contactin-2 by preclinical experimentation or modern computational approaches) were identified from independent sources. Additionally, gene expression data from 98 brain regions have been retrieved from the databases of the Allen Institute for Brain Science, while the absolute values of gene expression intensity per brain region have been normalized by the whole-brain expression intensity of the corresponding gene (relative gene expression values). These relative gene expression values have been used to visualize the across-brain *Cntn2* expression intensity and to perform a spatial correlation analysis between the across-brain expression patterns of *Cntn2* and the other genes of interest. Finally, using Tabula Muris, we specified the brain cell types responsible for expressing *Cntn2* and the spatially correlated and anticorrelated genes (Figure 13).

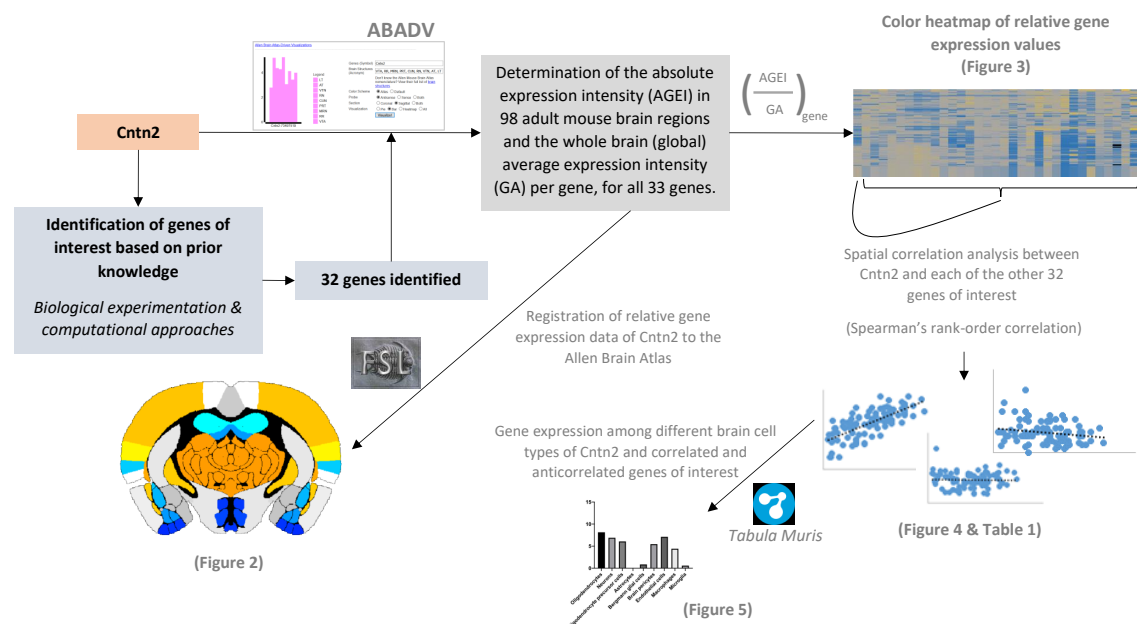


Figure 13: Pipeline of the methodology implemented in this work. ABADV: Allen Brain Atlas-driven visualizations tool, *Cntn2*: Contactin-2/TAG-1 gene, FSL: FMRI Software Library, Tabula Muris: <https://tabula-muris.ds.czbiohub.org>. (Kalafatakis et al., 2020)

## F.2 Technical aspects of the Allen Institute ISH experiments

For all ISH experiments, where the data regarding gene expression derive from, adult male mice of the C57BL/6J inbred strain (aged 56 weeks) have been used. Antisense RNA probes have been used on brain sagittal sections. More detailed information regarding the technical aspects of the ISH experiments can be found in Lein et al., 2017. All genes, mentioned in this work, have been studied under these specific settings in at least one experiment. In eight cases (Bace1, L1cam, Map1b, Apc, Ntrk2, Cldn11, Myrf, Reln) two identical experiments per gene have been performed and, in another case (Plp1), eighteen; the final dataset derives from the average between the two or three experiments per gene. The 58 experiments (raw data) included in this paper can be found in <http://mouse.brain-map.org/>, while experiment IDs can be found in Table 1.

Gene Nomenclature ( <a href="http://www.informatics.jax.org/">http://www.informatics.jax.org/</a> )	Experiment ID ( <a href="http://mouse.brain-map.org/">http://mouse.brain-map.org/</a> )	
	1 <sup>st</sup> experiment	2 <sup>nd</sup> experiment
Cntn2	73497519	
Lyn	68563122	
Bace1	69528046	70813149
Cntnap2	76098407	
Kcna1	69735688	
Kcna2	69257999	
L1cam	621	80342072
Nrcam	173	
Ncam1	80342134	
Ncam2	683	
Ncan	69608154	
Ptprz1	71487157	
Tnc	69817007	
Gnb2l1	71021172	
App	107	
Reln	79394359	892
Map1b	73834355	71570737
Map2	69549641	
Mapt	80525654	
Kif1b	74003383	
Apc	69526725	71148004
Apc2	69526731	
Pdgfra	79354743	
Cspg4	69608160	
Cd24a	70719038	
Ntrk2	747	79360318
Sema6a	68844851	
Nfasc	68844086	
Plp1		*
Mbp	79632288	
Mog	70946633	
Cldn11	74581223	77924438
Myrf	70295805	71161357

**Table 1:** IDs of the *in situ* hybridization experiments performed by Allen Institute on adult (56 weeks) male C57BL/6J mice, corresponding to the 33 genes of interest. In all experiments antisense RNA probes have been used on brain sections cut in the sagittal plane. (Kalafatakis et al., 2020)

\* 18 identical experiments have been performed on *Plp1*. The IDs are: 2490, 69117382, 75457512/-3/-4/-5, 75492714/-15/-25/-44, 75496145/-6/-7/-8, 75496499/-500/-510/-529

### F.3 Gene identification

Genes of interest were identified based on their encoding proteins having a potential relationship with Contactin-2. More specifically, either previous studies (Masuda, 2017; Traka et al., 2003; Poliak et al., 2003) have showed that these proteins directly or indirectly interact with Contactin-2 or have theoretical interactions with Contactin-2, based on the output of UniRed, which is a computational prediction tool that analyses biomedical literature suggesting protein-protein interactions (<http://bioinformatics.med.uoc.gr/unired/>) (Theodosiou et al., 2020). All genes of interest are listed in Table 2.

<b>Cntn2</b>	Contactin-2
<b>Markers of oligodendrocytic physiology</b>	
<b>Pdgfra</b>	Platelet derived growth factor receptor, alpha polypeptide
<b>Cspg4</b>	Chondroitin sulfate proteoglycan 4
<b>Apc</b>	WNT signaling pathway regulator, Adenomatosis polyposis coli
<b>Apc2</b>	Adenomatosis polyposis coli 2
<b>Plp1</b>	Proteolipid protein (myelin) 1
<b>Mbp</b>	Myelin basic protein
<b>Mog</b>	Myelin oligodendrocyte glycoprotein
<b>Cldn11</b>	Claudin-11, oligodendrocyte-specific protein
<b>Myrf</b>	Myelin regulatory factor
<b>Genes, whose products interact functionally or structurally with Contactin-2</b>	
<b>Lyn</b>	Proto-oncogene, Src family tyrosine kinase
<b>Cntnap2</b>	Contactin associated protein-like 2
<b>Kcna1</b>	Potassium voltage-gated channel, shaker-related subfamily, member 1
<b>Kcna2</b>	Potassium voltage-gated channel, shaker-related subfamily, member 2
<b>L1cam</b>	L1 cell adhesion molecule
<b>Nrcam</b>	Neuronal cell adhesion molecule
<b>Ncam1</b>	Neural cell adhesion molecule 1
<b>Ncam2</b>	Neural cell adhesion molecule 2
<b>Ncan</b>	Neurocan
<b>Ptprz1</b>	Protein tyrosine phosphatase, receptor type Z, polypeptide 1
<b>Tnc</b>	Tenascin C
<b>Gnb2l1</b>	Receptor for activated C kinase 1
<b>App</b>	Amyloid beta (A4) precursor protein
<b>Bace1</b>	Beta-site APP cleaving enzyme 1
<b>Reln</b>	Reelin
<b>Map1b</b>	Microtubule-associated protein 1b
<b>Map2</b>	Microtubule-associated protein 2
<b>Mapt</b>	Microtubule-associated protein tau
<b>Kif1b</b>	Kinesin family member 1b

<b>Cd24a</b>	CD24a antigen
<b>Ntrk2</b>	Neurotrophic tyrosine kinase, receptor, type 2
<b>Sema6a</b>	Semaphorin 6a
<b>Nfasc</b>	Neurofascin

Table 2: Nomenclature of all genes involved in this report, based on <http://www.informatics.jax.org/>. (Kalafatakis et al., 2020)

#### F.4 Brain segmentation and data collection

Data collection was based on the Allen Brain Atlas-Driven Visualizations software (ABADV), which is a free access web-based tool created to recover and visualize expression energy data from mouse AGEA across multiple genes and brain structures (Zaldivar and Krichmar, 2014). The spatial segmentation of the mouse brain was performed according to Allen Institute’s taxonomic system and based on ABADV’s capabilities to provide gene expression energy data for all 33 genes under investigation by the 58 experiments mentioned above (as explained in Kalafatakis et al., 2019). Abbreviations of the all brain regions can be found in Table 3.

<b>BRAIN REGIONS (grey matter)</b>	
<i>Abbreviations</i>	<i>Full name</i>
<b>MOB</b>	Main olfactory bulb
<b>AOB</b>	Accessory olfactory bulb
<b>AON</b>	Anterior olfactory nucleus
<b>TT</b>	Taenia tecta
<b>PIR</b>	Piriform area
<b>EP</b>	Endopiriform nucleus
<b>DP</b>	Dorsal peduncular area
<b>OT</b>	Olfactory tubercle
<b>FRP</b>	Frontal pole
<b>MO</b>	Somatomotor areas
<b>GU</b>	Gustatory areas
<b>VISC</b>	Visceral area
<b>PL</b>	Prelimbic area
<b>ILA</b>	Infralimbic area
<b>ORB</b>	Orbital area
<b>AI</b>	Agranular insular area
<b>CLA</b>	Clastrum
<b>AUD</b>	Auditory areas
<b>TEa</b>	Temporal association areas
<b>PERI</b>	Perirhinal area
<b>SS</b>	Somatosensory areas
<b>ACA</b>	Anterior cingulate area
<b>RSP</b>	Retrosplenial area
<b>PTLp</b>	Posterior parietal association areas
<b>NLOT</b>	Nucleus of the lateral olfactory bulb
<b>PAA</b>	Piriform-amygdalar area
<b>TR</b>	Postpiriform transition area
<b>ENT</b>	Entorhinal area
<b>VIS</b>	Visual areas
<b>ECT</b>	Ectorhinal area

CB	Cerebellum
DG	Dentate gyrus
CA	Ammon's horn
FC	Fasciola cinerea
IG	Induseum griseum
SUB	Subiculum
PAR	Parasubiculum
POST	Postsubiculum
PRE	Presubiculum
STRd	Dorsal striatum
FS	Fundus of striatum
ACB	Nucleus accumbens
PALv	Ventral pallidum
NDB	Diagonal band nucleus
PALd	Dorsal pallidum
PALc	Caudal pallidum
LSX	Lateral septal complex
TRS	Triangular nucleus of septum
MS	Medial septal nucleus
sAMY	Striatum-like amygdalar nuclei
COA	Cortical amygdalar area
LA	Lateral amygdalar nucleus
BLA	Basolateral amygdalar nucleus
BMA	Basomedial amygdalar nucleus
PA	Posterior amygdalar nucleus
TH	Thalamus
PVZ	Periventricular zone
PVR	Periventricular region
LZ	Hypothalamic lateral zone
ME	Median eminence
AHN	Anterior hypothalamic nucleus
MPN	Medial preoptic nucleus
PMd	Dorsal premammillary nucleus
PMv	Ventral premammillary nucleus
PVHd	Paraventricular hypothalamic nucleus (descending division)
VMH	Ventromedial hypothalamic nucleus
PH	Posterior hypothalamic nucleus
MBO	Mammillary body
IF	Interfascicular nucleus raphe
RL	Rostral linear nucleus raphe
CLI	Central linear nucleus raphe
DR	Dorsal nucleus raphe
SNe	Substantia nigra (compact part)
PPN	Predunculopontine nucleus
SAG	Nucleus sagulum
PBG	Parabigeminal nucleus
SNr	Substantia nigra (reticular part)
VTA	Ventral tegmental area
RR	Midbrain reticular nucleus (retrobulbar area)
MRN	Midbrain reticular nucleus
PRT	Pretectal region
CUN	Cuneiform nucleus
RN	Red nucleus

<b>VTN</b>	Ventral tegmental nucleus
<b>AT</b>	Anterior tegmental nucleus
<b>LT</b>	Lateral terminal nucleus of the accessory optic tract
<b>SCm</b>	Superior colliculus (motor-related)
<b>SCs</b>	Superior colliculus (sensory-related)
<b>IC</b>	Inferior colliculus
<b>NB</b>	Nucleus of the brachium of the inferior colliculus
<b>PAG</b>	Periaqueductal gray
<b>MEV</b>	Midbrain trigeminal nucleus
<b>III</b>	Oculomotor nucleus
<b>EW</b>	Edinger-Westphal nucleus
<b>IV</b>	Trochlear nucleus
<b>IPN</b>	Interpeduncular nucleus
<b>P</b>	Pons
<b>MY</b>	Medulla

**Table 3:** The 98 regions of the grey matter of the adult mouse brain. Abbreviations have been adopted from the Allen Brain Atlas nomenclature (<http://mouse.brain-map.org/static/atlas>). Different colours are used for different major brain regions (red: cerebral cortex, yellow: hippocampal formation and related structures, green: basal ganglia, light blue: amygdala and neighboring structures, dark blue: hypothalamus, purple: midbrain). (Kalafatakis et al., 2020)

### F.5 Whole-brain relative gene expression data visualisation

The values representing the gene expression intensity of all genes of interest per brain region have been normalized by the mean expression intensity of the corresponding gene in the whole brain to give relative gene expression values. A color heatmap has been used for data visualization. In case of *Cntn2*, the relative gene expression data have been additionally registered to the Allen Brain Atlas for visualizing them in relation to the underlying mouse brain anatomy. Values between 0.85 – 1.15 have been considered as average. To visualize the data, we used sections of the Allen Mouse Brain volumetric atlas 2012 and the masks corresponding to the 95 brain regions in NIFTI file format (<https://scalablebrainatlas.incf.org/mouse/ABA12>). We used FMRI Software Library (FSL) for image processing and visualization (Jenkinson et al., 2012), Fsleyes for image inspection and fslutils to register the available genomic data of *Cntn2* to the corresponding brain region.

### F.6 *Cntn2* genomic spatial correlation analysis

We conducted correlation analysis of the gene expression intensities between *Cntn2* and all other genes under investigation. Normality in the distribution of data (Shapiro–Wilk test) has been used, and Spearman’s rank-order correlation was preferred due to the non-normality in the distribution of the relevant data. The level of significance has been set to 0.05.

## **F.7 Data collection regarding the expression of genes of interest among different brain cell populations**

Data, referring to the brain cell type-specific expression of *Cntn2* and its spatially correlated and anticorrelated genes of interest, were retrieved from Tabula Muris (<https://tabula-muris.ds.czbiohub.org>), and were captured by FACS-based full length transcript analysis, which provides high sensitivity and coverage (Tabula Muris Consortium et al., 2018). Brain myeloid and brain non-myeloid were selected as the examined tissues. Median values of the gene expression were retrieved. For data visualization, Prism8 software was used.

## G. RESULTS I

### G.1 BNN20 reduces myelin loss in the lesion area of the LPC-induced demyelination mouse model

Our first aim was to investigate the action of BNN20 *in vivo* using the LPC demyelinating model in which LPC is injected in the corpus callosum (CC) and very quickly causes local demyelination. The myelin sheath is directly destroyed, attracting an inflammatory microglia/macrophage and astrocyte response. Complete remyelination occurs later on, typically after the 2nd-3rd week post-injection (Miller et al., 2010). Our study consisted of 3 different groups (control, LPC, LPC/BNN20). We focused on 3 different time points, 5 days post injection (dpi), 10dpi and 15dpi. The 5 and 10dpi represented an early and a late point of demyelination respectively, while the 15dpi time point represented a remyelination period. The lesion area was clearly evident during the two time points of demyelination as shown in Figure 14A, B. To test if BNN20 has an actual effect in myelin, we evaluated the demyelinated area by densitometric analysis upon PLP immunohistochemistry. This analysis revealed significant demyelination in the LPC group compared with the control at 5 (Figure 15A, B, D, P) and 10dpi (Figure 15F, G, I, Q) while at 15dpi the lesion was less evident (Figure 15K, L, N, R). Administration of BNN20 reduced myelin loss at 5 (Figure 15C, E, P) and 10 dpi (Figure 15H, J, Q), while at 15dpi there was a higher amount of myelin in the lesion area compared with the LPC group (Figure 15M, O, R). Our results indicate a protective and possibly restorative role of BNN20 regarding demyelination and remyelination in this specific model.



5dpi

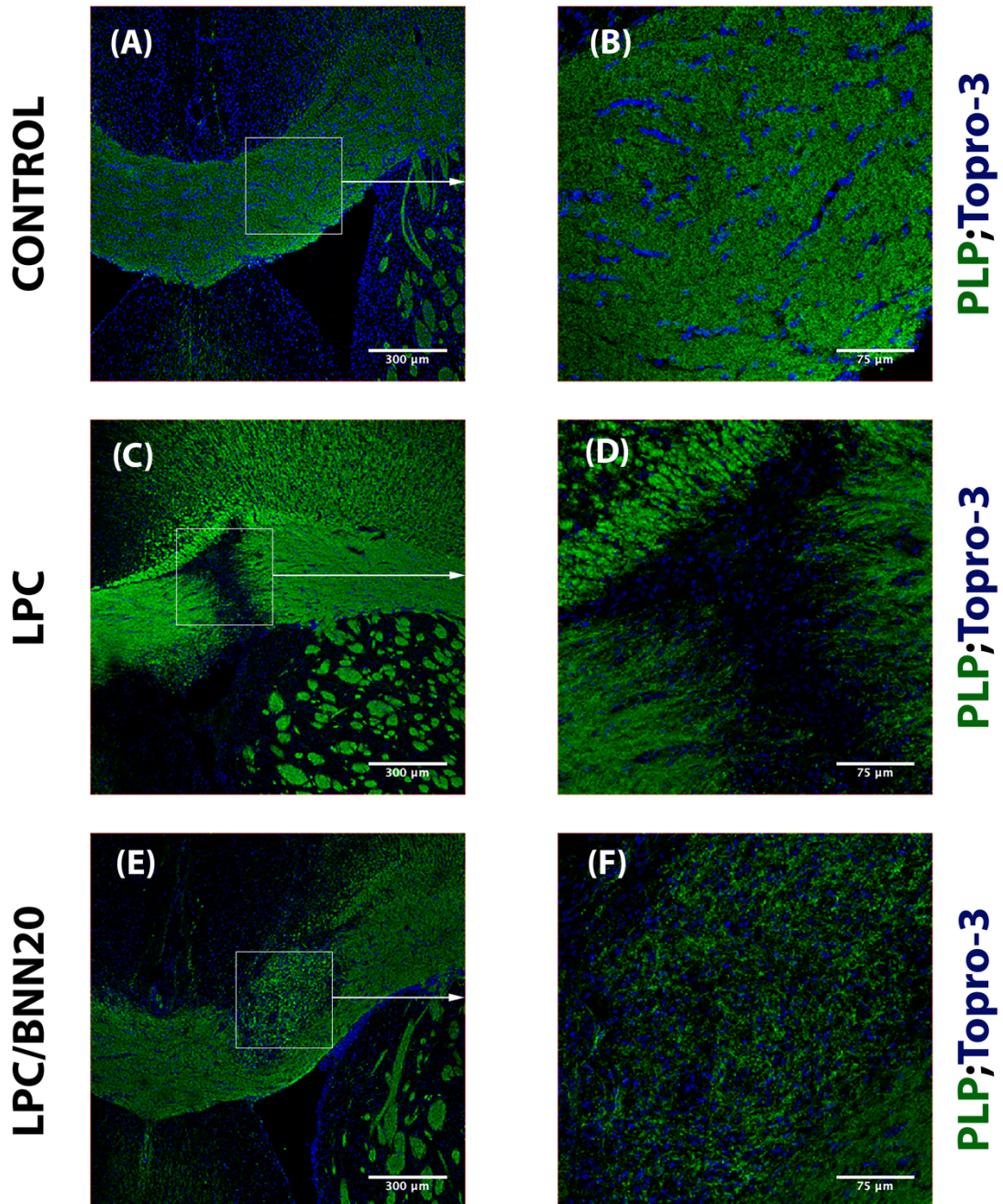


Figure 14A: (A-F) Representative immunohistochemical images of the corpus callosum labelled for PLP (green) and Topro-3 (blue), showing the lesion site in LPC and LPC/BNN20 treated mice at 5dpi. Scale bar in A, C, E: 300μm. Scale bar in B, D, F: 75μm.

10dpi

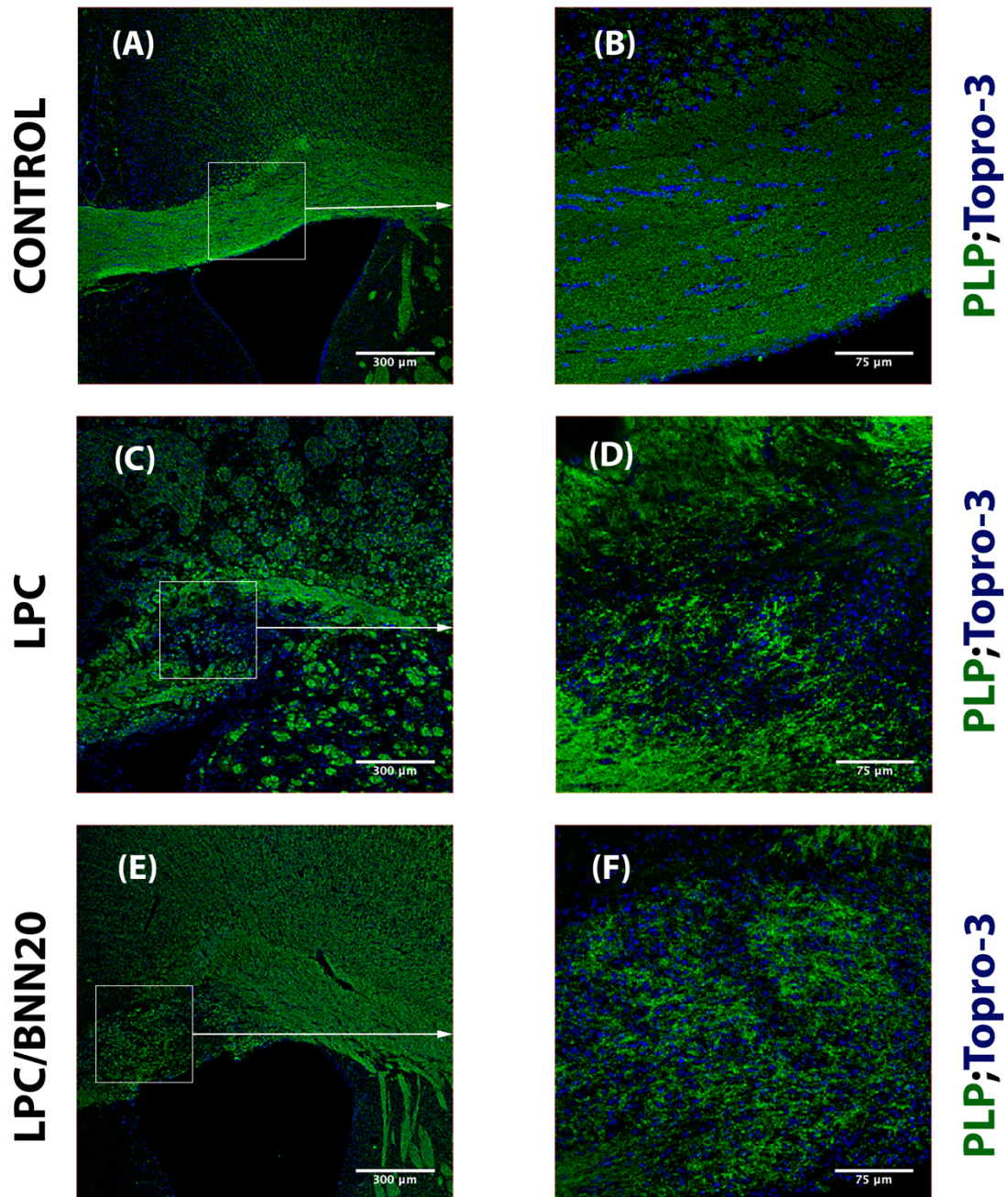


Figure 14B: (A-F) Representative immunohistochemical images of the corpus callosum labelled for PLP (green) and Topro-3 (blue), showing the lesion site in LPC and LPC/BNN20 treated mice at 10dpi. Scale bar in A, C, E: 300μm. Scale bar in B, D, F: 75μm.

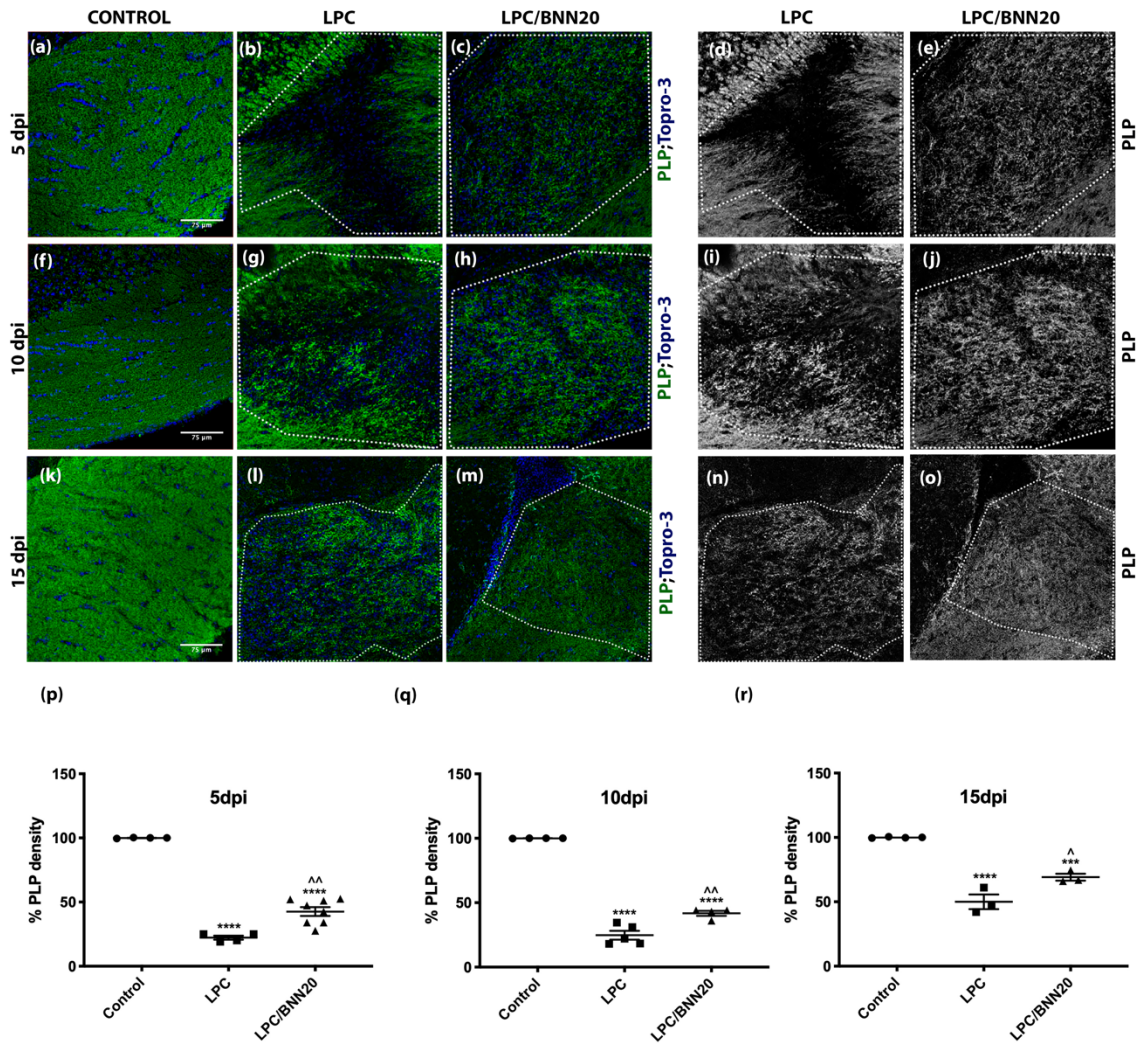


Figure 15: BNN20 ameliorates myelin loss in the lesion area of the LPC-induced demyelination mouse model: (A-O) Representative immunohistochemical images of the corpus callosum labelled for PLP (green) and Topro-3 (blue). The area surrounded by the dotted line denotes the lesion area. Lesion was recognized from the PLP staining and the accumulation of nuclei which represents the accumulation of astrocytes and microglia. (P-R) Quantification of the PLP densitometric analysis in control, LPC, and LPC/BNN20 groups at 5, 10 and 15dpi (control 5dpi n=4, control 10dpi n=4, control 15dpi n=4, LPC 5dpi n=4, LPC 10dpi n=5, LPC 15dpi n=3, LPC/BNN20 5dpi n=8, LPC/BNN20 10dpi n=4, LPC/BNN20 15dpi n=3). For the statistics, one-way ANOVA with post-hoc Tukey test was used. Data are expressed as mean  $\pm$  SEM. Regarding the statistics of 5dpi groups  $F(2, 13) = 127.5, p < 0.0001$ , of 10dpi groups  $F(2, 10) = 242.7, p < 0.0001$  and of 15dpi groups  $F(2, 7) = 65.95, p < 0.0001$ . Comparison with control group: \*\*\* $p < 0.001$ ; \*\*\*\* $p < 0.0001$ . Comparison with LPC group: ^ $p < 0.05$ ; ^^ $p < 0.01$ . Scale bar in A-O: 75 $\mu$ m.

## **G.2 BNN20 increases the number of mature OLs in the lesion area of LPC-induced demyelination mouse model**

Our next aim was to investigate which cell types are implicated in the reduced myelin loss observed upon BNN20 administration in the LPC model, so we first turned our attention to OLs. After LPC injection, mature OL loss is observed as revealed by CC-1 immunohistochemistry (Figure 17A, B, D, E, G, H, J, K, L), while PDGFRa<sup>+</sup> OPCs are recruited in the lesion area during demyelination phase (Figure 18A, B, D, E, J, K). We observed a reduced number of OLs in the LPC group compared with the control group, upon immunolabelling with the general marker for OLs, Olig2 (Figure 16A, B, D, E, G, H, J, K, L). However, upon BNN20 administration we noticed an increased number of OLs in the lesion area in all 3 time points (Figure 16C, F, I, J, K, L) indicating a beneficial role of BNN20 on OLs. In order to identify which population of OLs is affected by BNN20 administration, we used the CC-1 antibody, which marks mature OLs, and the PDGFRa antibody, which marks OPCs. We observed an increase in the number of mature OLs in the lesion area of BNN20 treated mice compared with the untreated ones in all 3 time points (Figure 17C, F, I, J, K, L), while BNN20 did not seem to significantly alter the recruitment of OPCs (Figure 18C, F, I, J, K, L). The beneficial role suggested for BNN20 by our results could arise either from reduced OL loss upon LPC treatment or due to enhanced maturation of OPCs to mature OLs.

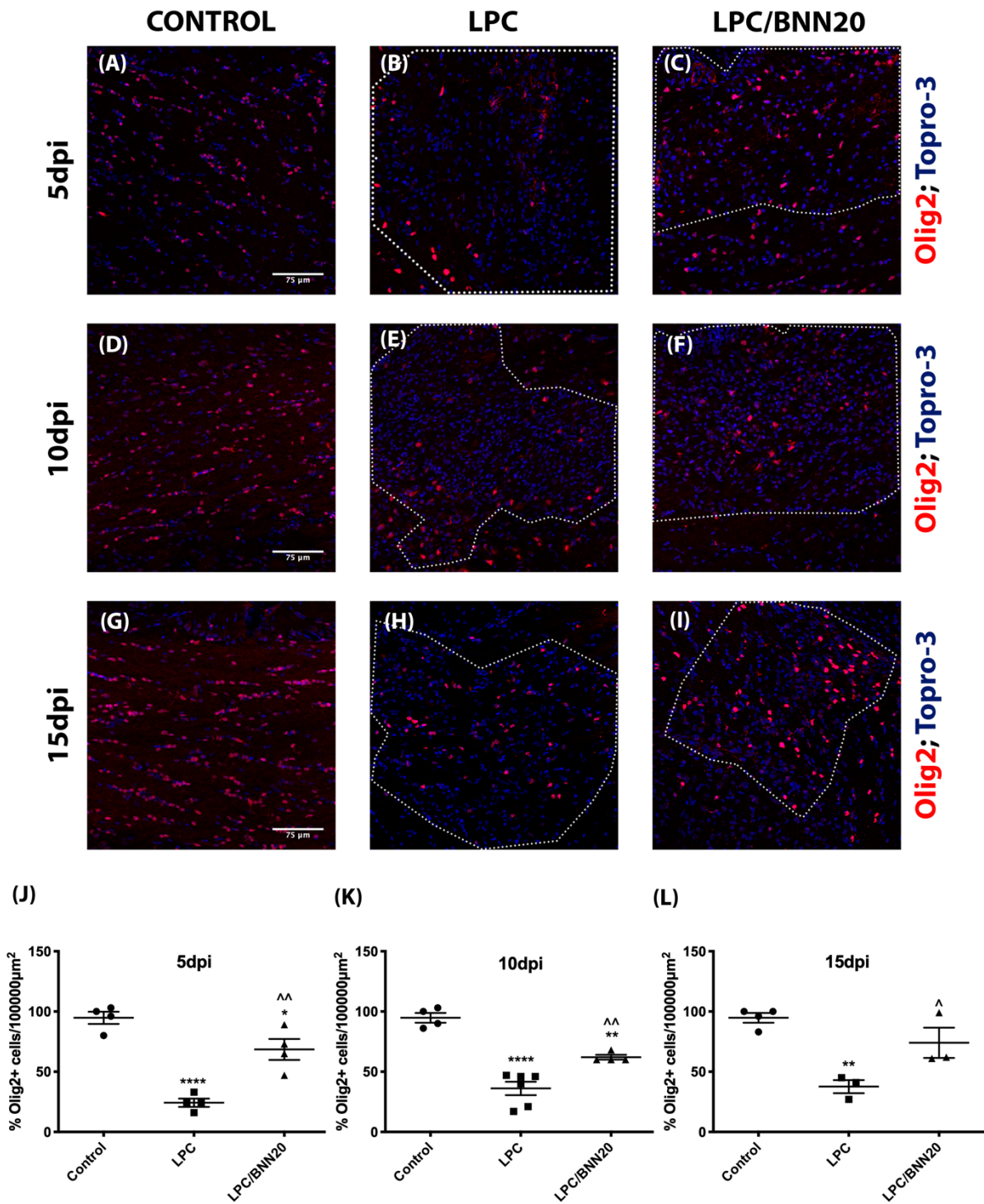


Figure 16: BNN20 increases the number of OLs in the lesion area of the LPC-induced demyelination mouse model: (A-I) Representative immunohistochemical images of the corpus callosum labelled for Olig2 (red) and Topro-3 (blue). The area surrounded by the dotted line denotes the lesion area. (J-L) Quantification of the percentage of oligodendrocytes stained with Olig2 in control, LPC and LPC/BNN20 groups, at 5, 10 and 15dpi (control 5dpi n=4, control 10dpi n=4, control 15dpi n=4, LPC 5dpi n=4, LPC 10dpi n=6, LPC 15dpi n=3, LPC/BNN20 5dpi n=4, LPC/BNN20 10dpi n=4, LPC/BNN20 15dpi n=3). For the statistics,

one-way ANOVA with post-hoc Tukey test was used. Data are expressed as mean  $\pm$  SEM. Regarding the statistics of 5dpi groups  $F(2, 9) = 33.25, p < 0.0001$ , of 10dpi groups  $F(2, 11) = 38.94, p < 0.0001$  and of 15dpi groups  $F(2, 7) = 14.99, p = 0.0030$ . Comparison with control group: \* $p < 0.05$ ; \*\* $p < 0.01$ ; \*\*\*\* $p < 0.0001$ . Comparison with LPC group: ^ $p < 0.05$ ; ^ $p < 0.01$ . Scale bar in A-I: 75 $\mu$ m.

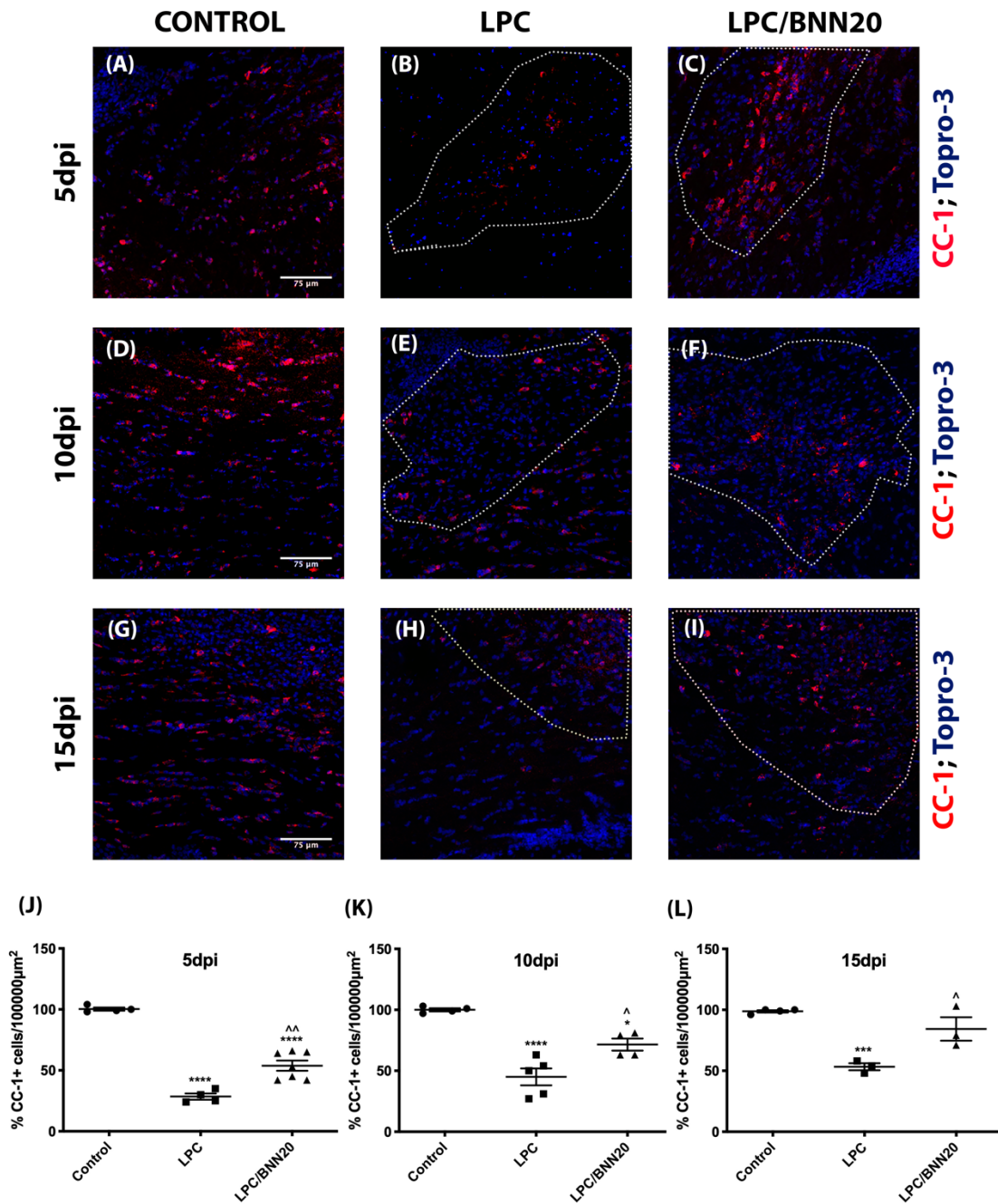
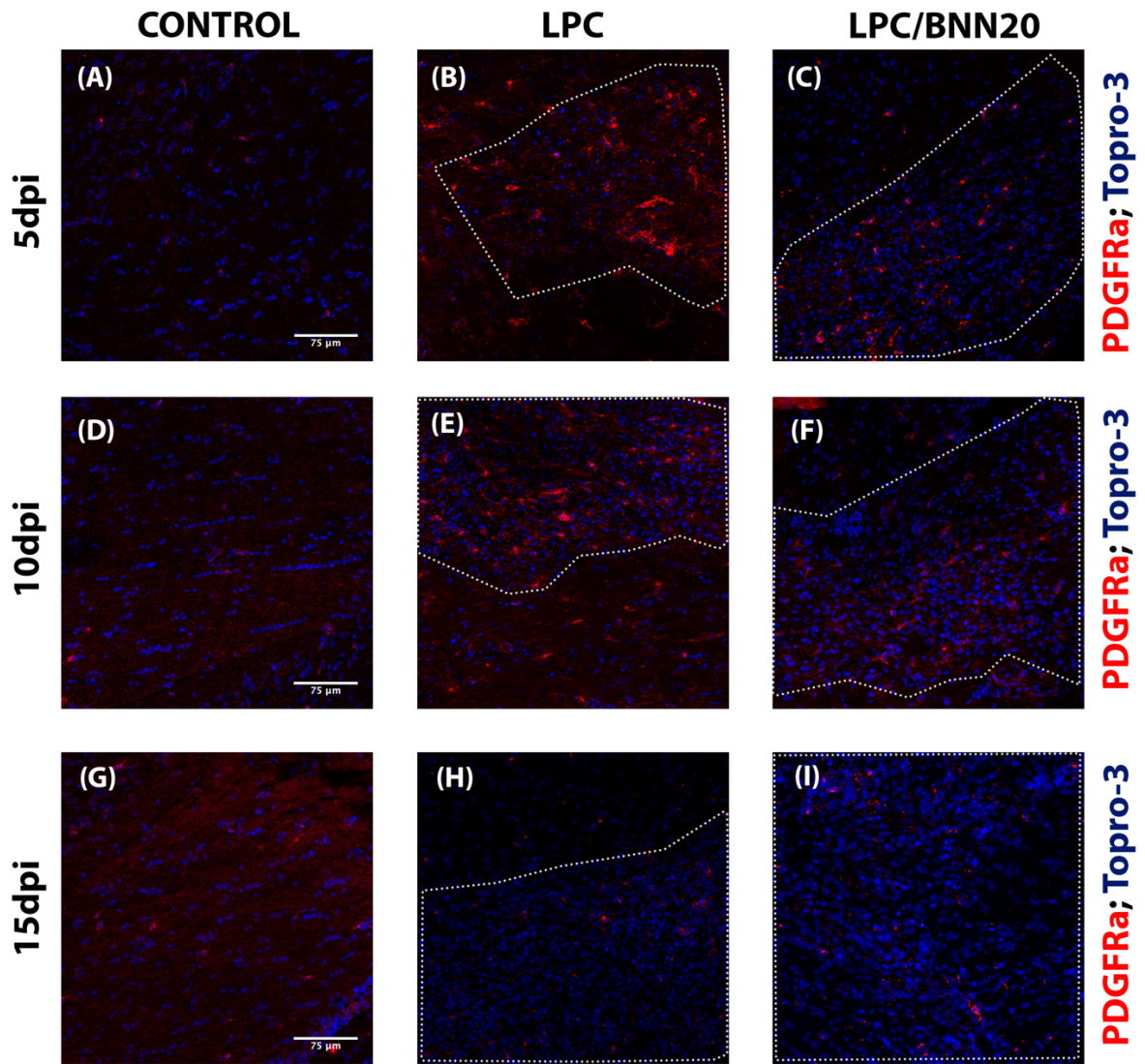


Figure 17: BNN20 increases the number of mature OLs in the lesion area of the LPC-induced demyelination mouse model: (A-I) Representative immunohistochemical images of the corpus

*callosum* labelled for CC-1 (red) and Topro-3 (blue). The area surrounded by the dotted line denotes the lesion area. (J-L) Quantification of the percentage of mature oligodendrocytes stained with CC-1 in control, LPC and LPC/BNN20 groups at 5, 10 and 15dpi (control 5dpi n=4, control 10dpi n=4, control 15dpi n=4, LPC 5dpi n=4, LPC 10dpi n=5, LPC 15dpi n=3, LPC/BNN20 5dpi n=7, LPC/BNN20 10dpi n=4, LPC/BNN20 15dpi n=3). Regarding the statistics, one-way ANOVA with post-hoc Tukey test was used. Data are expressed as mean  $\pm$  SEM. For the statistics of 5dpi groups  $F(2, 12) = 77.17, p < 0.0001$ , of 10dpi groups  $F(2, 10) = 26.70, p < 0.0001$  and of 15dpi groups  $F(2, 7) = 20.39, p = 0.0012$ . Comparison with control group: \* $p < 0.05$ ; \*\*\* $p < 0.001$ ; \*\*\*\* $p < 0.0001$ . Comparison with LPC group: ^ $p < 0.05$ ; ^ $p < 0.01$ . Scale bar in A-I: 75 $\mu$ m.



(J)

(K)

(L)

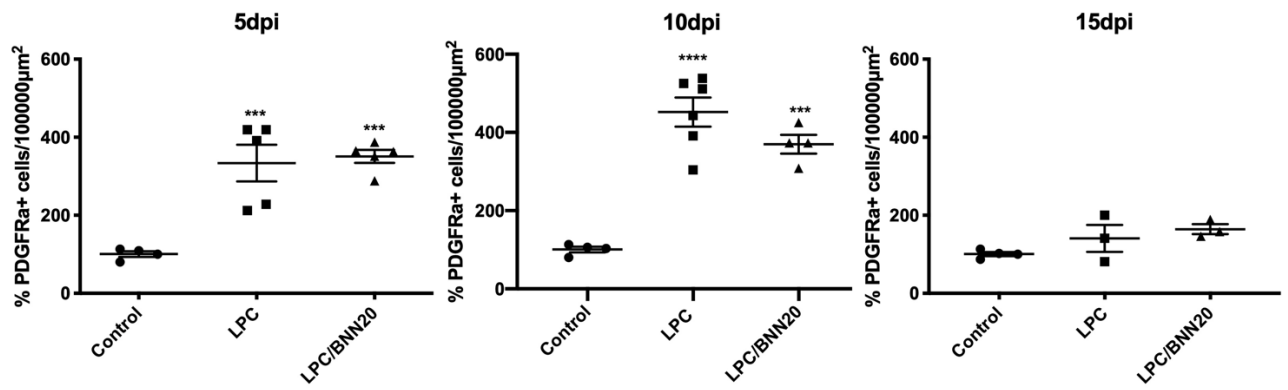




Figure 18: BNN20 does not affect OPC recruitment in the lesion area of the LPC-induced demyelination mouse model: (A-I) Representative immunohistochemical images of the corpus callosum labelled for PDGFR $\alpha$  (red) and Topro-3 (blue). The area surrounded by the dotted line denotes the lesion area. (J-L) Quantification of the percentage of OPCs stained with PDGFR $\alpha$  in control, LPC and LPC/BNN20 groups at 5, 10 and 15dpi (control 5dpi n=4, control 10dpi n=4, control 15dpi n=4, LPC 5dpi n=5, LPC 10dpi n=6, LPC 15dpi n=3, LPC/BNN20 5dpi n=5, LPC/BNN20 10dpi n=4, LPC/BNN20 15dpi n=3). For the statistics, one-way ANOVA with post-hoc Tukey test was used. Data are expressed as mean  $\pm$  SEM. Regarding the statistics of 5dpi groups  $F(2, 11) = 18.43, p = 0.0003$ , of 10dpi groups  $F(2, 11) = 34.09, p < 0.0001$  and of 15dpi groups  $F(2, 7) = 3.052, p = 0.1114$ . Comparison with control group: \*\*\* $p < 0.001$ ; \*\*\*\* $p < 0.0001$ . Scale bar in A-I: 75 $\mu$ m.

### **G.3 BNN20 reduces accumulation of astrocytes in the lesion area of LPC-induced demyelination mouse model with no effect on accumulation of microglia/macrophages.**

LPC injection in the CC leads to both activation and accumulation of astrocytes and microglia/macrophages in the lesion area, which, through the secretion of cytotoxic factors contribute to demyelination and mature OLs loss. Activation and accumulation of these glial populations is visible even from the first dpi. Taking into consideration that this event promotes demyelination and inflammation, we asked ourselves whether BNN20 has an effect in these populations. By performing immunohistochemistry for the astrocytic marker GFAP we observed a high activation and accumulation of astrocytes in the lesion area of LPC-injected mice when compared with the control group at 5, 10dpi (Figure 19A, B, D, E, J, K). BNN20 treatment caused a statistically significant reduction of this effect during demyelination (Figure 19C, F, J, K). At the start of remyelination (15dpi) the level of astrocyte accumulation in the lesion area is reduced compared with the other 2 time points (Figure 19B, E, H, J, K, L) as expected since demyelination period is over, but there is no difference between the LPC group that is treated with BNN20 and the untreated LPC group (Figure 19H, I, L). These results indicate that BNN20 reduces astrogliosis during demyelination *in vivo*.

We also performed immunohistochemistry for IBA-1, a microglia/macrophage marker. By densitometric analysis, we observed a statistically significant increase regarding the accumulation of microglia/macrophages in the lesion area of the LPC injected mice compared to the control group (Figure 20A, B, D, E, G, H, J, K, L). However, there was no statistically significant change, when LPC-treated mice were additionally treated with BNN20 (Figure 20C, F, I, J, K, L). Our results indicate that BNN20 does not affect the accumulation of microglia/macrophages in the lesion site during demyelination *in vivo*.

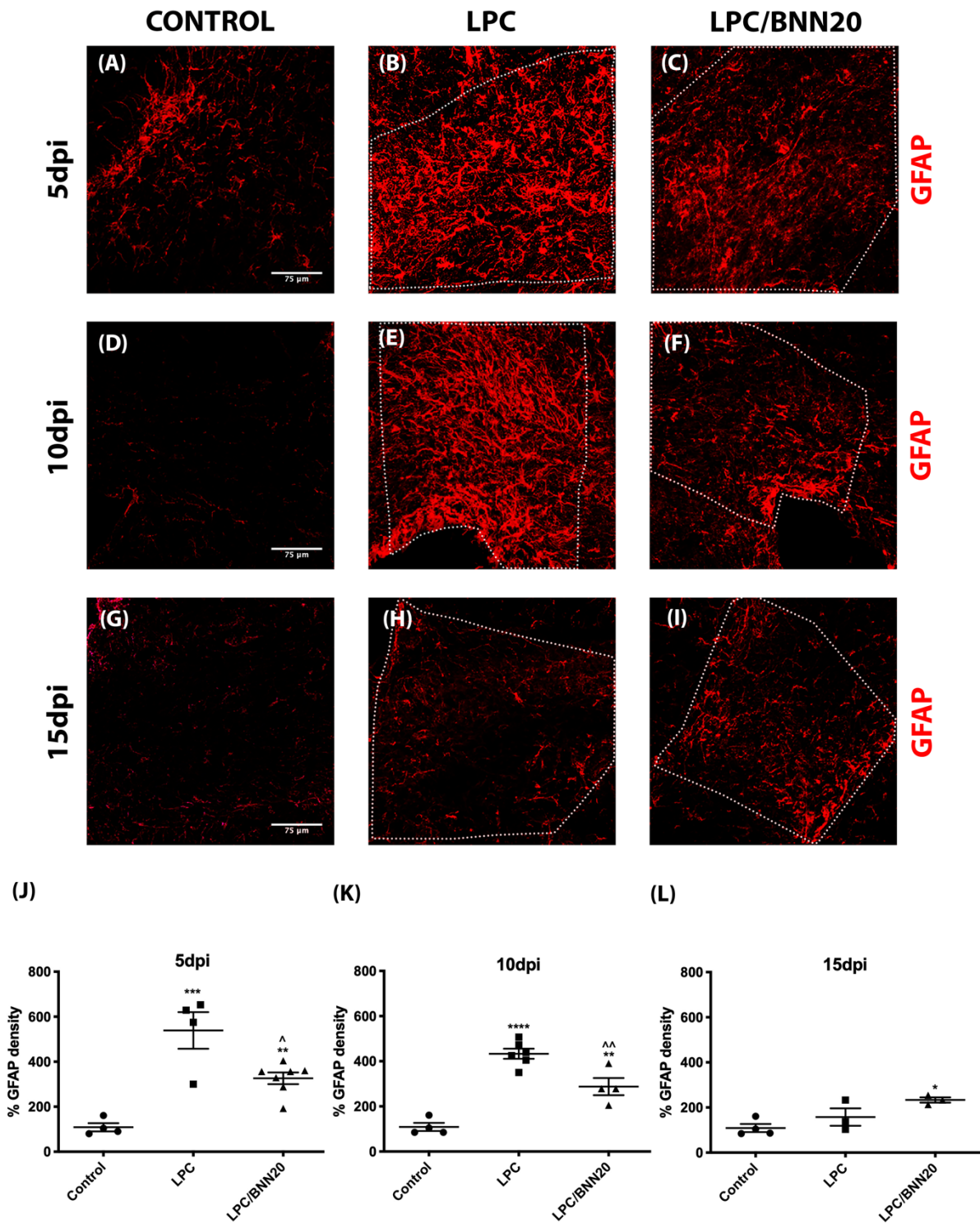


Figure 19: BNN20 reduces astrogliosis in the lesion area of the LPC-induced demyelination mouse model: (A-I) Representative immunohistochemical images of the corpus callosum labelled for GFAP (red). The area surrounded by the dotted line denotes the lesion area. (J-L) Quantification of the GFAP densitometric analysis in control, LPC and LPC/BNN20 groups at 5, 10 and 15dpi (control 5dpi n=4, control 10dpi n=4, control 15dpi n=4, LPC 5dpi n=4, LPC 10dpi n=6, LPC 15dpi n=3, LPC/BNN20 5dpi n=7, LPC/BNN20 10dpi n=4, LPC/BNN20

15dpi n=3). For the statistics, one-way ANOVA with post-hoc Tukey test was used. Data are expressed as mean  $\pm$  SEM. Regarding the statistics of 5dpi groups  $F(2, 12) = 19.88$ ,  $p = 0.0002$ , of 10dpi groups  $F(2, 11) = 38.46$ ,  $p < 0.0001$  and of 15dpi groups  $F(2, 7) = 6.752$ ,  $p = 0.0232$ . Comparison with CONTROL group: \* $p < 0.05$ ; \*\* $p < 0.01$ ; \*\*\* $p < 0.001$ ; \*\*\*\* $p < 0.0001$ . Comparison with LPC group: ^ $p < 0.05$ ; ^ $p < 0.001$ . Scale bar in A-I: 75 $\mu$ m.

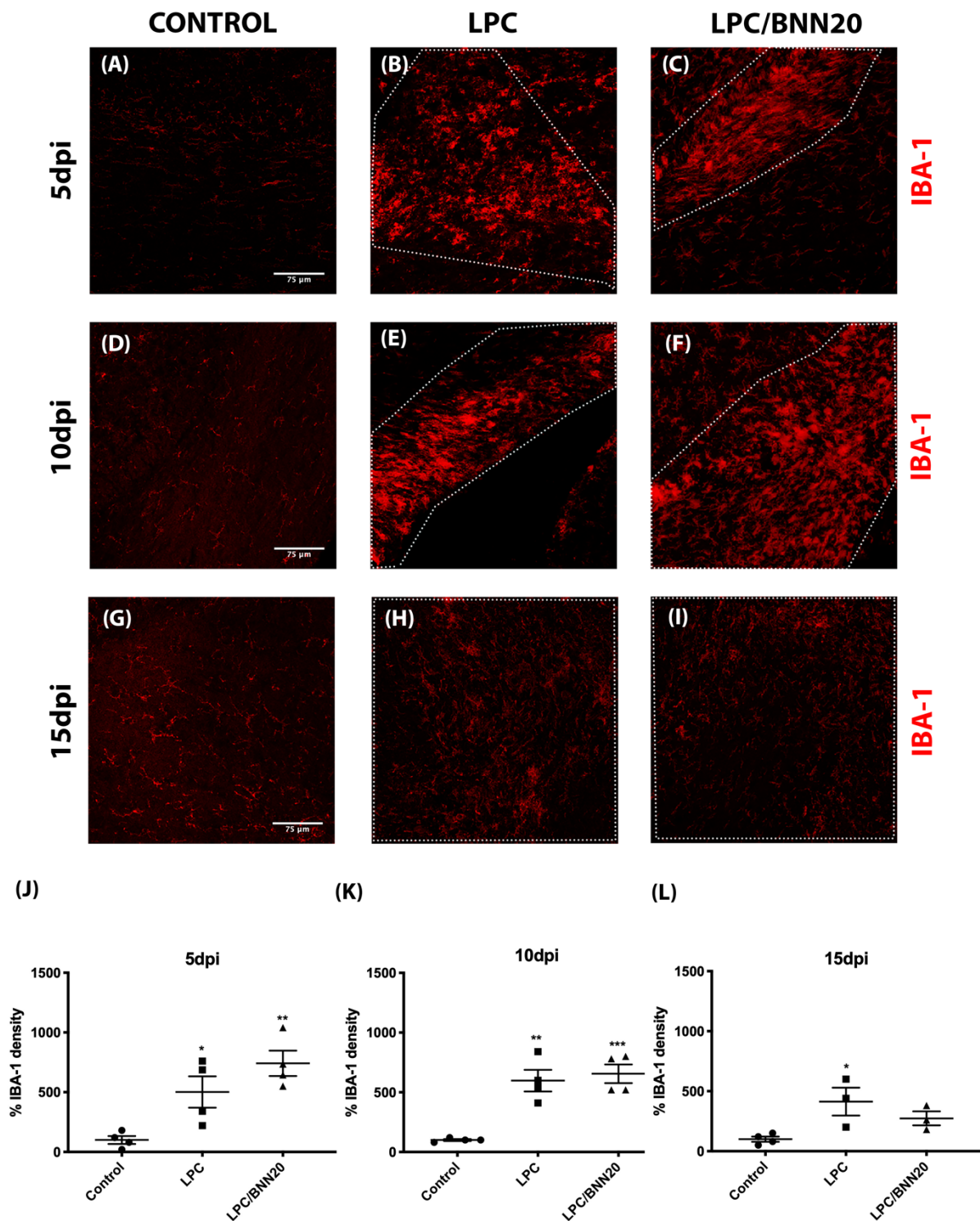


Figure 20: BNN20 does not affect the accumulation of microglia/macrophages that are present in the lesion area of LPC-induced demyelination mouse model: (A-I) Representative immunohistochemical images of the corpus callosum labelled for IBA-1 (red). The area surrounded by the dotted line denotes the lesion area. (J-L) Quantification of the IBA-1 densitometric analysis in control, LPC and LPC/BNN20 groups at 5, 10 and 15dpi (control 5dpi n=4, control 10dpi n=4, control 15dpi n=4, LPC 5dpi n=4, LPC 10dpi n=4, LPC 15dpi n=3, LPC/BNN20 5dpi n=4, LPC/BNN20 10dpi n=4, LPC/BNN20 15dpi n=3). For the

statistics, one-way ANOVA with post-hoc Tukey test was used. Data are expressed as mean  $\pm$  SEM. Regarding the statistics of 5dpi groups  $F(2, 9) = 10.66, p = 0.0042$ , of 10dpi groups  $F(2, 9) = 19.59, p = 0.0005$  and of 15dpi groups  $F(2, 7) = 5.603, p = 0.0352$ . Comparison with CONTROL group: \* $p < 0.05$ ; \*\* $p < 0.01$ ; \*\*\* $p < 0.001$ . Scale bar in A-I: 75 $\mu$ m.

#### **G.4 BNN20 reduces microglia activation and transition to their pro-inflammatory state upon LPS stimulation *in vitro***

Although the number of microglia seems to be unaffected by BNN20 addition *in vivo*, we hypothesized that their activation state might be altered. Microglia in their resting (non-active) form are characterized by small cell somata and long, highly ramified processes (Figure 21A-C, yellow arrow). Upon activation they change their morphology being characterized by large cell somata and an amoeboid shape (Figure 21A-C, white arrow). There are two different activated microglia polarization phenotypes, the anti-inflammatory and the pro-inflammatory microglia. The former type of cells secrete specific factors like IL-4, IL-10, IL-13, TGF $\beta$  and Arg1 and present an anti-inflammatory and neuroprotective response. On the other hand, pro-inflammatory microglia secrete factors like IL-1, IL-12, IL-23, TNF $\alpha$  and iNOS and they have an inflammatory and neurotoxic response (Tang and Le, 2016).

To study if BNN20 has an actual effect on microglial activation, we performed experiments on primary microglia cultures. For microglia activation the cultures were exposed for 24 or 48 hr to LPS inducing a shift in cellular morphology, from a ramified to an amoeboid one. Treatment with LPS stimulates the TLR4 receptor resulting in the activation of NF- $\kappa$ B and STAT1 and in the increase of the production of iNOS leading to the release of pro-inflammatory cytokines (Orihuela et al., 2015). Indeed, in the LPS group, we observed a decrease in the number of ramified and an increase in the number of amoeboid microglia when compared with the control, with significant differences observed at both 24 and 48 hr. BNN20 treatment reduced the number of amoeboid microglia at both time points with significant differences observed at 48hr (Figure 22A, B). To confirm our observations we performed Western blot analysis for iNOS, a specific marker of pro-inflammatory microglia. We observed a low expression of iNOS in our control group, a high expression of iNOS in the LPS group, as expected, while when BNN20 was added together with LPS, the expression of iNOS was decreased compared with the LPS group (Figure 22C, D). Overall, these results indicate that BNN20 holds a direct effect on microglia *in vitro* by reducing their activation and their transition to the pro-inflammatory state upon LPS stimulation.

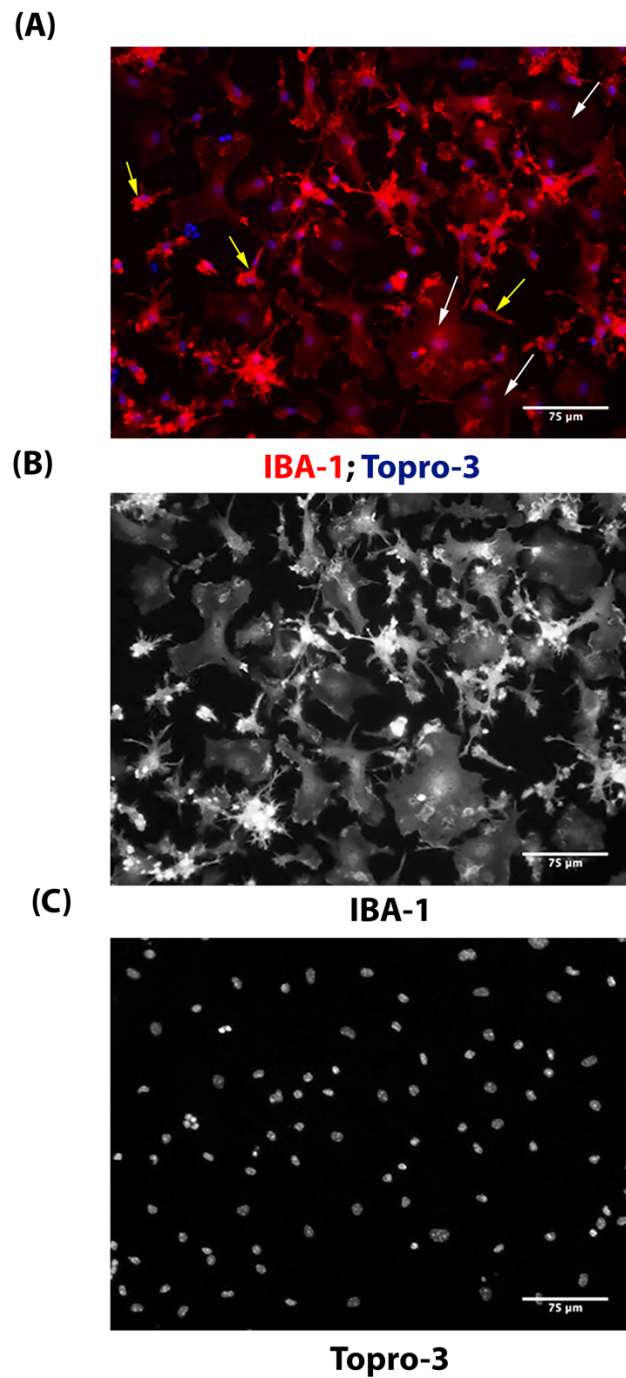


Figure 21: (A-C) Representative immunocytochemical images of primary microglia cells labelled for IBA-1 (red) and Topro-3 (blue), showing both ramified (non-active) and amoeboid (active) microglia cells with yellow and white arrow respectively. Scale bar: 75 $\mu$ m

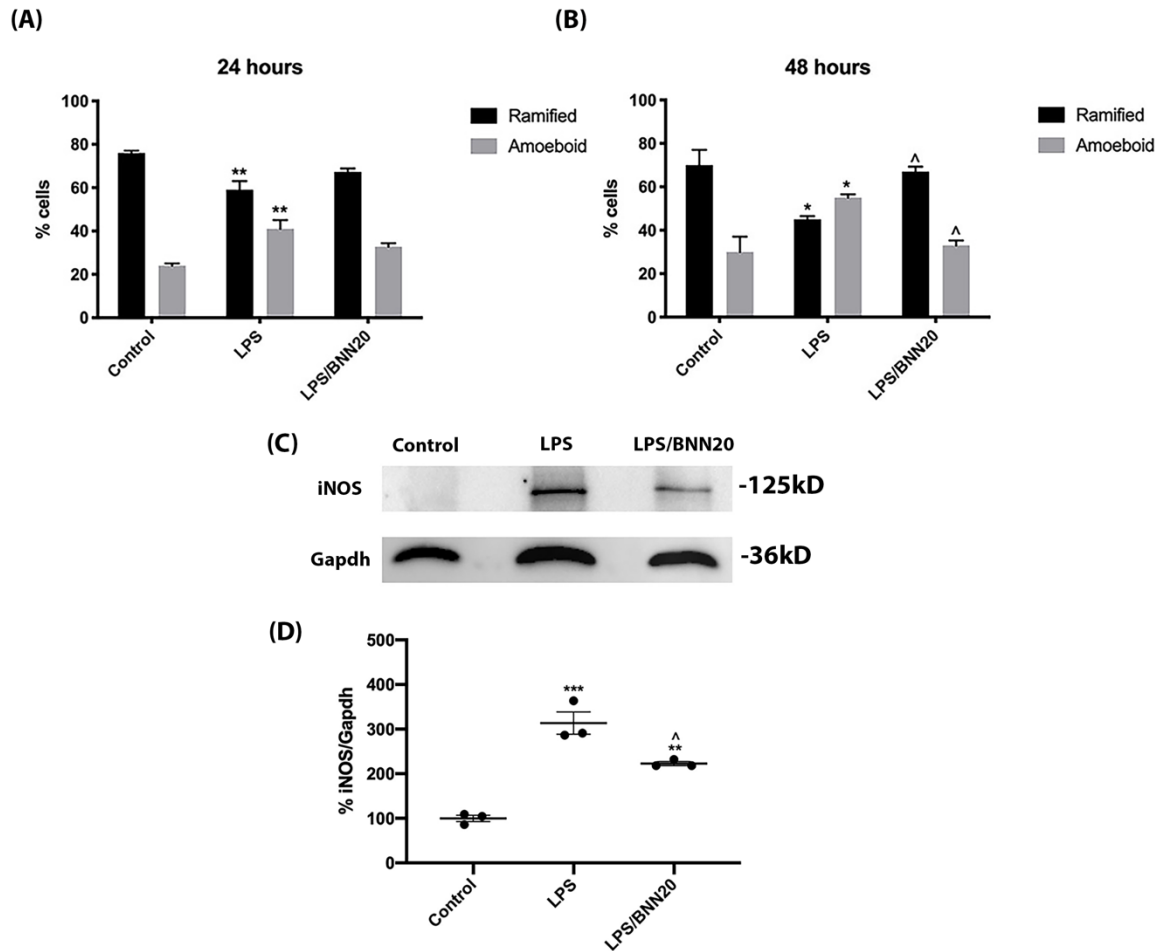


Figure 22: BNN20 reduces microglia activation and transition to their pro-inflammatory state upon LPS stimulation in vitro: (A, B) Quantification of the percentage of IBA-1+ cells showing a specific morphology (ramified/ amoeboid) in control, LPS and LPS/BNN20 treated primary microglia at 24 and 48 hours. Every group of each experiment was in triplicates, while 3 independent experiments were performed. For the statistics, one-way ANOVA with post-hoc Tukey test was used. Data are expressed as mean  $\pm$  SEM. Regarding the statistics of 24 hours treated groups  $F(5, 14) = 73.01$ ,  $p < 0.0001$  and of 48 hours treated groups  $F(5, 12) = 14.43$ ,  $p = 0.0001$ . Comparison with control group: \* $p < 0.05$ ; \*\* $p < 0.01$ . Comparison with LPS group: <sup>^</sup> $p < 0.05$ . (C) Representative Western Blot for iNOS and Gapdh in control, LPS treated and LPS/BNN20 treated primary microglia. (D) Quantification of iNOS/Gapdh protein levels in primary microglia lysates of control, LPS and LPS/BNN20 treated primary microglia. Every group of each experiment was in triplicates, while 3 independent experiments were performed. The intensity of the bands was measured with Fiji Image J software and normalized using Gapdh as loading control. For the statistics, one-way ANOVA with post-hoc Tukey test was used. Data are expressed as mean  $\pm$  SEM. Regarding the statistics  $F(2, 6) = 49.57$ ,  $p = 0.0002$ . Comparison with control group: \*\* $p < 0.01$ ; \*\*\* $p < 0.001$ . Comparison with LPS group: <sup>^</sup> $p < 0.05$ .

### **G.5 BNN20 increases the number of mature OLs even after LPC treatment, while it does not affect the proliferation of OPCs *in vitro***

To study if BNN20 has a direct effect in OLs, we performed *in vitro* experiments by isolating OPCs from P2 mice. First, we investigated if BNN20 affects OPC proliferation. OPCs were cultured for one day in proliferation medium (d1), while at d2 BNN20 was added. At d3 cells were fixed and labelled for the proliferation marker Ki-67 and PDGFRa (Figure 23A, B). Ki-67<sup>+</sup> PDGFRa<sup>+</sup> cells were counted over the total number of untreated and BNN20-treated cells. Our analysis did not reveal any difference between these two groups (Figure 23C), indicating that BNN20 does not affect the proliferation of OPCs *in vitro*. In order to investigate the role of BNN20 in mature OLs, OPCs were cultured for two days (d1-2) with proliferation medium. At d3 proliferation medium was replaced by differentiation medium, while at d4 BNN20 was added. At d5 cells were fixed and immunolabeled for MBP (Figure 23D, E), a marker for mature myelinating OLs. Our analysis showed that BNN20 treatment increased the number of MBP<sup>+</sup> cells compared with the untreated group (Figure 23F). Our results showed that BNN20 has no effect on OPCs, while it is able to increase the number of mature OLs *in vitro* possibly by enhancing their maturation.

After showing that BNN20 increases the number of mature OLs, we treated OL cultures with LPC, which is able to disrupt myelin lipids by inducing cell membrane permeability and thus resulting in mature OL cell death under *in vitro* conditions as well (Fressinaud, 2005; Plemel et al., 2017). For this experiment OPCs were cultured for two days (d1-2) with proliferation medium. At d3 proliferation medium was replaced by differentiation medium, while at d4 LPC or BNN20 or both were added to the medium. At d5, the medium was removed and replaced by normal differentiation medium, while at d6 cells were fixed and immunolabeled for MBP (Figure 23G-I). Our analysis showed that LPC decreased the number of MBP<sup>+</sup> cells, while treatment with BNN20 reversed this reduction (Figure 23J). In order to investigate if BNN20 has a prophylactic role in OLs, we performed Propidium iodide (PI) staining for cell death determination. Our analysis showed that PI<sup>+</sup> cells (which included all types of cells in the culture, OPCs, immature and mature OLs) are increased when treated with LPC compared to the untreated ones and remained increased even when they were treated with BNN20 together with LPC (Figure 23K), suggesting that the restored effect observed after BNN20 addition is because of the ability of this molecule to enhance the maturation of OLs as mentioned above.



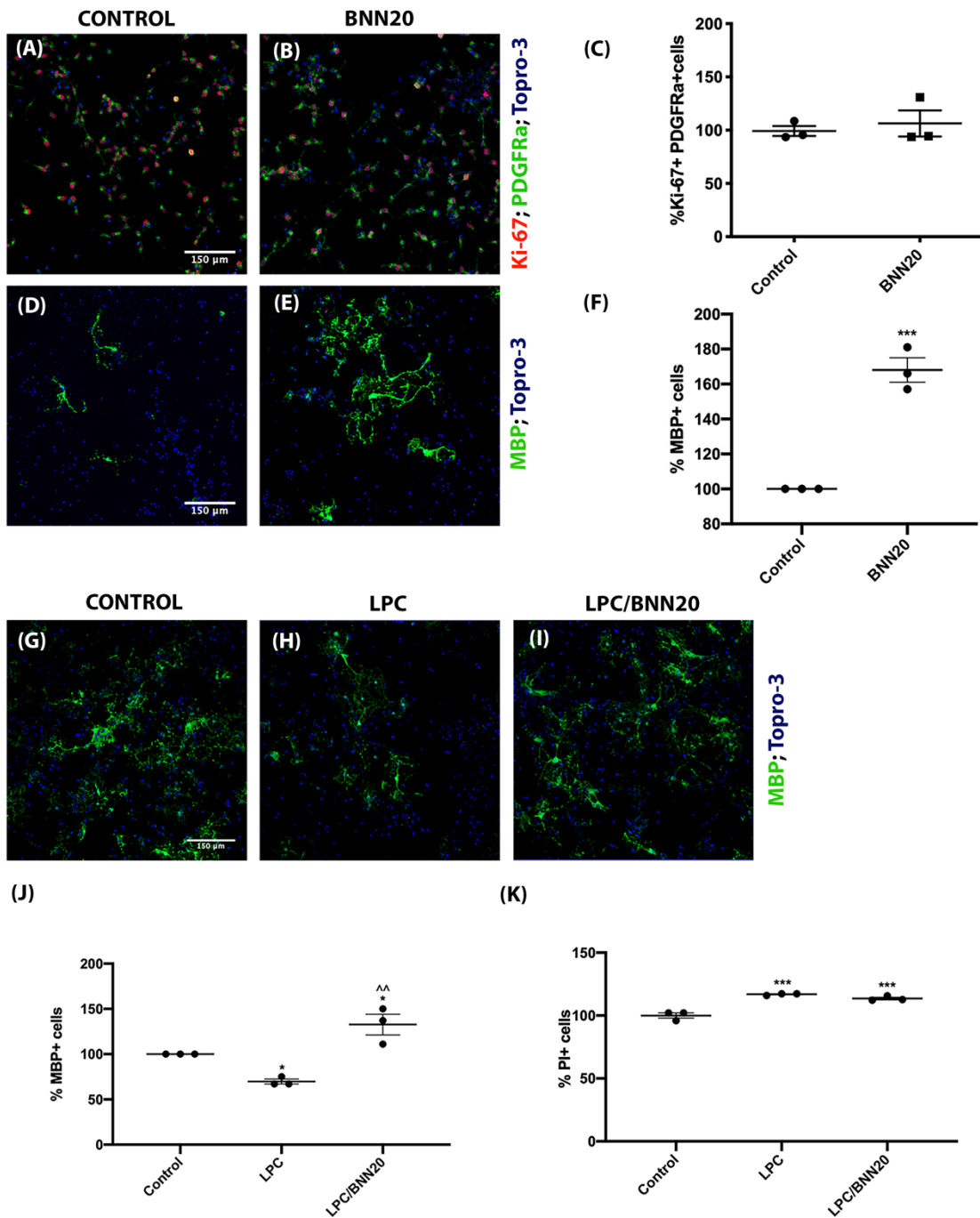


Figure 23: BNN20 increases the number of mature OLs even after LPC treatment, while it does not affect proliferation of OPCs in vitro: (A, B) Representative immunocytochemical images of primary OPCs labelled for Ki-67 (red), PDGFRα (green) and Topro-3 (blue). (C) Quantification of Ki-67+ PDGFRα+ cells over the total number of cells in control and BNN20 treated primary OPCs. Every group of each experiment was in triplicates, while 3 independent experiments were performed. For the statistics, unpaired t-test was used ( $p = 0.2606$ ). Data

are expressed as mean  $\pm$  SEM. (D, E) Representative immunocytochemical images of primary OLs labelled for MBP (green) and Topro-3 (blue). (F) Quantification of MBP<sup>+</sup> cells over the total number of cells in control and BNN20 treated primary OLs. Every group of each experiment was in triplicates, while 3 independent experiments were performed. For the statistics, unpaired *t*-test was used. Data are expressed as mean  $\pm$  SEM. Comparison with control group: \*\*\**p* < 0.001. (G-I) Representative immunocytochemical images of primary OLs labelled for MBP (green) and Topro-3 (blue). (J) Quantification of MBP<sup>+</sup> cells over the total number of cells in control, LPC and LPC/BNN20 treated primary OLs. Every group of each experiment was in triplicates, while 3 independent experiments were performed. For the statistics, one-way ANOVA with post-hoc Tukey test was used. Data are expressed as mean  $\pm$  SEM. Regarding the statistics  $F(2, 6) = 21.49$ ,  $p = 0.0018$ . Comparison with control group: \**p* < 0.05. Comparison with LPC group: ^*p* < 0.01. (K) Quantification of PI<sup>+</sup> cells over the total number of cells in control, LPC and LPC/BNN20 treated primary OLs. Every group of each experiment was in triplicates, while 3 independent experiments were performed. For the statistics, one-way ANOVA with post-hoc Tukey test was used. Data are expressed as mean  $\pm$  SEM. Regarding the statistics  $F(2, 6) = 44.15$ ,  $p = 0.0003$ . Comparison with control group: \*\*\**p* < 0.001. Scale bar in A-B, D-E and G-I: 150 $\mu$ m.

## **G.6 BNN20 increases the number of mature OLs after LPC treatment *in vitro* in a TrkA-dependent manner**

To investigate the molecular mechanism through which BNN20 exerts its beneficial role on mature myelinating OLs *in vitro* and since it was already shown that BNN20 activates p75<sup>NTR</sup>, TrkA and TrkB receptors (Botsakis et al., 2017), we used inhibitors for these receptors. We focused to both TrkA and TrkB receptors, because p75 receptor is mainly inducing cell death signals (Chao, 2003). Moreover, previous studies about the role of BNN27, which is another synthetic neurosteroid in OLs, showed that the absence of p75 receptor did not block the beneficial effect of this molecule (Bonetto et al., 2017). TrkA and TrkB receptors are both expressed in mature OLs (Bonetto et al., 2017; Wong et al., 2014). Our results showed that inhibition of TrkA reduced the number of mature OLs when treated with BNN20, while inhibition of TrkB did not change the beneficial effect of this molecule (Figure 24A-F). To ensure that TrkA and TrkB inhibitors specifically block TrkA and TrkB receptors respectively, we used as positive controls NGF and BDNF. NGF specifically activates TrkA receptor (Minnone et al., 2017), while BDNF specifically activates TrkB receptor (Sasi et al., 2017). It has been previously shown that both neurotrophins have a beneficial role in OLs either through protecting them or through enhancing their maturation (Bonetto et al., 2017; Fletcher et al., 2018). Indeed, addition of NGF or BDNF increased the number of mature OLs in LPC-treated OL primary cultures. Addition of TrkA inhibitor or TrkB inhibitor abolished the beneficial role of NGF and BDNF respectively (Figure 25A-J). Our results indicate that BNN20 increases the number of mature OLs *in vitro*, primarily, in a TrkA-dependent manner.

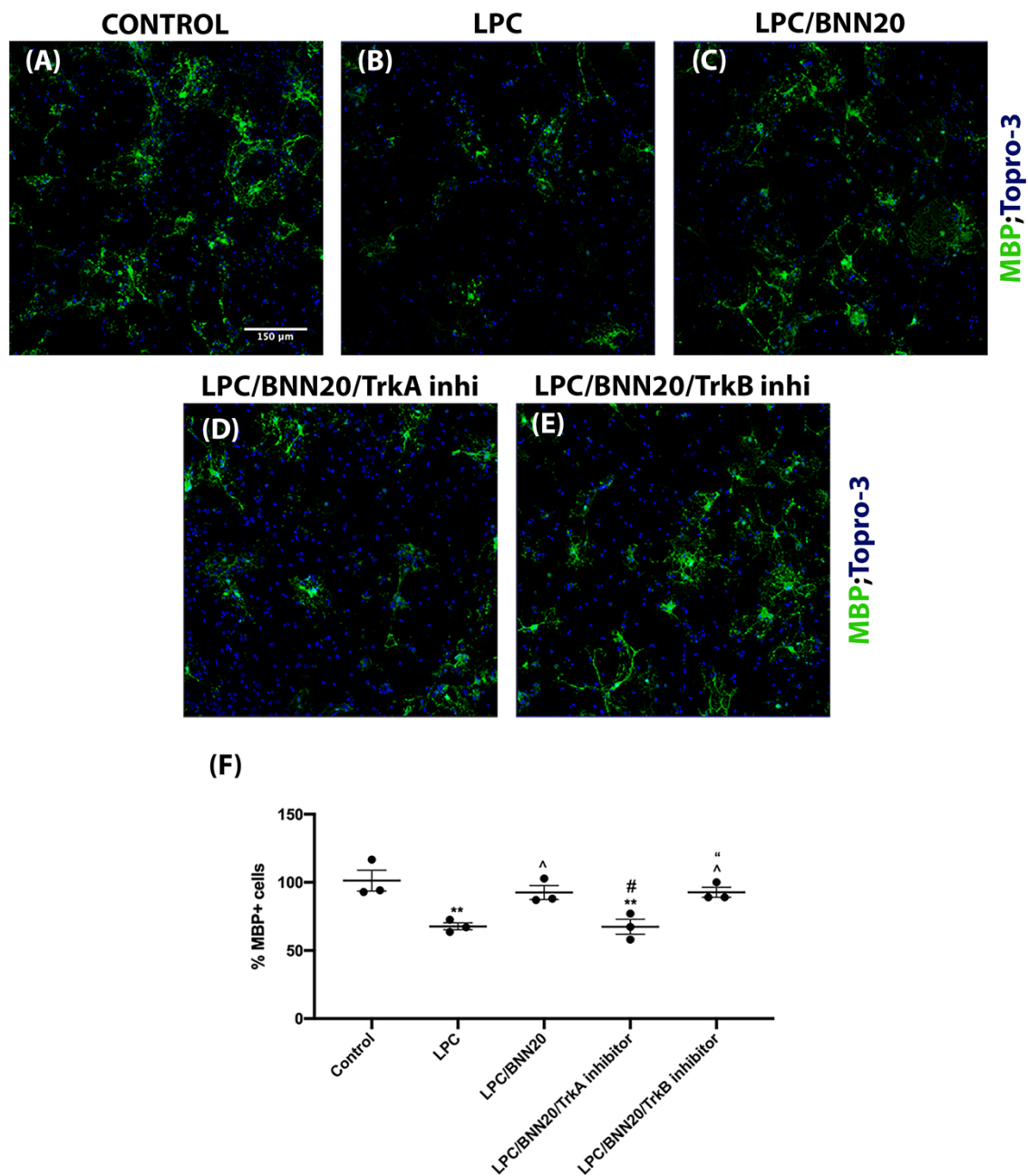
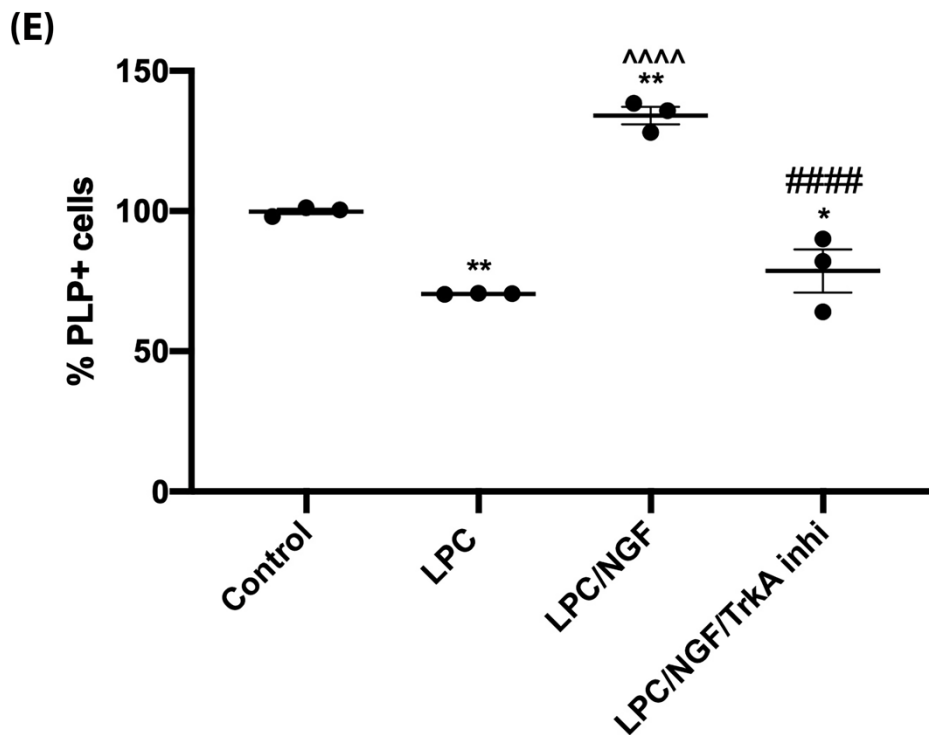
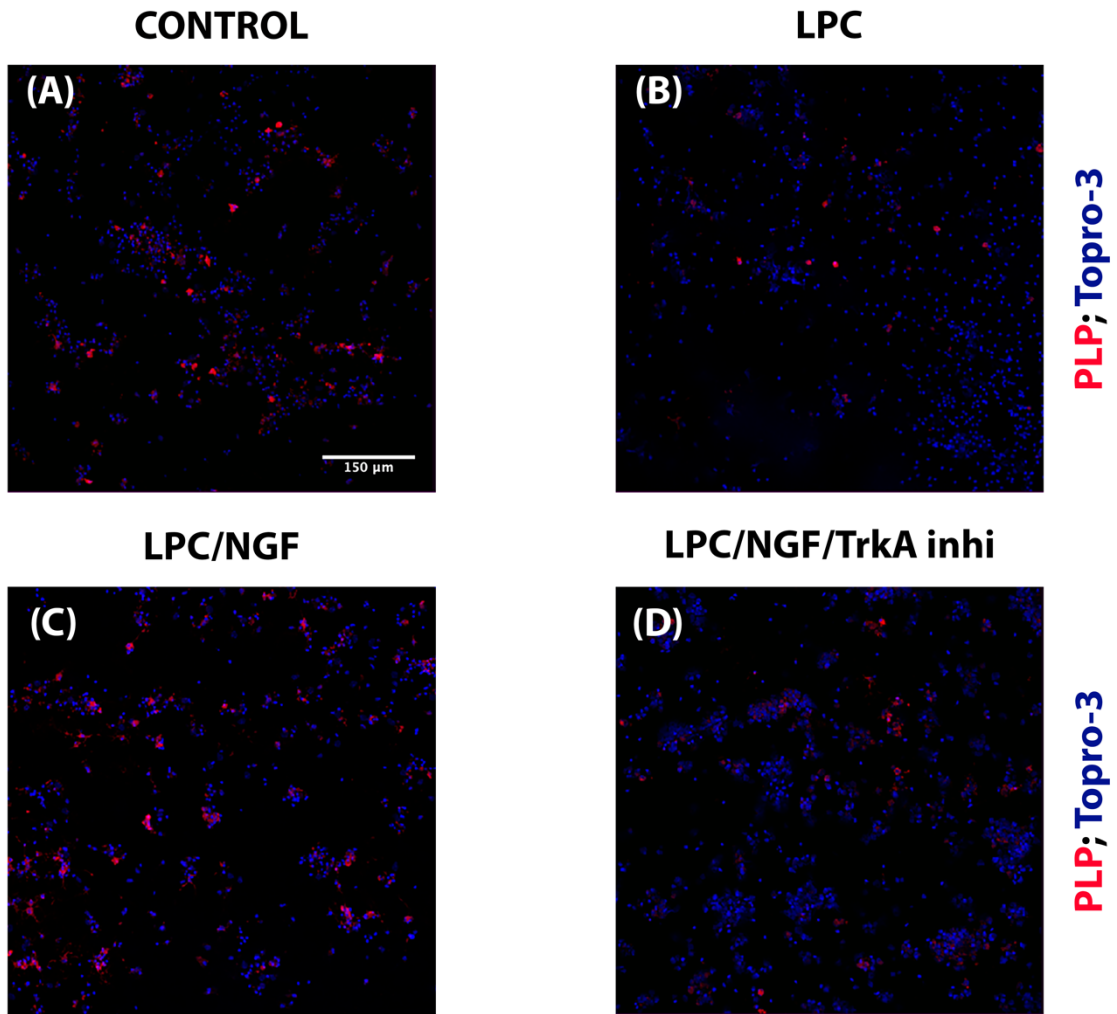


Figure 24: BNN20 increases the number of mature OLs after LPC treatment *in vitro* in a TrkA-dependent manner: (A-E) Representative immunocytochemical images of primary OLs labelled for MBP (green) and Topro-3 (blue). (F) Quantification of MBP+ cells over the total number of cells in control, LPC and LPC/BNN20, LPC/BNN20/TrkA inhibitor and LPC/BNN20/TrkB inhibitor treated primary OLs. Every group of each experiment was in triplicates, while 3 independent experiments were performed. For the statistics, one-way ANOVA with post-hoc Tukey test was used. Data are expressed as mean  $\pm$  SEM. Regarding the statistics  $F(4, 10) = 9.055$ ,  $p = 0.0023$ . Comparison with control group: \*\* $p < 0.01$ . Comparison with LPC group: ^ $p < 0.05$ . Comparison with LPC/BNN20 group: # $p < 0.05$ . Comparison with LPC/BNN20/TrkA inhibitor group: “ $p < 0.05$ . Scale bar in A-E: 150μm.



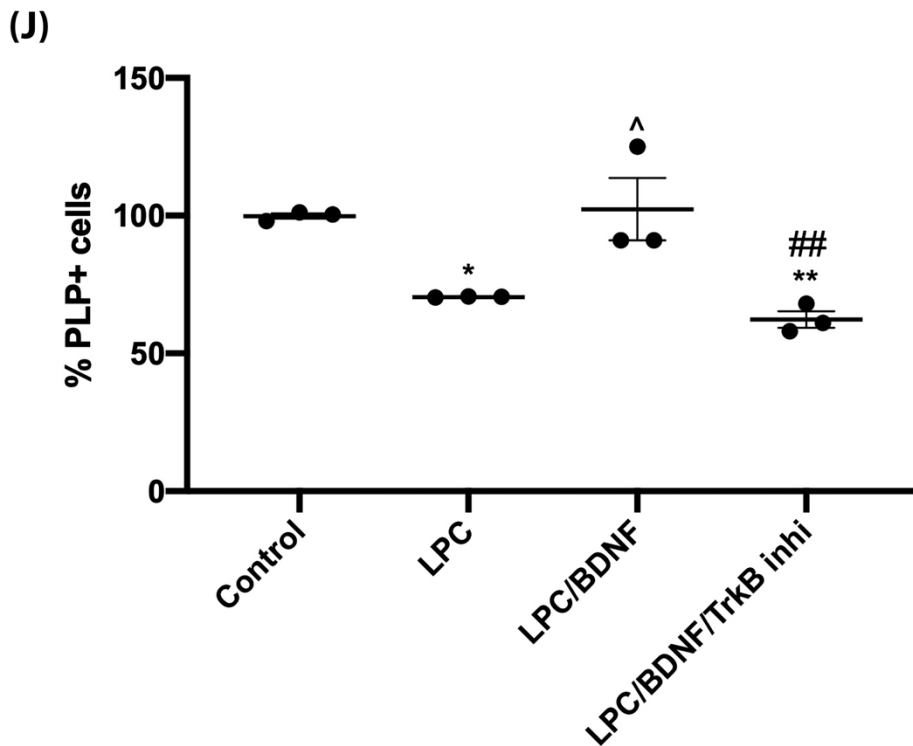
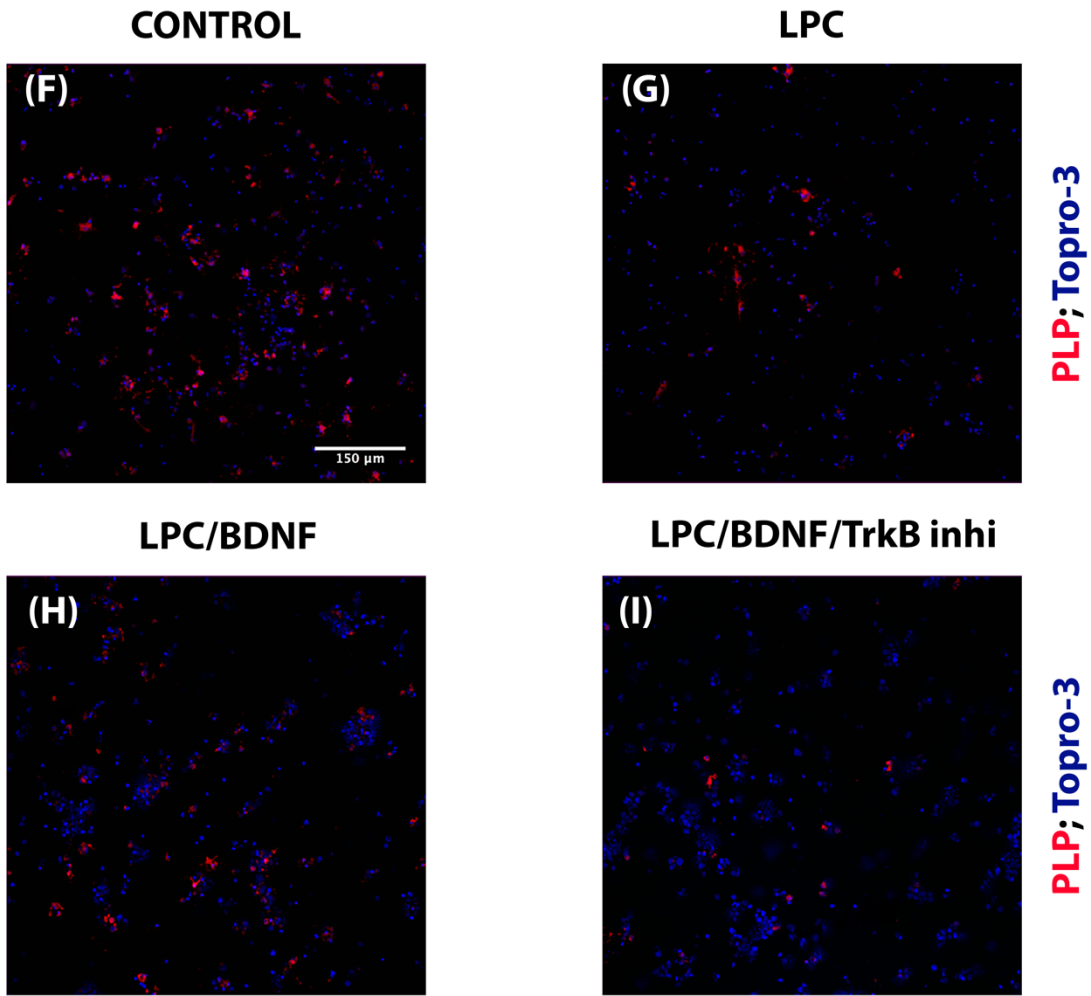


Figure 25: NGF and BDNF increases the number of mature OLs after LPC treatment in vitro, an effect that is abolished by TrkA and TrkB inhibitor respectively: (A-D, F-I) Representative immunocytochemical images of primary OLs labelled for PLP (red) and Topro-3 (blue). (E) Quantification of PLP+ cells over the total number of cells in control, LPC, LPC/NGF and LPC/NGF/TrkA inhibitor treated primary OLs. Every group of each experiment was in triplicates, while 3 independent experiments were performed. For the statistics, one-way ANOVA with post-hoc Tukey test was used. Data are expressed as mean  $\pm$  SEM. Regarding the statistics  $F(3, 8) = 46.12, p < 0.0001$ . Comparison with control group: \* $p < 0.05$ ; \*\* $p < 0.01$ . Comparison with LPC group: ^^^ $p < 0.0001$ . Comparison with LPC/NGF group: ##### $p < 0.0001$ . (J) Quantification of PLP+ cells over the total number of cells in control, LPC, LPC/BDNF and LPC/BDNF/TrkB inhibitor treated primary OLs. Every group of each experiment was in triplicates, while 3 independent experiments were performed. For the statistics, one-way ANOVA with post-hoc Tukey test was used. Data are expressed as mean  $\pm$  SEM. Regarding the statistics  $F(3, 8) = 11.96, p = 0.0025$ . Comparison with control group: \* $p < 0.05$ ; \*\* $p < 0.01$ . Comparison with LPC group: ^ $p < 0.05$ . Comparison with LPC/BDNF group: ## $p < 0.01$ . Scale bar in A-H: 150 $\mu$ m.

## H. RESULTS II

### H.1 Cntn2 gene expression across the brain

As a first step in our study, we focused on the expression of our primary gene of interest, *Cntn2*, across the brain. The relative gene expression data of *Cntn2* across the adult mouse brain, under baseline conditions, showed a lower expression in cerebellum, the diagonal band nucleus, most parts of the hippocampus (dentate gyrus, fasciola cinerea, parasubiculum and Ammon's horn), amygdalar nuclei and cortical amygdalar area, hypothalamus, medial nuclei of the midbrain (interpeduncular nucleus, interfascicular nucleus raphe, rostral linear nucleus raphe) and mainly medial parts of the cerebral cortex not related to the long ascending/descending pathways (prelimbic and infralimbic areas, visual areas, some olfactory areas, temporal association areas, frontal poles, anterior cingulate with surrounding areas). On the contrary, the relative gene expression data of *Cntn2* across the adult mouse brain, under baseline conditions, showed a higher expression in medulla, pons, thalami, most midbrain nuclei, dorsal pallidum, some parts of the hippocampus (presubiculum, indusium griseum) and various parts of the cerebral cortex related to the long ascending/ descending pathways (somatosensory areas, visceral areas), as well as parts of the olfactory areas, gustatory and auditory cortices, entorhinal areas, anterior insula, claustrum and endopiriform nucleus (Figure 26).

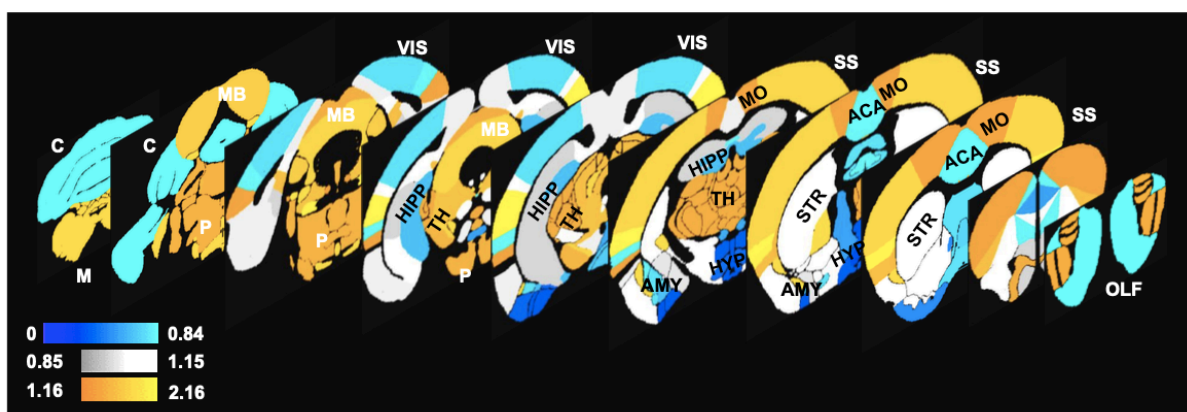


Figure 26: Colormaps of the relative gene expression data of *Cntn2* across the adult mouse brain under baseline conditions. Regions on a shade of blue show a relatively lower expression ( $< 0.85$ ), those on a shade of grey show a gene expression around the global mean ( $0.85-1.15$ ), while those on the orange-yellow scale show a relatively higher expression ( $> 1.15$ ). The first category of brain regions includes cerebellum (C), the diagonal band nucleus, most parts of the hippocampus (HIPP) (dentate gyrus, fasciola cinerea, Ammon's horn, parasubiculum), amygdalar nuclei and cortical amygdalar area (AMY), hypothalamus (HYP), medial nuclei of the midbrain (MB) (interpeduncular nucleus, interfascicular nucleus raphe, rostral linear nucleus raphe) and medial parts of the cerebral cortex like prelimbic and infralimbic areas, visual areas (VIS), some olfactory areas (OLF), temporal association areas, frontal poles, anterior cingulate and surrounding regions (ACA). The second category of brain regions involves the hypothalamic lateral zone, the striatum-like amygdalar nuclei and most other striatal nuclei (STR), periaqueductal grey, ventral tegmental area, red nucleus, parabigeminal

*nucleus and anterior tegmental nucleus from the midbrain, and parts of the cerebral cortex (somatomotor areas [MO], ectorhinal and corticolimbic areas, posterior parietal association areas and the piriform area). Finally, the third category of brain regions includes medulla (M), pons (P), thalami (TH), most midbrain nuclei, dorsal pallidum, some parts of the hippocampus (presubiculum, induseum griseum) and the remaining parts of the cerebral cortex like the somatosensory areas (SS), visceral areas, parts of the olfactory areas, gustatory and auditory cortices, anterior insula, claustrum and endopiriform nucleus. Ten different slices at the coronal level are demonstrated, starting from the most posterior part of the adult mouse brain (Y = 0) in the far left and going progressively to more anterior parts (Y = 10, 100, 135, 170, 200, 250, 300, 350, 400, 450 respectively). The nomenclature of all brain regions can be found in the coronal mouse Allen Brain Atlas (<http://mouse.brain-map.org/static/atlas>). (Kalafatakis et al., 2020)*

## **H.2 Gene identification encoding proteins related to Contactin-2 based on current knowledge**

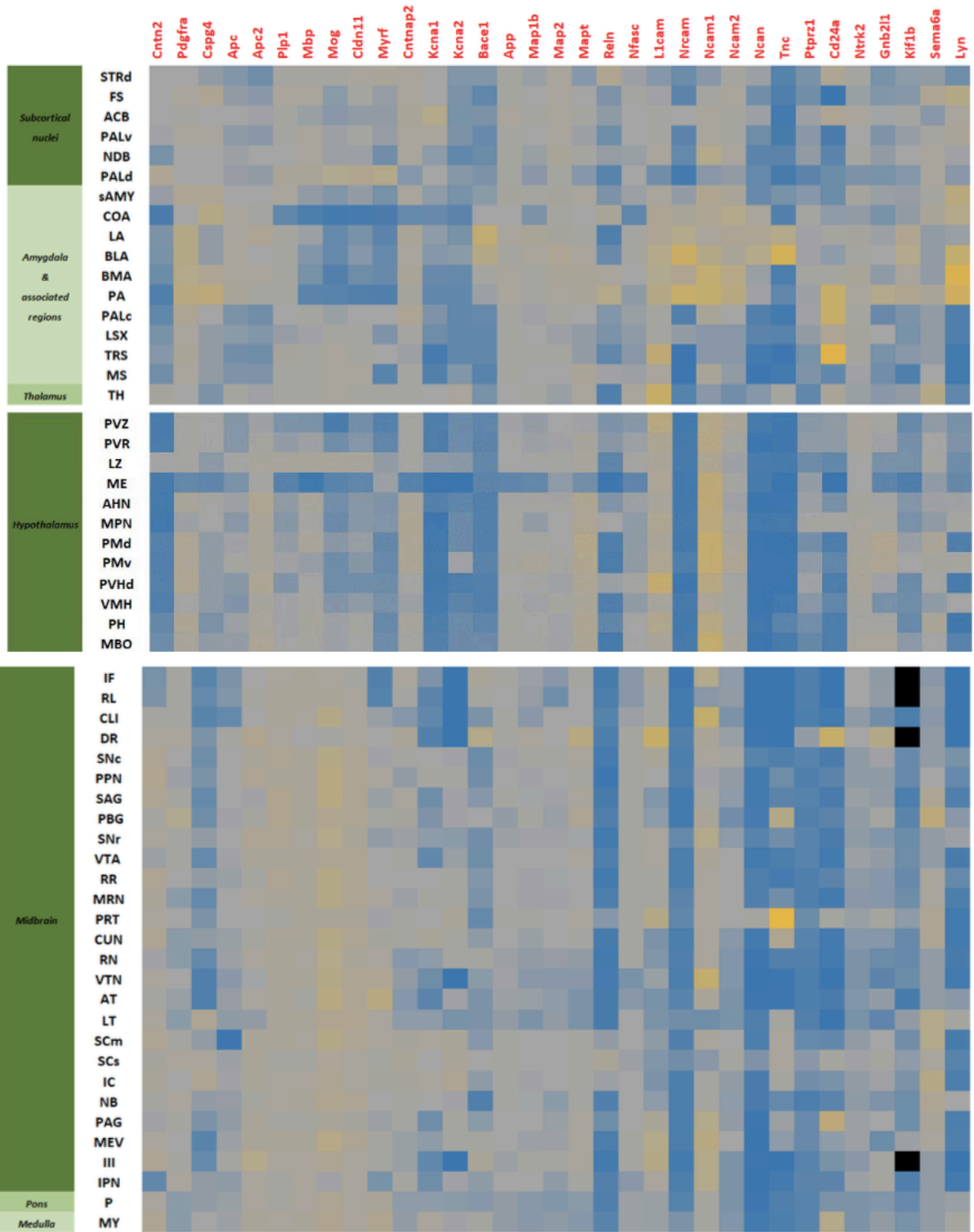
Our next step was to identify genes, whose products are potentially associated with Contactin-2, based on previous experimental studies or the predictions of UniRed. Through these methods, we identified 23 genes (Table 2), including the tyrosine-protein kinase Lyn (involved in signal transduction related to Contactin-2) (Kasahara et al., 2002), beta-secretase 1 (Bace1, which cleaves Contactin-2 to soluble forms) (Gautam et al., 2014), Contactin-associated protein-like 2 (Cntnap2, which interacts with Contactin-2) (Poliak et al., 2003; Traka et al., 2003), potassium channels (Kcna1 and Kcna2, regulated by Contactin-2) (Traka et al., 2003; Savvaki et al., 2008), various cell adhesion molecules found in neurons or extracellular matrix glycoproteins which might interact with Contactin-2 (L1cam, Nrcam, Ncam1, Ncam2, Ncan, Tnc, Reln) (Karagogeos, 2003; UniRed), phosphacan (Ptporz1, particularly expressed in remyelinating oligodendrocytes) (Milev et al., 1996), receptor for activated C kinase 1 (Gnb2l1, also involved in Contactin-2 related signaling) (Yan et al., 2016), amyloid precursor protein (App, which binds to Contactin-2) (Ma et al., 2008), markers of cytoskeletal homeostasis, which stabilize microtubules and promote axonal transport (like Map1b, Map2, Mapt), kinesin-like protein (Kif1b, essential for the transport of materials within cells, and also involved in apoptosis, interacts with Contactin-2) and signal transducer Cd24a (which possibly interacts with Contactin-2) (Lieberoth et al., 2009), the target receptor of brain-derived neurotrophic factor Trk-B (Ntrk2) (Savvaki et al., unpublished data), Semaphorin 6A (Sema6a, a transmembrane protein expressed in developing neural tissue, required for proper development of the thalamocortical projection) (UniRed), and finally neurofascin (Nfasc, an L1 family immunoglobulin cell adhesion molecule involved in axon subcellular targeting and synapse formation during neural development) (Hadas et al., 2013).

Moreover, given the fact that there is a functional relationship between Contactin-2 and myelinated axons (Traka et al., 2003; Poliak et al., 2003) in the adult mouse brain, we wondered whether there is a genomic association between the expression of Contactin-2 and markers of oligodendrocytes at various stages of their maturation (Fancy et al., 2011); either immature (Pdgfra, Cspg4), or mature, non-specific (Apc, Apc2, which are also expressed in neurons) (Brakeman et al. 1999), or specific for that cell type, pre- and myelinating oligodendrocytes



(Plp1, Myrf, Mbp, Mog, Cldn11). The relative expression intensity of all 33 genes identified (including Cntn2) in the grey matter of each of the 95 mouse brain regions is presented in the form of a color heatmap in Figure 27.





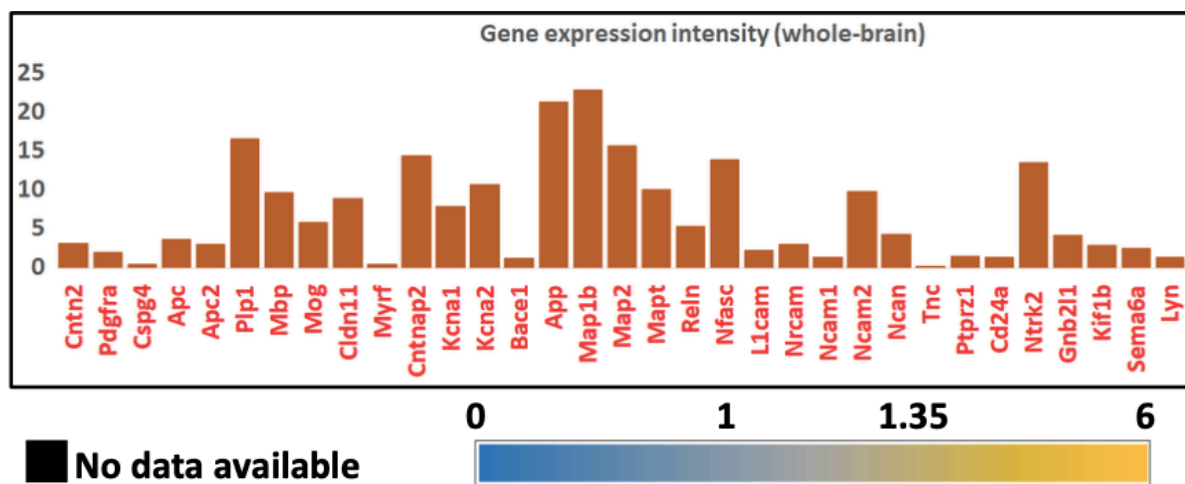


Figure 27: Heatmaps of the relative expression intensities (ranging from 0 to 6) of the 33 genes of interest (Cntn2 included) across 95 grey matter regions of the adult mouse brain. To acquire the relative gene expression value, raw data per brain region have been normalized based on the mean expression intensity of the corresponding gene at the whole brain level (shown inside the black frame). Abbreviations of brain regions have been adopted from the Allen Brain Atlas nomenclature (<http://mouse.brainmap.org/static/atlas>) and are also listed in Table 3. Abbreviations of the genes have been adopted from mouse genome informatics (<http://www.informatics.jax.org/>) and are also explained in Table 2. Blue color indicates gene expression close to zero, while lighter shades of blue indicate relative gene expressions below the corresponding global (whole brain) average (i.e. below 1). Shades of grey indicate relative gene expressions between 1 and 1.35, while greater values are expressed as shades of yellow. The brighter the yellow color the higher the value (maximum value 6). (Kalafatakis et al., 2020)

### H.3 Cntn2 genomic spatial correlation analysis with the 23 genes, whose products interact functionally or structurally with Contactin-2

After collecting all the data regarding the expression of the 32 genes of interest across the brain, we wondered if there was a spatial correlation of their relative expression values between them and Cntn2. The across-brain correlation analysis on the gene expression intensities between Cntn2 and the first 23 genes of interest of the adult mouse brain showed a positive spatial correlation for Cntn2 with 5 of them, and a negative spatial correlation for Cntn2 with another 4. In particular, the spatial patterns of the relative gene expression of Bace1, Kcna1 and Kcna2 show a strong correlation with the corresponding spatial pattern of Cntn2, while the spatial patterns of the relative gene expression of App and Nfasc show a lesser but also significant correlation with that of Cntn2. On the contrary, the spatial pattern of the relative gene expression of L1cam, Ncam1, Ncam2 and Ptprrz1 are strongly anticorrelated with that of Cntn2 (Table 4).

Cntn2								
Gene	r	Sig.	Gene	r	Sig.	Gene	r	Sig.
<i>Lyn</i>	0,059	0,57	<i>Ncam2</i>	-0,270	0,01	<i>Map2</i>	-0,008	0,94
<i>Bace1</i>	0,299	0,00	<i>Ncan</i>	0,023	0,82	<i>Mapt</i>	-0,077	0,46
<i>Cntnap2</i>	0,037	0,72	<i>Ptprz1</i>	-0,281	0,01	<i>Kif1b</i>	-0,084	0,43
<i>Kcna1</i>	0,599	0,00	<i>Tnc</i>	0,092	0,37	<i>Cd24a</i>	-0,058	0,57
<i>Kcna2</i>	0,428	0,00	<i>Gnb2l1</i>	-0,159	0,12	<i>Ntrk2</i>	0,148	0,15
<i>L1cam</i>	-0,252	0,01	<i>App</i>	0,212	0,04	<i>Sema6a</i>	0,167	0,11
<i>Nrcam</i>	-0,057	0,58	<i>Reln</i>	-0,095	0,36	<i>Nfasc</i>	0,215	0,04
<i>Ncam1</i>	-0,322	0,00	<i>Map1b</i>	0,170	0,10			

Table 4: Spatial correlations of *Cntn2* gene expression across the adult mouse brain with other genes, whose products have been (functionally or structurally) related to *Tag-1/Contactin-2*. Among the 23 genes of interest, 9 have been found to strongly correlate with *Cntn2*. The gene expressions of *Bace1*, *Kcna1*, *Kcna2*, *App* and *Nfasc* have a positive spatial association with that of *Cntn2* (green color), while the gene expressions of *L1cam*, *Ncam1*, *Ncam2* and *Ptprz1* have a negative spatial association with that of *Cntn2* (pink color). For further details on the nomenclature of the various genes, please refer to Table 2. (*r*: Spearman correlation coefficient, *Sig.*: level of significance) (Kalafatakis et al., 2020)

#### H.4 *Cntn2* genomic spatial correlation analysis with markers of oligodendrocytes

The myelination process begins when a pool of immature oligodendrocyte precursor cells is differentiated to mature pre-myelinating oligodendrocytes that eventually form myelin sheaths around multiple neurons. During all the stages of this process, oligodendrocytes express a variety of proteins, which constitute maturation stage-dependent markers, either specific for that cell type or not. For example, OPCs express *Cspg4* and *Pdgfra*, while mature oligodendrocytes express *Plp1*, *Mbp*, *Mog*, *Cldn11* and *Myrf*. *Apc* isoforms (*Apc*, *Apc2*) are expressed by both mature oligodendrocytes and neurons. The across-brain correlation analysis on the relative gene expression intensities between *Cntn2* and the 9 markers of oligodendrocyte physiology of the adult mouse brain showed a negative genomic spatial correlation for *Cntn2* with the two markers of immature oligodendrocytes (*Pdgfra*, *Cspg4*), no correlation between *Cntn2* and the non-specific markers of mature oligodendrocytes (*Apc*, *Apc2*), and a very strong positive correlation of *Cntn2* with all specific markers of mature oligodendrocytes (*Plp1*, *Myrf*, *Mbp*, *Mog*, *Cldn11*) (Figure 28).

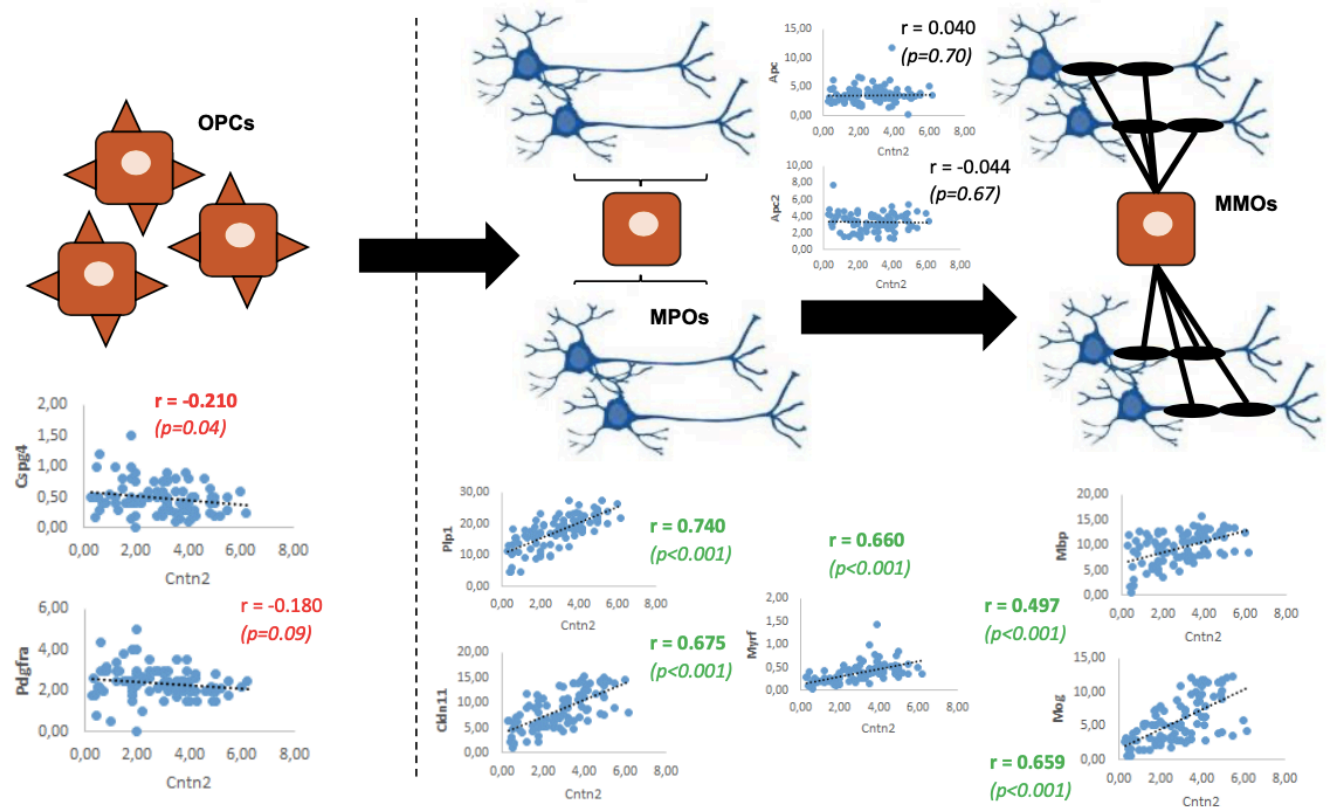


Figure 28: Spatial correlation of *Cntn2* gene expression across the adult mouse brain with genes related to immature and mature oligodendrocytes. The pattern of the gene expression intensity of *Cntn2* across the adult mouse brain is negatively correlated with the markers of OPCs and positively with the specific markers of mature oligodendrocytes. No correlation exists between *Cntn2* and *Apc* (or *Apc2*). Abbreviations of the genes have been adopted from mouse genome informatics (<http://www.informatics.jax.org/>) and are also explained in Table 2. (MMOs: mature myelinating oligodendrocytes, MPOs: pre-myelinating oligodendrocytes, OPCs: oligodendrocyte progenitor cells,  $r$  = Spearman correlation coefficient) (Kalafatakis et al., 2020)

## H.5 Expression of genes spatially correlated or anti-correlated with *Cntn2* among different brain cell populations

After finding a spatial correlation of 10 genes of interest and a spatial anti-correlation of 6 genes of interest with *Cntn2*, we investigated which brain cell populations (oligodendrocytes, OPCs, neurons, astrocytes, Bergmann glial cells, brain pericytes, endothelial cells, macrophages and microglia) preferably express these genes, by utilizing the relevant data from Tabula Muris. Median values were chosen over mean values with standard deviations to reduce the variance of the results. *Cntn2*, as expected, is mainly expressed by oligodendrocytes (it is also expressed by neurons but at much lower levels). Apart from *Kcna2*, oligodendrocytes are the brain cell type with the highest median value for expressing all other genes of interest, which share a similar spatial expression pattern with *Cntn2*, and for which data were available to retrieve from Tabula Muris. *Kcna2* on the contrary is mainly expressed in neurons and to a

much lesser degree in Bergmann glial cells (Figure 29A). All genes of interest, which have an opposing spatial expression pattern from *Cntn2*, and for which data were available to retrieve from Tabula Muris, show the highest median expression values in OPCs compared to the other brain cell types (Figure 29B).

Median expression of **Cntn2** among different brain cell types

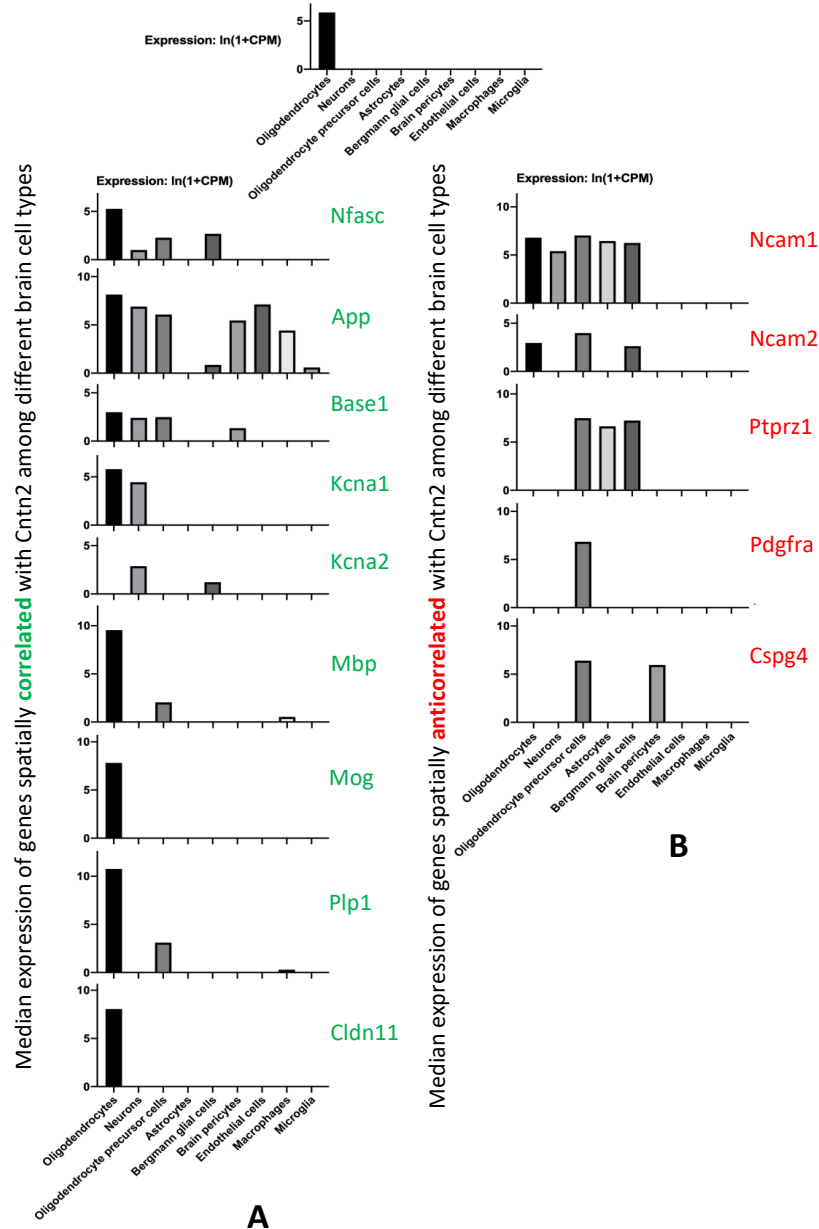


Figure 29: Expression of *Cntn2*, and genes spatially correlated (A) and anticorrelated (B) with *Cntn2* among different brain cell populations. Data were retrieved from Tabula Muris (<https://tabula-muris.ds.czbiohub.org>) using the median values. (Kalafatakis et al., 2020)

## I. DISCUSSION I

In this study, we investigated the putative role of BNN20 in de- and re-myelination using *in vivo* and *in vitro* approaches. We showed that the synthetic steroidal microneurotrophin BNN20, a chemical analogue of DHEA, reduces myelin loss, increases the number of mature OLs and decreases astrogliosis in the lesion site of LPC-induced demyelination mouse model, leading to faster remyelination. Furthermore, our results showed that BNN20 enhances maturation of OLs *in vitro*, counteracting the detrimental effects of LPC treatment in a TrkA-dependent manner. Finally, BNN20 decreases the activation and transition of microglia to their pro-inflammatory state upon LPS stimulation *in vitro*. These results suggest that BNN20 could be potentially used as a lead molecule for the development of BBB-permeable agents with clinical applications in the treatment of demyelinating diseases, such as MS.

According to the literature the neurosteroid DHEA presents similar beneficial effects with neurotrophins acting through their receptors (Lazaridis et al., 2011, Padiaditakis et al., 2015). Although this steroid is able to cross the BBB, it exerts important endocrine side effects limiting its therapeutic potential (Calogeropoulou et al., 2009; Compagnone and Mellon, 2000). To bypass the limitations of DHEA regarding its putative clinical application, we synthesized DHEA derivatives, that were chemically modified (C-17 substitutions) blocking their interaction with the classical steroid receptors and avoiding their interaction with metabolizing enzymes of DHEA (Calogeropoulou et al., 2009). These molecules, called BNNs or microneurotrophins (MNT), could still cross the BBB due to their small size and sustained the ability of DHEA to interact with Trk and p75 receptors leading to the activation of their downstream pathways (Padiaditakis et al., 2016a, 2016b). The most promising BNNs have been implicated in different studies regarding their role in neurodegeneration. For example, BNN27, a DHEA analog with strong neuroprotective effects acting through TrkA and p75 receptors (Padiaditakis et al., 2016a), was shown to decrease the loss of motor neurons when co-cultured with astrocytes derived from Amyotrophic Lateral Sclerosis (ALS) patients (Glajch et al., 2016). Additionally, BNN27 was shown to have anti-apoptotic and anti-inflammatory properties in rat streptozotocin (STZ)- model of diabetic retinopathy. More specifically, regarding the anti-apoptotic properties of BNN27 it was shown that administration of this molecule reduced the activation of Caspase 3, while regarding its anti-inflammatory properties it was shown that BNN27 reduced the pro-inflammatory (TNF $\alpha$ , IL-1) and increased the anti-inflammatory (IL-1-, IL-4) cytokine levels (Ibán-Arias et al., 2017). Moreover, recent studies showed that this microneurotrophin is able to affect locomotion, progesterone, and testosterone levels, as well as the glutamatergic and GABAergic systems of the hippocampus and prefrontal cortex in a sex-dependent way (Kokras et al., 2020). Furthermore, previous studies from our research group showed that BNN27 protects mature oligodendrocytes in cuprizone-induced demyelination mouse model, reduces accumulation of astrocytes and



microglia in the lesion sites, resulting in a decreased level of demyelination without a beneficial role during remyelination. *In vitro* studies showed that BNN27 protects OLs in a TrkA dependent manner, while it reduces activation of microglia upon LPS stimulation (Bonetto et al., 2017).

BNN20 is another DHEA derivative which according to previous studies binds and activates not only TrkA and p75<sup>NTR</sup> like BNN27, but also TrkB. More specifically, BNN20 was able to stimulate the tyrosine phosphorylation of TrkA and TrkB in CHO cell lines transfected with TrkA and TrkB plasmid respectively, while it was also able to induce the association of p75<sup>NTR</sup> with its effector RIP2 in transfected HEK293 cells. In this study, it was shown that BNN20 protects dopaminergic neurons, possibly, through TrkB-PI3K-Akt-NF- $\kappa$ B signaling pathway in the weaver mouse mutant, a mouse model for Parkinson's disease (Botsakis et al., 2017). Moreover, it was also shown that this compound exerts strong anti-inflammatory activity and restores BDNF levels in this specific mouse model. More specifically, BNN20 reversed microglia hyperactivation, observed in the "untreated" weaver mouse and induced a shift in microglia polarization towards the neuroprotective M2 phenotype, suggesting a possible beneficial shifting of microglia activity (Panagiotakopoulou et al., 2020).

In the present study we investigated the action of BNN20 on glial populations under de- and re-myelinating conditions using *in vivo* (LPC-induced demyelination) and *in vitro* approaches (primary OLs and microglia cultures). LPC is a membrane-dissolving chemical injected in the white matter of CNS inducing focal demyelination. Injection with this chemical leads to rapid loss of myelin and mature OLs, while there is OPC recruitment and accumulation of astrocytes and microglia/macrophages in the lesion site. Demyelination occurs rapidly (2-3 dpi), while remyelination starts after 10-14 days dpi. After 30 dpi remyelination is complete (Blakemore and Franklin, 2008).

BNN20 treatment reduced demyelination and increased the number of mature OLs in the lesion area of the LPC-induced demyelination model. Our *in vitro* experiments showed that BNN20 acts directly on OLs by enhancing their maturation and increasing the number of mature myelinating OLs even after they were treated with LPC. No effect was observed regarding OPC proliferation. Our results showed that this differentiation-promoting effect of BNN20 is mediated through the TrkA receptor.

OLs are responsible for myelin production in the CNS (Grinspan, 2002). Under demyelinating conditions like in MS, myelin is disrupted leading to OL loss and neurodegeneration. Remyelination acts as a repair process and involves the recruitment of OPCs at the lesion site and their differentiation to mature myelinating OLs. However, remyelination is insufficient in most cases, since either not enough OPCs are present in the lesion area or the OPCs that are recruited do not differentiate in mature myelinating OLs (D'Amico et al., 2016; Ontaneda et al., 2015). The promotion of OPC proliferation or/and their differentiation could be a step

towards a more efficient restoration of myelin. Our results propose a beneficial role of BNN20 regarding OL differentiation and maturation without an obvious effect on OPC proliferation.

Another important therapeutic aim in demyelinating diseases like MS is to find ways to decrease inflammation. In our study, BNN20 decreases astrogliosis *in vivo*, while it reduces activation of pro-inflammatory microglia indicating reduction of inflammation *in vitro*, without significantly affecting the accumulation of microglia/macrophages in the LPC model. The inability to observe a change in microglia activation *in vivo* probably arises from the fact that in the lesion site of the LPC-injected animals there is also infiltration of macrophages sharing the same antigenic markers (like IBA-1 used in our experiments) and the same morphology as microglia. Our observation is also in accordance with recent studies suggesting an anti-inflammatory and protective role of BNN20 in the advanced dopaminergic neurodegeneration of the Weaver mutant mouse. In this study, BNN20 reduced the activation of pro-inflammatory microglia inducing a shift in microglia polarization towards the anti-inflammatory, neuroprotective phenotype as mentioned above (Panagiotakopoulou et al., 2020).

Under normal conditions, microglia are characterized by ramified processes and their role is to “scan” CNS for any possible threats. Upon CNS injury, these cells are activated changing from a ramified to an amoeboid morphology. The activated microglia can be either pro-inflammatory secreting factors like IL-1, IL-12, IL-23, TNF $\alpha$  and iNOS promoting inflammation and cytotoxicity or anti-inflammatory secreting factors like IL-4, IL-10, IL-13, TGF $\beta$  and Arg1 reducing inflammation and promoting a neuroprotective response (Gordon and Taylor, 2005; Colton, 2009). Generally, microglia shift functions to retain tissue homeostasis influenced by the environment (Orihuela et al., 2015). In demyelinating conditions pro-inflammatory microglia promote inflammation, neurodegeneration and OLs loss, while anti-inflammatory microglia are associated with remyelination by promoting OPC differentiation through their secreted factors (Miron et al., 2013). Microglia are also responsible for myelin debris clearance, which is a crucial process for remyelination (Jurevics et al., 2002; Olah et al., 2012). Future experiments could focus in the LPC *in vivo* model, investigating if BNN20 alters the expression of specific microglia factors, like for example iNOS, TNF $\alpha$ , IL-1, TGF $\beta$ , IL-4 or IL-10.

Under normal conditions, astrocytes participate in a number of important physiological functions, like the maintenance of the BBB integrity, the regulation of axonal outgrowth and myelination (Kiray et al., 2016) and the formation of intracellular communication networks (Kimelberg and Nedergaard, 2010; Volterra and Meldolesi, 2005). Upon CNS injury, astrocytes are activated (Sofroniew and Vinters, 2010) leading to changes in morphology, increased expression of GFAP, proliferation and secretion of pro-inflammatory factors, which result in cell death of OLs and neurons (Jensen et al., 2013; Pekny et al., 2016). Reactive

astrocytes are responsible for the glial scar formation (Nash et al., 2011) and according to the literature they can have detrimental effects regarding OL differentiation, regeneration and remyelination (Silver and Miller, 2004).

In our study, BNN20 reduced the activation of astrocytes *in vivo*, while it decreased the activation of pro-inflammatory microglia, proposing reduction of inflammation *in vitro*. We suggested that this reduction of inflammation leads to reduced OLs loss and in combination with the direct effect of BNN20 through TrkA receptor in promoting OLs differentiation, leads to the increased number of mature OLs in the LPC-induced demyelination mouse model. These effects could explain the tendency for reduced numbers of OPCs observed during demyelination (10dpi) in the LPC-injected animals, treated with BNN20. The increased number of mature OLs could explain the decreased myelin loss observed during demyelination and the enhanced remyelination at 15 days post LPC injection, observed in BNN20 treated animals. Meanwhile, we cannot exclude the possibility of an indirect effect of BNN20 in OLs through other cell populations, like astrocytes or microglia, which could be TrkA or/and TrkB mediated since it is already known that BNN20 activates both receptors (Botsakis et al., 2017). Indeed, astrocytes and microglia express both neurotrophin receptors (Climent et al., 2000; Fodelianaki et al., 2019; Miao et al., 2018; Ruiz-Eddera et al., 2003). It is of note that microglial inflammation is reduced through activation of both TrkA or TrkB receptors. More specific, minocycline promotes M2 microglia polarization through upregulation of TrkB/BDNF pathway (Miao et al., 2018), apelin-13 suppresses neuroinflammation (microglia and astrocyte activation) through TrkB/BDNF pathway in a Streptozotocin-Induced rat model of Alzheimer's Disease (Luo et al., 2019), while DHEA reduces microglia mediated inflammation through activation of TrkA pathway (Alexaki et al., 2018). Future studies will focus on the mechanism through which BNN20 acts in microglia and on investigating if BNN20 affects astrocytes directly. Additionally, we could also investigate if BNN20 is able to change the expression of specific factors, secreted by astrocytes.

In conclusion, our results suggest that BNN20 could serve as a lead molecule to develop in the future, BBB-permeable synthetic agonists of neurotrophin receptors that could reduce inflammation and increase the number of OLs by promoting their differentiation/maturation. Such molecules could be tested to investigate their potential beneficial actions on glial populations and neurons together and could prove effective in demyelinating and neurodegenerative diseases.

## J. DISCUSSION II

The massive AGEA of the adult mouse brain, alone or in combination with other relevant, complementary data sources such as Tabula Muris, can be carefully interrogated (in a targeted, prior knowledge-driven manner) to confirm or question some of our views on mouse brain physiology and reveal new domains of potential neuroscientific interest for future translational research. According to the data presented in this study, and in accordance with our current understanding on the relationship between Contactin-2 and myelin physiology (Karagogeos, 2003; Paz Soldán and Pirko, 2012; Zoupi et al., 2011), the expression of Contactin-2 mainly follows the myelinated pathways of the central nervous system. More specific, this observation is supported firstly by the neuroanatomical distribution of the regions with the higher Cntn2 expression intensities, involving pathways controlling sensory processing and executive control functions, characterized by an increased degree of myelination, secondly by the fact that Cntn2 is mainly expressed by mature oligodendrocytes, and thirdly by the strong spatial genomic association between Cntn2 and specific markers of mature oligodendrocytes. This last observation is in accordance with previous studies that showed that the expression of the transcription factor Myrf positively regulates the expression of Contactin-2 as well as the expression of myelin genes and oligodendrocyte markers like MBP, PLP and MOG (Koenning et al., 2012). Moreover, the negative spatial association between the gene expressions of Cntn2 and markers of premature oligodendrocytes is in accordance with recent findings from our team showing that Contactin-2 is expressed only in mature oligodendrocytes and not in oligodendrocyte progenitor cells (Zoupi et al., 2018).

The fact that Contactin-2 plays a crucial role in the adult mammalian brain by ensuring the integrity, as well as proper function, of myelinated fibers is further supported by the close spatial genomic association of Cntn2 with Kcna1, Kcna2, and Nfasc. The relationship of Contactin-2 with Kcna1 and Kcna2, i.e. the genes that encode the voltage-gated potassium channels Kv1.1 and Kv1.2, confirms the importance of the co-presence of these biomolecules in exerting their physiological role. These potassium channels are found at the axonal initial segment and juxtaparanodes of myelinated fibers, modulating the action potential initiation and frequency (Pinatel et al., 2017; Traka et al., 2002). Contactin-2 also localizes at the juxtaparanodes (Traka et al., 2002) and, according to previous experimental findings, interacts with these potassium channels and Caspr2 forming a complex which is crucial for the axonal-glial interactions and for the proper function of myelinated fibers. Absence of Contactin-2 results in an impaired juxtaparanodal localization of Kv1.1/1.2 and Caspr2 as they diffuse into the internode (Traka et al., 2003; Savvaki et al., 2008). In particular, glial Contactin-2 is able to rescue this phenotype (Savvaki et al., 2010).

Moreover, the genomic relationship between Contactin-2 and Neurofascin shown in this work is in accordance with other sources of experimental evidence supporting their biological relevance. The latter is a transmembrane-linked adhesion molecule (encoded by the *Nfasc* gene) having a very similar structure to Contactin-2. According to previous studies, just like the data presented in this work, show a similar expression pattern (Brümmendorf T and Rathjen FG, 1996). Both Neurofascin and Contactin-2 are co-expressed in a variety of neuronal cell types promoting neurite outgrowth, while being also responsible for the architecture and function of the nodes of Ranvier, albeit in distinct ways. Moreover, the genes of these two proteins are adjacent in the genome, a feature that is evolutionary conserved. The data from this work strengthen the belief that Contactin-2 and Neurofascin could share the same regulatory mechanisms (Hadas et al., 2013).

Data from this work have also revealed a positive spatial association on the gene expression intensities between *Cntn2*, *Bace1* and APP. *Bace1* is a type I transmembrane aspartyl protease, which is expressed in neuronal tissue with Contactin-2 consisting one of the main substrates of this protease (Gautam et al., 2014). *Bace1* cleaves Contactin-2 near its GPI anchor site to produce its soluble form, found throughout the brain, able to bind to other cell surface axonal molecules thus regulating a variety of events (Kuhn et al., 2012). Therefore, *Bace1* is able to modify the function of Contactin-2 by regulating the expression levels of the two different forms (transmembrane and soluble) of this molecule (Gautam et al., 2014).

Amyloid  $\beta$  precursor protein (APP) is a type I transmembrane protein acting like a receptor and being responsible for many different biological activities in neuronal and non-neuronal cells (Austin, Sens, and Combs, 2009). According to previous studies, one of its ligands is TGF $\beta$ -2. The binding of TGF $\beta$ -2 with cell surface APP induces neuronal cell death through an intracellular death signal transduction pathway. Contactin-2 also is able to bind APP leading to a release of the APP intracellular domain, triggering FE65-dependent transcriptional activity in a  $\gamma$ -secretase-dependent manner. In this way, Contactin-2 inhibits the APP-dependent TGF $\beta$ 2-mediated neuronal cell death by reducing the binding of TGF $\beta$ -2 to APP (Tachi et al., 2010). In parallel, the interaction between Contactin-2 and APP is also responsible for the negative modulation of neurogenesis and also occurs via Fe65-dependent pathways (Ma et al., 2008).

Finally, the spatial pattern of the gene expression intensity of Contactin-2 correlates negatively with four genes (*Ncam1*, *Ncam2*, *L1cam*, *Ptptr1*) whose products have been related to anabolic processes in the adult brain, like neurogenesis (for *Ncam*) (Gascon E et al., 2010) or activity-dependent *de novo* myelination (for *L1cam*) (Fields 2015) or remyelination in lesion sites (for *Ptptr1*) (Levy et al., 1993). Tabula Muris data additionally show that, contrary to what is happening with *Cntn2*, one of the main brain cell types – source of their expression are OPCs.

Given the negative regulation of Contactin-2 in adult neurogenesis (in collaboration with APP, whose spatial patterns of gene expression correlate as mentioned above), we speculate that not only does the adult brain rely on Contactin-2-independent pathways for mediating plasticity of any form (being either via neurogenesis or *de novo* myelination or synaptic plasticity), but also the presence of Contactin-2 (contrary to what is happening during neurodevelopment) constitutes a negative signal for such processes. This opinion is in accordance with previous work from our group showing that absence of Contactin-2 leads to improved conduction velocity of axons during remyelination after cuprizone-induced demyelination in adult mice (Zoupi et al., 2018) and to increased axonal regeneration after injury (Savvaki et al., unpublished data).

In an effort to put together all the pieces of information related to the physiological significance of Contactin-2 during development and in adulthood, we suggest that while this molecule is expressed in essential functions of neurons such as the proximal part of the outgrowing axons/ neurites during development, in adulthood its expression is correlated with low plasticity events. For example, Contactin-2 is involved in the formation of long ascending/ descending pathways during development (Dodd et al., 1988; Furley et al., 1990), and possibly contributes to their functional/ electrolytic homeostasis thereafter (by interacting with the potassium channels Kv1.1 and Kv1.2, and other molecules like Neurofascin). Contactin-2 seems to contribute to the low plasticity of these pathways (for instance by downregulating any neurogenic events), and in regions characterized by higher degrees of plasticity or regenerative potential, the adult brain relies on the expression of different cell adhesion molecules to promote anabolic activities like neurogenesis, *de novo* myelination or remyelination. The post-genomic interplay between Contactin-2 and some of these other cell adhesion molecules (like Ncam) observed by prior experimentation (Milev et al., 1996) is not contradictory to the results of this work (showing a negative spatial genomic correlation among them). The adult brain could differentiate neural pathways of low and high plasticity or low and high regenerative potential based on which groups of proteins get preferably expressed, but at a functional level these different groups of proteins need to interact with each other, since all these neural pathways reciprocally interact with each other independent of the degree of plasticity or the regenerative potential.

Future studies are required in order to find possible transcription factors that regulate the expression of Contactin-2 together with the expression of genes correlated with Contactin-2, to further elucidate the physiological role of the molecule, and to investigate whether this protein can be used either as a target for novel treatments or as a marker for discriminating between neural pathways showing a different severity in the clinical outcome if damaged or a different regenerative potential in the context of demyelinating and neurodegenerative disorders.

## REFERENCES I

- Ackerman, S. D., C. Garcia, X. Piao, D. H. Gutmann and K. R. Monk (2015). "The adhesion GPCR Gpr56 regulates oligodendrocyte development via interactions with Galpha12/13 and RhoA." *Nat Commun* 6: 6122.
- Aggelakopoulou, M., E. Kourepini, N. Paschalidis, D. C. Simoes, D. Kalavrizioti, N. Dimisianos, P. Papathanasopoulos, A. Mouzaki and V. Panoutsakopoulou (2016). "ERbeta-Dependent Direct Suppression of Human and Murine Th17 Cells and Treatment of Established Central Nervous System Autoimmunity by a Neurosteroid." *J Immunol* 197(7): 2598-2609.
- Alexaki, V. I., Fodelianaki, G., Neuwirth, A., Mund, C., Kourgiantaki, A., Ieronimaki, E., . . . Chavakis, T. (2018). DHEA inhibits acute microglia-mediated inflammation through activation of the TrkA-Akt1/2-CREB-Jmjd3 pathway. *Mol Psychiatry*, 23(6), 1410-1420.
- Akdemir, E. S., Huang, A. Y., & Deneen, B. (2020). Astrocytogenesis: where, when, and how. *F1000Research*, 9, F1000 Faculty Rev-233.
- Anastasia, A., P. A. Barker, M. V. Chao and B. L. Hempstead (2015). "Detection of p75<sup>NTR</sup> Trimers: Implications for Receptor Stoichiometry and Activation." *J Neurosci* 35(34): 11911-11920.
- Althaus, H. H. (2004). Remyelination in multiple sclerosis: a new role for neurotrophins? *Prog Brain Res*, 146, 415-432.
- Amor, S., P. A. Smith, B. Hart and D. Baker (2005). "Biozzi mice: of mice and human neurological diseases." *J Neuroimmunol* 165(1-2): 1-10.
- Antony, J. M., G. van Marle, W. Opii, D. A. Butterfield, F. Mallet, V. W. Yong, J. L. Wallace, R. M. Deacon, K. Warren and C. Power (2004). "Human endogenous retrovirus glycoprotein-mediated induction of redox reactants causes oligodendrocyte death and demyelination." *Nat Neurosci* 7(10): 1088-1095.
- Bacallao, K. and P. V. Monje (2015). "Requirement of cAMP signaling for Schwann cell differentiation restricts the onset of myelination." *PLoS One* 10(2): e0116948.
- Bacmeister, C. M., Barr, H. J., McClain, C. R., Thornton, M. A., Nettles, D., Welle, C. G., & Hughes, E. G. (2020). Motor learning promotes remyelination via new and surviving oligodendrocytes. *Nature neuroscience*, 10.1038/s41593-020-0637-3. Advance online publication.
- Barateiro, A. and A. Fernandes (2014). "Temporal oligodendrocyte lineage progression: in vitro models of proliferation, differentiation and myelination." *Biochim Biophys Acta* 1843(9): 1917- 1929.
- Barde, Y. A., D. Edgar and H. Thoenen (1982). "Purification of a new neurotrophic factor from mammalian brain." *EMBO J* 1(5): 549-553.

- Barnett, M. H. and J. W. Prineas (2004). "Relapsing and remitting multiple sclerosis: pathology of the newly forming lesion." *Ann Neurol* 55(4): 458-468.
- Barres, B. A. (2008). "The mystery and magic of glia: a perspective on their roles in health and disease." *Neuron* 60(3): 430-440.
- Barres, B. A., I. K. Hart, H. S. Coles, J. F. Burne, J. T. Voyvodic, W. D. Richardson and M. C. Raff (1992). "Cell death and control of cell survival in the oligodendrocyte lineage." *Cell* 70(1): 31-46.
- Baulieu, E. E. and P. Robel (1990). "Neurosteroids: a new brain function?" *J Steroid Biochem Mol Biol* 37(3): 395-403.
- Baulieu, E. E. and P. Robel (1998). "Dehydroepiandrosterone (DHEA) and dehydroepiandrosterone sulfate (DHEAS) as neuroactive neurosteroids." *Proc Natl Acad Sci U S A* 95(8): 4089-4091.
- Baulieu, E. E., Robel, P., & Schumacher, M. (2001). Neurosteroids: beginning of the story. *Int Rev Neurobiol*, 46, 1-32.
- Bélanger, N., Grégoire, L., Bédard, P. J., & Di Paolo, T. (2006). DHEA improves symptomatic treatment of moderately and severely impaired MPTP monkeys. *Neurobiol Aging*, 27(11), 1684-1693.
- Belelli, D., N. L. Harrison, J. Maguire, R. L. Macdonald, M. C. Walker and D. W. Cope (2009). "Extrasynaptic GABAA receptors: form, pharmacology, and function." *J Neurosci* 29(41): 12757-12763.
- Belelli, D. and J. J. Lambert (2005). "Neurosteroids: endogenous regulators of the GABA(A) receptor." *Nat Rev Neurosci* 6(7): 565-575.
- Bennett, F. C., Bennett, M. L., Yaqoob, F., Mulinyawe, S. B., Grant, G. A., Hayden Gephart, M., Plowey, E. D., & Barres, B. A. (2018). A Combination of Ontogeny and CNS Environment Establishes Microglial Identity. *Neuron*, 98(6), 1170–1183.e8.
- Bennett, J. L., & Stüve, O. (2009). Update on inflammation, neurodegeneration, and immunoregulation in multiple sclerosis: therapeutic implications. *Clin Neuropharmacol*, 32(3), 121-132.
- Blakemore, W. F., & Franklin, R. J. (2008). Remyelination in experimental models of toxin-induced demyelination. *Curr Top Microbiol Immunol*, 318, 193-212.
- Bogler, O., D. Wren, S. C. Barnett, H. Land and M. Noble (1990). "Cooperation between two growth factors promotes extended self-renewal and inhibits differentiation of oligodendrocyte-type-2 astrocyte (O-2A) progenitor cells." *Proc Natl Acad Sci U S A* 87(16): 6368-6372.
- Bonetto, G., Charalampopoulos, I., Gravanis, A., & Karagogeos, D. (2017). The novel synthetic microneurotrophin BNN27 protects mature oligodendrocytes against cuprizone-induced death, through the NGF receptor TrkA. *Glia*, 65(8), 1376-1394.



- Botsakis, K., Mourtzi, T., Panagiotakopoulou, V., Vreka, M., Stathopoulos, G. T., Padiaditakis, I., . . . Angelatou, F. (2017). BNN-20, a synthetic microneurotrophin, strongly protects dopaminergic neurons in the "weaver" mouse, a genetic model of dopamine-denervation, acting through the TrkB neurotrophin receptor. *Neuropharmacology*, *121*, 140-157.
- Bourque, M., Morissette, M., Al Sweidi, S., Caruso, D., Melcangi, R. C., & Di Paolo, T. (2016). Neuroprotective Effect of Progesterone in MPTP-Treated Male Mice. *Neuroendocrinology*, *103*(3-4), 300-314.
- Briscoe J, Novitch BG. (2008). Regulatory pathways linking progenitor patterning, cell fates and neurogenesis in the ventral neural tube. *Philos. Trans. R Soc. Lond. B Biol. Sci.* 363:57–70
- Calogeropoulou, T., Avlonitis, N., Minas, V., Alexi, X., Pantzou, A., Chara-lampopoulos, I., . . . Alexis, M.N. (2009). Novel dehydroepiandrosterone derivatives with antiapoptotic, neuroprotective activity. *Journal of Medicinal Chemistry* 52:6569–87
- Chang, A., Nishiyama, A., Peterson, J., Prineas, J., & Trapp, B. D. (2000). NG2-positive oligodendrocyte progenitor cells in adult human brain and multiple sclerosis lesions. *J Neurosci*, *20*(17), 6404-6412.
- Chang, A., Tourtellotte, W. W., Rudick, R., & Trapp, B. D. (2002). Premyelinating oligodendrocytes in chronic lesions of multiple sclerosis. *N Engl J Med*, *346*(3), 165-173.
- Chao, M. V. (2003). Neurotrophins and their receptors: A convergence point for many signalling pathways. *Nature Reviews Neuroscience* 4: 299–309
- Chao, M. V., R. Rajagopal and F. S. Lee (2006). "Neurotrophin signalling in health and disease." *Clin Sci (Lond)* 110(2): 167-173.
- Charalampopoulos, I., A. N. Margioris and A. Gravanis (2008). "Neurosteroid dehydroepiandrosterone exerts anti-apoptotic effects by membrane-mediated, integrated genomic and non-genomic pro-survival signaling pathways." *J Neurochem* 107(5): 1457-1469.
- Charalampopoulos, I., Tsatsanis, C., Dermitzaki, E., Alexaki, V. I., Castanas, E., Margioris, A. N., & Gravanis, A. (2004). Dehydroepiandrosterone and allopregnanolone protect sympathoadrenal medulla cells against apoptosis via antiapoptotic Bcl-2 proteins. *Proc Natl Acad Sci U S A*, *101*(21), 8209-8214.
- Chen, J. Y., J. R. Lin, K. A. Cimprich and T. Meyer (2012). "A two-dimensional ERK-AKT signaling code for an NGF-triggered cell-fate decision." *Mol Cell* 45(2): 196-209.
- Ciccarelli, O., F. Barkhof, B. Bodini, N. De Stefano, X. Golay, K. Nicolay, D. Pelletier, P. J. Pouwels, S. A. Smith, C. A. Wheeler-Kingshott, B. Stankoff, T. Youstry and D. H. Miller (2014). "Pathogenesis of multiple sclerosis: insights from molecular and metabolic imaging." *Lancet Neurol* 13(8): 807-822.
- Clemente, D., Ortega, M. C., Melero-Jerez, C., & de Castro, F. (2013). The effect of glia-glia interactions on oligodendrocyte precursor cell biology during development and in demyelinating diseases. *Frontiers in cellular neuroscience*, *7*, 268.

- Climent, E., Sancho-Tello, M., Miñana, R., Baretino, D., & Guerri, C. (2000). Astrocytes in culture express the full-length Trk-B receptor and respond to brain derived neurotrophic factor by changing intracellular calcium levels: effect of ethanol exposure in rats. *Neurosci Lett*, 288(1), 53-56.
- Cohen, R. I., Marmur, R., Norton, W. T., Mehler, M. F., & Kessler, J. A. (1996). Nerve growth factor and neurotrophin-3 differentially regulate the proliferation and survival of developing rat brain oligodendrocytes. *Journal of Neuroscience* 16:6433–42
- Colognato, H. and I. D. Tzvetanova (2011). "Glia unglued: how signals from the extracellular matrix regulate the development of myelinating glia." *Dev Neurobiol* 71(11): 924-955.
- Colombo, F., G. Racchetti and J. Meldolesi (2014). "Neurite outgrowth induced by NGF or L1CAM via activation of the TrkA receptor is sustained also by the exocytosis of enlargeosomes." *Proc Natl Acad Sci U S A* 111(47): 16943-16948.
- Colton, C. A. (2009). Heterogeneity of microglial activation in the innate immune response in the brain. *J Neuroimmune Pharmacol*, 4(4), 399-418.
- Compagnone, N. A., & Mellon, S. H. (2000). Neurosteroids: Biosynthesis and function of these novel neuromodulators. *Frontiers in Neuroendocrinology* 21:1–56
- Compston, A., & Coles, A. (2008). Multiple sclerosis. *Lancet (London, England)*, 372(9648), 1502–1517.
- Corley, S. M., U. Ladiwala, A. Besson and V. W. Yong (2001). "Astrocytes attenuate oligodendrocyte death in vitro through an alpha(6) integrin-laminin-dependent mechanism." *Glia* 36(3): 281-294.
- Corpechot, C., P. Robel, M. Axelson, J. Sjoval and E. E. Baulieu (1981). "Characterization and measurement of dehydroepiandrosterone sulfate in rat brain." *Proc Natl Acad Sci U S A* 78(8): 4704-4707.
- Crang, A. J., R. J. Franklin, W. F. Blakemore, J. Trotter, M. Schachner, S. C. Barnett and M. Noble (1991). "Transplantation of normal and genetically engineered glia into areas of demyelination." *Ann N Y Acad Sci* 633: 563-565.
- Cunningham, C. L., Martínez-Cerdeño, V., & Noctor, S. C. (2013). Microglia regulate the number of neural precursor cells in the developing cerebral cortex. *The Journal of neuroscience : the official journal of the Society for Neuroscience*, 33(10), 4216–4233.
- D'Amico, E., Patti, F., Zanghi, A., & Zappia, M. (2016). A personalized approach in progressive multiple sclerosis: The current status of disease modifying therapies (DMTs) and future perspectives. *International Journal of Molecular Sciences* 17
- D'Astous, M., Morissette, M., Tanguay, B., Callier, S., & Di Paolo, T. (2003). Dehydroepiandrosterone (DHEA) such as 17beta-estradiol prevents MPTP-induced dopamine depletion in mice. *Synapse*, 47(1), 10-14. doi:10.1002/syn.10145
- de Castro, F. and A. Bribian (2005). "The molecular orchestra of the migration of oligodendrocyte precursors during development." *Brain Res Brain Res Rev* 49(2): 227-241.

- Dendrou, C. A., Fugger, L., & Friese, M. A. (2015). Immunopathology of multiple sclerosis. *Nature reviews. Immunology*, *15*(9), 545–558. <https://doi.org/10.1038/nri3871>
- Du, C., M. W. Khalil and S. Sriram (2001). "Administration of dehydroepiandrosterone suppresses experimental allergic encephalomyelitis in SJL/J mice." *J Immunol* *167*(12): 7094-7101.
- Du, J., L. Feng, F. Yang and B. Lu (2000). "Activity- and Ca(2+)-dependent modulation of surface expression of brain-derived neurotrophic factor receptors in hippocampal neurons." *J Cell Biol* *150*(6): 1423-1434.
- Du, Y., Fischer, T. Z., Lee, L. N., Lercher, L. D., & Dreyfus, C. F. (2003). Regionally specific effects of BDNF on oligodendrocytes. *Developmental neuroscience*, *25*(2-4), 116–126.
- Fancy, S. P., Chan, J. R., Baranzini, S. E., Franklin, R. J., & Rowitch, D. H. (2011). Myelin regeneration: a recapitulation of development?. *Annual review of neuroscience*, *34*, 21–43.
- Ferent, J., Zimmer, C., Durbec, P., Ruat, M., & Traiffort, E. (2013). Sonic Hedgehog signaling is a positive oligodendrocyte regulator during demyelination. *J Neurosci*, *33*(5), 1759-1772.
- Fletcher, J. L., Murray, S. S., & Xiao, J. (2018). Brain-Derived Neurotrophic Factor in Central Nervous System Myelination: A New Mechanism to Promote Myelin Plasticity and Repair. *Int J Mol Sci*, *19*(12).
- Fodelianaki, G., Lansing, F., Bhattarai, P., Troullinaki, M., Zeballos, M. A., Charalampopoulos, I., . . . Alexaki, V. I. (2019). Nerve Growth Factor modulates LPS - induced microglial glycolysis and inflammatory responses. *Exp Cell Res*, *377*(1-2), 10-16.
- Frade, J. M. and Y. A. Barde (1998). "Microglia-derived nerve growth factor causes cell death in the developing retina." *Neuron* *20*(1): 35-41.
- Frade, J. M. and Y. A. Barde (1999). "Genetic evidence for cell death mediated by nerve growth factor and the neurotrophin receptor p75 in the developing mouse retina and spinal cord." *Development* *126*(4): 683-690.
- Franklin, R. J., A. J. Crang and W. F. Blakemore (1991). "Transplanted type-1 astrocytes facilitate repair of demyelinating lesions by host oligodendrocytes in adult rat spinal cord." *J Neurocytol* *20*(5): 420-430.
- Franklin, R. J., & Ffrench-Constant, C. (2008). Remyelination in the CNS: from biology to therapy. *Nat Rev Neurosci*, *9*(11), 839-855.
- Franklin, R. J. and S. A. Goldman (2015). "Glia Disease and Repair-Remyelination." *Cold Spring Harb Perspect Biol* *7*(7): a020594.
- Fressinaud, C. (2005). Repeated injuries dramatically affect cells of the oligodendrocyte lineage: effects of PDGF and NT-3 in vitro. *Glia*, *49*(4), 555-566.

- Fressinaud, C., & Eyer, J. (2013). Axoskeletal proteins prevent oligodendrocyte from toxic injury by upregulating survival, proliferation, and differentiation in vitro. *Neurochem Int*, 62(3), 306-313.
- Fulmer, C. G., VonDran, M. W., Stillman, A. A., Huang, Y., Hempstead, B. L., & Dreyfus, C. F. (2014). Astrocyte-derived BDNF supports myelin protein synthesis after cuprizone-induced demyelination. *J Neurosci*, 34(24), 8186-8196.
- Funfschilling, U., L. M. Supplie, D. Mahad, S. Boretius, A. S. Saab, J. Edgar, B. G. Brinkmann, C. M. Kassmann, I. D. Tzvetanova, W. Mobius, F. Diaz, D. Meijer, U. Suter, B. Hamprecht, M. W. Sereda, C. T. Moraes, J. Frahm, S. Goebbels and K. A. Nave (2012). "Glycolytic oligodendrocytes maintain myelin and long-term axonal integrity." *Nature* 485(7399): 517-521.
- Gard, A. L., M. R. Burrell, S. E. Pfeiffer, J. S. Rudge and W. C. Williams, 2nd (1995). "Astroglial control of oligodendrocyte survival mediated by PDGF and leukemia inhibitory factor-like protein." *Development* 121(7): 2187-2197.
- Gensert, J. M. and J. E. Goldman (1997). "Endogenous progenitors remyelinate demyelinated axons in the adult CNS." *Neuron* 19(1): 197-203.
- Ghosh A. (2010). Brain APCs including microglia are only differential and positional polymorphs. *Annals of neurosciences*, 17(4), 191–199.
- Gibon, J., S. M. Buckley, N. Unsain, V. Kaartinen, P. Seguela and P. A. Barker (2015). "proBDNF and p75<sup>NTR</sup> Control Excitability and Persistent Firing of Cortical Pyramidal Neurons." *J Neurosci* 35(26): 9741-9753.
- Giedd, J. N. (2004). "Structural magnetic resonance imaging of the adolescent brain." *Ann N Y Acad Sci* 1021: 77-85.
- Glajch, K. E., Ferraiuolo, L., Mueller, K. A., Stopford, M. J., Prabhkar, V., Gravanis, A., ... Sadri-Vakili, G. (2016). Microneurotrophins improve survival in motor neuron-astrocyte co-cultures but do not improve disease phenotypes in a mutant SOD1 mouse model of amyotrophic lateral sclerosis. *PLoS One* 11:e0164103-
- Gold, R., Linington, C., & Lassmann, H. (2006). Understanding pathogenesis and therapy of multiple sclerosis via animal models: 70 years of merits and culprits in experimental autoimmune encephalomyelitis research. *Brain* 129:1953–71
- Gordon, S., & Taylor, P. R. (2005). Monocyte and macrophage heterogeneity. *Nat Rev Immunol*, 5(12), 953-964.
- Grinspan, J. (2002). Cells and signaling in oligodendrocyte development. *J Neuropathol Exp Neurol*, 61(4), 297-306.
- Guo, W., Y. Ji, S. Wang, Y. Sun and B. Lu (2014). "Neuronal activity alters BDNF-TrkB signaling kinetics and downstream functions." *J Cell Sci* 127(Pt 10): 2249-2260.
- Hagemeyer, N., Hanft, K. M., Akriditou, M. A., Unger, N., Park, E. S., Stanley, E. R., Staszewski, O., Dimou, L., & Prinz, M. (2017). Microglia contribute to normal

myelinogenesis and to oligodendrocyte progenitor maintenance during adulthood. *Acta neuropathologica*, 134(3), 441–458.

Hall, S. M. (1972). "The effect of injections of lysophosphatidyl choline into white matter of the adult mouse spinal cord." *J Cell Sci* 10(2): 535-546.

Hallbook, F. (1999). "Evolution of the vertebrate neurotrophin and Trk receptor gene families." *Curr Opin Neurobiol* 9(5): 616-621.

Hamilton, S. P. and L. H. Rome (1994). "Stimulation of in vitro myelin synthesis by microglia." *Glia* 11(4): 326-335.

Hammond, T. R., Gadea, A., Dupree, J., Kerninon, C., Nait-Oumesmar, B., Aguirre, A., & Gallo, V. (2014). Astrocyte-Derived Endothelin-1 Inhibits Remyelination through Notch Activation. *Neuron*, 81(6), 1442.

Hammond, T. R., McEllin, B., Morton, P. D., Raymond, M., Dupree, J., & Gallo, V. (2015). Endothelin-B Receptor Activation in Astrocytes Regulates the Rate of Oligodendrocyte Regeneration during Remyelination. *Cell reports*, 13(10), 2090–2097.

Hanamsagar, R., Alter, M. D., Block, C. S., Sullivan, H., Bolton, J. L., & Bilbo, S. D. (2017). Generation of a microglial developmental index in mice and in humans reveals a sex difference in maturation and immune reactivity. *Glia*, 65(9), 1504–1520.

Hannan, M. A., Haque, M. N., Dash, R., Alam, M., & Moon, I. S. (2019). 3 $\beta$ , 6 $\beta$ -dichloro-5-hydroxy-5 $\alpha$ -cholestane facilitates neuronal development through modulating TrkA signaling regulated proteins in primary hippocampal neuron. *Sci Rep*, 9(1), 18919.

Havelock, J. C., R. J. Auchus and W. E. Rainey (2004). "The rise in adrenal androgen biosynthesis: adrenarche." *Semin Reprod Med* 22(4): 337-347.

He, X. L. and K. C. Garcia (2004). "Structure of nerve growth factor complexed with the shared neurotrophin receptor p75." *Science* 304(5672): 870-875.

Herculano-Houzel, S. (2014). "The glia/neuron ratio: how it varies uniformly across brain structures and species and what that means for brain physiology and evolution." *Glia* 62(9): 1377- 1391.

Holtman, I. R., Skola, D., & Glass, C. K. (2017). Transcriptional control of microglia phenotypes in health and disease. *The Journal of clinical investigation*, 127(9), 3220–3229.

Hong, S., Dissing-Olesen, L., & Stevens, B. (2016). New insights on the role of microglia in synaptic pruning in health and disease. *Current opinion in neurobiology*, 36, 128–134.

Huang, E. J., & Reichardt, L. F. (2001). Neurotrophins: roles in neuronal development and function. *Annual review of neuroscience*, 24, 677–736.

Huang, E. J. and L. F. Reichardt (2003). "Trk receptors: roles in neuronal signal transduction." *Annu Rev Biochem* 72: 609-642.

- Huebner, E. A. and S. M. Strittmatter (2009). "Axon regeneration in the peripheral and central nervous systems." *Results Probl Cell Differ* 48: 339-351.
- Ibán-Arias, R., Lisa, S., Mastrodimou, N., Kokona, D., Koulakis, E., Iordanidou, P., . . . Thermos, K. (2018). The Synthetic Microneurotrophin BNN27 Affects Retinal Function in Rats With Streptozotocin-Induced Diabetes. *Diabetes*, 67(2), 321-333.
- Jean, I., Laviaille, C., Barthelaix-Pouplard, A., & Fressinaud, C. (2003). Neurotrophin-3 specifically increases mature oligodendrocyte population and enhances remyelination after chemical demyelination of adult rat CNS. *Brain Res*, 972(1-2), 110-118.
- Jensen, C. J., Massie, A., & De Keyser, J. (2013). Immune players in the CNS: the astrocyte. *J Neuroimmune Pharmacol*, 8(4), 824-839.
- Joo, W., S. Hippenmeyer and L. Luo (2014). "Neurodevelopment. Dendrite morphogenesis depends on relative levels of NT-3/TrkC signaling." *Science* 346(6209): 626-629.
- Jurevics, H., Largent, C., Hostettler, J., Sammond, D. W., Matsushima, G. K., Kleindienst, A., ... Morell, P. (2002). Alterations in metabolism and gene expression in brain regions during cuprizone-induced demyelination and remyelination. *Journal of Neurochemistry* 82:126–36
- Kastriti, M. E., Sargiannidou, I., Kleopa, K. A., & Karagozeos, D. (2015). Differential modulation of the juxtapanodal complex in Multiple Sclerosis. *Molecular and cellular neurosciences*, 67, 93–103.
- Kawakami, N., S. Lassmann, Z. Li, F. Odoardi, T. Ritter, T. Ziemssen, W. E. Klinkert, J. W. Ellwart, M. Bradl, K. Krivacic, H. Lassmann, R. M. Ransohoff, H. D. Volk, H. Wekerle, C. Linington and A. Flugel (2004). "The activation status of neuroantigen-specific T cells in the target organ determines the clinical outcome of autoimmune encephalomyelitis." *J Exp Med* 199(2): 185-197.
- Kessaris, N., N. Pringle and W. D. Richardson (2008). "Specification of CNS glia from neural stem cells in the embryonic neuroepithelium." *Philos Trans R Soc Lond B Biol Sci* 363(1489): 71-85.
- Kimelberg, H. K., & Nedergaard, M. (2010). Functions of astrocytes and their potential as therapeutic targets. *Neurotherapeutics*, 7(4), 338-353.
- Kıray, H., Lindsay, S. L., Hosseinzadeh, S., & Barnett, S. C. (2016). The multifaceted role of astrocytes in regulating myelination. *Exp Neurol*, 283(Pt B), 541-549.
- Kirby, B. B., N. Takada, A. J. Latimer, J. Shin, T. J. Carney, R. N. Kelsh and B. Appel (2006). "In vivo time-lapse imaging shows dynamic oligodendrocyte progenitor behavior during zebrafish development." *Nat Neurosci* 9(12): 1506-1511.
- Kokras, N., Dioli, C., Paravatou, R., Sotiropoulos, M. G., Delis, F., Antoniou, K., Calogeropoulou, T., Charalampopoulos, I., Gravanis, A., & Dalla, C. (2020). Psychoactive properties of BNN27, a novel neurosteroid derivative, in male and female rats. *Psychopharmacology*, 10.1007/s00213-020-05545-5. Advance online publication.

Kotter, M. R., W. W. Li, C. Zhao and R. J. Franklin (2006). "Myelin impairs CNS remyelination by inhibiting oligodendrocyte precursor cell differentiation." *J Neurosci* 26(1): 328-332.

Kucenas, S., H. Snell and B. Appel (2008). "nkx2.2a promotes specification and differentiation of a myelinating subset of oligodendrocyte lineage cells in zebrafish." *Neuron Glia Biol* 4(2): 71-81.

Kuhlmann, T., V. Miron, Q. Cui, C. Wegner, J. Antel and W. Bruck (2008). "Differentiation block of oligodendroglial progenitor cells as a cause for remyelination failure in chronic multiple sclerosis." *Brain* 131(Pt 7): 1749-1758.

Kumar, S., J. C. Biancotti, M. Yamaguchi and J. de Vellis (2007). "Combination of growth factors enhances remyelination in a cuprizone-induced demyelination mouse model." *Neurochem Res* 32(4-5): 783-797.

Kuno, R., Y. Yoshida, A. Nitta, T. Nabeshima, J. Wang, Y. Sonobe, J. Kawanokuchi, H. Takeuchi, T. Mizuno and A. Suzumura (2006). "The role of TNF-alpha and its receptors in the production of NGF and GDNF by astrocytes." *Brain Res* 1116(1): 12-18.

Lassmann, H. (1998). "Neuropathology in multiple sclerosis: new concepts." *Mult Scler* 4(3): 93-98.

Lau, L. W., Cua, R., Keough, M. B., Haylock-Jacobs, S., & Yong, V. W. (2013). Pathophysiology of the brain extracellular matrix: a new target for remyelination. *Nature reviews*.

Laudiero, L. B., L. Aloe, R. Levi-Montalcini, C. Buttinelli, D. Schilter, S. Gillessen and U. Otten (1992). "Multiple sclerosis patients express increased levels of beta-nerve growth factor in cerebrospinal fluid." *Neurosci Lett* 147(1): 9-12.

Lazaridis, I., Charalampopoulos, I., Alexaki, V. I., Avlonitis, N., Pediaditakis, I., Efstathopoulos, P., . . . Gravanis, A. (2011). Neurosteroid dehydroe- piandrosterone interacts with nerve growth factor (NGF) receptors, preventing neuronal apoptosis. *PLoS Biology* 9:e1001051-

Lee, J. K. and B. Zheng (2012). "Role of myelin-associated inhibitors in axonal repair after spinal cord injury." *Exp Neurol* 235(1): 33-42.

Lee, R., P. Kermani, K. K. Teng and B. L. Hempstead (2001). "Regulation of cell survival by secreted proneurotrophins." *Science* 294(5548): 1945-1948.

Lee, S., M. K. Leach, S. A. Redmond, S. Y. Chong, S. H. Mellon, S. J. Tuck, Z. Q. Feng, J. M. Corey and J. R. Chan (2012). "A culture system to study oligodendrocyte myelination processes using engineered nanofibers." *Nat Methods* 9(9): 917-922.

Lee, S., S. Y. Chong, S. J. Tuck, J. M. Corey and J. R. Chan (2013). "A rapid and reproducible assay for modeling myelination by oligodendrocytes using engineered nanofibers." *Nat Protoc* 8(4): 771-782.

- Le Moan, N., D. M. Houslay, F. Christian, M. D. Houslay and K. Akassoglou (2011). "Oxygen-dependent cleavage of the p75 neurotrophin receptor triggers stabilization of HIF-1alpha." *Mol Cell* 44(3): 476-490.
- Levi-Montalcini, R. (1987). "The nerve growth factor 35 years later." *Science* 237(4819): 1154-1162. Leon, A., A. Buriani, R. Dal Toso, M. Fabris, S. Romanello, L. Aloe and R. Levi-Montalcini (1994). "Mast cells synthesize, store, and release nerve growth factor." *Proc Natl Acad Sci U S A* 91(9): 3739-3743.
- Li, Q., & Barres, B. A. (2018). Microglia and macrophages in brain homeostasis and disease. *Nature reviews. Immunology*, 18(4)
- Li, J., E. R. Ramenaden, J. Peng, H. Koito, J. J. Volpe and P. A. Rosenberg (2008). "Tumor necrosis factor alpha mediates lipopolysaccharide-induced microglial toxicity to developing oligodendrocytes when astrocytes are present." *J Neurosci* 28(20): 5321-5330.
- Lieberman, S. (1995). "An abbreviated account of some aspects of the biochemistry of DHEA, 1934-1995." *Ann N Y Acad Sci* 774: 1-15.
- Longo, F. M. and S. M. Massa (2013). "Small-molecule modulation of neurotrophin receptors: a strategy for the treatment of neurological disease." *Nat Rev Drug Discov* 12(7): 507-525.
- Lucchinetti, C. F., Brück, W., Rodriguez, M., & Lassmann, H. (1996). Distinct patterns of multiple sclerosis pathology indicates heterogeneity on pathogenesis. *Brain Pathol*, 6(3), 259-274.
- Luo, H., Xiang, Y., Qu, X., Liu, H., Liu, C., Li, G., . . . Qin, X. (2019). Apelin-13 Suppresses Neuroinflammation Against Cognitive Deficit in a Streptozotocin-Induced Rat Model of Alzheimer's Disease Through Activation of BDNF-TrkB Signaling Pathway. *Front Pharmacol*, 10, 395.
- Makar, T. K., Bever, C. T., Singh, I. S., Royal, W., Sahu, S. N., Sura, T. P., Sultana, S., Sura, K. T., Patel, N., Dhib-Jalbut, S., & Trisler, D. (2009). Brain-derived neurotrophic factor gene delivery in an animal model of multiple sclerosis using bone marrow stem cells as a vehicle. *Journal of neuroimmunology*, 210(1-2), 40–51.
- Makar, T. K., Trisler, D., Sura, K. T., Sultana, S., Patel, N., & Bever, C. T. (2008). Brain derived neurotrophic factor treatment reduces inflammation and apoptosis in experimental allergic encephalomyelitis. *Journal of the neurological sciences*, 270(1-2), 70–76.
- Maninger, N., Wolkowitz, O. M., Reus, V. I., Epel, E. S., & Mellon, S. H. (2009). Neurobiological and neuropsychiatric effects of dehydroepiandrosterone (DHEA) and DHEA sulfate (DHEAS). *Front Neuroendocrinol*, 30(1), 65-91.
- Mason, J. L., C. Langaman, P. Morell, K. Suzuki and G. K. Matsushima (2001). "Episodic demyelination and subsequent remyelination within the murine central nervous system: changes in axonal calibre." *Neuropathol Appl Neurobiol* 27(1): 50-58.



- Martinez-Serrano, A. and A. Bjorklund (1996). "Protection of the neostriatum against excitotoxic damage by neurotrophin-producing, genetically modified neural stem cells." *J Neurosci* 16(15): 4604-4616.
- Matsushima, G. K. and P. Morell (2001). "The neurotoxicant, cuprizone, as a model to study demyelination and remyelination in the central nervous system." *Brain Pathol* 11(1): 107-116.
- McCarthy, K. D., & de Vellis, J. (1980). Preparation of separate astroglial and oligodendroglial cell cultures from rat cerebral tissue. *The Journal of Cell Biology* 85:890–902
- McFarland, H. F., & Martin, R. (2007). Multiple sclerosis: a complicated picture of autoimmunity. *Nat Immunol*, 8(9), 913-919.
- Mellon, S. H. (2007). Neurosteroid regulation of central nervous system development. *Pharmacol Ther*, 116(1), 107-124.
- Mellon, S. H., & Griffin, L. D. (2002). Neurosteroids: biochemistry and clinical significance. *Trends Endocrinol Metab*, 13(1), 35-43.
- Menn, B., J. M. Garcia-Verdugo, C. Yaschine, O. Gonzalez-Perez, D. Rowitch and A. Alvarez-Buylla (2006). "Origin of oligodendrocytes in the subventricular zone of the adult brain." *J Neurosci* 26(30): 7907-7918.
- Mesiano, S. and R. B. Jaffe (1997). "Developmental and functional biology of the primate fetal adrenal cortex." *Endocr Rev* 18(3): 378-403.
- Miao, H., Li, R., Han, C., Lu, X., & Zhang, H. (2018). Minocycline promotes posthemorrhagic neurogenesis via M2 microglia polarization via upregulation of the TrkB/BDNF pathway in rats. *J Neurophysiol*, 120(3), 1307-1317.
- Micera, A., R. De Simone and L. Aloe (1995). "Elevated levels of nerve growth factor in the thalamus and spinal cord of rats affected by experimental allergic encephalomyelitis." *Arch Ital Biol* 133(2): 131-142.
- Micera, A., F. Properzi, V. Triaca and L. Aloe (2000). "Nerve growth factor antibody exacerbates neuropathological signs of experimental allergic encephalomyelitis in adult lewis rats." *J Neuroimmunol* 104(2): 116-123.
- Miller, D. J., K. Asakura and M. Rodriguez (1996). "Central nervous system remyelination clinical application of basic neuroscience principles." *Brain Pathol* 6(3): 331-344.
- Miller, D. J., T. Duka, C. D. Stimpson, S. J. Schapiro, W. B. Baze, M. J. McArthur, A. J. Fobbs, A. M. Sousa, N. Sestan, D. E. Wildman, L. Lipovich, C. W. Kuzawa, P. R. Hof and C. C. Sherwood (2012). "Prolonged myelination in human neocortical evolution." *Proc Natl Acad Sci U S A* 109(41): 16480-16485.

Miller, R. H., & Fyffe-Maricich, S. L. (2010). Restoring the balance between disease and repair in multiple sclerosis: insights from mouse models. *Dis Model Mech*, 3(9-10), 535-539. doi:10.1242/dmm.001958

Minnone, G., De Benedetti, F., & Bracci-Laudiero, L. (2017). NGF and Its Receptors in the Regulation of Inflammatory Response. *Int J Mol Sci*, 18(5).

Miron, V. E., Boyd, A., Zhao, J. W., Yuen, T. J., Ruckh, J. M., Shadrach, J. L., . . . Ffrench-Constant, C. (2013). M2 microglia and macrophages drive oligodendrocyte differentiation during CNS remyelination. *Nat Neurosci*, 16(9), 1211-1218.

Mirsky, R., J. Winter, E. R. Abney, R. M. Pruss, J. Gavrilovic and M. C. Raff (1980). "Myelin-specific proteins and glycolipids in rat Schwann cells and oligodendrocytes in culture." *J Cell Biol* 84(3): 483-494.

Mishchenko, T. A., Mitroshina, E. V., Usenko, A. V., Voronova, N. V., Astrakhanova, T. A., Shirokova, O. M., . . . Vedunova, M. V. (2018). Features of Neural Network Formation and Their Functions in Primary Hippocampal Cultures in the Context of Chronic TrkB Receptor System Influence. *Front Physiol*, 9, 1925.

Mitew, S., C. M. Hay, H. Peckham, J. Xiao, M. Koenning and B. Emery (2014). "Mechanisms regulating the development of oligodendrocytes and central nervous system myelin." *Neuroscience* 276: 29-47.

Mo, L., Yang, Z., Zhang, A., & Li, X. (2010). The repair of the injured adult rat hippocampus with NT-3-chitosan carriers. *Biomaterials* 31:2184–92

Morgan, L., K. R. Jessen and R. Mirsky (1991). "The effects of cAMP on differentiation of cultured Schwann cells: progression from an early phenotype (04+) to a myelin phenotype (P0+, GFAP-, N-CAM-, NGF-receptor-) depends on growth inhibition." *J Cell Biol* 112(3): 457-467.

Nash, B., Ioannidou, K., & Barnett, S. C. (2011). Astrocyte phenotypes and their relationship to myelination. *J Anat*, 219(1), 44-52.

Nicholas, R. S., M. G. Wing and A. Compston (2001). "Nonactivated microglia promote oligodendrocyte precursor survival and maturation through the transcription factor NF-kappa B." *Eur J Neurosci* 13(5): 959-967.

Noble, M. and K. Murray (1984). "Purified astrocytes promote the in vitro division of a bipotential glial progenitor cell." *EMBO J* 3(10): 2243-2247.

Offner, H., A. Zamora, H. Drought, A. Matejuk, D. L. Auci, E. E. Morgan, A. A. Vandenbark and C. L. Reading (2002). "A synthetic androstene derivative and a natural androstene metabolite inhibit relapsing-remitting EAE." *J Neuroimmunol* 130(1-2): 128-139.

Oh, L. Y. and V. W. Yong (1996). "Astrocytes promote process outgrowth by adult human oligodendrocytes in vitro through interaction between bFGF and astrocyte extracellular matrix." *Glia* 17(3): 237-253.

- Olah, M., Amor, S., Brouwer, N., Vinet, J., Eggen, B., Biber, K., & Bod-deke, H. W. (2012). Identification of a microglia phenotype supportive of remyelination. *Glia* 60:306–21.
- Oleszak, E. L., J. R. Chang, H. Friedman, C. D. Katsetos and C. D. Platsoucas (2004). "Theiler's virus infection: a model for multiple sclerosis." *Clin Microbiol Rev* 17(1): 174-207.
- Ontaneda, D., Fox, R. J., & Chataway, J. (2015). Clinical trials in progressive multiple sclerosis: Lessons learned and future perspectives. *Lancet Neurology* 14:208–23
- Orentas, D. M., J. E. Hayes, K. L. Dyer and R. H. Miller (1999). "Sonic hedgehog signaling is required during the appearance of spinal cord oligodendrocyte precursors." *Development* 126(11): 2419-2429.
- Orentreich, N., J. L. Brind, J. H. Vogelman, R. Andres and H. Baldwin (1992). "Long-term longitudinal measurements of plasma dehydroepiandrosterone sulfate in normal men." *J Clin Endocrinol Metab* 75(4): 1002-1004.
- Orihuela, R., McPherson, C. A., & Harry, G. J. (2016). Microglial M1/M2 polarization and metabolic states. *Br J Pharmacol*, 173(4), 649-665.
- Oudega, M. and T. Hagg (1996). "Nerve growth factor promotes regeneration of sensory axons into adult rat spinal cord." *Exp Neurol* 140(2): 218-229.
- Panagiotakopoulou, V., Botsakis, K., Delis, F., Mourtzi, T., Tzatzarakis, M. N., Dimopoulou, A., . . . Angelatou, F. (2020). Anti-neuroinflammatory, protective effects of the synthetic microneurotrophin BNN-20 in the advanced dopaminergic neurodegeneration of "weaver" mice. *Neuropharmacology*, 165, 107919.
- Pang, Y., L. Campbell, B. Zheng, L. Fan, Z. Cai and P. Rhodes (2010). "Lipopolysaccharide-activated microglia induce death of oligodendrocyte progenitor cells and impede their development." *Neuroscience* 166(2): 464-475.
- Pang, Y., L. W. Fan, L. T. Tien, X. Dai, B. Zheng, Z. Cai, R. C. Lin and A. Bhatt (2013). "Differential roles of astrocyte and microglia in supporting oligodendrocyte development and myelination in vitro." *Brain Behav* 3(5): 503-514.
- Pang, Y., Z. Cai and P. G. Rhodes (2000). "Effects of lipopolysaccharide on oligodendrocyte progenitor cells are mediated by astrocytes and microglia." *J Neurosci Res* 62(4): 510-520.
- Papadopoulos, D., D. Pham-Dinh and R. Reynolds (2006). "Axon loss is responsible for chronic neurological deficit following inflammatory demyelination in the rat." *Exp Neurol* 197(2): 373-385.
- Patel, J. R., J. L. Williams, M. M. Muccigrosso, L. Liu, T. Sun, J. B. Rubin and R. S. Klein (2012). "Astrocyte TNFR2 is required for CXCL12-mediated regulation of oligodendrocyte progenitor proliferation and differentiation within the adult CNS." *Acta Neuropathol* 124(6): 847-860.

- Pediaditakis, I., Efstathopoulos, P., Prousis, K. C., Zervou, M., Arevalo, J. C., Alexaki, V. I., ... Gravanis, A. (2016a). Selective and differential interactions of BNN27, a novel C17-spiroepoxy steroid derivative, with TrkA receptors, regulating neuronal survival and differentiation. *Neuropharmacology* 111:266–282
- Pediaditakis, I., Iliopoulos, I., Theologidis, I., Delivanoglou, N., Margioris, A. N., Charalampopoulos, I., & Gravanis, A. (2015). Dehydroepiandrosterone: An ancestral ligand of neurotrophin receptors. *Endocrinology* 156:16–23
- Pediaditakis, I., Kourgiantaki, A., Prousis, K. C., Potamitis, C., Xanthopoulos, K. P., Zervou, M., ... Gravanis, A. (2016b). BNN27, a 17-spiroepoxy steroid derivative, interacts with and activates p75 neurotrophin receptor, rescuing cerebellar granule neurons from apoptosis. *Frontiers in Pharmacology* 7:512
- Pekny, M., Pekna, M., Messing, A., Steinhäuser, C., Lee, J. M., Parpura, V., . . . Verkhratsky, A. (2016). Astrocytes: a central element in neurological diseases. *Acta Neuropathol*, 131(3), 323-345.
- Pfeiffer, S. E., A. E. Warrington and R. Bansal (1993). "The oligodendrocyte and its many cellular processes." *Trends Cell Biol* 3(6): 191-197.
- Philippidou, P., G. Valdez, W. Akmentin, W. J. Bowers, H. J. Federoff and S. Halegoua (2011). "Trk retrograde signaling requires persistent, Pincher-directed endosomes." *Proc Natl Acad Sci U S A* 108(2): 852-857.
- Pitsikas, N., & Gravanis, A. (2017). The novel dehydroepiandrosterone (DHEA) derivative BNN27 counteracts delay-dependent and scopolamine-induced recognition memory deficits in rats. *Neurobiology of learning and memory*, 140, 145–153.
- Plemel, J. R., Michaels, N. J., Weishaupt, N., Caprariello, A. V., Keough, M. B., Rogers, J. A., . . . Yong, V. W. (2018). Mechanisms of lysophosphatidylcholine-induced demyelination: A primary lipid disrupting myelinopathy. *Glia*, 66(2), 327-347.
- Poliak, S. and E. Peles (2003). "The local differentiation of myelinated axons at nodes of Ranvier." *Nat Rev Neurosci* 4(12): 968-980.
- Poliani, P. L., Y. Wang, E. Fontana, M. L. Robinette, Y. Yamanishi, S. Gilfillan and M. Colonna (2015). "TREM2 sustains microglial expansion during aging and response to demyelination." *J Clin Invest* 125(5): 2161-2170.
- Prineas, J. W., E. E. Kwon, P. Z. Goldenberg, A. A. Ilyas, R. H. Quarles, J. A. Benjamins and T. J. Sprinkle (1989). "Multiple sclerosis. Oligodendrocyte proliferation and differentiation in fresh lesions." *Lab Invest* 61(5): 489-503.
- Prineas, J. W. and F. Connell (1979). "Remyelination in multiple sclerosis." *Ann Neurol* 5(1): 22-31.
- Pringle, N. P. and W. D. Richardson (1993). "A singularity of PDGF alpha-receptor expression in the dorsoventral axis of the neural tube may define the origin of the oligodendrocyte lineage." *Development* 117(2): 525-533.

- Prinz, M., Erny, D., & Hagemeyer, N. (2017). Ontogeny and homeostasis of CNS myeloid cells. *Nature immunology*, 18(4), 385–392.
- Prinz, M. and J. Priller (2014). "Microglia and brain macrophages in the molecular age: from origin to neuropsychiatric disease." *Nat Rev Neurosci* 15(5): 300-312.
- Raine, C. S., L. Scheinberg and J. M. Waltz (1981). "Multiple sclerosis. Oligodendrocyte survival and proliferation in an active established lesion." *Lab Invest* 45(6): 534-546.
- Rawji, K. S., Gonzalez Martinez, G. A., Sharma, A., & Franklin, R. (2020). The Role of Astrocytes in Remyelination. *Trends in neurosciences*, S0166-2236(20)30124-7. Advance online publication.
- Reddy, D. S. (2010). "Neurosteroids: endogenous role in the human brain and therapeutic potentials." *Prog Brain Res* 186: 113-137.
- Richardson, W. D., H. K. Smith, T. Sun, N. P. Pringle, A. Hall and R. Woodruff (2000). "Oligodendrocyte lineage and the motor neuron connection." *Glia* 29(2): 136-142.
- Richardson, W. D., N. Kessaris and N. Pringle (2006). "Oligodendrocyte wars." *Nat Rev Neurosci* 7(1): 11-18.
- Robinson, A. P., C. T. Harp, A. Noronha and S. D. Miller (2014). "The experimental autoimmune encephalomyelitis (EAE) model of MS: utility for understanding disease pathophysiology and treatment." *Handb Clin Neurol* 122: 173-189.
- Rodriguez-Tebar, A., G. Dechant and Y. A. Barde (1990). "Binding of brain-derived neurotrophic factor to the nerve growth factor receptor." *Neuron* 4(4): 487-492.
- Rosen, C. L., R. P. Bunge, M. D. Ard and P. M. Wood (1989). "Type 1 astrocytes inhibit myelination by adult rat oligodendrocytes in vitro." *J Neurosci* 9(10): 3371-3379.
- Rosenberg, S. S., E. E. Kelland, E. Tokar, A. R. De la Torre and J. R. Chan (2008). "The geometric and spatial constraints of the microenvironment induce oligodendrocyte differentiation." *Proc Natl Acad Sci U S A* 105(38): 14662-14667.
- Rotola, A., I. Merlotti, L. Caniatti, E. Caselli, E. Granieri, M. R. Tola, D. Di Luca and E. Cassai (2004). "Human herpesvirus 6 infects the central nervous system of multiple sclerosis patients in the early stages of the disease." *Mult Scler* 10(4): 348-354.
- Rowitch, D. H. (2004). "Glial specification in the vertebrate neural tube." *Nat Rev Neurosci* 5(5): 409-419.
- Rowitch, D. H. and A. R. Kriegstein (2010). "Developmental genetics of vertebrate glial-cell specification." *Nature* 468(7321): 214-222.
- Ruiz-Ederra, J., Hitchcock, P. F., & Vecino, E. (2003). Two classes of astrocytes in the adult human and pig retina in terms of their expression of high affinity NGF receptor (TrkA). *Neurosci Lett*, 337(3), 127-130.

- Saijo, K., J. G. Collier, A. C. Li, J. A. Katzenellenbogen and C. K. Glass (2011). "An ADIOL- ERbeta-CtBP transrepression pathway negatively regulates microglia-mediated inflammation." *Cell* 145(4): 584-595.
- Sakurai, Y., D. Nishimura, K. Yoshimura, Y. Tsuruo, C. Seiwa and H. Asou (1998). "Differentiation of oligodendrocyte occurs in contact with astrocyte." *J Neurosci Res* 52(1): 17-26.
- Samanta, J., E. M. Grund, H. M. Silva, J. J. Lafaille, G. Fishell and J. L. Salzer (2015). "Inhibition of Gli1 mobilizes endogenous neural stem cells for remyelination." *Nature* 526(7573): 448-452.
- Santambrogio, L., M. Benedetti, M. V. Chao, R. Muzaffar, K. Kulig, N. Gabellini and G. Hochwald (1994). "Nerve growth factor production by lymphocytes." *J Immunol* 153(10): 4488-4495.
- Sasi, M., Vignoli, B., Canossa, M., & Blum, R. (2017). Neurobiology of local and intercellular BDNF signaling. *Pflugers Arch*, 469(5-6), 593-610. doi:10.1007/s00424-017-1964-4
- Schumacher, M., Weill-Engerer, S., Liere, P., Robert, F., Franklin, R. J., Garcia-Segura, L. M., . . . Akwa, Y. (2003). Steroid hormones and neurosteroids in normal and pathological aging of the nervous system. *Prog Neurobiol*, 71(1), 3-29.
- Scolding, N., R. Franklin, S. Stevens, C. H. Heldin, A. Compston and J. Newcombe (1998). "Oligodendrocyte progenitors are present in the normal adult human CNS and in the lesions of multiple sclerosis." *Brain* 121 ( Pt 12): 2221-2228.
- Shooter, E. M. (2001). "Early days of the nerve growth factor proteins." *Annu Rev Neurosci* 24: 601-629.
- Silver, J., & Miller, J. H. (2004). Regeneration beyond the glial scar. *Nat Rev Neurosci*, 5(2), 146-156.
- Skripuletz and M. Stangel (2013). "Cuprizone [bis(cyclohexylidenehydrazide)] is selectively toxic for mature oligodendrocytes." *Neurotox Res* 24(2): 244-250.
- Sloane, J. A., C. Batt, Y. Ma, Z. M. Harris, B. Trapp and T. Vartanian (2010). "Hyaluronan blocks oligodendrocyte progenitor maturation and remyelination through TLR2." *Proc Natl Acad Sci U S A* 107(25): 11555-11560.
- Snaidero, N., W. Mobius, T. Czopka, L. H. Hekking, C. Mathisen, D. Verkleij, S. Goebbels, J. Edgar, D. Merkler, D. A. Lyons, K. A. Nave and M. Simons (2014). "Myelin membrane wrapping of CNS axons by PI(3,4,5)P3-dependent polarized growth at the inner tongue." *Cell* 156(1-2): 277-290.
- Sofroniew, M. V., & Vinters, H. V. (2010). Astrocytes: biology and pathology. *Acta Neuropathol*, 119(1), 7-35.
- Soulet, D. and S. Rivest (2008). "Microglia." *Curr Biol* 18(12): R506-508.

Stadelmann, C., Timmler, S., Barrantes-Freer, A., & Simons, M. (2019). Myelin in the Central Nervous System: Structure, Function, and Pathology. *Physiol Rev*, *99*(3), 1381-1431.

Stankoff, B., M. S. Aigrot, F. Noel, A. Wattilliaux, B. Zalc and C. Lubetzki (2002). "Ciliary neurotrophic factor (CNTF) enhances myelin formation: a novel role for CNTF and CNTF-related molecules." *J Neurosci* *22*(21): 9221-9227.

Stassart, R. M., Möbius, W., Nave, K. A., & Edgar, J. M. (2018). The Axon-Myelin Unit in Development and Degenerative Disease. *Front Neurosci*, *12*, 467.

Strohmaier, C., B. D. Carter, R. Urfer, Y. A. Barde and G. Dechant (1996). "A splice variant of the neurotrophin receptor trkB with increased specificity for brain-derived neurotrophic factor." *EMBO J* *15*(13): 3332-3337.

Sun, T., N. P. Pringle, A. P. Hardy, W. D. Richardson and H. K. Smith (1998). "Pax6 influences the time and site of origin of glial precursors in the ventral neural tube." *Mol Cell Neurosci* *12*(4-5): 228-239.

Swinnen, N., Smolders, S., Avila, A., Notelaers, K., Paesen, R., Ameloot, M., Brône, B., Legendre, P., & Rigo, J. M. (2013). Complex invasion pattern of the cerebral cortex by microglial cells during development of the mouse embryo. *Glia*, *61*(2), 150–163.

Takano, R., S. Hisahara, K. Namikawa, H. Kiyama, H. Okano and M. Miura (2000). "Nerve growth factor protects oligodendrocytes from tumor necrosis factor-alpha-induced injury through Akt- mediated signaling mechanisms." *J Biol Chem* *275*(21): 16360-16365.

Tamashiro, T. T., Dalgard, C. L., & Byrnes, K. R. (2012). Primary microglia isolation from mixed glial cell cultures of neonatal rat brain tissue. *Journal of Visualized Experiment* e3814

Tang, Y., & Le, W. (2016). Differential Roles of M1 and M2 Microglia in Neurodegenerative Diseases. *Mol Neurobiol*, *53*(2), 1181-1194.

Taveggia, C., P. Thaker, A. Petrylak, G. L. Caporaso, A. Toews, D. L. Falls, S. Einheber and J. L. Salzer (2008). "Type III neuregulin-1 promotes oligodendrocyte myelination." *Glia* *56*(3): 284- 293.

Thion, M. S., & Garel, S. (2017). On place and time: microglia in embryonic and perinatal brain development. *Current opinion in neurobiology*, *47*, 121–130.

Thion, M. S., Ginhoux, F., & Garel, S. (2018). Microglia and early brain development: An intimate journey. *Science (New York, N.Y.)*, *362*(6411), 185–189.

Thion, M. S., Low, D., Silvin, A., Chen, J., Grisel, P., Schulte-Schrepping, J., Blecher, R., Ulas, T., Squarzoni, P., Hoeffel, G., Couplier, F., Siopi, E., David, F. S., Scholz, C., Shihui, F., Lum, J., Amoyo, A. A., Larbi, A., Poidinger, M., Buttgerit, A., ... Garel, S. (2018). Microbiome Influences Prenatal and Adult Microglia in a Sex-Specific Manner. *Cell*, *172*(3), 500–516.e16.

Thoenen H. (2000). Neurotrophins and activity-dependent plasticity. *Progress in brain research*, *128*, 183–191.

Tomassy, G. S. and V. Fossati (2014). "How big is the myelinating orchestra? Cellular diversity within the oligodendrocyte lineage: facts and hypotheses." *Front Cell Neurosci* 8: 201.

Tsiperson, V., Huang, Y., Bagayogo, I., Song, Y., VonDran, M. W., DiCicco-Bloom, E., & Dreyfus, C. F. (2015). Brain-derived neurotrophic factor deficiency restricts proliferation of oligodendrocyte progenitors following cuprizone-induced demyelination. *ASN Neuro*, 7(1).

Tsoka, P., Matsumoto, H., Maidana, D. E., Kataoka, K., Naoumidi, I., Gravanis, A., Vavvas, D. G., & Tsilimbaris, M. K. (2018). Effects of BNN27, a novel C17-spiroepoxy steroid derivative, on experimental retinal detachment-induced photoreceptor cell death. *Scientific reports*, 8(1), 10661.

Trapp, B. D. (2004). "Pathogenesis of multiple sclerosis: the eyes only see what the mind is prepared to comprehend." *Ann Neurol* 55(4): 455-457.

Trapp, B. D., A. Nishiyama, D. Cheng and W. Macklin (1997). "Differentiation and death of premyelinating oligodendrocytes in developing rodent brain." *J Cell Biol* 137(2): 459-468.

Trebst, C., F. Konig, R. Ransohoff, W. Bruck and M. Stangel (2008). "CCR5 expression on macrophages/microglia is associated with early remyelination in multiple sclerosis lesions." *Mult Scler* 14(6): 728-733.

Trigos, A. S., M. Longart, L. Garcia, C. Castillo, P. Forsyth and R. Medina (2015). "ProNGF derived from rat sciatic nerves downregulates neurite elongation and axon specification in PC12 cells." *Front Cell Neurosci* 9: 364.

Villa, A., Gelosa, P., Castiglioni, L., Cimino, M., Rizzi, N., Pepe, G., Lolli, F., Marcello, E., Sironi, L., Vegeto, E., & Maggi, A. (2018). Sex-Specific Features of Microglia from Adult Mice. *Cell reports*, 23(12), 3501–3511.

Villoslada, P., S. L. Hauser, I. Bartke, J. Unger, N. Heald, D. Rosenberg, S. W. Cheung, W. C. Mobley, S. Fisher and C. P. Genain (2000). "Human nerve growth factor protects common marmosets against autoimmune encephalomyelitis by switching the balance of T helper cell type 1 and 2 cytokines within the central nervous system." *J Exp Med* 191(10): 1799-1806.

Volterra, A., & Meldolesi, J. (2005). Astrocytes, from brain glue to communication elements: the revolution continues. *Nat Rev Neurosci*, 6(8), 626-640.

Vondran, M. W., Clinton-Luke, P., Honeywell, J. Z., & Dreyfus, C. F. (2010). BDNF<sup>±</sup> mice exhibit deficits in oligodendrocyte lineage cells of the basal forebrain. *Glia*, 58(7), 848–856.

VonDran, M. W., Singh, H., Honeywell, J. Z., & Dreyfus, C. F. (2011). Levels of BDNF impact oligodendrocyte lineage cells following a cuprizone lesion. *J Neurosci*, 31(40), 14182-14190.

Wang, H., S. Liu, Y. Tian, X. Wu, Y. He, C. Li, M. Namaka, J. Kong, H. Li and L. Xiao (2015). "Quetiapine Inhibits Microglial Activation by Neutralizing Abnormal STIM1-



Mediated Intercellular Calcium Homeostasis and Promotes Myelin Repair in a Cuprizone-Induced Mouse Model of Demyelination." *Front Cell Neurosci* 9: 492.

Wang, L., X. Chang, L. She, D. Xu, W. Huang and M. M. Poo (2015). "Autocrine action of BDNF on dendrite development of adult-born hippocampal neurons." *J Neurosci* 35(22): 8384-8393.

Wang, Y., X. Cheng, Q. He, Y. Zheng, D. H. Kim, S. R. Whittemore and Q. L. Cao (2011). "Astrocytes from the contused spinal cord inhibit oligodendrocyte differentiation of adult oligodendrocyte precursor cells by increasing the expression of bone morphogenetic proteins." *J Neurosci* 31(16): 6053-6058.

Warf, B. C., J. Fok-Seang and R. H. Miller (1991). "Evidence for the ventral origin of oligodendrocyte precursors in the rat spinal cord." *J Neurosci* 11(8): 2477-2488.

Watkins, T. A., B. Emery, S. Mulinyawe and B. A. Barres (2008). "Distinct stages of myelination regulated by gamma-secretase and astrocytes in a rapidly myelinating CNS coculture system." *Neuron* 60(4): 555-569.

Weill-Engerer, S., David, J. P., Sazdovitch, V., Liere, P., Eychenne, B., Pianos, A., . . . Akwa, Y. (2002). Neurosteroid quantification in human brain regions: comparison between Alzheimer's and nondemented patients. *J Clin Endocrinol Metab*, 87(11), 5138-5143.

Weill-Engerer, S., David, J. P., Sazdovitch, V., Liere, P., Schumacher, M., Delacourte, A., . . . Akwa, Y. (2003). In vitro metabolism of dehydroepiandrosterone (DHEA) to 7alpha-hydroxy-DHEA and Delta5-androstene-3beta,17beta-diol in specific regions of the aging brain from Alzheimer's and non-demented patients. *Brain Res*, 969(1-2), 117-125.

Wolswijk, G. (1998). "Chronic stage multiple sclerosis lesions contain a relatively quiescent population of oligodendrocyte precursor cells." *J Neurosci* 18(2): 601-609.

Wolswijk, G. (1998). "Oligodendrocyte regeneration in the adult rodent CNS and the failure of this process in multiple sclerosis." *Prog Brain Res* 117: 233-247.

Wong, A. W., Giuffrida, L., Wood, R., Peckham, H., Gonsalvez, D., Murray, S. S., . . . Xiao, J. (2014). TDP6, a brain-derived neurotrophic factor-based trkB peptide mimetic, promotes oligodendrocyte myelination. *Mol Cell Neurosci*, 63, 132-140.

Xiao, J., Wong, A. W., Willingham, M. M., van den Buuse, M., Kilpatrick, T. J., & Murray, S. S. (2010). Brain-derived neurotrophic factor promotes central nervous system myelination via a direct effect upon oligodendrocytes. *Neuro-Signals*, 18(3), 186–202.

Yajima, K. and K. Suzuki (1979). "Demyelination and remyelination in the rat central nervous system following ethidium bromide injection." *Lab Invest* 41(5): 385-392.

Yan, Q., Elliott, J., & Snider, W. D. (1992). Brain-derived neurotrophic factor rescues spinal motor neurons from axotomy-induced cell death. *Nature* 360:753–5.

Yang, J., L. C. Harte-Hargrove, C. J. Siao, T. Marinic, R. Clarke, Q. Ma, D. Jing, J. J. Lafrancois, K. G. Bath, W. Mark, D. Ballon, F. S. Lee, H. E. Scharfman and B. L.

- Hempstead (2014). "proBDNF negatively regulates neuronal remodeling, synaptic transmission, and synaptic plasticity in hippocampus." *Cell Rep* 7(3): 796-806.
- Yeung, M. S., S. Zdunek, O. Bergmann, S. Bernard, M. Salehpour, K. Alkass, S. Perl, J. Tisdale, G. Possnert, L. Brundin, H. Druid and J. Frisen (2014). "Dynamics of oligodendrocyte generation and myelination in the human brain." *Cell* 159(4): 766-774.
- Yi, X., Manickam, D. S., Brynskikh, A., & Kabanov, A. V. (2014). Agile delivery of protein therapeutics to CNS. *Journal of Controlled Release* 190:637–63
- Young, K. M., K. Psachoulia, R. B. Tripathi, S. J. Dunn, L. Cossell, D. Attwell, K. Tohyama and W. D. Richardson (2013). "Oligodendrocyte dynamics in the healthy adult CNS: evidence for myelin remodeling." *Neuron* 77(5): 873-885.
- Zalc, B. and D. R. Colman (2000). "Origins of vertebrate success." *Science* 288(5464): 271-272.
- Zawadzka, M., L. E. Rivers, S. P. Fancy, C. Zhao, R. Tripathi, F. Jamen, K. Young, A. Goncharevich, H. Pohl, M. Rizzi, D. H. Rowitch, N. Kessaris, U. Suter, W. D. Richardson and R. J. Franklin (2010). "CNS-resident glial progenitor/stem cells produce Schwann cells as well as oligodendrocytes during repair of CNS demyelination." *Cell Stem Cell* 6(6): 578-590.
- Zeger, M., G. Popken, J. Zhang, S. Xuan, Q. R. Lu, M. H. Schwab, K. A. Nave, D. Rowitch, A. J. D'Ercole and P. Ye (2007). "Insulin-like growth factor type 1 receptor signaling in the cells of oligodendrocyte lineage is required for normal in vivo oligodendrocyte development and myelination." *Glia* 55(4): 400-411.
- Zhao, L., M. L. Yeh and E. S. Levine (2015). "Role for Endogenous BDNF in Endocannabinoid-Mediated Long-Term Depression at Neocortical Inhibitory Synapses." *eNeuro* 2(2).
- Zhu, Q., X. Zhao, K. Zheng, H. Li, H. Huang, Z. Zhang, T. Mastracci, M. Wegner, Y. Chen, L. Sussel and M. Qiu (2014). "Genetic evidence that Nkx2.2 and Pdgfra are major determinants of the timing of oligodendrocyte differentiation in the developing CNS." *Development* 141(3): 548-555.
- Zoupa, E., Gravanis, A., & Pitsikas, N. (2019). The novel dehydroepiandrosterone (DHEA) derivative BNN27 counteracts behavioural deficits induced by the NMDA receptor antagonist ketamine in rats. *Neuropharmacology*, 151, 74–83.  
<https://doi.org/10.1016/j.neuropharm.2019.04.001>
- Zwain, I. H. and S. S. Yen (1999). "Neurosteroidogenesis in astrocytes, oligodendrocytes, and neurons of cerebral cortex of rat brain." *Endocrinology* 140(8): 3843-3852.

## REFERENCES II

- Austin SA, Sens MA, Combs CK (2009) Amyloid precursor protein mediates a tyrosine kinase-dependent activation response in endothelial cells. *J Neurosci* 29(46): 14451-62. doi: 10.1523/JNEUROSCI.3107-09.2009
- Bailly, Y., Kyriakopoulou, K., Delhaye-Bouchaud, N., Mariani, J., & Karagogeos, D. (1996). Cerebellar granule cell differentiation in mutant and X-irradiated rodents revealed by the neural adhesion molecule TAG-1. *The Journal of comparative neurology*, 369(1), 150–161. [https://doi.org/10.1002/\(SICI\)1096-9861\(19960520\)369:1<150::AID-CNE11>3.0.CO;2-V](https://doi.org/10.1002/(SICI)1096-9861(19960520)369:1<150::AID-CNE11>3.0.CO;2-V)
- Brakeman JS, Gu SH, Wang XB, Dolin G, Baraban JM (1999) Neuronal localization of the Adenomatous polyposis coli tumor suppressor protein. *Neuroscience* 91(2): 661-72
- Brümmendorf T, Rathjen FG (1996) Structure/function relationships of axon-associated adhesion receptors of the immunoglobulin superfamily. *Curr Opin Neurobiol* 6(5): 584-93
- Buttiglione, M., Revest, J. M., Pavlou, O., Karagogeos, D., Furley, A., Rougon, G., & Faivre-Sarrailh, C. (1998). A functional interaction between the neuronal adhesion molecules TAG-1 and F3 modulates neurite outgrowth and fasciculation of cerebellar granule cells. *The Journal of neuroscience : the official journal of the Society for Neuroscience*, 18(17), 6853–6870.
- Chatzopoulou E, Miguez A, Savvaki M, Levasseur G, Muzerelle A, Muriel MP, Goureau O, Watanabe K, Goutebroze L, Gaspar P, Zalc B, Karagogeos D, Thomas JL (2008) Structural requirement of TAG-1 for retinal ganglion cell axons and myelin in the mouse optic nerve. *J Neurosci* 28(30): 7624-36. doi: 10.1523/JNEUROSCI.1103-08.2008
- Denaxa, M., Chan, C. H., Schachner, M., Parnavelas, J. G., & Karagogeos, D. (2001). The adhesion molecule TAG-1 mediates the migration of cortical interneurons from the ganglionic eminence along the corticofugal fiber system. *Development (Cambridge, England)*, 128(22), 4635–4644.
- Denaxa, M., Kyriakopoulou, K., Theodorakis, K., Trichas, G., Vidaki, M., Takeda, Y., Watanabe, K., & Karagogeos, D. (2005). The adhesion molecule TAG-1 is required for proper migration of the superficial migratory stream in the medulla but not of cortical interneurons. *Developmental biology*, 288(1), 87–99.
- Denaxa, M., Pavlou, O., Tsiotra, P., Papadopoulos, G. C., Liapaki, K., Theodorakis, K., Papadaki, C., Karagogeos, D., & Papamatheakis, J. (2003). The upstream regulatory region of the gene for the human homologue of the adhesion molecule TAG-1 contains elements driving neural specific expression in vivo. *Brain research. Molecular brain research*, 118(1-2), 91–101.
- Derfuss T, Parikh K, Velhin S, Braun M, Mathey E, Krumbholz M, Kümpfel T, Moldenhauer A, Rader C, Sonderegger P, Pöllmann W, Tiefenthaller C, Bauer J, Lassmann H, Wekerle H, Karagogeos D, Hohlfeld R, Linington C, Meinl E (2009) Contactin-2/TAG-1-directed autoimmunity is identified in multiple sclerosis patients and mediates gray matter pathology in animals. *Proc Natl Acad Sci U S A* 106(20): 8302-7.

Dodd J, Morton SB, Karagogeos D, Yamamoto M, Jessell TM (1988) Spatial regulation of axonal glycoprotein expression on subsets of embryonic spinal neurons. *Neuron* 1(2): 105-116

Fancy SP, Chan JR, Baranzini SE, Franklin RJ, Rowitch DH (2011) Myelin regeneration: a recapitulation of development? *Annu Rev Neurosci* 34: 21-43. doi: 10.1146/annurev-neuro-061010-113629

Fields RD (2015) A new mechanism of nervous system plasticity: activity-dependent myelination. *Nat Rev Neurosci* 16(12): 756-67.

Furley AJ, Morton SB, Manalo D, Karagogeos D, Dodd J, Jessell TM (1990) The axonal glycoprotein TAG-1 is an immunoglobulin superfamily member with neurite outgrowth-promoting activity. *Cell* 61(1): 157-70.

Gascon E, Vutskits L, Kiss JZ (2010) The role of PSA-NCAM in adult neurogenesis. *Adv Exp Med Biol* 663: 127-36.

Gautam V, D'Avanzo C, Hebisch M, Kovacs DM, Kim DY (2014) BACE1 activity regulates cell surface contactin-2 levels. *Mol Neurodegener* 9: 4.

Gennarini G, Furley A (2017) Cell adhesion molecules in neural development and disease. *Mol Cell Neurosci* 81: 1-3.

Hadas Y, Nitzan N, Furley AJ, Kozlov SV, Klar A (2013) Distinct cis regulatory elements govern the expression of TAG1 in embryonic sensory ganglia and spinal cord. *PLoS One* 8(2): e57960.

Iijima M, Tomita M, Morozumi S, Kawagashira Y, Nakamura T, Koike H, Katsuno M, Hattori N, Tanaka F, Yamamoto M, Sobue G (2009) Single nucleotide polymorphism of TAG-1 influences IVIg responsiveness of Japanese patients with CIDP. *Neurology* Oct 27;73(17):1348-52. Epub 2009 Sep 23. PubMed PMID: 19776380

Jenkinson M, Beckmann CF, Behrens TE, Woolrich MW, Smith SM (2012) FSL. *Neuroimage* 62(2): 782-90.

Kalafatakis, I., Kalafatakis, K., Tsimpolis, A., Giannakeas, N., Tsipouras, M., Tzallas, A., & Karagogeos, D. (2020). Using the Allen gene expression atlas of the adult mouse brain to gain further insight into the physiological significance of TAG-1/Contactin-2. *Brain structure & function*, 10.1007/s00429-020-02108-4. Advance online publication.

Kalafatakis K, Giannakeas N, Lightman SL, Charalampopoulos I, Russell GM, Tsipouras M, Tzallas A (2019) Utilization of the allen gene expression atlas to gain further insight into glucocorticoid physiology in the adult mouse brain. *Neurosci Lett* 706: 194-200.

Karagogeos D (2003) Neural GPI-anchored cell adhesion molecules. *Front Biosci* 8: s1304-20.

Karagogeos D, Morton SB, Casano F, Dodd J, Jessell TM (1991) Developmental expression of the axonal glycoprotein TAG-1: differential regulation by central and peripheral neurons in vitro. *Development* 112(1): 51-67

- Kasahara K, Watanabe K, Kozutsumi Y, Oohira A, Yamamoto T, Sanai Y (2002) Association of GPI-anchored protein TAG-1 with src-family kinase Lyn in lipid rafts of cerebellar granule cells. *Neurochem Res* 27(7-8): 823-9
- Koenning M, Jackson S, Hay CM, Faux C, Kilpatrick TJ, Willingham M, Emery B (2012) Myelin gene regulatory factor is required for maintenance of myelin and mature oligodendrocyte identity in the adult CNS. *J Neurosci* 32(36): 12528-42.
- Kuhn PH, Koroniak K, Hogl S, Colombo A, Zeitschel U, Willem M, Volbracht C, Schepers U, Imhof A, Hoffmeister A, Haass C, Roßner S, Bräse S, Lichtenthaler SF (2012) Secretome protein enrichment identifies physiological BACE1 protease substrates in neurons. *EMBO J* 31(14): 3157-68.
- Kyriakopoulou, K., de Diego, I., Wassef, M., & Karagogeos, D. (2002). A combination of chain and neurophilic migration involving the adhesion molecule TAG-1 in the caudal medulla. *Development (Cambridge, England)*, 129(2), 287–296.
- Lein ES, Hawrylycz MJ, Ao N, Ayres M, Bensinger A, Bernard A, Boe AF, Boguski MS, Brockway KS, Byrnes EJ, Chen L, Chen L, Chen TM, Chin MC, Chong J, Crook BE, Czaplinska A, Dang CN, Datta S, Dee NR, Desaki AL, Desta T, Diep E, Dolbeare TA, Donelan MJ, Dong HW, Dougherty JG, Duncan BJ, Ebbert AJ, Eichele G, Estin LK, Faber C, Facer BA, Fields R, Fischer SR, Fliss TP, Frensley C, Gates SN, Glattfelder KJ, Halverson KR, Hart MR, Hohmann JG, Howell MP, Jeung DP, Johnson RA, Karr PT, Kawal R, Kidney JM, Knapik RH, Kuan CL, Lake JH, Laramie AR, Larsen KD, Lau C, Lemon TA, Liang AJ, Liu Y, Luong LT, Michaels J, Morgan JJ, Morgan RJ, Mortrud MT, Mosqueda NF, Ng LL, Ng R, Orta GJ, Overly CC, Pak TH, Parry SE, Pathak SD, Pearson OC, Puchalski RB, Riley ZL, Rockett HR, Rowland SA, Royall JJ, Ruiz MJ, Sarno NR, Schaffnit K, Shapovalova NV, Sivisay T, Slaughterbeck CR, Smith SC, Smith KA, Smith BI, Sodt AJ, Stewart NN, Stumpf KR, Sunkin SM, Sutram M, Tam A, Teemer CD, Thaller C, Thompson CL, Varnam LR, Visel A, Whitlock RM, Wohnoutka PE, Wolkey CK, Wong VY, Wood M, Yaylaoglu MB, Young RC, Youngstrom BL, Yuan XF, Zhang B, Zwingman TA, Jones AR (2007) Genome-wide atlas of gene expression in the adult mouse brain. *Nature* 445(7124): 10573-81
- Levy JB, Canoll PD, Silvennoinen O, Barnea G, Morse B, Honegger AM, Huang JT, Cannizzaro LA, Park SH, Druck T, et al. (1993) The cloning of a receptor-type protein tyrosine phosphatase expressed in the central nervous system. *J Biol Chem* 268(14): 10573-81
- Lieberoth A, Splittstoesser F, Katagihallimath N, Jakovcevski I, Loers G, Ranscht B, Karagogeos D, Schachner M, Kleene R (2009) Lewis(x) and alpha2,3-sialyl glycans and their receptors TAG-1, Contactin, and L1 mediate CD24-dependent neurite outgrowth. *J Neurosci* 29(20): 6677-90.
- Ma QH, Futagawa T, Yang WL, Jiang XD, Zeng L, Takeda Y, Xu RX, Bagnard D, Schachner M, Furley AJ, Karagogeos D, Watanabe K, Dawe GS, Xiao ZC (2008) A TAG1-APP signalling pathway through Fe65 negatively modulates neurogenesis. *Nat Cell Biol* 10(3): 283-94.
- Masuda T (2017) Contactin-2/TAG-1, active on the front line for three decades. *Cell Adh Migr* 11(5-6): 524-531.

Masuda T, Okado N, Shiga T (2000) The involvement of axonin-1/SC2 in mediating notochord-derived chemorepulsive activities for dorsal root ganglion neurites. *Dev Biol* 224: 112-21.

Milev P, Maurel P, Häring M, Margolis RK, Margolis RU (1996) TAG-1/axonin-1 is a high-affinity ligand of neurocan, phosphacan/protein-tyrosine phosphatase-zeta/beta, and N-CAM. *J Biol Chem* 271(26): 15716-23

Namba T, Kibe Y, Funahashi Y, Nakamuta S, Takano T, Ueno T, Shimada A, Kozawa S, Okamoto M, Shimoda Y, Oda K, Wada Y, Masuda T, Sakakibara A, Igarashi M, Miyata T, Faivre-Sarrailh C, Takeuchi K, Kaibuchi K (2014) Pioneering axons regulate neuronal polarization in the developing cerebral cortex. *Neuron* 81: 814-29.

Ng L, Bernard A, Lau C, Overly CC, Dong HW, Kuan C, Pathak S, Sunkin SM, Dang C, Bohland JW, Bokil H, Mitra PP, Puellas L, Hohmann J, Anderson DJ, Lein ES, Jones AR, Hawrylycz M (2009) An anatomic gene expression atlas of the adult mouse brain. *Nat Neurosci* 12(3): 356-62.

Okamoto M, Namba T, Shinoda T, Kondo T, Watanabe T, Inoue Y, Takeuchi K, Enomoto Y, Ota K, Oda K, Wada Y, Sagou K, Saito K, Sakakibara A, Kawaguchi A, Nakajima K, Adachi T, Fujimori T, Ueda M, Hayashi S, Kaibuchi K, Miyata T (2013) TAG-1-assisted progenitor elongation streamlines nuclear migration to optimize subapical crowding. *Nat Neurosci* 16: 1556-66.

Pinatel D, Hivert B, Saint-Martin M, Noraz N, Savvaki M, Karagogeos D, Faivre-Sarrailh C (2017) The Kv1-associated molecules TAG-1 and Caspr2 are selectively targeted to the axon initial segment in hippocampal neurons. *J Cell Sci* 130(13): 2209-2220.

Poliak S, Salomon D, Elhanany H, Sabanay H, Kiernan B, Pevny L, Stewart CL, Xu X, Chiu SY, Shrager P, Furley AJ, Peles E (2003) Juxtaparanodal clustering of Shaker-like K<sup>+</sup> channels in myelinated axons depends on Caspr2 and TAG-1. *J Cell Biol* 162(6): 1149-60

Savvaki M, Panagiotaropoulos T, Stamatakis A, Sargiannidou I, Karatzioula P, Watanabe K, Stylianopoulou F, Karagogeos D, Kleopa KA (2008) Impairment of learning and memory in TAG-1 deficient mice associated with shorter CNS internodes and disrupted juxtaparanodes. *Mol Cell Neurosci* 39(3): 478-90.

Savvaki, M., Theodorakis, K., Zoupi, L., Stamatakis, A., Tivodar, S., Kyriacou, K., Stylianopoulou, F., & Karagogeos, D. (2010). The expression of TAG-1 in glial cells is sufficient for the formation of the juxtaparanodal complex and the phenotypic rescue of tag-1 homozygous mutants in the CNS. *The Journal of neuroscience : the official journal of the Society for Neuroscience*, 30(42), 13943–13954.

Stoeckli ET, Kuhn TB, Duc CO, Ruegg MA, Sonderegger P (1991) The axonally secreted protein axonin-1 is a potent substratum for neurite growth. *J Cell Biol* 112:449-55.

Stogmann E, Reinthaler E, Eltawil S, El Etribi MA, Hemeda M, El Nahhas N, Gaber AM, Fouad A, Edris S, Benet-Pages A, Eck SH, Patariaia E, Mei D, Brice A, Lesage S, Guerrini R, Zimprich F, Strom TM, Zimprich A (2013) Autosomal recessive cortical myoclonic tremor and epilepsy: association with a mutation in the potassium channel associated gene CNTN2. *Brain* Apr;136(Pt 4):1155-60. Epub 2013 Mar 21. PubMed PMID: 23518707

Paz Soldán MM, Pirko I (2012) Biogenesis and significance of central nervous system myelin. *Semin Neurol* 32(1): 9-14.

Tabula Muris Consortium, Overall coordination, Logistical coordination, Organ collection and processing, Library preparation and sequencing, Computational data analysis, Cell type annotation, Writing group, Supplemental text writing group, & Principal investigators (2018). Single-cell transcriptomics of 20 mouse organs creates a Tabula Muris. *Nature*, 562(7727), 367–372.

Tachi N, Hashimoto Y, Nawa M, Matsuoka M (2010) TAG-1 is an inhibitor of TGFbeta2-induced neuronal death via amyloid beta precursor protein. *Biochem Biophys Res Commun* 394(1): 119-25.

Theodosiou T, Papanikolaou N, Savvaki M, Bonetto G, Maxouri S, Fakourelis E, Elioupoulos AG, Tavernarakis N, Amoutzias GD, Pavlopoulos GA, Aivaliotis M, Nikolettou V, Tzamarias D, Karagogeos D, Iliopoulos I (2020) UniProt-Related Documents (UniReD): assisting wet lab biologists in their quest on finding novel counterparts in a protein network. *NAR Genomics and Bioinformatics*, 2020, Vol. 2, No. 1

Traka M, Dupree JL, Popko B, Karagogeos D (2002) The neuronal adhesion protein TAG-1 is expressed by Schwann cells and oligodendrocytes and is localized to the juxtaparanodal region of myelinated fibers. *J Neurosci* 22(8): 3016-24

Traka M, Goutebroze L, Denisenko N, Bessa M, Nifli A, Havaki S, Iwakura Y, Fukamauchi F, Watanabe K, Soliven B, Girault JA, Karagogeos D (2003) Association of TAG-1 with Caspr2 is essential for the molecular organization of juxtaparanodal regions of myelinated fibers. *J Cell Biol* 162(6): 1161-72

Wang, W., Karagogeos, D., & Kilpatrick, D. L. (2011). The effects of Tag-1 on the maturation of mouse cerebellar granule neurons. *Cellular and molecular neurobiology*, 31(3), 351–356.

Xenaki D, Martin IB, Yoshida L, Ohyama K, Gennarini G, Grumet M, Sakurai T, Furley AJ (2011) F3/contactin and TAG1 play antagonistic roles in the regulation of sonic hedgehog-induced cerebellar granule neuron progenitor proliferation. *Development* 138: 519-29.

Yamamoto M, Boyer AM, Crandall JE, Edwards M, Tanaka H (1986) Distribution of stage-specific neurite-associated proteins in the developing murine nervous system recognized by a monoclonal antibody. *J Neurosci* 6(12): 3576-94

Yan Y, Jiang Y (2016) RACK1 affects glioma cell growth and differentiation through the CNTN2-mediated RTK/Ras/MAPK pathway. *Int J Mol Med* 37(1): 251-7.

Zaldivar A, Krichmar JL (2014) Allen Brain Atlas-Driven Visualizations: a web-based gene expression energy visualization tool. *Front Neuroinform* 8: 51.

Zhou L, Barão S, Laga M, Bockstael K, Borgers M, Gijssen H, Annaert W, Moechars D, Mercken M, Gevaert K, De Strooper B (2012) The neural cell adhesion molecules L1 and CHL1 are cleaved by BACE1 protease in vivo. *J Biol Chem* 287(31): 25927-40.

Zoupi L, Savvaki M, Kalemaki K, Kalafatakis I, Sidiropoulou K, Karagogeos D (2018) The function of contactin-2/TAG-1 in oligodendrocytes in health and demyelinating pathology. *Glia* 66(3): 576-591.

Zoupi L, Savvaki M, Karagogeos D (2011) Axons and myelinating glia: An intimate contact. *IUBMB Life* 63(9): 730-5.



## APPENDIX

Table 1: Primary antibodies used in this study

Antibody	Source	Type	Directed against	Working dilution	Application
a-PLP	Abcam (ab28486)	Rabbit, polyclonal	Human, Mouse, Rabbit, Rat	1/1000	ICC, IHC
a-MBP	Serotec	Rat, monoclonal	Human, Mouse, Rabbit, Rat	1/200	ICC, IHC
a-APC/CC-1	Millipore (OP80)	Mouse, monoclonal	Human, Mouse, Rabbit, Rat	1/100	IHC
a-PDGFRa	Millipore (CBL1366)	Rat, monoclonal	Mouse, Rat	1/100	ICC, IHC
a-Olig2	Abcam (ab42453)	Rabbit, polyclonal	Human, Rhesus monkey	1/500	IHC
a-IBA-1	Waco (019-19741)	Rabbit, polyclonal	Human, Mouse, Rabbit, Rat	1/500	ICC, IHC
a-GFAP	Sigma-Aldrich (G3893)	Mouse, monoclonal	Human, Mouse, Pig, Rat	1/2000	ICC, IHC
a-Ki-67	Thermo Fisher Scientific (PA1-21520)	Rabbit, polyclonal	Human, Mouse, Rat, Zebrafish	1/200	ICC
a-iNOS	Millipore (ABN26)	Rabbit, polyclonal	Human, Mouse	1/2000	WB
a-Gapdh	Millipore (ABS16)	Rabbit, polyclonal	Human, Mouse, Rat	1/2000	WB






Table 2: Secondary antibodies and fluorescent-conjugated probes used in the study

Antibody	Source	Working dilution	Application
a-Rabbit IgG-Cy3	Jackson ImmunoResearch Laboratories	1/800	ICC, IHC
a-Rat IgG-Alexa Fluor 488 or 555	Molecular Probes, Thermo Fisher Scientific	1/800	ICC, IHC
a-Mouse IgG-Alexa Fluor 488 or 555	Molecular Probes, Thermo Fisher Scientific	1/800	ICC, IHC
$\alpha$ -rabbit IgG horseradish- conjugated	Jackson, ImmunoResearch Laboratories	1/5000	WB

## **PRINTED VERSIONS OF PUBLICATIONS**

## RESEARCH ARTICLE

# The function of contactin-2/TAG-1 in oligodendrocytes in health and demyelinating pathology

Lida Zoupi<sup>1</sup>  | Maria Savvaki<sup>1</sup>  | Katerina Kalemaki<sup>1</sup>  | Ilias Kalafatakis<sup>1</sup>  |  
 Kyriaki Sidiropoulou<sup>2</sup>  | Domna Karageos<sup>1</sup> 

<sup>1</sup>Department of Basic Science, Faculty of Medicine, University of Crete, Voutes University Campus, GR-70013, P.O. Box 2208, Heraklion, Crete, Greece and

<sup>1</sup>Institute of Molecular Biology & Biotechnology - FoRTH, Nikolaou Plastira 100 GR-70013, Heraklion, Crete, Greece

<sup>2</sup>Neurophysiology & Behavior Laboratory, Department of Biology, University of Crete, Voutes University Campus, GR-70013, P.O. Box 2208, Heraklion, Crete, Greece

## Correspondence

Domna Karageos, Department of Basic Science, Faculty of Medicine, University of Crete and Institute of Molecular Biology and Biotechnology - Foundation for Research and Technology, Voutes University Campus, GR-70013, P.O. Box 2208, Greece.  
 Email: karageos@imbb.forth.gr

## Funding information

Fondation pour l'Aide à la Recherche sur la Sclérose en Plaques; General Secretariat for Research and Technology; ARISTEIA I/ MyelinTag 593

## Abstract

The oligodendrocyte maturation process and the transition from the pre-myelinating to the myelinating state are extremely important during development and in pathology. In the present study, we have investigated the role of the cell adhesion molecule CNTN2/TAG-1 on oligodendrocyte proliferation, differentiation, myelination, and function during development and under pathological conditions. With the combination of *in vivo*, *in vitro*, ultrastructural, and electrophysiological methods, we have mapped the expression of CNTN2 protein in the oligodendrocyte lineage during the different stages of myelination and its involvement on oligodendrocyte maturation, branching, myelin-gene expression, myelination, and axonal function. The cuprizone model of central nervous system demyelination was further used to assess CNTN2 in pathology. During development, CNTN2 can transiently affect the expression levels of myelin and myelin-regulating genes, while its absence results in reduced oligodendrocyte branching, hypomyelination of fiber tracts and impaired axonal conduction. In pathology, CNTN2 absence does not affect the extent of de- and remyelination. However during remyelination, a novel, CNTN2-independent mechanism is revealed that is able to recluster voltage gated potassium channels (VGKCs) resulting in the improvement of fiber conduction.

## KEYWORDS

conduction velocity, cuprizone, demyelination, juxtaparanode, myelin

## 1 | INTRODUCTION

During development, designated oligodendrocyte precursor cells (OPCs) are generated in the sub-ventricular zones of the brain and the spinal cord and subsequently migrate in waves to the different central nervous system (CNS) regions, where they differentiate into mature oligodendrocytes (OLCs; Bergles & Richardson, 2015; Kessaris et al. 2006; Kessaris, Pringle, & Richardson, 2008; Richardson, Kessaris, & Pringle, 2006). These processes are achieved via the regulated expression of numerous transcription factors like Nkx2.2, Nkx6.1, Sox10, Olig1, Olig2, Ascl1/Mash1, and YY1 (Cai et al., 2010; Fu et al., 2002; He et al., 2007; Küspert, Hammer, Bösl, & Wegner, 2011; Lu, Cai, Rowitch, Cepko, & Stiles, 2001; Qi et al., 2001; Stolt et al., 2002; Sugimori et al., 2008; Wang et al., 2006; Zhou & Anderson, 2002). OLC maturation is necessary for the transition from pre-myelinating to myelinating

OLC, as is reflected in major morphological changes and the formation of an extensive branching network. The final maturation step requires the expression of transcription factors zinc-finger protein 191 (zfp191) and myelin regulatory factor (Myrf) leading to the upregulation of myelin genes and the formation of membranous sheaths (Emery et al., 2009; Howng et al., 2010). Mature, myelinating OLCs will eventually contact different axons and extend their processes to specific sites, synthesizing and transporting large amounts of membrane while rearranging their cytoskeleton to create consecutive wrappings around the axonal segment (Chang, Redmond, & Chan, 2016; Simons & Trotter, 2007; Snaidero & Simons, 2017).

Subsequently, healthy myelinated fibers are segregated into distinct domains (perinodal areas) that ensure the rapid propagation of action potentials, such as the node of Ranvier, the paranodal junction, the juxtaparanode and the internode (Rasband & Peles, 2015; Sherman

& Brophy, 2005; Susuki & Rasband, 2008; Zoupi, Savvaki, & Karagogeos, 2011). At the node, the accumulation of sodium channels is responsible for the generation of action potentials. Adjacent to the node, glial membrane contacts the axon via the interaction of glial NF155 with the axonal immunoglobulin superfamily (IgSF) protein contactin-1 and the neurexin member Caspr/Paranodin, resulting in the formation of paranodal junctions and thus creating a physical barrier that prevents the lateral diffusion of molecular constituents (Charles et al., 2002; Labasque & Fainre-Sarrailh, 2010; Rasband & Peles, 2015; Sherman & Brophy, 2005; Sherman et al., 2005). Juxtaparanodes are characterized by the accumulation of Shaker-type voltage gated potassium channels (VGKCs) that are necessary for membrane repolarization. Their interaction with the neurexin member Caspr2 and the IgSF molecule CNTN2/TAG-1 ensure and maintain the localization of the complex at the region (Poliak et al., 2003; Savvaki et al., 2008; Traka et al., 2003). The cytoskeletal protein 4.1B is expressed at both paranodal and juxtaparanodal domains (Denisenko-Nehrbass et al., 2003) and links the membrane with the spectrin/actin cytoskeleton, while membrane-associated guanylate-kinase (MAGUK) adapter proteins PSD93 and PSD95 are also expressed at the juxtaparanode ensuring the maintenance of VGKC localization in the mature fiber (Ogawa et al., 2008; Ogawa et al., 2010).

In demyelinating pathologies, the myelin sheath is destroyed leading to a severe impairment of nerve conduction (Coman et al., 2006; Howell et al., 2010; Kastriti, Sargiannidou, Kleopa, & Karagogeos, 2015; Zoupi, Markoullis, Kleopa, & Karagogeos, 2013). Remyelination acts as a repair process and involves the recruitment and differentiation of oligodendrocytes at the lesion site and the subsequent ensheathment of denuded axons. The extent of remyelination dictates also the molecular reorganization of perinodal components that is important for the restoration of nerve conduction (Coman et al., 2006; Fancy, Chan, Baranzini, Franklin, & Rowitch, 2011; Franklin & Ffrench-Constant, 2008; Zoupi et al., 2013). However, remyelination is usually insufficient (Kuhlmann et al., 2008).

We have previously reported that the loss of CNTN2 from both the axon and the glial cells, leads to a significant hypomyelination of the optic nerve (Chatzopoulou et al., 2008) and to the disruption of the juxtaparanodal complex in adult myelinated fibers (Chatzopoulou et al., 2008; Savvaki et al., 2008; Traka, Dupree, Popko, & Karagogeos, 2002; Traka et al., 2003). In addition, CNTN2 deficient animals (that will be referred in this paper as *Tag-1*<sup>-/-</sup>) exhibit significant impairment in motor coordination, learning and memory (Savvaki et al., 2008; Savvaki et al., 2010). However, the role of CNTN2 in oligodendrocyte development and myelination/demyelination has not been elucidated. In the present study, we report that CNTN2 is expressed by post-mitotic and mature oligodendrocytes and can transiently affect the expression levels of myelin and myelin-regulating genes. CNTN2 is also responsible for the formation of an extensive branching network at the mature oligodendrocyte. Under demyelinating conditions, CNTN2 does not affect the OLC number or the extent of remyelination. However, a CNTN2-independent and possibly compensatory mechanism was revealed during remyelination, that reclusters VGKCs on the remyelinating fiber, leading to increased conduction.

## 2 | MATERIALS & METHODS

### 2.1 | Animals

The generation of the *Tag-1*<sup>-/-</sup> line has been previously described (Fukamauchi et al., 2001; Savvaki et al., 2008; Traka et al., 2003). All mice were kept as heterozygote breeding pairs and the genotypes were confirmed by polymerase chain reaction (PCR). Genetically modified *Tag-1*<sup>loxP-GFP-loxP-DTA</sup> and *Tag-1*<sup>-/-</sup>; myelin proteolipid protein (*plp*)<sup>Tg(*Tag-1*)</sup> animals have been previously described (Bastakis, Savvaki, Stamatakis, Vidaki, & Karagogeos, 2015; Savvaki et al., 2010). All animals are of C57BL6/SV129 background and were kept at the animal unit of the Institute of Molecular Biology and Biotechnology, in a temperature-controlled facility on a 12 hr light/dark cycle, fed by standard chow diet and water *ad libitum*. All research activities strictly adhered to the EU adopted Directive 2010/63/EU on the protection of animals used for scientific purposes. Housing and animal procedures performed strictly according to the European Union adopted Directive 2010/63/EU on the protection of animals used for scientific purposes.

### 2.2 | Cuprizone administration

Eight-week old males (20–25 g each) were fed with 0.2% cuprizone (oxalic bis [cyclohexylidenehydrazide]; Sigma-Aldrich, St. Louis, MI) mixed with the animal's standard chow. The followed experimental setup was based on (Matsushima & Morell, 2001) and it is schematically depicted in Figures 4a and 5c. Briefly, cuprizone administration induces the full demyelination of the corpus callosum (CC) upon consecutive administration for 6 weeks (here demyelination time-points are referred as 5.5 and 6 weeks). Toxin removal leads to extensive remyelination (here remyelination time-points are referred as 9 or 12 weeks). All groups (10 animals/group) were compared with age- and sex-matched untreated controls.

### 2.3 | Immunohistochemistry, immunocytochemistry, and Luxol fast blue staining

For immunohistochemistry, brains were harvested from mice after transcardial perfusion with 4% paraformaldehyde (PFA) in 0.1 M phosphate buffer saline (PBS). Tissues were then post-fixed in the same fixative for 30 min at 4°C, cryo-protected overnight in 30% sucrose in 0.1 M PBS, embedded in 7.5% gelatin/15% sucrose gel. Cryosections of 10 μm were obtained and mounted on Superfrost Plus microscope slides (O. Kindler), post-fixed in ice-cold acetone for 10 min, blocked in 5% BSA (Sigma-Aldrich) in 0.1 M PBS, and incubated with primary and secondary antibodies in 5% BSA, 0.5% Triton-X in 0.1 M PBS. For immunocytochemistry, cells were fixed with 4% PFA for 30 min at RT, permeabilized for 10 min with 0.01% Triton-X in 0.1 M PBS and incubated with the primary antibody and secondary antibodies in 1% BSA in 0.1 M PBS. Slides and coverslips were mounted using MOWIOL Reagent (Merk-Millipore, Burlington, MA) and the samples were observed in a confocal microscope (TCS SP2; TCS SP8, Leica Microsystems, Wetzlar, Germany).



The following antibodies were used: Rabbit polyclonal antibodies against Olig2 (AB9610, Millipore, 1:1000), against Caspr2, Caspr, and 4.1B protein (kind gifts by Dr Laurence Goutebroze, Inserm 536, Paris, all 1:100); against Kv1.2 (APC-010, Alomone, 1:200) against ADAM23 (kind gift from Prof. D. Meijer, University of Edinburgh, UK, 1:200), against Iba1 (019-19741, Wako, 1:500) and against CNTN2 (TG1, [Traka et al., 2002], 1:1000). Mouse monoclonal PanNav (clone K58/35, S8809, Sigma-Aldrich, 1:50); Caspr (kind gift by Dr Peles, Weizmann Institute of Science, Israel, 1:1000), glial fibrillary acidic protein (GFAP; clone G-A-5, Sigma-Aldrich, 1:2000), CC-1 (APC clone CC-1, MABC200, Millipore, 1:100) and rat monoclonal antibody against myelin basic protein (MBP – MCA409S, AbD Serotec, Raleigh, NC, 1:200) and against CD140a (platelet-derived growth factor receptor [PDGFR $\alpha$ ], clone APA5, CBL1366, Millipore, 1:100). Fluorochrome-labeled secondary antibodies Alexa Fluor 488, 555 and 647 (Invitrogen, Carlsbad, CA, 1:800) were also used. To-Pro 3 iodide (Invitrogen) was finally used for the visualization of the nuclei.

For OPCs/OLCs density quantifications 5–6 different  $444 \times 364 \mu\text{m}$  images were obtained from the CC of each animal using confocal microscopy (TCS SP2, Leica Microsystems). The area of the tissue was calculated using Fiji/ImageJ software (<https://imagej.net/Fiji>) and the cell number was manually quantified. Cell densities were calculated as cell number/ $\text{mm}^2$ . For each group, 5 different animals were used for the quantification. For the quantification of Iba1 and GFAP<sup>+</sup> areas in the CC 3 different areas/animal were obtained (3 animals/group). For the individual Iba1 and GFAP channels, intensity threshold (“threshold” plugin) was applied and the total staining area was measured using the “analyze particles” plugin of Fiji/ImageJ software. For the quantification of VGKCs clustering and nodal density 5–6 different areas/animal were used (3 animals/group). VGKCs clustering and nodal density were quantified using Fiji software as previously described in (Zoupi et al., 2013).

Luxol fast blue (LFB) staining was performed on  $14 \mu\text{m}$  cortical cryosections. Sections were rinsed twice with 100% and 96% ethanol for 2 min and subsequently incubated for 1 hr in pre-heated LFB solution (0.1% LFB powder, 96% ethanol, and 0.5% glacial acetic acid) at  $60^\circ\text{C}$ . Staining differentiation was achieved with 0.05% Lithium Carbonate solution for 30 s and rinsing with 70% ethanol for additional 30 s. Sections were subsequently dehydrated with increasing concentrations of ethanol and mounted in xylene-based mounting medium. CC pictures were obtained using optical microscopy (Axioskop 2, Zeiss). Demyelination was evaluated via three independent and blinded observers. LFB-stained CC sections were scored between 0 (total demyelination) and 3 (control/untreated myelin levels).

## 2.4 | Western blot analysis and immunoprecipitation

Tissues were collected (3 animals/group) and homogenized in ice-cold 85 mM Tris, pH 7.5, 30 mM NaCl, 1 mM ethylenediaminetetraacetic acid, 120 mM glucose, 1% Triton X-100, 60 mM octyl Q-D glucopyranoside (Sigma-Aldrich), and protease inhibitor mixture diluted 1:1000 (Sigma-Aldrich), followed by a brief sonication on ice. The total protein in each sample was quantified with the Bradford kit (Bio-Rad

Laboratories, Hercules, CA). Protein extracts were analyzed by sodium dodecyl sulfate polyacrylamide gel electrophoresis (SDS-PAGE) and electro-transferred to  $0.45 \mu\text{m}$  Protran nitrocellulose transfer membrane (Whatman). Following 1 hr blocking (5% powdered skim milk and 0.1% Tween 20 in 0.1 M PBS); the membrane was incubated overnight with the primary antibodies. Samples were incubated with horseradish peroxidase-coupled secondary antibodies and proteins were visualized using enhanced chemiluminescence (Merk-Millipore). The following antibodies were used: rabbit polyclonal a-PLP (AB28488, Abcam, 1:1000), rat monoclonal a-MBP (MCA409S, AbD Serotec, 1:5000), rabbit polyclonal a-GAPDH (14C10, Cell Signaling, 1:1000), rabbit polyclonal anti-ADAM23 (kind gift from Prof. D. Meijer, University of Edinburgh, UK 1:1000), mouse monoclonal a-Kv1.1 (07-039, Upstate Biotechnologies, 1:1200), mouse monoclonal a-ACTIN (MAB1501, CHEMICON, 1:4000). The intensity of the bands was measured with Tinascan version 2.07d and normalized using actin as loading control.

For immunoprecipitation (IP), adult mouse brain protein extracts were obtained as described above. The lysates were centrifuged at 13,000 rpm at  $4^\circ\text{C}$  for 30 min and pre-cleared with protein G Sepharose beads (GE Healthcare, Chicago, IL) for 1 hr at  $4^\circ\text{C}$ . IP was performed by incubating the samples with  $3 \mu\text{l}$  of rabbit polyclonal anti-ADAM23 (kind gift from Prof. D. Meijer, University of Edinburgh, UK), and  $40 \mu\text{l}$  of protein G Sepharose beads on a rotating platform overnight at  $4^\circ\text{C}$ . After a brief centrifugation, the supernatants were removed, and the beads were washed with wash buffer (5 mM Tris-HCl, pH 8.0, 1% Triton X-100, 50 mM NaCl, 2.5 mM CaCl<sub>2</sub>, 2.5 mM MgCl), and re-suspended in equal volume of  $2\times$  SDS loading buffer.

## 2.5 | Real time PCR

Extraction of total RNA was performed on cortical samples from wild type (WT) and *Tag-1*<sup>-/-</sup> (3 animals/group) mice using the RNAiso-plus kit (Takara) according to the manufacturer's instructions. Total RNA was subjected to reverse transcription according to the protocol of Affinity Script Multiple Temperature cDNA synthesis kit (Agilent Technologies, Santa Clara, CA). Expression levels of genes encoding *plp* (forward primer: 5'-TCAGTCTATTGCCTCCCTA-3', reverse primer: 5'-AGCATTCCATGGGAGAACAC-3'), *mbp* (Pernet, Joly, Christ, Dimou, & Schwab, 2008; forward primer: 5'-CACACACGAGAACTACCCA-3', reverse primer: 5'-GGTGTTTCGAGGTGCACAA-3'), myelin associated glycoprotein (*mag*) (forward primer: 5'-CTGCTCTGTGGGCTGACAG-3', reverse primer: 5'-AGGTAGAGGCTCTTGCAACT-3'), *zfp191* (forward primer: 5'-CTGGTCAGCCGTTTCTCT-3', reverse primer: 5'-TTCCCAGGATGCCCACTTGA-3'), *myrf* (forward primer: 5'-GCAC TACAGATACAAGCCTGAG-3', reverse primer: 5'-AAGATTCGCTCT TGTTCCT-3'), 2',3'-Cyclic-nucleotide 3'-phosphodiesterase (*cnp*) (Pernet et al., 2008; forward primer: 5'-AGGAGAAGCTTGAGCTGGTC-3', reverse primer: 5'-CGATCTCTTACCACCTCT-3') were examined by real-time PCR analysis using a StepOnePlus real-time PCR system (Applied Biosystems, Life Technologies, Thermo Fisher Scientific Inc., Waltham, MA). *Gapdh* was used as the internal control (forward primer: 5'-ATTGTCAGCAATGCATCCTG-3', reverse primer: 5'-ATGGAC TGTGGTCATGAGCC-3'). Real-Time PCR was performed in a 15  $\mu\text{l}$



reaction containing 7.5  $\mu$ l iTaq Universal SYBR Green Supermix (Bio-rad), 2  $\mu$ l forward primer (2 pmol/ $\mu$ l), 2  $\mu$ l reverse primer (2 pmol/ $\mu$ l), and 3.5  $\mu$ l cDNA sample. PCR conditions were 95°C for 20 s, followed by 40 cycles of 95°C for 3 s, 58°C (*plp*, *zfp191*, *mbp*, *myrf* and *cnp*)/57°C (*mag*) for 45 s and 95°C for 15 s, and a final step of 60°C for 1 min and 95°C for 15 s.

For all genes tested, we performed comparative real-time PCR analysis, with the exception of *myrf* and *cnp*, where a relative standard curve was performed (due to different efficiencies between them and the control gene). PCR runs were performed for each sample in triplicates using cDNA corresponding to 50 ng of total RNA regarding *plp*, *mbp*, *mag*, and *zfp191*, 100 ng regarding *cnp* and 200 ng regarding *myrf*. Expression levels for each gene were normalized according to the internal control.

## 2.6 | Primary OLC cultures

Primary OLC cultures were obtained from postnatal day 2 (P2) mouse cortices. Tissues were dissected in Hank's balanced salt solution (HBSS, ThermoFisher Scientific, Waltham, MA) and cleared completely of the meninges. They were subsequently trypsinized (1% trypsin, ThermoFisher Scientific) for 10 min at 37°C. Trypsin activity was neutralized with the addition of 10% fetal bovine serum (FBS, ThermoFisher Scientific) in 1 $\times$  HBSS. Cortices were then washed and re-suspended in Dulbecco's modified Eagle medium (DMEM, 10% FBS, 2% penicillin-streptomycin, ThermoFisher Scientific). Followed by mechanical homogenization, cell suspensions were transferred in pre-coated poly-D-lysine (Sigma-Aldrich) 75 cm<sup>2</sup> flasks at 37°C, 5% CO<sub>2</sub> for 14 days. Medium was replenished every second day. Microglial removal was achieved mechanically by culture shaking at 37°C for 1 hr at 200 rpm. Primary OPCs were obtained by subsequent culture shaking at 37°C over night at 250 rpm. OPCs were then washed and plated on pre-coated poly-D-lysine 18 mm glass coverslips in DMEM (High glucose-pyruvate, ThermoFisher Scientific), 1% N2 (ThermoFisher Scientific), 1  $\mu$ M D-biotin (Sigma-Aldrich), 1% BSA fatty acid-free (Sigma-Aldrich), 5  $\mu$ g/ml N-acetylcysteine (Sigma-Aldrich), 1% penicillin-streptomycin (ThermoFisher Scientific), 10 ng/ml fibroblast growth factors (FGF; Peprotech, Rocky Hill, NJ), 10 ng/ml PDGF $\alpha$  (Peprotech) for 48 hr, when FGF and PDGF $\alpha$  were removed from the medium and 40 ng/ml T3 (Sigma-Aldrich) was added to allow the differentiation of OPCs toward mature OLCs. OLC cultures were then immunostained and analyzed after 8 days *in vitro*. Operetta High-Content Imaging System (Perkin Elmer, Waltham, MA) was used for the visualization of OLCs. Image processing was performed with Harmony 4.1 (Perkin Elmer) and OLCs were manually distributed in the different categories in continuous fields. A total number of 300–500 MBP<sup>+</sup> cells were evaluated per experiment and per condition ( $n = 3$  independent experiments). Scholl analysis was performed using Fiji/ImageJ plugin ([http://imagej.net/Scholl\\_Analysis](http://imagej.net/Scholl_Analysis)) for the automatic measuring of the number of intersections occurring in each segmented Sholl ring.

## 2.7 | Electrophysiology

CC compound action potential (CAP) recordings from acute brain slices of 5-month old male mice (Untreated: WT = 6 and *Tag-1*<sup>-/-</sup> = 7, demyelination: WT = 8 and *Tag-1*<sup>-/-</sup> = 8, remyelination: WT = 7 and *Tag-1*<sup>-/-</sup> = 5) were obtained similarly to previously described protocols (Crawford, Mangiardi, & Tiwari-Woodruff, 2009; Reeves, Phillips, & Povlishock, 2005). In short, mice were decapitated under halothane anesthesia. The brain was sectioned into 450- $\mu$ m thick coronal sections while submerged in ice-cold oxygenated (95% O<sub>2</sub> 5% CO<sub>2</sub>) artificial cerebrospinal fluid (aCSF) containing (in mM): 125 NaCl, 3.5 KCl, 26 NaHCO<sub>3</sub>, 1.42 MgCl<sub>2</sub> and 10 glucose (pH = 7.4, 315 mOsm/l), using a vibratome (Leica, VT1000S, Leica Biosystems). Slices were transferred and incubated for at least 1 hr at room temperature (RT) in oxygenated (95% O<sub>2</sub> 5% CO<sub>2</sub>) aCSF containing (in mM): NaCl 124, KCl 5, NaH<sub>2</sub>PO<sub>4</sub> 1.25, NaHCO<sub>3</sub> 26, MgSO<sub>4</sub> 1.3, CaCl<sub>2</sub> 2, glucose 10; adjusted to pH 7.4, 315 mOsm/l. Brain slices containing the midline-crossing segments of the CC were used for recordings and corresponded to Bregma 0.26 mm to -2.06 mm of the atlas of (Franklin & Paxinos, 1997). Slices were then transferred to a submerged recording chamber, which was continuously superfused with oxygenated (95% O<sub>2</sub>/5% CO<sub>2</sub>) aCSF (same constitution as the one used for maintenance of brain slices) at RT. The extracellular recording electrode, filled with NaCl (3 M), was placed in the CC at  $\sim$ 1.5 mm from the stimulating electrode (Platinum/iridium metal microelectrodes, Harvard apparatus UK). Evoked CC CAPs extracellular field potentials were amplified with a Dagan BVC-700A amplifier (Dagan Corporation, Minneapolis, MN), digitized with the ITC-18 board (Instrutech, Inc, Longmont, CO) on a PC using custom-made procedures in IgorPro (Wavemetrics, Inc, Lake Oswego, OR). The electrical stimulus consisted of a single square waveform of 100  $\mu$ s duration given at intensities of 0.3–4 mA generated by a stimulator equipped with a stimulus isolation unit (World Precision Instruments Inc, Sarasota, FL).

## 2.8 | Data acquisition and analysis

Data were acquired and analyzed using custom-written procedures in IgorPro software (Wavemetrics, Inc). The evoked CC CAPs extracellular field potentials were characterized by relatively fast-conducting myelinated axons (CC CAPs of myelinated axons) between 1 and 2 ms, and a later occurring component reflecting mainly slower unmyelinated axons (CC CAPs of unmyelinated axons) appeared at 3–6 ms. We specifically analyzed the CC CAPs and conduction velocity of myelinated axons as we were interested in axonal conduction and functional consequences of recovered remyelinated *Tag-1*<sup>-/-</sup> mice. The CAPs amplitude was quantified as the vertical distance from the local negative peak to a tangent joining preceding and following positives. A stimulus-response curve was determined using stimulation intensities between 0.3 and 4 mA. For each different intensity level, two traces were acquired and averaged. The CC conduction velocity was estimated by changing the distance between the stimulating and recording electrodes from 0.5 to 1.5 mm while holding the stimulus intensity constant. Then, the CC conduction velocity for each animal was measured by dividing the



change in distance of the stimulating electrode (for example 1.5–0.5 mm) with the corresponding difference in peak latency (time A–time B). The average conduction velocity was calculated by using different distances between electrodes. Two sections from each animal was used in each experimental group.

## 2.9 | Electron microscopy

Anesthetized animals were perfused with 2% glutaraldehyde and 2% PFA in 0.1 M phosphate buffer (PB), pH 7.3. Dissected brains were transferred in the same fixative overnight at 4°C. Fixed brains were washed in 0.1 M PB, post-fixed in 1% osmium tetroxide for 1 h, dehydrated with increasing concentrations of ethanol and embedded in epoxy resin (Durcupan ACM, Fluka). Ultrathin sections (70–80 nm) were obtained using the EM UC6 (Leica) ultramicrotome, contrasted with lead and viewed using a transmission electron microscope (100C, JEOL) operating at 80 kV. For the analysis, 10–20 randomly chosen electron micrographs of the CC were obtained at 12,000 magnification for each animal. In total 17 animals were used for the g ratio and axonal diameter quantification (3 WT untreated (5–6 mo), 3 *Tag-1*<sup>-/-</sup> untreated (5–6 mo), 2 WT 5.5 weeks, 3 *Tag-1*<sup>-/-</sup> 5.5 weeks, 3 WT 9 weeks and 3 *Tag-1*<sup>-/-</sup> 9 weeks). For g-ratio quantification 100 axons were measured for each animal using Fiji/ImageJ software. For the axon diameter distribution, 200 axons were analyzed and finally for the quantification of the percentage of myelinated axons for each experimental setup, 10 random electron micrographs per animal were manually quantified.

## 2.10 | Statistical analysis

All data are presented as mean ± SEM. Normality distribution and equality of variances of data were tested with the D'Agostino-Pearson normality test. Statistical analysis of the measured values for each group was performed using two-tailed, unpaired Student's *t* test or One-way analysis of variance (ANOVA) with Bonferroni or Tuckey *post-hoc* tests for multiple comparisons. In the case of non-normally distributed values, non-parametric Mann-Whitney test or Kruskal-Wallis test with Dunn's *post hoc* tests for multiple comparisons were used. Statistical analysis was performed using GraphPad Prism version 5.00 for Windows (Prism, GraphPad). *p* < .05 was considered statistically significant.

## 3 | RESULTS

### 3.1 | CNTN2 is expressed by mature oligodendrocytes but not oligodendrocyte precursor cells

In the adult, CNTN2 is expressed both by the axon and the myelin-forming glial cells in the peripheral nervous system (PNS) and CNS (Traka et al., 2002; Traka et al., 2003). Since the onset of expression of the protein in different cellular populations differs, we examined this aspect specifically in the oligodendrocytic lineage *in vivo*. We used a transgenic mouse line that drives the expression of the green fluorescent protein (GFP) under the *Cntn2* (*Tag-1*) promoter (*Tag-1*<sup>loxP-GFP-loxP</sup>;

<sup>DTA</sup>; Bastakis et al., 2015). We used Olig-2 as an oligodendroglial lineage marker, PDGFR $\alpha$  as an OPC marker and CC-1 (Figure 1) that stains mature, pre-myelinating and myelinating oligodendrocytes. At P10, a period coincident with the onset of myelination, a few GFP<sup>+</sup>/Olig2<sup>+</sup> cells are observed (Supporting Information, Figure S1).

At the peak of myelination (P23), double immunolabeling for GFP and PDGFR $\alpha$  (Figure 1a), Olig2 (Figure 1b) or CC-1 (Figure 1c) revealed GFP<sup>+</sup>/Olig2<sup>+</sup> and GFP<sup>+</sup>/CC-1<sup>+</sup> oligodendrocytes in the CC. No co-labeling of GFP and PDGFR $\alpha$  was detected (Figure 1a), although all GFP<sup>+</sup> cells were Olig2<sup>+</sup> and CC-1<sup>+</sup> (comprising 24.42% ± 7.34% of the total CC-1<sup>+</sup> population), a finding underlying the specific expression of CNTN2 in mature oligodendrocytes (Figure 1b,c,k).

As the process of myelination progresses (P30), an increasing percentage (36.88% ± 6.51% of the total CC-1<sup>+</sup> population) of GFP was observed in the CC (Figure 1e,f,k). In addition, GFP expression was also noted in MBP-expressing OLCs in primary OLCs cultures *in vitro* (data not shown). Still, no expression was detected by OPCs (Figure 1d). In the adult CC (Figure 1g,h,i) mature oligodendrocytes expressing CNTN2 included over half of the CC-1<sup>+</sup> population with GFP<sup>+</sup>/CC-1<sup>+</sup> oligodendrocytes reaching a 61.38% ± 2.96% (Figure 1k). As at earlier time points, none of the PDGFR $\alpha$ <sup>+</sup> cells was positive for GFP (Figure 1g). When we evaluated the efficiency of GFP expression in CNTN2<sup>+</sup> OLCs by quantifying the GFP<sup>+</sup>/TG1<sup>+</sup> (CNTN2 specific antibody) cells we found that on average 46.01% ± 13.81% of the TG1<sup>+</sup> cells were also GFP<sup>+</sup>, but all of the TG1<sup>+</sup> cells were also CC-1<sup>+</sup> (Figure 1j). Hence, we believe that the limited efficiency of GFP expression in the transgenic animal is a possible explanation for the percentage of CNTN2<sup>+</sup> mature OLCs in the adult. In conclusion, CNTN2 is expressed by mature oligodendrocytes and not by OPCs during development and in the adult CNS.

### 3.2 | CNTN2 absence transiently affects the expression of myelin genes during active myelination

Our previous work has shown that the absence of CNTN2 in the adult brain of *Tag-1*<sup>-/-</sup> mice is responsible for the mislocalization of the juxtaparanodal components and the hypomyelination of myelinated fibers (Chatzopoulou et al., 2008; Savvaki et al., 2008; Savvaki et al., 2010; Traka et al., 2003). However, the effect of the protein loss on the oligodendroglial population and the regulation of myelin genes during myelination have not been addressed. We asked whether the lack of CNTN2 protein during the process of myelination had any impact on oligodendrocyte subpopulations thus accounting for the observed hypomyelination (Chatzopoulou et al., 2008). We compared PDGFR $\alpha$ <sup>+</sup> and CC-1<sup>+</sup> oligodendrocyte densities in the CC from P10, P21, and P30 WT and *Tag-1*<sup>-/-</sup> animals (Figure 2a). No differences in the OPCs and mature oligodendrocyte numbers were detected at all ages tested between *Tag-1*<sup>-/-</sup> animals and controls (Figure 2a).

We then examined if the absence of CNTN2 affects the transcriptional levels of myelin or myelin-regulating genes. By using quantitative real-time PCR on brain extracts from WT and *Tag-1*<sup>-/-</sup> animals we measured the mRNA levels of the *plp*, *mbp*, *cnp*, *mag*, and of factors important for oligodendrocyte maturation like the *zfp191* and *myrf*



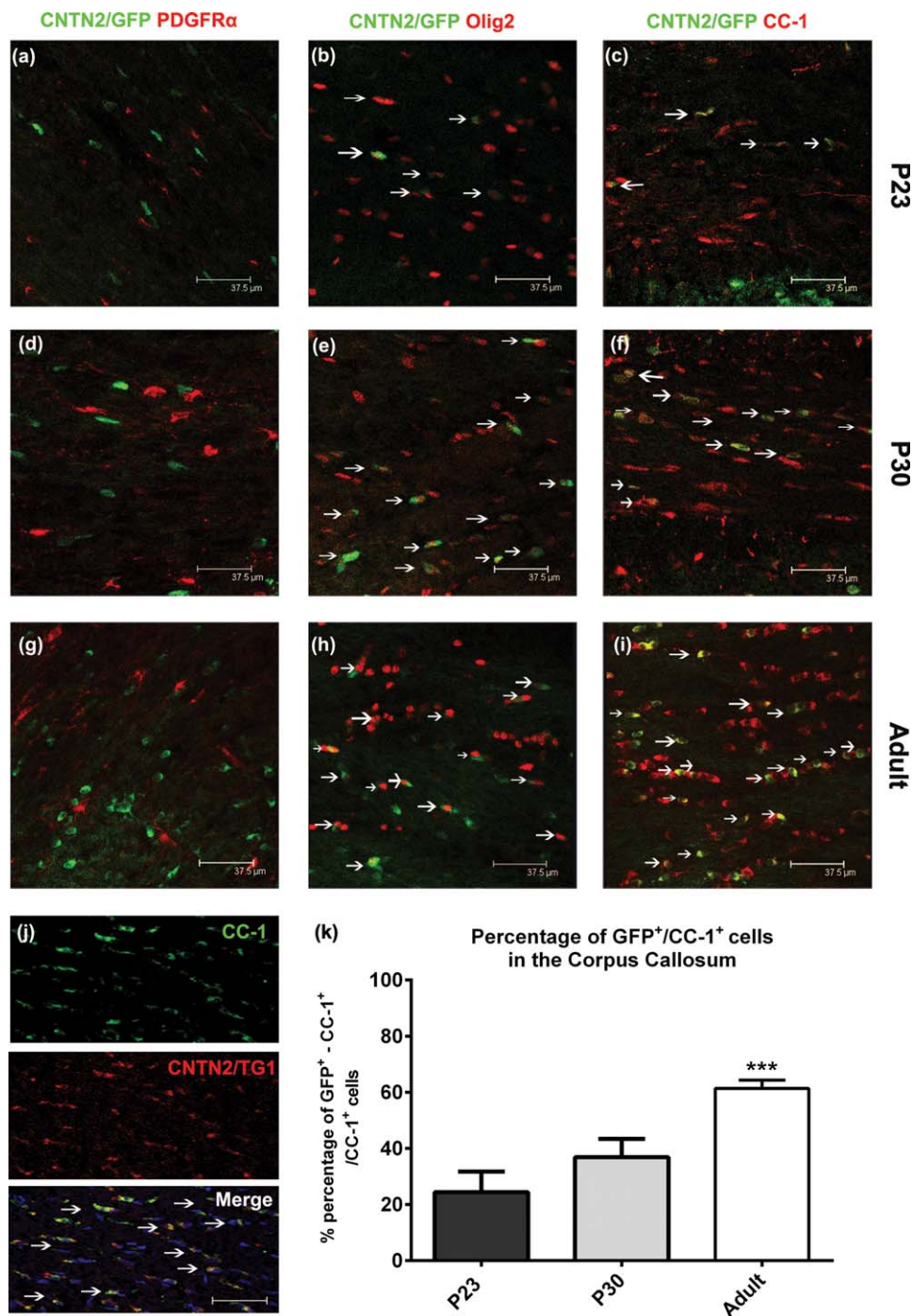


**FIGURE 1** Lineage mapping of CNTN2<sup>+</sup> oligodendrocytes reveals expression by mature oligodendrocytes and not OPCs. (a–i) Immunohistochemical analysis of rostral CC cryosections from P23 (a–c), P30 (d–f) and adult (g–i) transgenic animals expressing GFP under the promoter of *Cntn2* gene (here referred as *Tag-1*<sup>loxP-GFP-loxP-DTA</sup>). Three oligodendrocyte lineage markers were used in each case: PDGFR $\alpha$  (a, d, and g) for oligodendrocyte precursors, Olig2 (b, e, and h), expressed throughout the oligodendrocyte lineage and CC-1 (c, f, and i) for mature oligodendrocytes. In all images GFP/CNTN2 is in green and the OLC markers in red. CNTN2 was never co-expressed in PDGFR $\alpha$ <sup>+</sup> precursors. In contrast, CNTN2<sup>+</sup>/Olig2<sup>+</sup> (arrows) and CNTN2<sup>+</sup>/CC-1<sup>+</sup> oligodendrocytes (arrows) were identified in increasing percentages with age (k and i, \*\*\* $p < .001$ ). (j) CC cryosections from adult *Tag-1*<sup>loxP-GFP-loxP-DTA</sup> stained for CC-1 (green) and a CNTN2 specific antibody (CNTN2/TG1, red). All TG1<sup>+</sup> cells co-localize with the CC-1 antibody (merge, arrows). Insert scheme in (k) depicts the areas of quantification. Scale bar: 37.5  $\mu$ m

genes at different developmental stages (P10, P21, P30, and P75; Figure 2b). Although the number of oligodendrocytes does not differ at P10, the mRNA levels of some myelin genes displayed significant

alterations (Figure 2b). Specifically, three out of four myelin genes (*plp*, *cnp*, and *mbp*) showed a significant reduction at the transcript level with *mag* mRNA also showing a tendency toward reduction in the *Tag-*

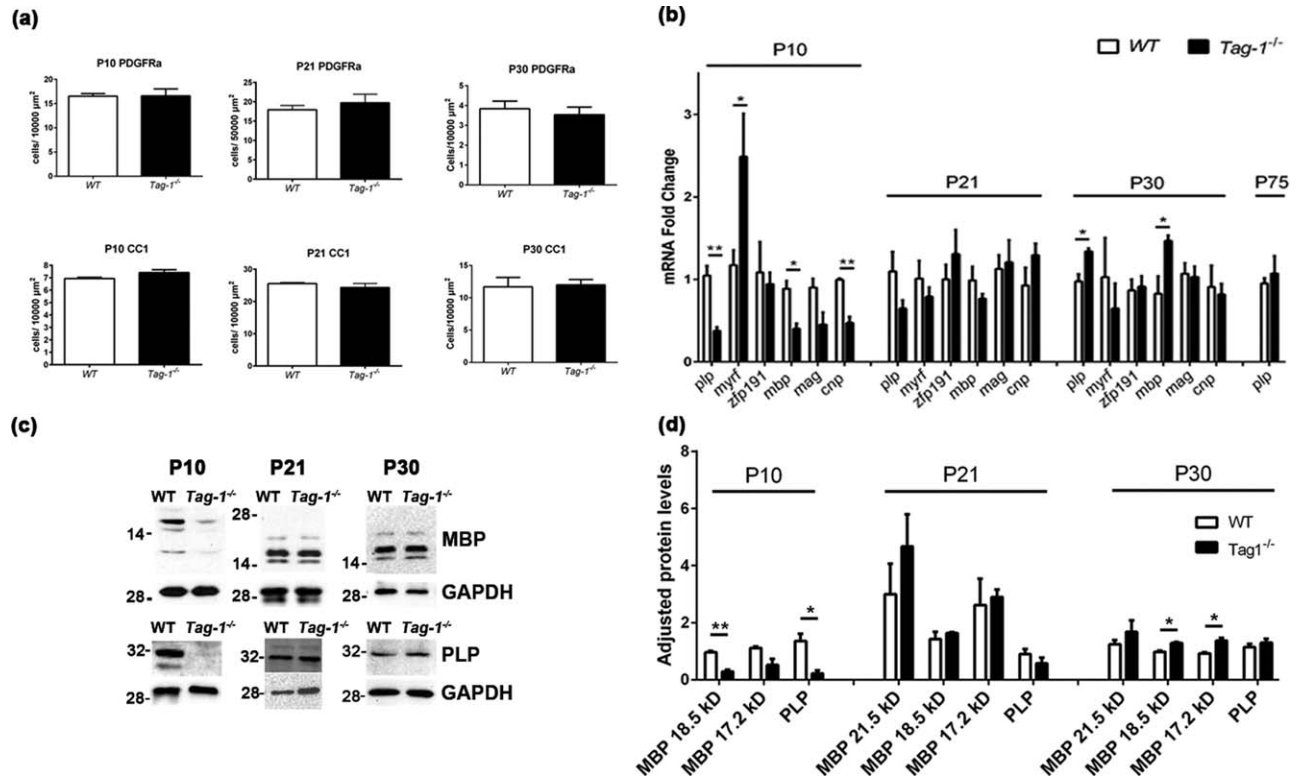


**FIGURE 2** CNTN2 transiently affects the expression of myelin and myelin-regulating genes during myelination. (a) Cell density quantification for PDGFR $\alpha^+$  and CC-1 $^+$  cells in the rostral part of the CC at P10, P21, and P30. No difference was observed. (b) Analysis of transcriptional levels of myelin and myelin-regulating genes using quantitative real-time PCR in mouse brains at P10, P21, P30, and P75. Fold changes in the mRNA levels of tested genes (*plp*, *mbp*, *cnp*, *myrf*, *zfp191*, and *mag*) were quantified in *Tag-1* $^{-/-}$  mice compared with WT control littermates. Significant downregulation of myelin genes and upregulation of *myrf* at P10 that is restored from P21 onwards. (c) Western blot analysis for PLP and MBP proteins of brain lysates from P10, P21, and P30 mice. Representative images are depicted. (d) Quantification of the adjusted relative protein levels of MBP isoforms and PLP. Significant reduction was detected for both proteins at P10 mutant cortices, which was fully compensated by P21. At P30, MBP expression was slightly but significantly increased in *Tag-1* $^{-/-}$  brains, compared with WT controls (\*\* $p < .001$ , \*\* $p < .01$ , \* $p < .05$ )

*1* $^{-/-}$  animals (Figure 2b). In parallel, the *myrf* transcription factor shown to be important for the final differentiation of oligodendrocytes and the activation of myelin genes (Emery et al., 2009; Koenning et al., 2012), was significantly upregulated in CNTN2 deficient animals (Figure 2b). We observed that myelin transcriptional levels were restored by P21 and at P30, when myelination is extensive and nearly complete, with *mbp* and *plp* appearing slightly upregulated in the *Tag-1* $^{-/-}$  brains. However, the effect seemed to be restored at later stages (P75; Figure 2b).

These differences in the transcriptional levels of myelin and myelin-regulating genes point toward a molecular and/or physiological dysregulation rather than a proliferation phenotype in the *Tag-1* $^{-/-}$  oligodendrocytes. Hence, we tested if there was any correlation between these transcriptional differences and the respective protein levels in the *Tag-1* $^{-/-}$  brains (Figure 2c,d). In accordance with the mRNA results, both *plp* and *mbp* protein levels were significantly reduced in *Tag-1* $^{-/-}$  brain lysates at P10 (Figure 2c,d) a phenotype that was restored by P21 (Figure 2c,d). At the end of the myelination process (P30), similarly to the gene expression analysis, MBP and PLP levels were slightly increased in *Tag-1* $^{-/-}$  animals when compared with controls (Figure 2c,d). Western blot for MBP in brain lysates from P10 WT, *Tag-1* $^{-/-}$  and *Tag-*

*1* $^{-/-};plp^{Tg(Tag-1)}$  animals that exclusively express CNTN2 from the OLCs has shown that MBP levels are restored by the expression of CNTN2 from the glial cell during the initiation of myelination, pointing toward a cell autonomous regulation of myelin genes without the involvement of the axonal compartment (Supporting Information, Figure S2).

Thus, CNTN2 is expressed by mature oligodendrocytes and its absence can transiently alter the expression of myelin genes at the onset of myelination.

### 3.3 | CNTN2 is essential for the later stages in oligodendrocyte maturation, myelin sheath formation and affects axonal conduction velocity in the adult

Our previous study showing hypomyelination in *Tag-1* $^{-/-}$  mice was performed in the optic nerve (Chatzopoulou et al., 2008). In order to verify that it was not a tissue-specific effect, we analyzed the CC of adult *Tag-1* $^{-/-}$  animals by using g-ratio measurements (g-ratio WT:  $0.7552 \pm 0.020$ , g ratio *Tag-1* $^{-/-}$ :  $0.8225 \pm 0.050$ ,  $p = 0.09$ ) of semithin EM sections (Figure 3a,b). Although the difference did not reach statistical significance between the groups (Figure 3a), a clear trend in both the average g-ratio values and the ratio distribution in different

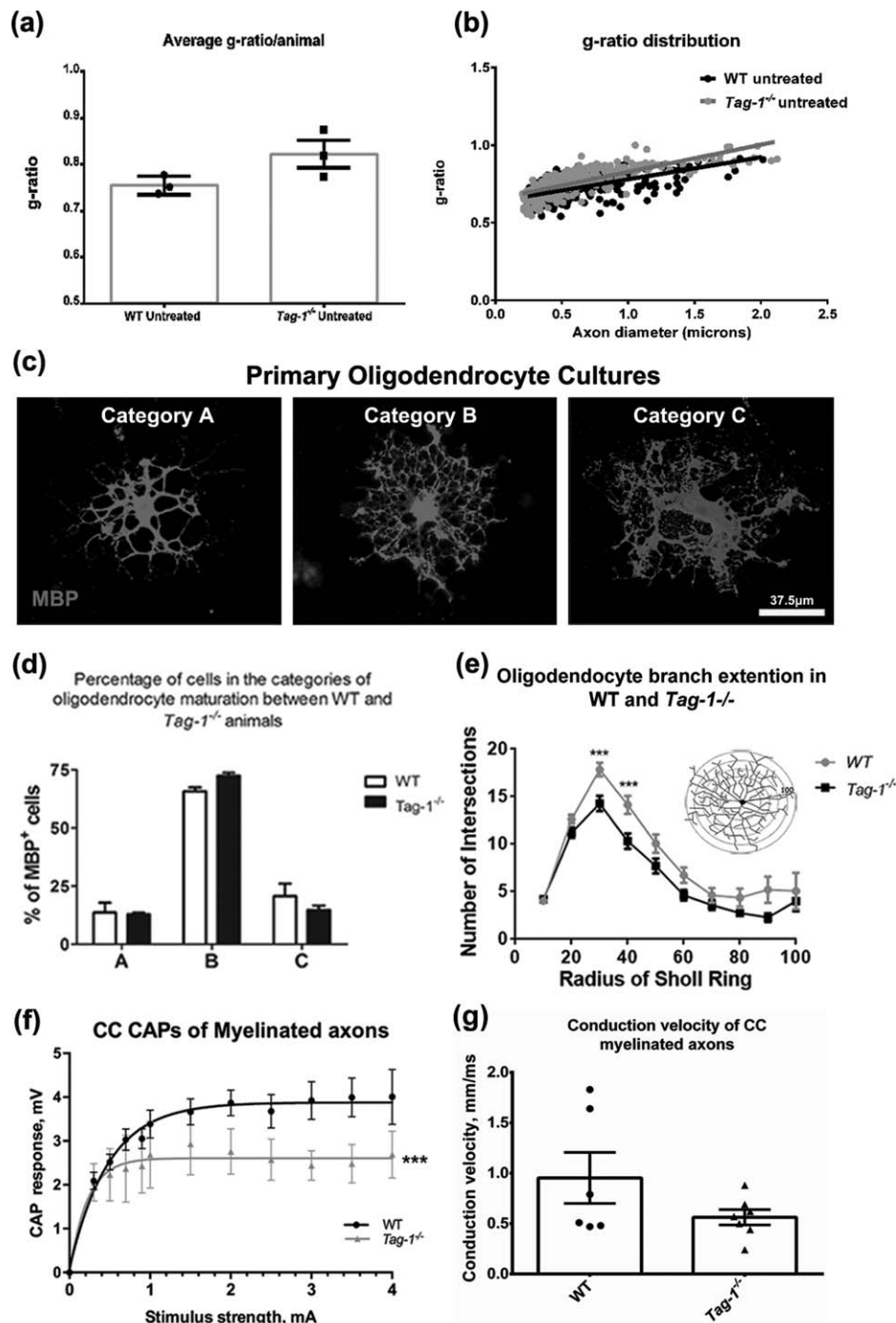


**FIGURE 3** CNTN2 is essential for the later stages in oligodendrocyte maturation, myelin sheath formation and affects conduction velocity in the adult. (a) Myelin sheath thickness was assessed using *g*-ratio measurement of EM images from adult WT and *Tag-1*<sup>-/-</sup> animals. Box-plot of mean *g*-ratio values per animal group. Each point represents an animal. *Tag-1*<sup>-/-</sup> animals show a trend of increased *g*-ratio values when compared with WT ( $p = .09$ ). (b) *g*-ratio distribution to different axonal diameters of WT and *Tag-1*<sup>-/-</sup> untreated animals. (c) Primary oligodendrocyte cultures from WT and *Tag-1*<sup>-/-</sup> animals immunostained for MBP. Three morphological categories (Category A, B, and C) of mature, MBP-expressing oligodendrocytes were further analyzed with the Operetta High-Content Imaging System. (d) Quantification of the percentage of oligodendrocytes found in the categories described above. (e) Sholl analysis of category B oligodendrocytes between WT and *Tag-1*<sup>-/-</sup> animals showed a significant reduction of branch network in CNTN2-deficient OLCs. (f) Corpus callosum compound action potential responses (CC CAPs) from acute slices containing the CC of WT and *Tag-1*<sup>-/-</sup> animals. Quantification of average stimulus-response from each animal showed significantly reduced CC CAPs in myelinated axons from *Tag-1*<sup>-/-</sup> animals compared with controls. (g) Quantification of the CC conduction velocity for each animal. *Tag-1*<sup>-/-</sup> show a tendency toward reduced conduction velocity values when compared with WT (\*\* $p < .001$ )



axonal diameters was noted (Figure 3b), verifying the previously observed result in the optic nerve.

Subsequently, we tested if the loss of CNTN2 can lead to an OLC differentiation arrest at the final maturation stages (Figure 3c,d,e). Consequently, we performed primary oligodendrocyte cultures from P2 WT and *Tag-1*<sup>-/-</sup> cortices. After 8DIV, these cultures were immunostained for MBP (Figure 3c). Three morphological categories (Category A,B,C) of mature oligodendrocytes were identified according to previously published work (Lourenço et al., 2016; Miron et al., 2013) and were further analyzed with the Operetta High-Content Imaging System (Figure 3c,d,e). No numerical differences among MBP<sup>+</sup> OLCs in the three categories between the two genotypes were observed, suggesting that there is no direct effect of CNTN2 on the progression toward the myelinating state (Figure 3d). By using the Sholl analysis plug-in ([http://imagej.net/Sholl\\_Analysis](http://imagej.net/Sholl_Analysis)) on category B oligodendrocytes (representing the majority of OLCs at 8 DIV) from WT and *Tag-1*<sup>-/-</sup> cultures, we were able to assess the extent of oligodendrocyte branching in both genotypes (Figure 3e). We found that in the case of mutant OLCs the branch extension was significantly reduced compared with controls (Figure 3e).

We subsequently asked whether the cellular phenotype of a defective oligodendrocyte branch network together with a slight hypomyelination and juxtaparanodal disruption impacts the physiology of the adult animal. Extracellular field recordings of callosal compound action potential responses (CC CAPs) were performed in acute brain slices from WT and *Tag-1*<sup>-/-</sup> adult animals (Figure 3f, Supporting Information, Figure S3a). The average CAP-response was quantified in both genotypes for myelinated callosal axons (Figure 3f, Supporting Information, Figure S3a). In the adult CC, the CAP responses to all electrical stimuli applied on myelinated axons were significantly reduced in *Tag-1*<sup>-/-</sup> animals compared with controls, strongly indicating a severe impairment of the functional properties of the total number of axons recruited into the CAP field potential (Figure 3f). When the peak latency to the stimulus distance was plotted and the mean value of conduction velocity was calculated for each animal, there was a trend toward decreased conduction velocity in *Tag-1*<sup>-/-</sup> animals (WT: 0.95 ± 0.25 mm/ms and *Tag-1*<sup>-/-</sup>: 0.56 ± 0.07 mm/ms, *p* = .08; Figure 3g).

### 3.4 | Improved conduction velocity of *Tag-1*<sup>-/-</sup> callosal axons during remyelination

Our analysis so far was focused on OLCs during the normal process of myelination in the adult CNS. However, we wished to investigate the protein's role under pathological conditions, such as in demyelination and remyelination. In order to study both these processes, simultaneously avoiding the involvement of the peripheral immune system, we chose to subject both WT and *Tag-1*<sup>-/-</sup> animals to the cuprizone model of toxic CNS demyelination (Matsushima & Morell, 2001) as shown in Figure 4a. Cuprizone administration leads to progressive demyelination, while the toxin removal allows remyelination of demyelinated tracts like the CC. In WT and *Tag-1*<sup>-/-</sup> animals, the myelin staining was nearly absent after 6 weeks of treatment (demyelination),

while this effect was restored after a period of remyelination (9 weeks), with no obvious differences between the genotypes (Figure 4b). We also investigated the CC ultrastructure at the two time points without observing differences between the genotypes (Demyelination: WT: 0.8134 ± 0.034, *Tag-1*<sup>-/-</sup>: 0.8258 ± 0.035, Remyelination: WT: 0.7938 ± 0.025, *Tag-1*<sup>-/-</sup>: 0.7911 ± 0.01) (Figure 4c,d, Supporting Information, Figure S4b,c). During demyelination, the number of the remaining myelinated axons was similar in both genotypes (Supporting Information, Figure S4a), indicating that neither the thickness of myelin nor the number of demyelinated axons were affected by the absence of CNTN2. Since remyelination was possible both in the presence and the absence of CNTN2, we first asked whether there was a difference in OPC and OLC populations, by quantifying the number of PDGFRα<sup>+</sup> and CC-1<sup>+</sup> cells per area in the CC after 9 weeks, without observing any difference (Supporting Information, Figure S4d). Furthermore, no significant difference was observed in the density of myelinated callosal axons or in the distribution of axonal diameters throughout the treatments (Supporting Information, Figure S4e,f).

Then we tested if there were functional differences in the tract's signal transduction capacity under these conditions. Callosal CAPs were recorded in acute brain slices of WT and *Tag-1*<sup>-/-</sup> animals after 6 and 9 weeks of treatment and the response to increasing electrical stimuli was plotted for myelinated axons (Figure 4e, Supporting Information, Figure S3b,c). CAP responses were similar between WT and *Tag-1*<sup>-/-</sup> animals in demyelination (Figure 4e, left graph) although significantly reduced compared with untreated responses (Supporting Information, Figure S3d,e). In remyelination, CAP responses were also similar between WT and *Tag-1*<sup>-/-</sup> (Figure 4e, right graph). CAP responses of WT remyelinated mice were reduced compared with untreated WT mice, while *Tag-1*<sup>-/-</sup> remyelinated mice were similar to *Tag-1*<sup>-/-</sup> untreated animals (Supporting Information Figure S3d,e). When we compared the conduction velocity of WT untreated to the remyelination group we found no significant difference (Figure 4f). Surprisingly, a significant increase in the velocity of *Tag-1*<sup>-/-</sup> remyelination group was observed when compared with the *Tag-1*<sup>-/-</sup> untreated state (WT untreated: 0.95 ± 0.25 mm/ms and *Tag-1*<sup>-/-</sup> untreated: 0.56 ± 0.07 mm/ms, WT 9 weeks: 0.75 ± 0.08 mm/ms and *Tag-1*<sup>-/-</sup> 9 weeks: 0.88 ± 0.07 mm/ms; Figure 4f). This phenomenon prompted us to hypothesize that an additional mechanism may exist in the *Tag-1*<sup>-/-</sup>, which is able to affect conduction irrespective of the remyelination status.

### 3.5 | Perinodal protein reorganization during remyelination reveals the presence of a CNTN2-independent mechanism of juxtaparanodal clustering of VGKCs

We hypothesized that an additional mechanism may be responsible for the physiological improvement of the conduction velocity of *Tag-1*<sup>-/-</sup> animals in remyelination, possibly at the level of the molecular organization of the fiber. We performed immunohistochemistry for the juxtaparanodal components Caspr2 (Figure 5a) and VGKCs (Figure 5b) in combination with the paranodal marker Caspr on CC cryosections from

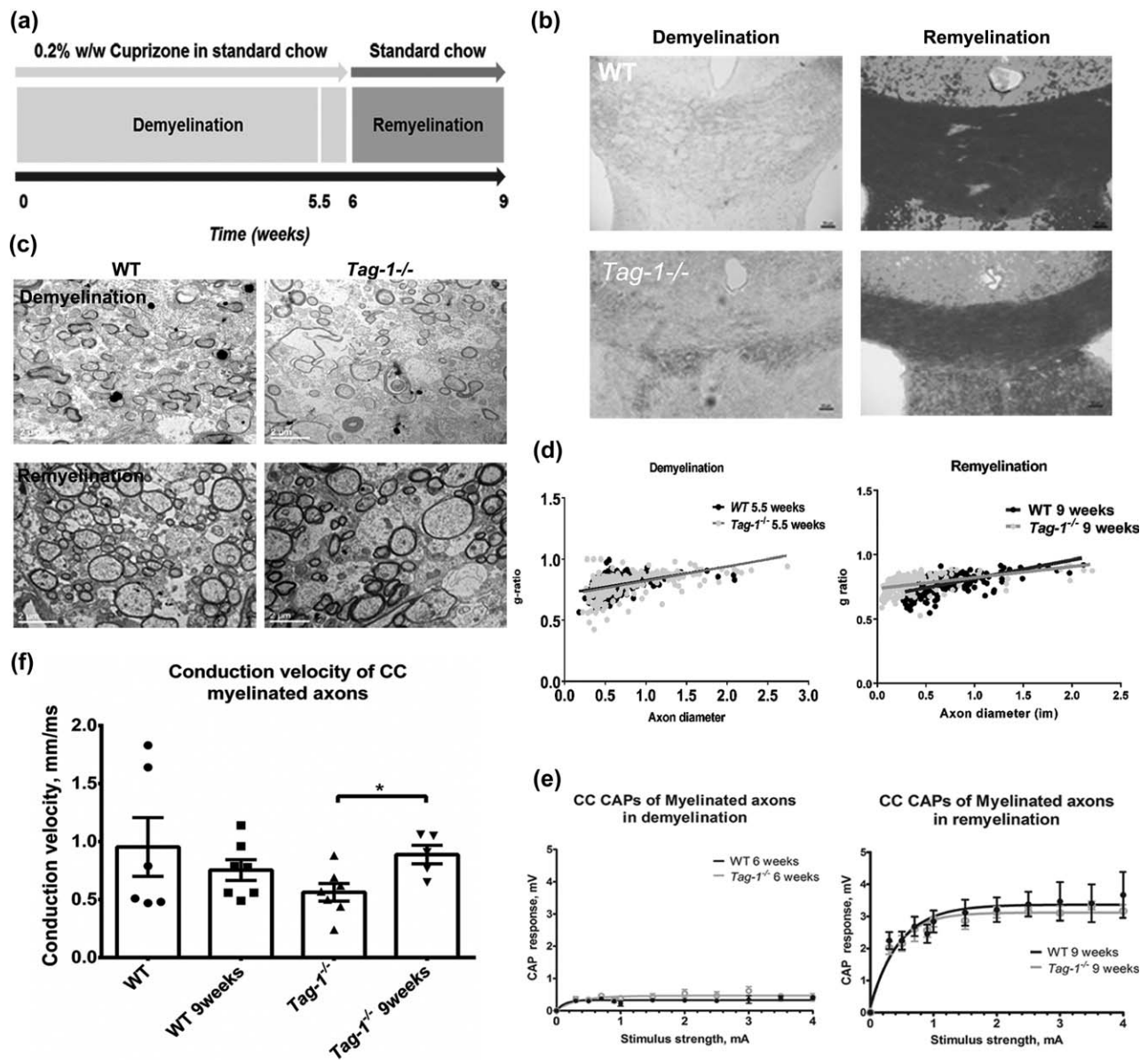


**FIGURE 4** Improved conduction velocity of *Tag-1*<sup>-/-</sup> callosal axons during remyelination. (a) Schematic representation of the cuprizone-induced CNS demyelination experimental protocol. Specific time points of demyelination (5.5 and 6 weeks) are indicated. By the end of the sixth week of cuprizone administration the animal groups were returned to the normal chow for three additional weeks (9 weeks), for remyelination to occur. (b) Luxol fast blue myelin staining on 6 and 9 weeks treated WT and *Tag-1*<sup>-/-</sup> animals. (c) Representative electron microscopy images of WT and *Tag-1*<sup>-/-</sup> CC at 5.5 weeks (demyelination) and 9 weeks (remyelination). (d) g-ratio distribution of myelin sheath thickness of WT and *Tag-1*<sup>-/-</sup> groups during demyelination (left scatter plot) and remyelination (right scatter plot). (e) CC CAPs stimulus-responses curves from demyelinated (left graph) and remyelinated (right graph) WT and *Tag-1*<sup>-/-</sup> animals. No difference on the stimulus response is observed between genotypes in both treatments. (f) Box-plot of conduction velocity comparison for WT and *Tag-1*<sup>-/-</sup> untreated and remyelinated animal groups. Each point represents a different animal. *Tag-1*<sup>-/-</sup> 9-week group showed a significant increase in conduction velocity values when compared with *Tag-1*<sup>-/-</sup> untreated animals (\**p* < .05)

WT and *Tag-1*<sup>-/-</sup> animals. For the purpose of this analysis, untreated adult animals were compared with one demyelinating (6 weeks) and two remyelinating time points (9 and 12 weeks) as depicted at the experimental setup scheme (Figure 5c). As previously described (Zoupi et al., 2013), demyelination of the WT adult callosal tract, caused paranodal disruption and juxtaparanodal component diffusion (6 weeks, Figure 5a,b). The myelinated fibers of the *Tag-1*<sup>-/-</sup> animals are characterized by Caspr2 loss and VGKCs diffusion from the juxtaparanodal

domain (Figure 5a,b, untreated). Demyelination of the *Tag-1*<sup>-/-</sup> CC resulted in the disruption of the paranodal area similarly to the WT controls (Figure 5a,b, 6 weeks). In remyelination (9 and 12 weeks), the disruption of the juxtaparanodal area in *Tag-1*<sup>-/-</sup> animals did not affect the paranodal area. However, we observed that in contrast to the juxtaparanodal Caspr2 (Figure 5a, 9 and 12 weeks) which is dependent on CNTN2 protein for its localization, VGKCs were able to recluster at the JXP domain of *Tag-1*<sup>-/-</sup> mice, (Figure 5b, 9 weeks). In order to test

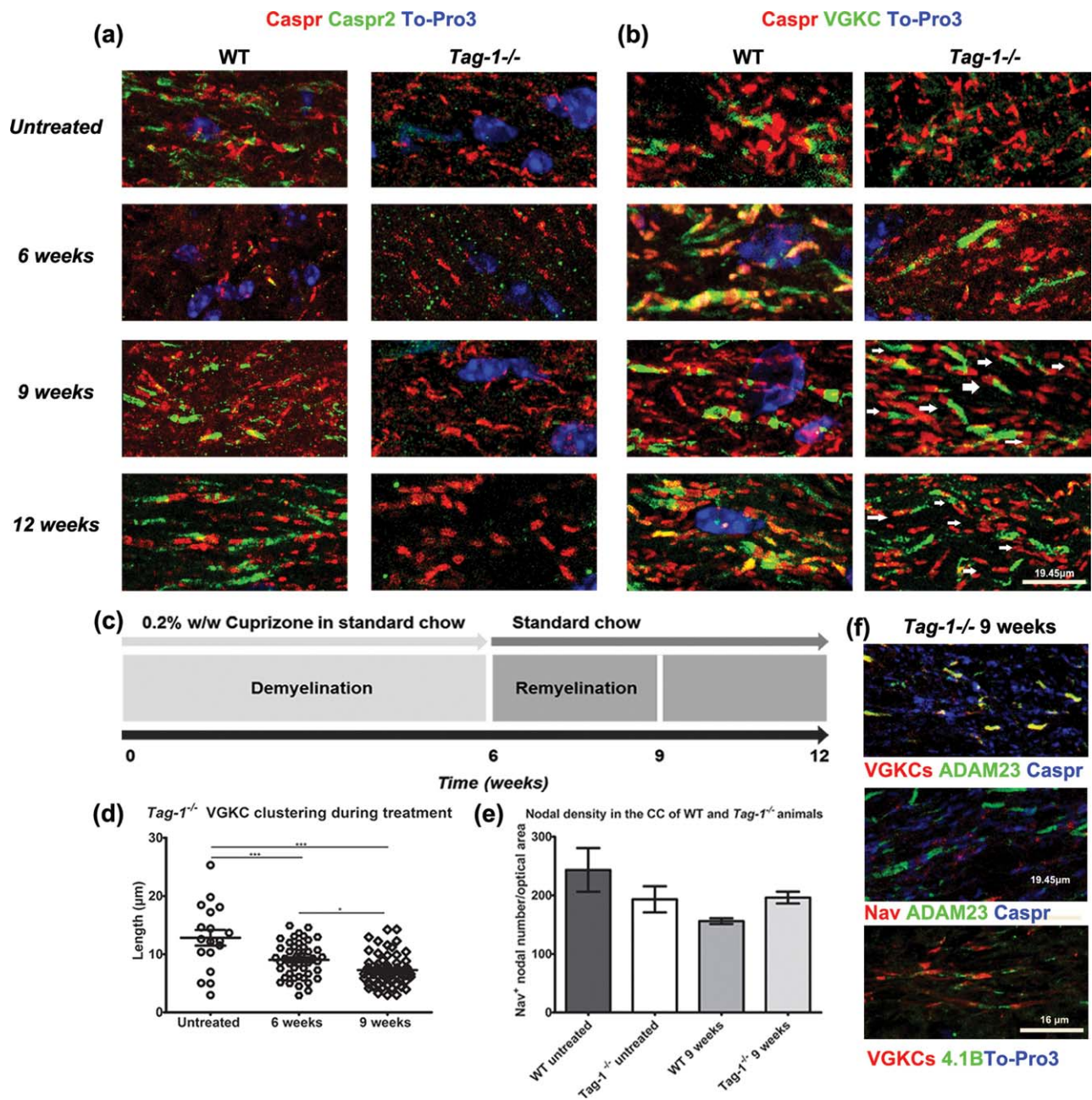


**FIGURE 5** CNTN2-independent mechanism of VGKCs juxtapanodal clustering during remyelination. (a) Immunohistochemical analysis of CC cryosections from untreated and cuprizone treated WT and *Tag-1*<sup>-/-</sup> animals for paranodal Caspr (red) and juxtapanodal Caspr2 (green) proteins. (b) Immunohistochemical analysis of CC cryosections from untreated and cuprizone treated WT and *Tag-1*<sup>-/-</sup> animals for paranodal Caspr (red) and juxtapanodal VGKCs (green). VGKC staining is adjacent to the paranodal Caspr staining (arrows). (c) Schematic representation of the cuprizone-induced CNS demyelination experimental protocol. Time-points for demyelination (6 weeks) and remyelination (9 or 12 weeks) are depicted. (d) Dot plot chart of the measured VGKCs staining length between untreated, 6 and 9 weeks *Tag-1*<sup>-/-</sup> myelinated fibers. The mean length of VGKCs juxtapanodal localization was quantified in each experimental category. (e) Bar graph of the mean nodal density in untreated and remyelinated WT and *Tag-1*<sup>-/-</sup> animals, as assessed by pan-sodium channel immunohistochemical staining of CCs (f) Immunohistochemical analysis of CC cryosections from 9 weeks treated *Tag-1*<sup>-/-</sup> animals for nodal sodium channels (red), paranodal Caspr (blue) and ADAM23 (green) proteins (middle panel), paranodal Caspr (blue), juxtapanodal VGKCs (red), and ADAM23 (green) proteins (first panel) or 4.1B protein (green) and juxtapanodal VGKCs (red; lower panel). In remyelination ADAM23 was detected at the juxtapanodal domain next to paranodal Caspr, co-localizing with VGKCs in *Tag-1*<sup>-/-</sup> myelinated fibers. 4.1B was also properly localized at paranodes and juxtapanodes, where it co-localized with VGKCs (\*\*\**p* < .001, \**p* < .05)

whether this phenomenon was transient, we studied a second time-point of remyelination, at 12 weeks (Figure 5c), where we observed that the VGKCs clustering is maintained (Figure 5b, 12 weeks).

The extent of VGKCs clustering was subsequently measured in the *Tag-1*<sup>-/-</sup> animals by quantifying the length of the VGKCs signal in each experimental condition (Figure 5d). To our surprise, the area of the signal

was reduced in the mutants in the remyelinated condition when compared with untreated *Tag-1<sup>-/-</sup>* animals, suggesting an ongoing recluster-ing process (Figure 5d). This implies that spontaneous remyelination can trigger the initiation of VGKCs clustering at the juxtaparanode possibly by a CNTN2-independent mechanism. In contrast, nodal density as assessed by sodium channel clustering showed no significant difference between the two genotypes and at both de- and re-myelination stages (Figure 5e).

Recent work by Kegel et al. (2014) has identified a novel mechanism of VGKCs clustering during PNS myelination involving the cell surface receptor ADAM23. We have verified the presence of ADAM23 at the CNS juxtaparanodes of the adult WT as well as *Tag-1<sup>-/-</sup>* callosal fibers during remyelination, co-localized with VGKCs (Figure 5f). However, when we performed co-immunoprecipitation experiment on brain lysates from WT and *Tag-1<sup>-/-</sup>* 9 weeks for ADAM23 and VGKCs an interaction was not detected (data not shown).

The adapter protein 4.1B has also been implicated in the formation of the juxtaparanodal complex (Denisenko-Nehrbass et al., 2003; Hivert et al., 2016; Horresh, Bar, Kissil, & Peles, 2010). We observed 4.1B co-localization with VGKCs in the juxtaparanodal domains of *Tag-1<sup>-/-</sup>* 9 weeks callosal fibers (Figure 5f).

In remyelination, the juxtaparanodal VGKCs recluster-ing can contribute to the improvement of axonal conduction velocity observed in *Tag-1<sup>-/-</sup>* animals. However, other glial populations like astrocytes and microglia have been implicated in regulating conduction (Goldstein, Church, Hesp, Popovich, & McTigue, 2016; Salter & Stevens, 2017) and we therefore asked if any of these cellular groups is differentially affected in *Tag-1<sup>-/-</sup>* CC (Supporting Information, Figure S5). In order to address this question, we stained WT and *Tag-1<sup>-/-</sup>* untreated and 9 weeks CCs for the astrocytic marker GFAP (Supporting Information, Figure S5a) and the microglia marker Iba1 (Supporting Information, Figure S5c). Subsequently, the percentage of the area covered by staining was quantified in all groups (Supporting Information, Figure S5b,d). No difference was observed in the GFAP<sup>+</sup> areas for both untreated and 9 weeks groups (Supporting Information, Figure S5b). In contrast, a significant increase in Iba1<sup>+</sup> areas was observed in both untreated and 9 weeks *Tag-1<sup>-/-</sup>* animals when compared with WT (Supporting Information, Figure S5d).

These results imply that during remyelination, alternative CNTN2-independent molecular mechanisms can be initiated in order to compensate for the functional impairment caused after a demyelinating insult.

## 4 | DISCUSSION

In the present study we report on the role of the cell adhesion molecule CNTN2 on oligodendrocyte proliferation, differentiation, myelination and function during development and under pathological conditions. During development, CNTN2 absence can transiently affect the expression levels of myelin and myelin-regulating genes, and results in impaired oligodendrocyte branching and hypomyelination of fiber tracts. During de- and remyelination, *Cntn2* absence did not affect oligodendrocyte survival or the extent of remyelination. However, a

novel, molecular, CNTN2-independent and possibly compensatory mechanism was revealed during remyelination that is able to recluster VGKCs on the remyelinating fiber. We suggest that this recluster-ing results in the improvement of the fiber's conduction.

### 4.1 | CNTN2 is specifically expressed by mature oligodendrocytes

Oligodendrocyte differentiation and maturation is marked by morphological and molecular changes. Factors like Nkx2.2, Nkx6.1, Sox10, Olig1, Olig2, Ascl1/Mash1, and YY1 have been implicated in promoting OPC specification and oligodendrocyte differentiation which morphologically coincides with the extension of thin processes (Cai et al., 2010; Fu et al., 2002; He et al., 2007; Küspert et al., 2011; Lu et al., 2001; Qi et al., 2001; Stolt et al., 2002; Sugimori et al., 2008; Wang et al., 2006; Zhou & Anderson, 2002). As the oligodendrocyte matures, the processes thicken and progressively flat myelin sheaths are formed. At these late stages the oligodendrocyte initially expresses proteins like CC-1, CNP, and MAG and later structural myelin proteins such as MBP, PLP, and MOG (Baumann & Pham-Dinh 2001; Lang et al., 2013).

Here we show that the cell adhesion protein CNTN2/TAG-1 is expressed on mature oligodendrocytes and excluded from OPCs. We detect CNTN2 expression in Olig2<sup>+</sup> oligodendrocytes from P10 onwards using a specific reporter mouse line. Since P10 the numbers of CNTN2<sup>+</sup> mature OLCs were increased, as shown by quantification of CC-1<sup>+</sup> OLCs in the CC white matter tract. Our findings complement the results of a previous study by Çolakoglu and colleagues, where the involvement of the IgSF Contactin-1 during OPC and OLC development and myelination is investigated (Çolakoglu, Bergstrom-Tyrberg, Berglund, & Ranscht, 2014). Contactin-1 was expressed by OPCs and down-regulated in mature OLCs (Çolakoglu et al. 2014). We hypothesize that Contactin-1 and CNTN2 expression by OLCs is a temporally regulated event *in vivo*.

We observed that approximately 60% of the mature OLC population expressed CNTN2 in the adult CC, although this number can be also attributed to GFP expression efficiency in adult transgenic animal. Nevertheless, CNTN2 expression by mature OLCs is a useful observation since the discovery of factors that drive or mark the later stages of oligodendrocyte differentiation/maturation is important especially in pathology. It has been shown that in pathological, demyelinating conditions, failure of remyelination is not only attributed to the lack of proliferation or OPC recruitment at the lesion site, but to the inability of oligodendrocytes to reach their final maturation and myelination states (Chang, Tourtellotte, Rudick, & Trapp, 2002; Kuhlmann et al., 2008).

### 4.2 | CNTN2 can transiently affect the expression of myelin/myelin-regulating genes

*Cntn2* genetic ablation had no effect in the numbers of both OPCs and mature OLCs populations. In contrast, *Cntn2* absence resulted in the transcriptional downregulation of the majority of myelin genes like *mbp*, *plp* and *cnp* at P10, a phenotype that was reversed for *plp* and *mbp* in later stages of myelination. Thus we propose that CNTN2 can



transiently affect the expression of myelin genes although its effect may be compensated by additional mechanisms.

Recently, two main transcription factors have been proven to be necessary for driving the expression of myelin genes thus marking the oligodendrocyte's passage to the myelinating stage. The first one, the zinc-finger protein 191 (*zfp191*) is a nuclear localized transcription factor, responsible for the late-stage of oligodendrocyte maturation and myelination (Howng et al., 2010). Our results showed no alteration in the *zfp191* levels throughout the myelination process.

The second factor is myelin regulatory factor (*Myrf*; Cahoy et al., 2008; Emery et al., 2009; Koenning et al., 2012). Mutant animals with disrupted *Myrf* function can form mature oligodendrocytes that fail to express the necessary myelin genes and eventually undergo apoptotic cell death (Emery et al., 2009). *Myrf* is also an important factor for the maintenance of myelination and the formation of mature oligodendrocytes. Its conditional ablation from myelinating oligodendrocytes leads to the downregulation of myelin genes and a progressive loss of myelin (Koenning et al., 2012). *Myrf* can undergo auto-proteolytic cleavage that results in the nuclear translocation of its N-terminal domain, while with the C-terminal domain can act as a membrane-associated transcription factor. Interestingly, *Myrf* can directly target genes important in oligodendrocyte development like *mag*, *plp1* and *mbp* while an active *myrf* binding region was identified for the *Cntn2* gene (Bujalka et al., 2013). We examined the putative alterations in *Myrf* transcription at the same time points during myelination in both WT and *Tag-1*<sup>-/-</sup> animals. *Myrf* levels were significantly increased at P10 when all myelin genes tested were downregulated. Since *Myrf* can bind and induce the transcription of *Cntn2* gene (Bujalka et al., 2013), *Cntn2* absence may result in the compensatory upregulation of *myrf*. Subsequently, the increased *Myrf* levels can lead to the upregulation of myelin genes that we observe toward the late stages of myelination.

#### 4.3 | CNTN2 affects the morphology of myelinating oligodendrocytes, the extent of myelination and the axonal conduction properties of CC white matter tract

We have shown that regardless of the myelin gene restoration, the production of a sufficient branching network required for the proper enwrapping of the axon was impaired in the mutant animals. Our *in vitro* analysis showed that upon *Cntn2* absence a sufficient number of mature and myelinating oligodendrocytes can be formed. Nevertheless, these myelinating oligodendrocytes exhibit a significantly shorter network of myelin processes. *In vivo* the thickness of myelin sheaths in the adult CC showed a tendency toward higher g-ratio values in the mutant animals. These observations lead us to hypothesize that this cell autonomous defect in the oligodendrocyte branching network can contribute to the final production of thinner myelin sheaths (Chatzopoulou et al., 2008; Savvaki et al., 2008) in the adult.

Finally, our extracellular field recordings of the CC fibers from *Tag-1*<sup>-/-</sup> animals versus adult WT, showed a significant reduction of the CAP responses (reduction of fast conducting myelinating component) in all applied electrical stimuli in the mutants. The decrease of CAP amplitude may reflect reduced numbers of responsive axons or

alterations to callosal axons such as pathological depolarization. Specifically, this impairment can be the result of two CNTN2-dependent mechanisms: First, the afore-mentioned deficit in oligodendrocyte branching and production of thinner myelin sheaths and second, the disassembly of the juxtaparanodal complex that results in the diffusion of VGKCs toward the internodal domain (Savvaki et al., 2008; Traka et al., 2003).

#### 4.4 | Improved conduction velocity of *Tag-1*<sup>-/-</sup> callosal axons during remyelination. No impact in myelin sheath thickness

The effect of CNTN2 on the process network of the myelinating oligodendrocyte led us to investigate its involvement in de/remyelinating conditions, using the well-established cuprizone model of toxic CNS demyelination (Benetti et al., 2010; Matsushima & Morell, 2001).

No differences on cell distribution or myelination were observed between the groups in all parameters tested during de- and remyelination. It is of note that in remyelination, the myelin sheaths that are produced are always thinner and shorter in size compared with the control state (Fancy et al., 2011; Franklin & Ffrench-Constant 2008). At that stage, no difference was detected between WT and *Tag-1*<sup>-/-</sup> fibers regarding their CAP responses. However they were reduced compared with the untreated state, suggesting only a partial recovery. Nevertheless, when the conduction velocity was measured, in *Tag-1*<sup>-/-</sup> animals, a significant increase was noted, suggesting an underlying compensatory mechanism. Since conduction velocity can be affected by the myelin sheath thickness, the axonal numbers and health and the distribution of ion channels along the axon, we hypothesized that a possible molecular re-organization in the areas around the node of Ranvier could contribute in the observed changes in signal transduction.

#### 4.5 | VGKCs recluster during remyelination in a CNTN2/Caspr2-independent manner

The molecular clustering of VGKCs on the remyelinating fiber along with the presence of sufficient sodium channel concentration at the node of Ranvier could be responsible for the observed improvement in conduction in the *Tag-1*<sup>-/-</sup> animals. Indeed, we have identified the existence of a molecular compensatory mechanism resulting in the reassembly of VGKCs at the juxtaparanodal domain during remyelination, in a CNTN2/Caspr2-independent manner.

Myelin loss leads to a progressive disruption of the perinodal architecture initiating from the paranodal domain and followed by the juxtaparanodal disassembly (Zoupi et al., 2013). On the other hand, the extent of remyelination seems to dictate the molecular assembly of perinodal components that also begins from the paranode (Zoupi et al., 2013). Loss of CNTN2 protein from the juxtaparanode leads to the disruption of the tripartite molecular complex that includes Caspr2 protein and the VGKCs (Chatzopoulou et al., 2008; Savvaki et al., 2008; Traka et al., 2003). However, CNTN2 expression from the oligodendrocyte can completely restore the mutant phenotype and therefore is an



indispensable protein for both Caspr2 and VGKCs clustering (Savvaki et al., 2010).

In addition, 4.1B protein acts as a linker protein that connects a number of membrane proteins to the spectrin/actin cytoskeleton (Baines, 2010), like the paranodal Caspr and the juxtaparanodal Caspr2 via a PDZ-binding motif (Denisenko-Nehrbass et al., 2003). 4.1B KO animals display perturbed paranodal protein localization and a severe disruption of the juxtaparanodal complex (Cifuentes-Diaz et al., 2011). At the juxtaparanode, MAGUK adapter proteins PSD93 and PSD95 are also expressed along with ADAM22 (a disintegrin and metalloprotease 22; Ogawa et al., 2008; Ogawa et al., 2010). Loss of Caspr2 or CNTN2 affects MAGUK protein and ADAM22 assembly at the juxtaparanode (Horresh, Poliak, Grant, Bredt, Rasband, & Peles, 2008; Ogawa et al., 2010), but it does not affect the localization of 4.1B protein (Horresh et al., 2010).

Interestingly, previous work from Duflocq et al. (2011) has shown that the clustering of VGKCs was independent of the CNTN2/Caspr2 complex and of the membrane-associated guanylate-kinase (MAGUK) adapter protein PSD93 in the axon initial segment (AIS) of motor neurons. In that study, when the AIS of *Tag-1*<sup>-/-</sup> animals was analyzed it has been found that VGKCs were normally localized although Caspr2 localization was abolished, in contrast to juxtaparanodal VGKCs from the spinal cord ventral horn which were diffused. Instead, 4.1B/Caspr protein complex was responsible for the formation of the appropriate barrier that led to the correct VGKCs localization at the respective AIS area (Duflocq et al., 2011).

A recent study has revealed the existence of an additional molecule at the juxtaparanode, ADAM23, which was found to co-localize with Caspr2, CNTN2, and VGKCs at the area (Kegel et al., 2014). It has been suggested that ADAM22 and ADAM23 expression in apposing cell membranes at the juxtaparanode might be an additional mechanism of juxtaparanodal complex organization and/or stability possibly in an LGI4-dependent manner, although this hypothesis needs further investigation (Kegel et al., 2014).

We have shown that upon remyelination, VGKCs clustering at the juxtaparanodal domain is evident irrespective of the absence of both juxtaparanodal CNTN2 and Caspr2. Furthermore, the absence of these proteins had no impact on paranodal Caspr, 4.1B protein localization and juxtaparanodal ADAM23 distribution, molecules that have been described to indirectly affect VGKCs localization. We have verified the presence of ADAM23 protein at the CNS juxtaparanode and therefore, hypothesize that, during remyelination in the absence of CNTN2/Caspr2, ADAM23 and 4.1B could be responsible for VGKC clustering. In parallel, the formation of an intact paranodal barrier by Caspr and 4.1B proteins, allows the correct segregation of VGKCs at the juxtaparanode which along with the existence of intact sodium channel accumulation at the nodes of Ranvier, allow for the increase of conduction velocities in the remyelinated fibers. Although an interaction between ADAM23 and VGKCs was not evident biochemically, indirect interactions with additional candidates like ADAM22, LGI4, MMPs and Nectin-like proteins (neclns) (Horresh et al., 2008; Shingai et al., 2003; Spiegel et al., 2007), implicated in interactions with paranodal/juxtaparanodal proteins, cannot be excluded.

The axonal conduction velocity can be also affected by the different glial populations (i.e. astrocytes and microglia) that are recruited as a response to the demyelinating insult. Microglia and astrocytes have been shown to stimulate both inflammatory and anti-inflammatory pathways, engulfment of myelin debris at the area of the lesion and regulation of synaptic activity (Goldstein et al., 2016; Salter & Stevens, 2017). In our case, we noted that the microglial population was increased in both untreated and remyelinating *Tag-1*<sup>-/-</sup> animals, while the astrocytes did not show any difference between the genotypes. Although the involvement of microglia to the functional restoration of conduction velocity is possible, its exact role in the *Tag-1*<sup>-/-</sup> needs further investigation.

We propose that the combination of intact nodal domains combined with the observed reclustering of VGKCs, important for the membrane's resting potential and the involvement of the microglial population in the *Tag-1*<sup>-/-</sup> fibers during remyelination is a candidate mechanism for the improved conductivity observed in the particular animal group, irrespective of the remyelinating state of the callosal tract.

#### ACKNOWLEDGMENT

We are thankful to members of the Karageos lab for critical reading of the manuscript, Dr A. Stamatakis for his help and advice, Prof. G. Chalepakis, Mr S. Papadakis, Mrs S. Papadogiorgaki and Mrs A. Siakouli for the preparation and acquisition of EM samples and Dr E. Deligianni for her assistance on the Operetta High-Content Imaging System. We would like to acknowledge support from the General Secretariat for Research & Technology (GSRT), program ARISTEIA I "Myelin Tag" Project 593, the Fondation ARSEP grant «Assembly of the juxtaparanodal complex under normal and pathological conditions», the GSRT for the Franco-Hellenic project «Juxtamyelin» and the Manasaki graduate fellowships of the University of Crete (to K. K.).

#### REFERENCES

- Baines, A. J. (2010). The spectrin-ankyrin-4.1-adducin membrane skeleton: Adapting eukaryotic cells to the demands of animal life. *Proto-plasma*, 244, 99–131.
- Bastakis, G. G., Savvaki, M., Stamatakis, A., Vidaki, M., & Karageos, D. (2015). Tag1 deficiency results in olfactory dysfunction through impaired migration of mitral cells. *Development*, 142, 4318–4328.
- Baumann, N., & Pham-Dinh, D. (2001). Biology of oligodendrocyte and myelin in the mammalian central nervous system. *Physiological Reviews*, 81, 871–927.
- Benetti, F., Ventura, M., Salmini, B., Ceola, S., Carbonera, D., Mammi, S., ... Spisni, E. (2010). Cuprizone neurotoxicity, copper deficiency and neurodegeneration. *Neurotoxicology*, 31, 509–517.
- Bergles, D. E., & Richardson, W. D. (2015). Oligodendrocyte development and plasticity. *Cold Spring Harbor Perspectives in Biology*, 8, a020453.
- Bujalka, H., Koenning, M., Jackson, S., Perreau, V. M., Pope, B., Hay, C. M., ... Emery, B. (2013). MYRF is a membrane-associated transcription factor that autoproteolytically cleaves to directly activate myelin genes. *PLoS Biology*, 11, e1001625.



- Cahoy, J. D., Emery, B., Kaushal, A., Foo, L. C., Zamanian, J. L., Christopherson, K. S., ... Barres, B. A. (2008). A transcriptome database for astrocytes, neurons, and oligodendrocytes: A new resource for understanding brain development and function. *Journal of Neuroscience*, 28, 264–278.
- Cai, J., Zhu, Q., Zheng, K., Li, H., Qi, Y., Cao, Q., & Qiu, M. (2010). Colocalization of Nkx6.2 and Nkx2.2 homeodomain proteins in differentiated myelinating oligodendrocytes. *Glia*, 58, 458–468.
- Chang, A., Tourtellotte, W. W., Rudick, R., & Trapp, B. D. (2002). Pre-myelinating oligodendrocytes in chronic lesions of multiple sclerosis. *The New England Journal of Medicine*, 346, 165–173.
- Chang, K. J., Redmond, S. A., & Chan, J. R. (2016). Remodeling myelination: Implications for mechanisms of neural plasticity. *Nature Neuroscience*, 19, 190–197.
- Charles, P., Tait, S., Faivre-Sarrailh, C., Barbin, G., Gunn-Moore, F., Denisenko-Nehrbass, N., ... Lubetzki, C. (2002). Neurofascin is a glial receptor for the paranodin/Caspr-contactin axonal complex at the axoglial junction. *Current Biology*, 12, 217–220.
- Chatzopoulou, E., Miguez, A., Savvaki, M., Levasseur, G., Muzerelle, A., Muriel, M. P., ... Thomas, J. L. (2008). Structural requirement of TAG-1 for retinal ganglion cell axons and myelin in the mouse optic nerve. *Journal of Neuroscience*, 28, 7624–7636.
- Cifuentes-Diaz, C., Chareyre, F., Garcia, M., Devaux, J., Carnaud, M., Levasseur, G., ... Goutebroze, L. (2011). Protein 4.1B contributes to the organization of peripheral myelinated axons. *PLoS One*, 6, e25043.
- Çolakoglu, G., Bergstrom-Tyrberg, U., Berglund, E. O., & Ranscht, B. (2014). Contactin-1 regulates myelination and nodal/paranodal domain organization in the central nervous system. *Proceedings of the National Academy of Sciences of the United States of America*, 111, E394–E403.
- Coman, I., Aigrot, M. S., Seilhean, D., Reynolds, R., Girault, J. A., Zalc, B., & Lubetzki, C. (2006). Nodal, paranodal and juxtaparanodal axonal proteins during demyelination and remyelination in multiple sclerosis. *Brain*, 129, 3186–3195.
- Crawford, D. K., Mangiardi, M., & Tiwari-Woodruff, S. K. (2009). Assaying the functional effects of demyelination and remyelination: Revisiting field potential recordings. *The Journal of Neuroscience Methods*, 182, 25–33.
- Denisenko-Nehrbass, N., Oguievetskaia, K., Goutebroze, L., Galvez, T., Yamakawa, H., Ohara, O., ... Girault, J. A. (2003). Protein 4.1B associates with both Caspr/paranodin and Caspr2 at paranodes and juxtaparanodes of myelinated fibres. *European Journal of Neuroscience*, 17, 411–416.
- Duflocq, A., Chareyre, F., Giovannini, M., Couraud, F., & Davenne, M. (2011). Characterization of the axon initial segment (AIS) of motor neurons and identification of a para-AIS and a juxtapara-AIS, organized by protein 4.1B. *BMC Biology*, 9, 66.
- Emery, B., Agalliu, D., Cahoy, J. D., Watkins, T. A., Dugas, J. C., Mulinnyaw, S. B., ... Barres, B. A. (2009). Myelin gene regulatory factor is a critical transcriptional regulator required for CNS myelination. *Cell*, 138, 172–185.
- Fancy, S. P., Chan, J. R., Baranzini, S. E., Franklin, R. J., & Rowitch, D. H. (2011). Myelin regeneration: A recapitulation of development? *Annual Review of Neuroscience*, 34, 21–43.
- Franklin, K. B. J., & Paxinos, G. (1997). *The mouse brain in stereotaxic coordinates*. San Diego: Academic Press.
- Franklin, R. J., & Ffrench-Constant, C. (2008). Remyelination in the CNS: From biology to therapy. *Nature Reviews Neuroscience*, 9, 839–855.
- Fu, H., Qi, Y., Tan, M., Cai, J., Takebayashi, H., Nakafuku, M., ... Qiu, M. (2002). Dual origin of spinal oligodendrocyte progenitors and evidence for the cooperative role of Olig2 and Nkx2.2 in the control of oligodendrocyte differentiation. *Development*, 129, 681–693.
- Fukamauchi, F., Aihara, O., Wang, Y. J., Akasaka, K., Takeda, Y., Horie, M., ... Iwakura, Y. (2001). TAG-1-deficient mice have marked elevation of adenosine A1 receptors in the hippocampus. *Biochemical and Biophysical Research Communications*, 281, 220–226.
- Goldstein, E. Z., Church, J. S., Hesp, Z. C., Popovich, P. G., & McTigue, D. M. (2016). A silver lining of neuroinflammation: Beneficial effects on myelination. *Experimental Neurology*, 283, 550–559.
- He, Y., Dupree, J., Wang, J., Sandoval, J., Li, J., Liu, H., ... Casaccia-Bonnel, P. (2007). The transcription factor Yin Yang 1 is essential for oligodendrocyte progenitor differentiation. *Neuron*, 55, 217–230.
- Hivert, B., Pinatel, D., Labasque, M., Tricaud, N., Goutebroze, L., & Faivre-Sarrailh, C. (2016). Assembly of juxtaparanodes in myelinating DRG culture: Differential clustering of the Kv1/Caspr2 complex and scaffolding protein 4.1B. *Glia*, 64, 840–852.
- Horresh, I., Bar, V., Kissil, J. L., & Peles, E. (2010). Organization of myelinated axons by Caspr and Caspr2 requires the cytoskeletal adapter protein 4.1B. *Journal of Neuroscience*, 30, 2480–2489.
- Horresh, I., Poliak, S., Grant, S., Bredt, D., Rasband, M. N., & Peles, E. (2008). Multiple molecular interactions determine the clustering of Caspr2 and Kv1 channels in myelinated axons. *Journal of Neuroscience*, 28, 14213–14222.
- Howell, O. W., Rundle, J. L., Garg, A., Komada, M., Brophy, P. J., & Reynolds, R. (2010). Activated microglia mediate axoglial disruption that contributes to axonal injury in multiple sclerosis. *The Journal of Neuro-pathology & Experimental Neurology*, 69, 1017–1033.
- Howng, S. Y., Avila, R. L., Emery, B., Traka, M., Lin, W., Watkins, T., ... Popko, B. (2010). ZFP191 is required by oligodendrocytes for CNS myelination. *Genes Development*, 24, 301–311.
- Kastriti, M. E., Sargiannidou, I., Kleopa, K. A., & Karageorgos, D. (2015). Differential modulation of the juxtaparanodal complex in Multiple Sclerosis. *Molecular and Cellular Neuroscience*, 67, 93–103.
- Kegel, L., Jaegle, M., Driegen, S., Aunin, E., Leslie, K., Fukata, Y., ... Meijer, D. (2014). Functional phylogenetic analysis of LGI proteins identifies an interaction motif crucial for myelination. *Development*, 141, 1749–1756.
- Kessarar, N., Fogarty, M., Iannarelli, P., Grist, M., Wegner, M., & Richardson, W. D. (2006). Competing waves of oligodendrocytes in the fore-brain and postnatal elimination of an embryonic lineage. *Nature Neuroscience*, 9, 173–179.
- Kessarar, N., Pringle, N., & Richardson, W. D. (2008). Specification of CNS glia from neural stem cells in the embryonic neuroepithelium. *Philosophical Transactions of the Royal Society B: Biological Sciences*, 363, 71–85.
- Koenning, M., Jackson, S., Hay, C. M., Faux, C., Kilpatrick, T. J., Willingham, M., & Emery, B. (2012). Myelin gene regulatory factor is required for maintenance of myelin and mature oligodendrocyte identity in the adult CNS. *Journal of Neuroscience*, 32, 12528–12542.
- Kuhlmann, T., Miron, V., Cui, Q., Cuo, Q., Wegner, C., Antel, J., & Brück, W. (2008). Differentiation block of oligodendroglial progenitor cells as a cause for remyelination failure in chronic multiple sclerosis. *Brain*, 131, 1749–1758.
- Küspert, M., Hammer, A., Bösl, M. R., & Wegner, M. (2011). Olig2 regulates Sox10 expression in oligodendrocyte precursors through an evolutionary conserved distal enhancer. *Nucleic Acids Research*, 39, 1280–1293.
- Labasque, M., & Faivre-Sarrailh, C. (2010). GPI-anchored proteins at the node of Ranvier. *FEBS Letters*, 584, 1787–1792.
- Lang, J., Maeda, Y., Bannerman, P., Xu, J., Horiuchi, M., Pleasure, D., & Guo, F. (2013). Adenomatous polyposis coli regulates oligodendroglial development. *Journal of Neuroscience*, 33, 3113–3130.

- Lourenço, T., Paes de Faria, J., Bippes, C. A., Maia, J., Lopes-da-Silva, J. A., Relvas, J. B., & Grãos, M. (2016). Modulation of oligodendrocyte differentiation and maturation by combined biochemical and mechanical cues. *Science Reports*, *6*, 21563.
- Lu, Q. R., Cai, L., Rowitch, D., Cepko, C. L., & Stiles, C. D. (2001). Ectopic expression of Olig1 promotes oligodendrocyte formation and reduces neuronal survival in developing mouse cortex. *Nature Neuroscience*, *4*, 973–974.
- Matsushima, G. K., & Morell, P. (2001). The neurotoxicant, cuprizone, as a model to study demyelination and remyelination in the central nervous system. *Brain Pathology*, *11*, 107–116.
- Miron, V. E., Boyd, A., Zhao, J. W., Yuen, T. J., Ruckh, J. M., Shadrach, J. L., ... Ffrench-Constant, C. (2013). M2 microglia and macrophages drive oligodendrocyte differentiation during CNS remyelination. *Nature Neuroscience*, *16*, 1211–1218.
- Ogawa, Y., Horresh, I., Trimmer, J. S., Bredt, D. S., Peles, E., & Rasband, M. N. (2008). Postsynaptic density-93 clusters Kv1 channels at axon initial segments independently of Caspr2. *Journal of Neuroscience*, *28*, 5731–5739.
- Ogawa, Y., Oses-Prieto, J., Kim, M. Y., Horresh, I., Peles, E., Burlingame, A. L., ... Rasband, M. N. (2010). ADAM22, a Kv1 channel-interacting protein, recruits membrane-associated guanylate kinases to juxtaparanodes of myelinated axons. *Journal of Neuroscience*, *30*, 1038–1048.
- Pernet, V., Joly, S., Christ, F., Dimou, L., & Schwab, M. E. (2008). Nogo-A and myelin-associated glycoprotein differently regulate oligodendrocyte maturation and myelin formation. *Journal of Neuroscience*, *28*, 7435–7444.
- Poliak, S., Salomon, D., Elhanany, H., Sabanay, H., Kiernan, B., Pevny, L., ... Peles, E. (2003). Juxtaparanodal clustering of Shaker-like K<sup>+</sup> channels in myelinated axons depends on Caspr2 and TAG-1. *Journal of Cell Biology*, *162*, 1149–1160.
- Qi, Y., Cai, J., Wu, Y., Wu, R., Lee, J., Fu, H., ... Qiu, M. (2001). Control of oligodendrocyte differentiation by the Nkx2.2 homeodomain transcription factor. *Development*, *128*, 2723–2733.
- Rasband, M. N., & Peles, E. (2015). The nodes of Ranvier: Molecular assembly and maintenance. *Cold Spring Harbor Perspectives in Biology*, *8*, a020495.
- Reeves, T. M., Phillips, L. L., & Povlishock, J. T. (2005). Myelinated and unmyelinated axons of the corpus callosum differ in vulnerability and functional recovery following traumatic brain injury. *Experimental Neurology*, *196*, 126–137.
- Richardson, W. D., Kessar, N., & Pringle, N. (2006). Oligodendrocyte wars. *Nature Reviews Neuroscience*, *7*, 11–18.
- Salter, M. W., & Stevens, B. (2017). Microglia emerge as central players in brain disease. *Nature Medicine*, *23*, 1018–1027.
- Savvaki, M., Panagiotaropoulos, T., Stamatakis, A., Sargiannidou, I., Karatzioula, P., Watanabe, K., ... Kleopa, K. A. (2008). Impairment of learning and memory in TAG-1 deficient mice associated with shorter CNS internodes and disrupted juxtaparanodes. *Molecular and Cellular Neuroscience*, *39*, 478–490.
- Savvaki, M., Theodorakis, K., Zoupi, L., Stamatakis, A., Tivodar, S., Kyriacou, K., ... Karagogeos, D. (2010). The expression of TAG-1 in glial cells is sufficient for the formation of the juxtaparanodal complex and the phenotypic rescue of tag-1 homozygous mutants in the CNS. *Journal of Neuroscience*, *30*, 13943–13954.
- Sherman, D. L., & Brophy, P. J. (2005). Mechanisms of axon ensheathment and myelin growth. *Nature Reviews Neuroscience*, *6*, 683–690.
- Sherman, D. L., Tait, S., Melrose, S., Johnson, R., Zonta, B., Court, F. A., ... Brophy, P. J. (2005). Neurofascins are required to establish axonal domains for saltatory conduction. *Neuron*, *48*, 737–742.
- Shingai, T., Ikeda, W., Kakunaga, S., Morimoto, K., Takekuni, K., Itoh, S., ... Takai, Y. (2003). Implications of nectin-like molecule-2/IGSF4/RA175/SgIGSF/TSLC1/SynCAM1 in cell-cell adhesion and transmembrane protein localization in epithelial cells. *The Journal of Biological Chemistry*, *278*, 35421–35427.
- Simons, M., & Trotter, J. (2007). Wrapping it up: The cell biology of myelination. *Current Opinion in Neurobiology*, *17*, 533–540.
- Snaidero, N., & Simons, M. (2017). The logistics of myelin biogenesis in the central nervous system. *Glia*, *65*(7), 1021–1031. <https://doi.org/10.1002/glia.23116>.
- Spiegel, I., Adamsky, K., Eshed, Y., Milo, R., Sabanay, H., Sarig-Nadir, O., ... Peles, E. (2007). A central role for Necl4 (SynCAM4) in Schwann cell-axon interaction and myelination. *Nature Neuroscience*, *10*, 861–869.
- Stolt, C. C., Rehberg, S., Ader, M., Lommes, P., Riethmacher, D., Schachner, M., ... Wegner, M. (2002). Terminal differentiation of myelin-forming oligodendrocytes depends on the transcription factor Sox10. *Genes Development*, *16*, 165–170.
- Sugimori, M., Nagao, M., Parras, C. M., Nakatani, H., Lebel, M., Guillemot, F., & Nakafuku, M. (2008). Ascl1 is required for oligodendrocyte development in the spinal cord. *Development*, *135*, 1271–1281.
- Susuki, K., & Rasband, M. N. (2008). Molecular mechanisms of node of Ranvier formation. *Current Opinion in Cell Biology*, *20*, 616–623.
- Traka, M., Dupree, J. L., Popko, B., & Karagogeos, D. (2002). The neuronal adhesion protein TAG-1 is expressed by Schwann cells and oligodendrocytes and is localized to the juxtaparanodal region of myelinated fibers. *Journal of Neuroscience*, *22*, 3016–3024.
- Traka, M., Goutebroze, L., Denisenko, N., Bessa, M., Nifli, A., Havaki, S., ... Karagogeos, D. (2003). Association of TAG-1 with Caspr2 is essential for the molecular organization of juxtaparanodal regions of myelinated fibers. *The Journal of Cell Biology*, *162*, 1161–1172.
- Wang, S. Z., Dulin, J., Wu, H., Hurlock, E., Lee, S. E., Jansson, K., & Lu, Q. R. (2006). An oligodendrocyte-specific zinc-finger transcription regulator cooperates with Olig2 to promote oligodendrocyte differentiation. *Development*, *133*, 3389–3398.
- Zhou, Q., & Anderson, D. J. (2002). The bHLH transcription factors OLIG2 and OLIG1 couple neuronal and glial subtype specification. *Cell*, *109*, 61–73.
- Zoupi, L., Markoullis, K., Kleopa, K. A., & Karagogeos, D. (2013). Alterations of juxtaparanodal domains in two rodent models of CNS demyelination. *Glia*, *61*, 1236–1249.
- Zoupi, L., Savvaki, M., & Karagogeos, D. (2011). Axons and myelinating glia: An intimate contact. *IUBMB Life*, *63*, 730–735.

## SUPPORTING INFORMATION

Additional Supporting Information may be found online in the supporting information tab for this article.

**How to cite this article:** Zoupi L, Savvaki M, Kalemaki K, Kalafatakis I, Sidiropoulou K, Karagogeos D. The function of contactin-2/TAG-1 in oligodendrocytes in health and demyelinating pathology. *Glia*. 2018;66:576–591. <https://doi.org/10.1002/glia.23266>



# Using the Allen gene expression atlas of the adult mouse brain to gain further insight into the physiological significance of TAG-1/Contactin-2

Ilias Kalafatakis<sup>1</sup> · Konstantinos Kalafatakis<sup>1,2</sup> · Alexandros Tsimpolis<sup>1</sup> · Nikos Giannakeas<sup>2</sup> · Markos Tsipouras<sup>2</sup> · Alexandros Tzallas<sup>2</sup> · Domna Karagogeos<sup>1</sup>

Received: 7 December 2019 / Accepted: 21 June 2020  
© Springer-Verlag GmbH Germany, part of Springer Nature 2020

## Abstract

The anatomic gene expression atlas (AGEA) of the adult mouse brain of the Allen Institute for Brain Science is a transcriptome-based atlas of the adult C57Bl/6 J mouse brain, based on the extensive in situ hybridization dataset of the Institute. This spatial mapping of the gene expression levels of mice under baseline conditions could assist in the formation of new, reasonable transcriptome-derived hypotheses on brain structure and underlying biochemistry, which could also have functional implications. The aim of this work is to use the data of the AGEA (in combination with Tabula Muris, a compendium of single cell transcriptome data collected from mice, enabling direct and controlled comparison of gene expression among cell types) to provide further insights into the physiology of TAG-1/Contactin-2 and its interactions, by presenting the expression of the corresponding gene across the adult mouse brain under baseline conditions and to investigate any spatial genomic correlations between TAG-1/Contactin-2 and its interacting proteins and markers of mature and immature oligodendrocytes, based on the pre-existing experimental or bibliographical evidence. The across-brain correlation analysis on the gene expression intensities showed a positive spatial correlation of TAG-1/Contactin-2 with the gene expression of Plp1, Myrf, Mbp, Mog, Cldn11, Bace1, Kcna1, Kcna2, App and Nfasc and a negative spatial correlation with the gene expression of Cspg4, Pdgfra, L1cam, Ncam1, Ncam2 and Ptpnz1. Spatially correlated genes are mainly expressed by mature oligodendrocytes (like Cntn2), while spatially anticorrelated genes are mainly expressed by oligodendrocyte precursor cells. According to the data presented in this work, we propose that even though Contactin-2 expression during development correlates with high plasticity events, such as neurogenesis, in adulthood it correlates with pathways characterized by low plasticity.

**Keywords** Anatomic gene expression atlas (AGEA) · TAG-1/Contactin-2 · Interacting proteins · Oligodendrocytes · Myelination

---

**Electronic supplementary material** The online version of this article (<https://doi.org/10.1007/s00429-020-02108-4>) contains supplementary material, which is available to authorized users.

✉ Ilias Kalafatakis  
ilias\_kalafatakis@imbb.forth.gr

<sup>1</sup> Faculty of Medicine, University of Crete & Institute of Molecular Biology and Biotechnology, Foundation of Research and Technology Hellas, Heraklion, Crete, Greece

<sup>2</sup> Department of Informatics and Telecommunications, School of Informatics and Telecommunications, University of Ioannina, Arta, Greece

## Introduction

TAG-1/Contactin-2 (herein called Contactin-2) is a GPI-anchor glycoprotein that belongs to the immunoglobulin superfamily (IgSF). This group of proteins contains multiple extracellular immunoglobulin-like and fibronectin III-like domains and is mainly found in the nervous system (Dodd et al. 1988; Furley et al. 1990; Gennarini and Furley 2017; Karagogeos 2003; Yamamoto et al. 1986). Although Contactin-2 acts as a cell adhesion molecule and is normally found on the membrane surface during development, it can also be found in a soluble form throughout the brain due to its cleavable GPI linkage (Furley et al. 1990; Karagogeos et al. 1991; Zhou et al. 2012). It has a plethora of different functions in both the developing and the adult nervous system.

In the embryonic nervous system, Contactin-2 plays an important role in a lot of different developmental processes (Denaxa et al. 2003; Karagozeos 2003). It is highly expressed on the surface of axons of commissural neurons, while they approach the floor plate. Upon crossing it, Contactin-2 expression is highly reduced and L1 is expressed instead (Dodd et al. 1988). In addition, Contactin-2 is present on the surface of dorsal root ganglion (DRG) axons and plays a significant role in their elongation, fasciculation and guidance (Karagozeos et al. 1991; Masuda et al. 2000; Stoeckli et al. 1991). Contactin-2 is also responsible for the interactions between mature axons and immature neurons of the cerebral cortex, while it is also involved in the axonal formation of the latter (Namba et al. 2014). Moreover, Contactin-2 is essential for the migration of a variety of neurons in the cerebral cortex and the medulla (Denaxa et al. 2001; Denaxa et al. 2005; Kyriakopoulou et al. 2002; Okamoto et al. 2013); while in cerebellum, it is expressed on the surface of granule precursor cells preventing their premature differentiation (Bailly et al. 1996; Buttiglione et al. 1998; Xenaki et al. 2011; Wang et al. 2011).

In the adult nervous system, Contactin-2 is expressed in both axons and glial cells (Traka et al. 2002). It is essential for the clustering of potassium channels and Caspr2 at the juxtaparanodes of myelinated fibers (Savvaki et al. 2008; Traka et al. 2003), while absence of this protein is correlated with hypomyelination, abnormalities in the calibre distribution and cytoskeletal defects of axons (Chatzopoulou et al. 2008). In addition, absence of Contactin-2 leads to significant impairments in motor coordination as well as learning and memory (Savvaki et al. 2008). Lastly, it can transiently affect the expression of myelin genes and myelin-regulating genes and the morphology of myelinating oligodendrocytes, the extent of myelination and the axonal conduction properties of white matter tracts (Zoupi et al. 2018). Contactin-2 is recognized as an autoantigen in multiple sclerosis patients, contributing to the development of grey matter pathology (Derfuss et al. 2009), while there are some indications that this protein is also involved in other pathologies, such as gliomas, Alzheimer disease, epilepsy and chronic inflammatory demyelinating polyneuropathy (Iijima et al. 2009; Stogmann et al. 2013; Tachi et al. 2010; Yan and Jiang 2016).

Research on Contactin-2 has revealed various functional or structural interactions between this glycoprotein and other biomolecules. These interactions have been specified either by experimentation in biological systems or *in silico*, by modern computational tools. In this work, we have hypothesized that if the co-involvement of Contactin-2 and these other biomolecules was crucial for normal neuronal and/or glial function, the cells would want to ensure their co-presence by regulating their co-expression at a genomic level.

To establish any spatial genomic correlations between Contactin-2 with its functionally or structurally interacting

molecules in the adult mouse brain, we utilized the corresponding data from two sources: (i) the anatomic gene expression atlas (AGEA) of the adult mouse brain of the Allen Institute for Brain Science, an online transcriptome-based atlas of the adult C57Bl/6 J mouse brain, showing the spatial registration of the expression intensity of 4376 genes into 51,533, 200  $\mu\text{m}$ -diameter cubic voxels. All the information presented in the AGEA are based on extensive *in situ* hybridization (ISH) experiments of the Institute (Ng et al. 2009). And (ii) Tabula Muris, which is a compendium of single cell transcriptome data collected from mice. It contains nearly 100,000 cells from 20 organs and tissues. These data provide the option of direct and controlled comparison of gene expression among cell types of different tissues (Tabula Muris Consortium et al. 2018). Ultimately, our goal was to gain further insight into the physiological role of Contactin-2 and provide insights for more targeted hypotheses for future experimentation on the field.

## Materials and methods

### Pipeline of the methodology implemented in this work

Genes of interest were identified from independent sources; their corresponding proteins have been found to interact structurally or functionally with Contactin-2 by preclinical experimentation or modern computational (theoretical) approaches. Subsequently, gene expression data from 98 brain regions have been retrieved from the databases of the Allen Institute for Brain Science. Absolute values of gene expression intensity per brain region have been normalized by the whole-brain expression intensity of the corresponding gene (relative gene expression values). These relative gene expression values have been used to visualize the across-brain Cntn2 expression intensity and to perform a spatial correlation analysis between the across-brain expression patterns of Cntn2 and the other genes of interest. Finally, utilizing Tabula Muris, we specified the brain cell types responsible for expressing Cntn2 and the spatially correlated and anticorrelated genes (Fig. 1).

### Technical aspects of the Allen Institute ISH experiments

For all ISH experiments, where the data regarding gene expression derive from, adult male mice (*mus musculus*) of the C57BL/6 J inbred strain (aged 56 weeks) have been used. Antisense RNA probes have been used on brain sagittal sections. More detailed information regarding the

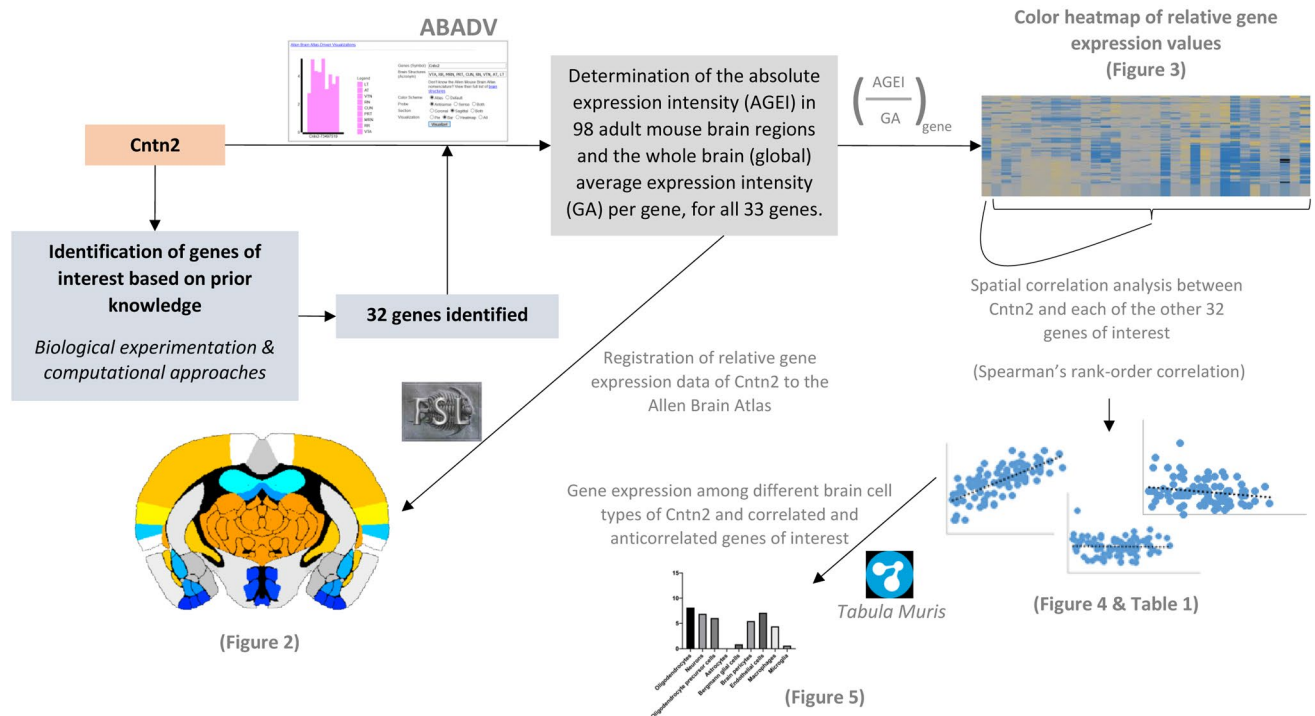


**Fig. 1** Pipeline of the methodology implemented in this work. *ABADV* Allen Brain Atlas-driven visualizations tool, *Cntn2* Contactin-2/TAG-1 gene, *FSL* FMRISoftware Library, Tabula Muris: <https://tabula-muris.ds.czbiohub.org>

technical aspects of the ISH experiments can be found in Lein et al. (2007). All genes, included in this work, have been studied under these settings in at least one experiment. In eight cases (*Bace1*, *L1cam*, *Map1b*, *Apc*, *Ntrk2*, *Cldn11*, *Myrf*, *Reln*) two identical experiments per gene have been conducted and, in another case (*Plp1*), eighteen; the final dataset derives from the average between the two or three experiments per gene. The 58 experiments (raw data) included in this paper can be found in <http://mouse.brain-map.org/>. Experiment IDs can be found in Supplementary Table 1.

## Gene identification

Genes of interest (aside *Cntn2*) were identified based on their encoding proteins having a potential relationship with Contactin-2; either prior research (Masuda 2017; Traka et al. 2003; Poliak et al. 2003) has indicated that these proteins directly or indirectly (physically or functionally) interact with Contactin-2, or have theoretical interactions (i.e. not tested yet experimentally) with the Contactin-2, based on the output of UniRed, a computational prediction tool which analyses biomedical literature to suggest undocumented protein–protein interactions (<http://bioinformatics.med.uoc.gr/unired/>) (Theodosiou et al. 2020). All genes of interest are listed in Supplementary Table 2.

## Brain segmentation and data collection

The data collection was based on the Allen Brain Atlas-Driven Visualizations software (*ABADV*), which is a free access web-based tool created to recover and visualize expression energy data from the mouse AGEA across multiple genes and brain structures (Zaldivar and Krichmar 2014). The spatial segmentation of the mouse brain was performed according to Allen Institute's taxonomic system and based on *ABADV*'s capabilities to provide gene expression energy data for all 33 genes under investigation by the 58 experiments mentioned above (as explained in Kalafatakis et al. 2019). Abbreviations of the all brain regions can be found in Supplementary Table 3.

## Whole-brain relative gene expression data visualization

The values representing the gene expression intensity of all genes of interest per brain region have been normalized by the mean expression intensity of the corresponding gene in the whole brain to give relative gene expression values. These data have been visualized in the form of a color heatmap. In the case of *Cntn2*, the relative gene expression data have been additionally registered to the Allen Brain Atlas for visualizing them in relation to the underlying mouse brain anatomy. Values between 0.85 and 1.15 have been

considered as average. To visualize the data, we used sections of the Allen Mouse Brain volumetric atlas 2012 and the masks corresponding to the 95 brain regions in NIFTI file format (<https://scalablebrainatlas.incf.org/mouse/ABA12>). We used FMRI Software Library (FSL) for image processing and visualization (Jenkinson et al. 2012), Fsleyes for image inspection and fslutils to register the available genomic data of *Cntn2* to the corresponding brain region.

### Cntn2 genomic spatial correlation analysis

We performed correlation analysis of the gene expression intensities between *Cntn2* and all other genes under investigation. Normality in the distribution of data (Shapiro–Wilk test) has been used and Spearman’s rank-order correlation was preferred due to the non-normality in the distribution of the relevant data. The level of significance has been set to 0.05.

### Data collection regarding the expression of genes of interest among different brain cell populations

The data, referring to the brain cell type-specific expression of *Cntn2* and its spatially correlated and anticorrelated genes of interest, were mined from Tabula Muris (<https://tabula-muris.ds.czbiohub.org>) and were captured by FACS-based full length transcript analysis, which provides high sensitivity and coverage (Tabula Muris Consortium et al. 2018). Brain myeloid and brain non-myeloid were selected as the examined tissues. Median values of the gene expression were retrieved. For data visualization, Prism8 software was used.

## Results

### Cntn2 gene expression across the brain

As a first step in our study, we investigated the expression of our primary gene of interest, *Cntn2*, across the brain. The relative gene expression data of *Cntn2* across the adult mouse brain, under baseline conditions, showed a lower expression ( $< 0.85$ ) in cerebellum, the diagonal band nucleus, most parts of the hippocampus (dentate gyrus, fasciola cinerea, parasubiculum and Ammon’s horn), amygdalar nuclei and cortical amygdalar area, hypothalamus, medial nuclei of the midbrain (interpeduncular nucleus, interfascicular nucleus raphe, rostral linear nucleus raphe) and mainly medial parts of the cerebral cortex not related to the long ascending/descending pathways (prelimbic and infralimbic areas, visual areas, some olfactory areas, temporal association areas, frontal poles, anterior cingulate with surrounding areas). In contrast, the relative gene expression

data of *Cntn2* across the adult mouse brain, under baseline conditions, showed a higher expression ( $> 1.15$ ) in medulla, pons, thalami, most midbrain nuclei, dorsal pallidum, some parts of the hippocampus (presubiculum, indusium griseum) and various parts of the cerebral cortex related to the long ascending/descending pathways (somatosensory areas, visceral areas), as well as parts of the olfactory areas, gustatory and auditory cortices, entorhinal areas, anterior insula, claustrum and endopiriform nucleus (Fig. 2).

### Gene identification encoding proteins related to Contactin-2 based on current knowledge

Our next point of interest was to identify genes, whose products are potentially associated with Contactin-2, based on prior experimentation or the predictions of UniRed. Via these methods, we identified 23 genes (Supplementary Table 2), including the tyrosine-protein kinase Lyn (involved in signal transduction related to Contactin-2) (Kasahara et al. 2002), beta-secretase 1 (*Bace1*, which cleaves Contactin-2 to soluble forms) (Gautam et al. 2014), Contactin-associated protein-like 2 (*Cntnap2*, which interacts with Contactin-2) (Poliak et al. 2003; Traka et al. 2003), potassium channels (*Kcna1* and *Kcna2*, regulated by Contactin-2) (Traka et al. 2003; Savvaki et al. 2008), various cell adhesion molecules found in neurons or extracellular matrix glycoproteins which might interact with Contactin-2 (*L1cam*, *Nrcam*, *Ncam1*, *Ncam2*, *Ncan*, *Tnc*, *Reln*) (Karagozeos 2003; UniRed), phosphacan (*Ptprz1*, particularly expressed in remyelinating oligodendrocytes) (Milev et al. 1996), receptor for activated C kinase 1 (*Gnb211*, also involved in Contactin-2 related signalling) (Yan and Jiang 2016), amyloid precursor protein (*App*, which binds to Contactin-2) (Ma et al. 2008), markers of cytoskeletal homeostasis, which stabilize microtubules and promote axonal transport (like *Map1b*, *Map2*, *Mapt*), kinesin-like protein (*Kif1b*, essential for the transport of materials within cells and also involved in apoptosis, interacts with Contactin-2) and signal transducer *Cd24a* (which possibly interacts with Contactin-2) (Lieberoth et al. 2009), the target receptor of brain-derived neurotrophic factor *Trk-B* (*Ntrk2*) (Savvaki et al. unpublished data), *Sema6a* (a transmembrane protein expressed in developing neural tissue, required for proper development of the thalamocortical projection) (UniRed) and finally neurofascin (*Nfasc*, an L1 family immunoglobulin cell adhesion molecule involved in axon subcellular targeting and synapse formation during neural development) (Hadas et al. 2013).

Moreover, given the functional relationship between Contactin-2 and myelinated axons (Traka et al. 2003; Poliak et al. 2003) in the adult mouse brain, we wanted to investigate whether there is a genomic association between the expression of Contactin-2 and markers of oligodendrocytes (the cells responsible for the formation of myelin in the

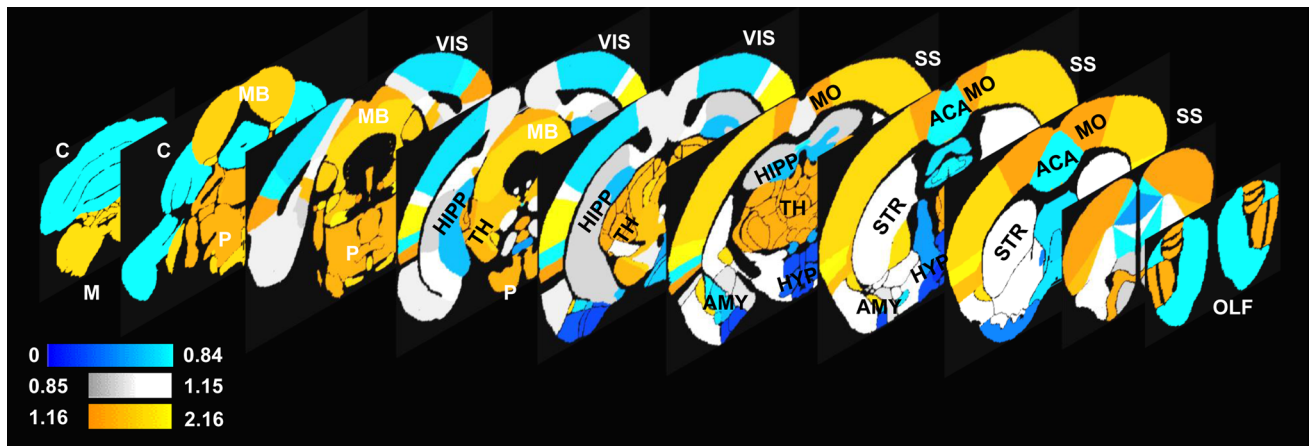


**Fig. 2** Colourmaps of the relative gene expression data of *Cntn2* across the adult mouse brain under baseline conditions. Regions on a shade of blue show a relatively lower expression ( $<0.85$ ), those on a shade of grey show a gene expression around the global mean ( $0.85\text{--}1.15$ ), while those on the orange-yellow scale show a relatively higher expression ( $>1.15$ ). The first category of brain regions includes cerebellum (C), the diagonal band nucleus, most parts of the hippocampus (HIPP) (dentate gyrus, fasciola cinerea, Ammon's horn, parasubiculum), amygdalar nuclei and cortical amygdalar area (AMY), hypothalamus (HYP), medial nuclei of the midbrain (MB) (interpeduncular nucleus, interfascicular nucleus raphe, rostral linear nucleus raphe) and medial parts of the cerebral cortex like prelimbic and infralimbic areas, visual areas (VIS), some olfactory areas (OLF), temporal association areas, frontal poles, anterior cingulate and surrounding regions (ACA). The second category of brain regions involves the hypothalamic lateral zone, the striatum-like amygdalar nuclei and most other striatal nuclei (STR), periaqueductal grey, ven-

tral tegmental area, red nucleus, parabigeminal nucleus and anterior tegmental nucleus from the midbrain and parts of the cerebral cortex (somatomotor areas [MO], ectorhinal and corticolimbic areas, posterior parietal association areas and the piriform area). Finally, the third category of brain regions includes medulla (M), pons (P), thalami (TH), most midbrain nuclei, dorsal pallidum, some parts of the hippocampus (presubiculum, induseum griseum) and the remaining parts of the cerebral cortex like the somatosensory areas (SS), visceral areas, parts of the olfactory areas, gustatory and auditory cortices, anterior insula, claustrum and endopiriform nucleus. Ten different slices at the coronal level are demonstrated, starting from the most posterior part of the adult mouse brain ( $Y=0$ ) in the far left and going progressively to more anterior parts ( $Y=10, 100, 135, 170, 200, 250, 300, 350, 400, 450$  respectively). The nomenclature of all brain regions can be found in the coronal mouse Allen Brain Atlas (<http://mouse.brain-map.org/static/atlas>)

central nervous system) at various stages of their maturation (Fancy et al. 2011); either immature (*Pdgfra*, *Cspg4*), or mature, non-specific (*Apc*, *Apc2*, which are also expressed in neurons) (Brakeman et al. 1999), or specific for that cell type, pre- and myelinating oligodendrocytes (*Plp1*, *Myrf*, *Mbp*, *Mog*, *Cldn11*). The relative expression intensity of all 33 genes identified (including *Cntn2*) in the grey matter of each of the 95 mouse brain regions is presented in the form of a color heatmap in Fig. 3.

### ***Cntn2* genomic spatial correlation analysis with the 23 genes, whose products interact functionally or structurally with Contactin-2**

After collecting all the data regarding the expression of the 32 genes of interest across the brain, we decided to investigate if there was a spatial correlation of their relative expression values between them and *Cntn2*. The across-brain correlation analysis on the gene expression intensities between *Cntn2* and the first 23 genes of interest of the adult mouse brain showed a positive spatial correlation for *Cntn2* with 5 of them and a negative spatial correlation for *Cntn2* with another 4. In particular, the spatial patterns of the relative

gene expression of *Bace1*, *Kcna1* and *Kcna2* show a strong correlation with the corresponding spatial pattern of *Cntn2* ( $p < 0.01$ ), while the spatial patterns of the relative gene expression of *App* and *Nfasc* show a lesser but also significant correlation ( $p = 0.04$ ) with that of *Cntn2*. On the other hand, the spatial pattern of the relative gene expression of *L1cam*, *Ncam1*, *Ncam2* and *Ptprz1* are strongly anticorrelated with that of *Cntn2* ( $p \leq 0.01$ ) (Table 1).

### ***Cntn2* genomic spatial correlation analysis with markers of oligodendrocytes**

The myelination process begins when a pool of immature oligodendrocytes (i.e. oligodendrocyte progenitor cells or OPCs) is differentiated to mature pre-myelinating oligodendrocytes which eventually form myelin sheaths around multiple neurons. At the various stages of this process, oligodendrocytes express a different combination of proteins, which constitute maturation stage-dependent markers, either specific for that cell type or not. For instance, OPCs express *Cspg4* and *Pdgfra*, while mature oligodendrocytes express *Plp1*, *Mbp*, *Mog*, *Cldn11* and *Myrf*. *Apc* isoforms (*Apc*, *Apc2*) are expressed by both mature oligodendrocytes and



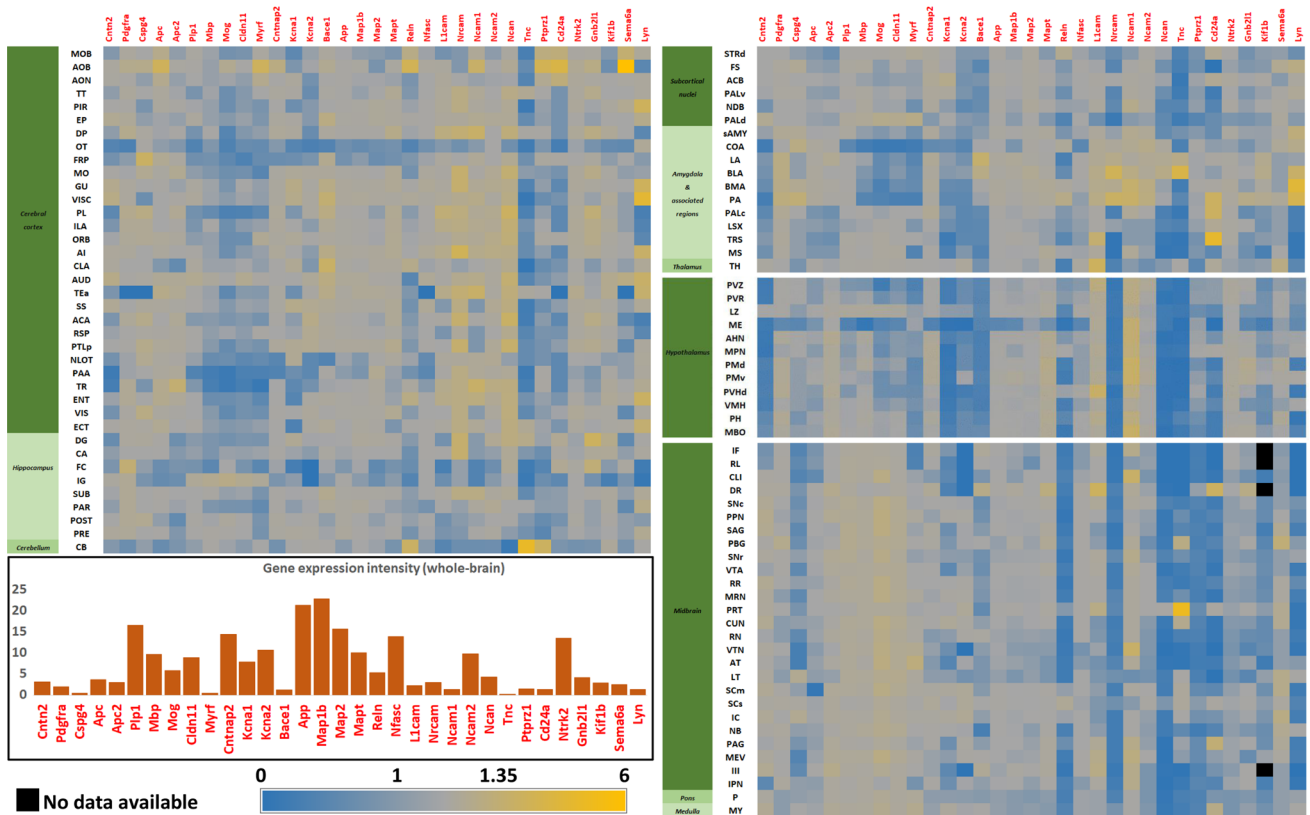


**Fig. 3** Heatmaps of the relative expression intensities (ranging from 0 to 6) of the 33 genes of interest (Cntn2 included) across 95 grey matter regions of the adult mouse brain. To acquire the relative gene expression value, raw data per brain region have been normalized based on the mean expression intensity of the corresponding gene at the whole brain level (shown inside the black frame). Abbreviations of brain regions have been adopted from the Allen Brain Atlas nomenclature (<http://mouse.brainmap.org/static/atlas>) and are also listed in Supplementary Table 3. Abbreviations of the genes have

been adopted from mouse genome informatics (<http://www.informatics.jax.org/>) and are also explained in the Supplementary Table 2. Blue color indicates gene expression close to zero, while lighter shades of blue indicate relative gene expressions below the corresponding global (whole brain) average (i.e. below 1). Shades of grey indicate relative gene expressions between 1 and 1.35, while greater values are expressed as shades of yellow. The brighter the yellow color the higher the value (maximum value 6)

**Table 1** Spatial correlations of Cntn2 gene expression across the adult mouse brain with other genes, whose products have been (functionally or structurally) related to Tag-1/Conntactin-2. Among the 23 genes of interest, 9 have been found to strongly correlate with Cntn2

		Cntn2						
<i>Lyn</i>	0.059	0.57	<i>Ncam2</i>	-0.270	0.01	<i>Map2</i>	-0.008	0.94
<i>Bace1</i>	0.299	0.00	<i>Ncan</i>	0.023	0.82	<i>Mapt</i>	-0.077	0.46
<i>Cntnap2</i>	0.037	0.72	<i>Pptrz1</i>	-0.281	0.01	<i>Kif1b</i>	-0.084	0.43
<i>Kcna1</i>	0.599	0.00	<i>Tnc</i>	0.092	0.37	<i>Cd24a</i>	-0.058	0.57
<i>Kcna2</i>	0.428	0.00	<i>Gnb2l1</i>	-0.159	0.12	<i>Ntrk2</i>	0.148	0.15
<i>L1cam</i>	-0.252	0.01	<i>App</i>	0.212	0.04	<i>Sema6a</i>	0.167	0.11
<i>Nrcam</i>	-0.057	0.58	<i>Reln</i>	-0.095	0.36	<i>Nfasc</i>	0.215	0.04
<i>Ncam1</i>	-0.322	0.00	<i>Map1b</i>	0.170	0.10			

The gene expressions of Bace1, Kcna1, Kcna2, App and Nfasc have a positive spatial association with that of Cntn2 (green color), while the gene expressions of L1cam, Ncam1, Ncam2 and Pptrz1 have a negative spatial association with that of Cntn2 (pink color). For further details on the nomenclature of the various genes, please refer to Supplementary Table 2

R Pearson correlation coefficient, Sig. (level of) significance

neurons. The across-brain correlation analysis on the relative gene expression intensities between *Cntn2* and the 9 markers of oligodendrocyte physiology of the adult mouse brain showed a negative genomic spatial correlation for *Cntn2* with the two markers of immature oligodendrocytes (*Pdgfra*, *Cspg4*), no correlation between *Cntn2* and the non-specific markers of mature oligodendrocytes (*Apc*, *Apc2*) and a very strong positive correlation of *Cntn2* with all specific markers of mature oligodendrocytes (*Plp1*, *Myrf*, *Mbp*, *Mog*, *Cldn11*) (Fig. 4).

### Expression of genes spatially correlated or anti-correlated with *Cntn2* among different brain cell populations

Having found a spatial correlation of 10 genes of interest and a spatial anti-correlation of 6 genes of interest with *Cntn2*, we wanted to investigate which brain cell

populations (oligodendrocytes, OPCs, neurons, astrocytes, Bergmann glial cells, brain pericytes, endothelial cells, macrophages and microglia) preferably express these genes, by utilizing the relevant data from Tabula Muris. Median values were chosen (over mean values with standard deviations) to reduce the variance of the results. *Cntn2*, as expected, is mainly expressed by oligodendrocytes (it is also expressed by neurons but at much lower levels). Apart from *Kcna2*, oligodendrocytes are the brain cell type with the highest median value for expressing all other genes of interest, which share a similar spatial expression pattern with *Cntn2* and for which data were available to retrieve from Tabula Muris. *Kcna2* on the contrary is mainly expressed in neurons and to a much lesser degree in Bergmann glial cells (Fig. 5a). All genes of interest, which have an opposing spatial expression pattern from *Cntn2* and for which data were available to retrieve from Tabula Muris, show the highest median expression values in OPCs as compared to the other brain cell types (Fig. 5b).

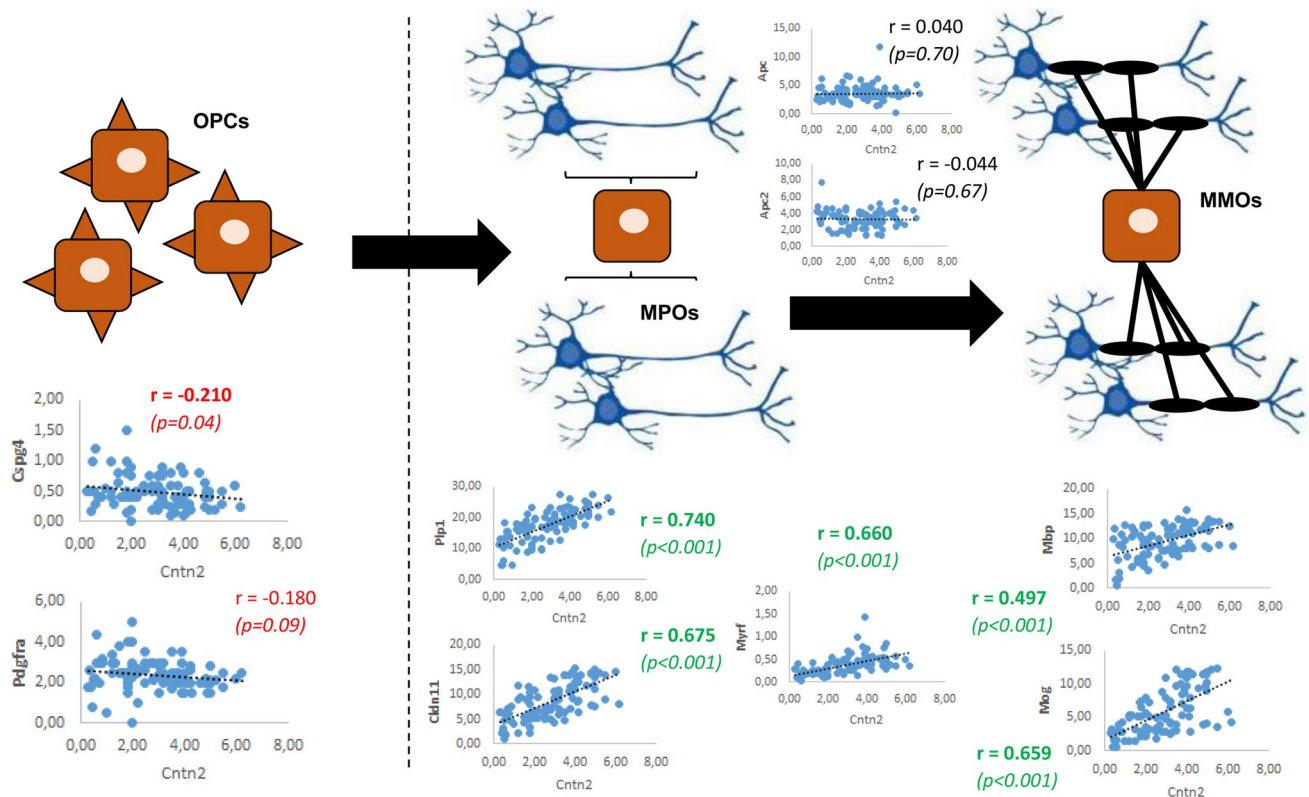
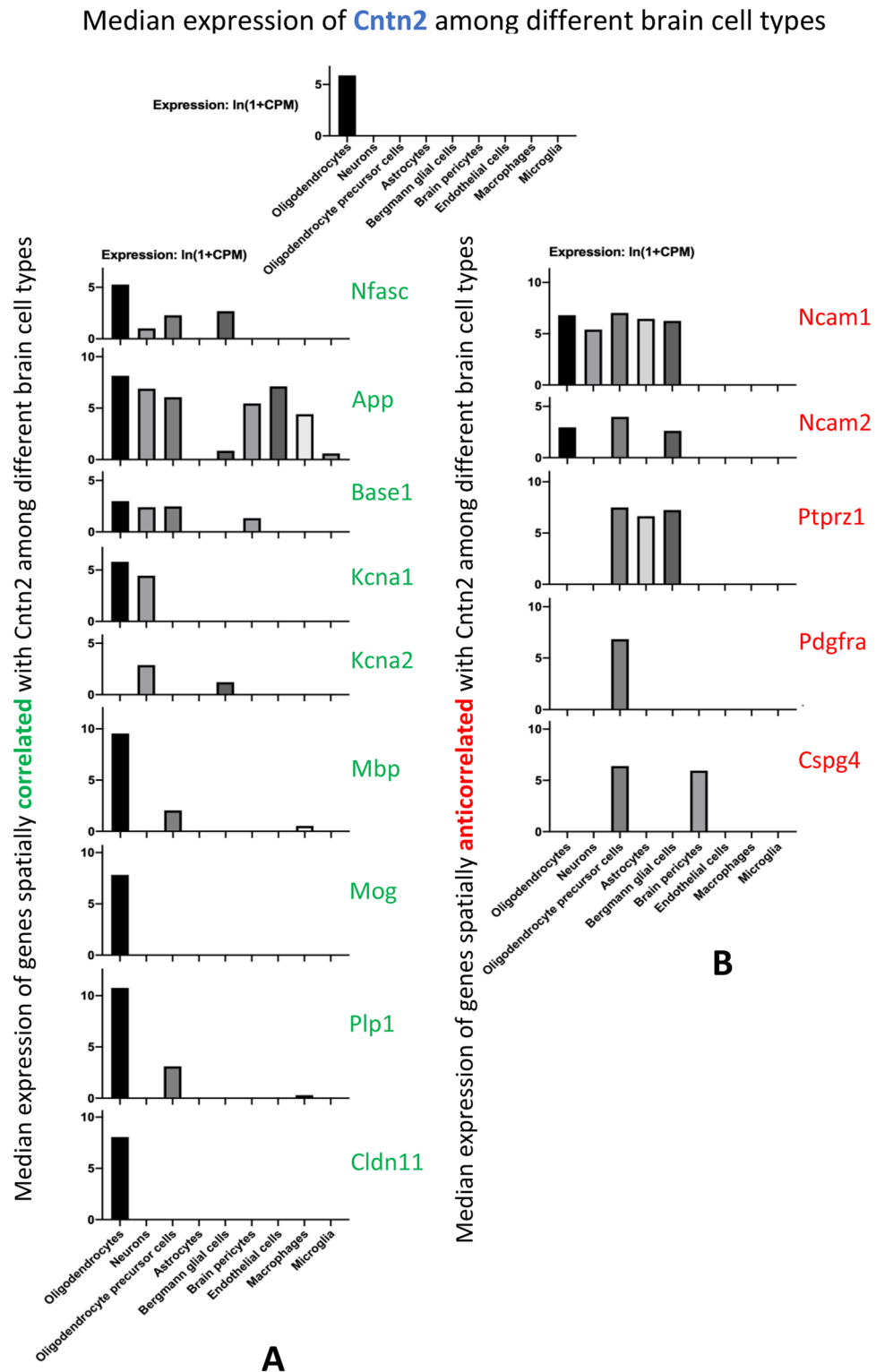


**Fig. 4** Spatial correlation of *Cntn2* gene expression across the adult mouse brain with genes related to immature and mature oligodendrocytes. The pattern of the gene expression intensity of *Cntn2* across the adult mouse brain is negatively correlated with the markers of OPCs and positively with the specific markers of mature oligodendrocytes. No correlation exists between *Cntn2* and *Apc* (or *Apc2*).

Abbreviations of the genes have been adopted from mouse genome informatics (<http://www.informatics.jax.org/>) and are also explained in the Supplementary Table 2. *MMOs* mature myelinating oligodendrocytes, *MPOs* pre-myelinating oligodendrocytes, *OPCs* oligodendrocyte progenitor cells, *r* Pearson correlation coefficient

**Fig. 5** Expression of *Cntn2* and genes spatially correlated (a) and anticorrelated (b) with *Cntn2* among different brain cell populations. Data were retrieved from Tabula Muris (<https://tabula-muris.ds.czbiohub.org>) using the median values



## Discussion

The massive AGEA of the adult mouse brain, alone or in combination with other relevant, complementary data sources, such as Tabula Muris, can be carefully interrogated

(in a targeted, prior knowledge-driven manner) to confirm or question some of our views on mouse brain physiology and reveal new domains of potential neuroscientific interest for future translational research. According to the data presented in this paper and in accordance with our current

understanding on the relationship between Contactin-2 and myelin physiology (Karagogeos 2003; Paz Soldán and Pirko 2012; Zoupi et al. 2011), the expression of Contactin-2 mainly follows the myelinated pathways of the central nervous system. Specifically, this observation is supported (a) by the neuroanatomical distribution of the regions with the (relatively) higher *Cntn2* expression intensities, involving pathways controlling sensory processing and executive control functions, characterized by an increased degree of myelination, (b) by the fact that *Cntn2* is mainly expressed by mature oligodendrocytes and (c) by the strong spatial genomic association between *Cntn2* and specific markers of mature oligodendrocytes. This last observation is in accordance with the previous studies showing that the expression of the transcription factor *Myrf* positively regulates the expression of Contactin-2 as well as the expression of myelin genes and oligodendrocyte markers like MBP, PLP and MOG (Koenning et al. 2012). Moreover, the negative spatial association between the gene expressions of *Cntn2* and markers of premature oligodendrocytes is in accordance with the recent findings from our team showing that Contactin-2 is expressed only in mature oligodendrocytes and not in oligodendrocyte progenitor cells (Zoupi et al. 2018).

The fact that Contactin-2 plays its main physiological role in the adult mammalian brain by stabilizing/ensuring the integrity, as well as proper function, of myelinated fibres is further supported by the close spatial genomic association of *Cntn2* with *Kcna1*, *Kcna2* and *Nfasc*. The relationship of Contactin-2 with *Kcna1* and *Kcna2*, i.e. the genes that encode the voltage-gated potassium channels *Kv1.1* and *Kv1.2*, confirms the importance of the co-presence of these biomolecules in exerting their physiological role. These potassium channels are found at the axonal initial segment and juxtaparanodes of myelinated fibres, modulating the action potential initiation and frequency (Pinatel et al. 2017; Traka et al. 2002). Contactin-2 also localizes at the juxtaparanodes (Traka et al. 2002) and, according to the previous experimental findings, interacts with these potassium channels and *Caspr2* forming a complex that is crucial for the axonal-glial interactions and for the proper function of myelinated fibres. The absence of Contactin-2 leads to an impaired juxtaparanodal localization of *Kv1.1/1.2* and *Caspr2* as they diffuse into the internode (Traka et al. 2003; Savvaki et al. 2008). In particular, glial Contactin-2 is able to rescue this phenotype (Savvaki et al. 2010).

Moreover, the genomic relationship between Contactin-2 and Neurofascin shown in this paper is in accordance with other sources of experimental evidence supporting their biological relevance. The latter is a transmembrane-linked adhesion molecule (encoded by the *Nfasc* gene). It has a very similar structure to Contactin-2 and previous studies, just like the data presented in this work, show a similar expression pattern (Brümmendorf and Rathjen 1996). Both

Neurofascin and Contactin-2 are co-expressed in numerous neuronal cell types and promote neurite outgrowth, while they are responsible for the architecture and function of the nodes of Ranvier, albeit in distinct ways. Moreover, the genes of these two proteins are adjacent in the genome, a feature that is evolutionary conserved. The data from this work strengthen the notion that Contactin-2 and Neurofascin could share the same regulatory mechanisms (Hadas et al. 2013).

Our data have also revealed a positive spatial association on the gene expression intensities between *Cntn2*, *Bace1* and APP. *Bace1* is a type I transmembrane aspartyl protease expressed in neuronal tissue and Contactin-2 consists one of the main substrates of this protease (Gautam et al. 2014). *Bace1* cleaves Contactin-2 near its GPI anchor site to produce its soluble form, found throughout the brain, able to bind to other cell surface axonal molecules thus regulating a variety of events (Kuhn et al. 2012). Therefore, *Bace1* may modify the function of Contactin-2 by regulating the expression levels of the two different forms (transmembrane and soluble) of this molecule (Gautam et al. 2014).

Amyloid  $\beta$  precursor protein (APP) is a type I transmembrane protein, which acts like a receptor and is responsible for many different biological activities in neuronal and non-neuronal cells (Austin et al. 2009). According to the previous publications one of its ligands is TGF $\beta$ -2. The binding of TGF $\beta$ -2 with cell surface APP induces neuronal cell death through an intracellular death signal transduction pathway. Contactin-2 also binds APP leading to a release of the APP intracellular domain, triggering FE65-dependent transcriptional activity in a  $\gamma$ -secretase-dependent manner. In this way, Contactin-2 inhibits the APP-dependent TGF $\beta$ 2-mediated neuronal cell death by reducing the binding of TGF $\beta$ -2 to APP (Tachi et al. 2010). In parallel, the interaction between Contactin-2 and APP is also responsible for the negative modulation of neurogenesis and also occurs via FE65-dependent pathways (Ma et al. 2008).

Finally, the spatial pattern of the gene expression intensity of Contactin-2 correlates negatively with four genes (*Ncam1*, *Ncam2*, *L1cam*, *Ptprz1*) whose products have been related to anabolic processes in the adult brain, like neurogenesis (for *Ncam*) (Gascon et al. 2010) or activity-dependent de novo myelination (for *L1cam*) (Fields 2015) or remyelination in lesion sites (for *Ptprz1*) (Levy et al. 1993). *Tabula Muris* data additionally show that, contrary to what is happening with *Cntn2*, one of the main brain cell types—source of their expression are OPCs. Given the negative regulation of Contactin-2 in adult neurogenesis (in collaboration with APP, whose spatial patterns of gene expression correlate as mentioned above), we could speculate that not only does the adult brain rely on Contactin-2-independent pathways for mediating plasticity of any form (being either via neurogenesis or de novo myelination or synaptic plasticity),

but also the presence of Contactin-2 (contrary to what is happening during neurodevelopment) constitutes a negative signal for such processes. This notion is in accordance with the previous work from our group showing that absence of Contactin-2 leads to improved conduction velocity of axons during remyelination after cuprizone-induced demyelination in adult mice (Zoupi et al. 2018) and to increased axonal regeneration after injury (Savvaki et al. unpublished data).

In an effort to put together all the pieces of information related to the physiological significance of Contactin-2 during development and in adulthood, we put forward the hypothesis that while this molecule is expressed in essential functions of neurons, such as the proximal part of the outgrowing axons/neurites during development, in adulthood its expression is correlated with low plasticity events. For example, Contactin-2 is involved in the formation of long ascending/descending pathways during development (Dodd et al. 1988; Furley et al. 1990) and possibly contributes to their functional/electrolytic homeostasis thereafter (by interacting with the potassium channels Kv1.1 and Kv1.2 and other molecules like Neurofascin). Contactin-2 seems to contribute to the low plasticity of these pathways (for instance by downregulating any neurogenic events) and in regions characterized by higher degrees of plasticity or regenerative potential, the adult brain relies on the expression of different cell adhesion molecules to promote anabolic activities like neurogenesis, de novo myelination or remyelination. The post-genomic (functional) interplay between Contactin-2 and some of these other cell adhesion molecules (like Ncam) observed by prior experimentation (Milev et al. 1996) is not contradictory to the results of this work (showing a negative spatial genomic correlation among them); the adult brain could differentiate neural pathways of low and high plasticity (or low and high regenerative potential) based on which groups of proteins get preferably expressed, but at a functional level (at least some members of) these different groups of proteins need to interact with each other, since all these neural pathways reciprocally interact with each other independent of the degree of plasticity (or the regenerative potential).

Future studies are required to find possible transcription factors that regulate the expression of Contactin-2 together with the expression of genes correlated with Contactin-2, to further elucidate the physiological role of the molecule and to investigate whether this protein can be used either as a target for novel treatments or as a marker for discriminating between neural pathways showing a different severity in the clinical outcome if damaged or a different regenerative potential in the context of demyelinating and neurodegenerative disorders.

**Acknowledgements** Dr Konstantinos Kalafatakis would like to express his gratitude to Bodossaki Foundation (<https://www.bodossaki.gr/en/>)

for supporting his research on modelling biological and biomedical data. Mr Ilias Kalafatakis would like to acknowledge that his research is co-financed by Greece and the European Union (European Social Fund- ESF) through the Operational Programme «Human Resources Development, Education and Lifelong Learning» in the context of the project “Strengthening Human Resources Research Potential via Doctorate Research” (MIS-5000432), implemented by the State Scholarships Foundation (IKY). Dr Domna Karageorgos acknowledges funding from Foundation ARSEP and ARISTEIA I (MyelinTag).

## Compliance of ethical standards

**Conflict of interest** The authors declare that the research was conducted in the absence of any commercial or financial relationships that could be construed as a potential conflict of interest.

## References

- Austin SA, Sens MA, Combs CK (2009) Amyloid precursor protein mediates a tyrosine kinase-dependent activation response in endothelial cells. *J Neurosci* 29(46):14451–14462. <https://doi.org/10.1523/JNEUROSCI.3107-09.2009>
- Bailly Y, Kyriakopoulou K, Delhay-Bouchaud N, Mariani J, Karageorgos D (1996) Cerebellar granule cell differentiation in mutant and X-irradiated rodents revealed by the neural adhesion molecule TAG-1. *J Comp Neurol* 369(1):150–161. [https://doi.org/10.1002/\(SICI\)1096-9861\(19960520\)369:1%3c150:AID-CNE11%3e3.0.CO;2-V](https://doi.org/10.1002/(SICI)1096-9861(19960520)369:1%3c150:AID-CNE11%3e3.0.CO;2-V)
- Brakeman JS, Gu SH, Wang XB, Dolin G, Baraban JM (1999) Neuronal localization of the Adenomatous polyposis coli tumor suppressor protein. *Neuroscience* 91(2):661–672
- Brümmendorf T, Rathjen FG (1996) Structure/function relationships of axon-associated adhesion receptors of the immunoglobulin superfamily. *Curr Opin Neurobiol* 6(5):584–593
- Buttiglione M, Revest JM, Pavlou O, Karageorgos D, Furley A, Rougon G, Faivre-Sarrailh C (1998) A functional interaction between the neuronal adhesion molecules TAG-1 and F3 modulates neurite outgrowth and fasciculation of cerebellar granule cells. *J Neurosci: Off J Soc Neurosci* 18(17):6853–6870. <https://doi.org/10.1523/JNEUROSCI.18-17-06853.1998>
- Chatzopoulou E, Miguez A, Savvaki M, Levasseur G, Muzerelle A, Muriel MP, Goureau O, Watanabe K, Goutebroze L, Gaspar P, Zalc B, Karageorgos D, Thomas JL (2008) Structural requirement of TAG-1 for retinal ganglion cell axons and myelin in the mouse optic nerve. *J Neurosci* 28(30):7624–7636. <https://doi.org/10.1523/JNEUROSCI.1103-08.2008>
- Denaxa M, Chan CH, Schachner M, Parnavelas JG, Karageorgos D (2001) The adhesion molecule TAG-1 mediates the migration of cortical interneurons from the ganglionic eminence along the corticofugal fiber system. *Development (Cambridge, England)* 128(22):4635–4644
- Denaxa M, Pavlou O, Tsiotra P, Papadopoulos GC, Liapaki K, Theodorakis K, Papadaki C, Karageorgos D, Papamatheakis J (2003) The upstream regulatory region of the gene for the human homologue of the adhesion molecule TAG-1 contains elements driving neural specific expression in vivo. *Brain Res Mol Brain Res* 118(1–2):91–101. <https://doi.org/10.1016/j.molbrainres.2003.07.004>
- Denaxa M, Kyriakopoulou K, Theodorakis K, Trichas G, Vidaki M, Takeda Y, Watanabe K, Karageorgos D (2005) The adhesion molecule TAG-1 is required for proper migration of the superficial migratory stream in the medulla but not of cortical interneurons. *Dev Biol* 288(1):87–99. <https://doi.org/10.1016/j.ydbio.2005.09.021>

- Derfuss T, Parikh K, Velhin S, Braun M, Mathey E, Krumbholz M, Kümpfel T, Moldenhauer A, Rader C, Sonderegger P, Pöllmann W, Tiefenthaler C, Bauer J, Lassmann H, Wekerle H, Karagogeos D, Hohlfeld R, Linington C, Meinl E (2009) Contactin-2/TAG-1-directed autoimmunity is identified in multiple sclerosis patients and mediates gray matter pathology in animals. *Proc Natl Acad Sci USA* 106(20):8302–8307. <https://doi.org/10.1073/pnas.0901496106>
- Dodd J, Morton SB, Karagogeos D, Yamamoto M, Jessell TM (1988) Spatial regulation of axonal glycoprotein expression on subsets of embryonic spinal neurons. *Neuron* 1(2):105–116
- Fancy SP, Chan JR, Baranzini SE, Franklin RJ, Rowitch DH (2011) Myelin regeneration: a recapitulation of development? *Annu Rev Neurosci* 34:21–43. <https://doi.org/10.1146/annurev-neuro-061010-113629>
- Fields RD (2015) A new mechanism of nervous system plasticity: activity-dependent myelination. *Nat Rev Neurosci* 16(12):756–767. <https://doi.org/10.1038/nrn4023>
- Furley AJ, Morton SB, Manalo D, Karagogeos D, Dodd J, Jessell TM (1990) The axonal glycoprotein TAG-1 is an immunoglobulin superfamily member with neurite outgrowth-promoting activity. *Cell* 61(1):157–170. [https://doi.org/10.1016/0092-8674\(90\)90223-2](https://doi.org/10.1016/0092-8674(90)90223-2)
- Gascon E, Vutskits L, Kiss JZ (2010) The role of PSA-NCAM in adult neurogenesis. *Adv Exp Med Biol* 663:127–136. [https://doi.org/10.1007/978-1-4419-1170-4\\_8](https://doi.org/10.1007/978-1-4419-1170-4_8)
- Gautam V, D'Avanzo C, Hebisch M, Kovacs DM, Kim DY (2014) BACE1 activity regulates cell surface contactin-2 levels. *Mol Neurodegener* 9:4. <https://doi.org/10.1186/1750-1326-9-4>
- Gennarini G, Furlay A (2017) Cell adhesion molecules in neural development and disease. *Mol Cell Neurosci* 81:1–3. <https://doi.org/10.1016/j.mcn.2017.03.010>
- Hadas Y, Nitzan N, Furley AJ, Kozlov SV, Klar A (2013) Distinct cis regulatory elements govern the expression of TAG1 in embryonic sensory ganglia and spinal cord. *PLoS ONE* 8(2):e57960. <https://doi.org/10.1371/journal.pone.0057960>
- Iijima M, Tomita M, Morozumi S, Kawagashira Y, Nakamura T, Koike H, Katsuno M, Hattori N, Tanaka F, Yamamoto M, Sobue G (2009) Single nucleotide polymorphism of TAG-1 influences IVIg responsiveness of Japanese patients with CIDP. *Neurology* 73(17):1348–1352. <https://doi.org/10.1212/wnl.0b013e3181bd1139>
- Jenkinson M, Beckmann CF, Behrens TE, Woolrich MW, Smith SM (2012) FSL. *Neuroimage* 62(2):782–790. <https://doi.org/10.1016/j.neuroimage.2011.09.015>
- Kalafatakis K, Giannakeas N, Lightman SL, Charalampopoulos I, Russell GM, Tshipouras M, Tzallas A (2019) Utilization of the allen gene expression atlas to gain further insight into glucocorticoid physiology in the adult mouse brain. *Neurosci Lett* 706:194–200. <https://doi.org/10.1016/j.neulet.2019.05.020>
- Karagogeos D (2003) Neural GPI-anchored cell adhesion molecules. *Front Biosci* 8:s1304–s1320. <https://doi.org/10.2741/1214>
- Karagogeos D, Morton SB, Casano F, Dodd J, Jessell TM (1991) Developmental expression of the axonal glycoprotein TAG-1: differential regulation by central and peripheral neurons in vitro. *Development* 112(1):51–67
- Kasahara K, Watanabe K, Kozutsumi Y, Oohira A, Yamamoto T, Sanai Y (2002) Association of GPI-anchored protein TAG-1 with src-family kinase Lyn in lipid rafts of cerebellar granule cells. *Neurochem Res* 27(7–8):823–829
- Koenning M, Jackson S, Hay CM, Faux C, Kilpatrick TJ, Willingham M, Emery B (2012) Myelin gene regulatory factor is required for maintenance of myelin and mature oligodendrocyte identity in the adult CNS. *J Neurosci* 32(36):12528–12542. <https://doi.org/10.1523/JNEUROSCI.1069-12.2012>
- Kuhn PH, Koroniak K, Hogl S, Colombo A, Zeitschel U, Willem M, Volbracht C, Schepers U, Imhof A, Hoffmeister A, Haass C, Roßner S, Bräse S, Lichtenthaler SF (2012) Secretome protein enrichment identifies physiological BACE1 protease substrates in neurons. *EMBO J* 31(14):3157–3168. <https://doi.org/10.1038/emboj.2012.173>
- Kyriakopoulou K, de Diego I, Wassef M, Karagogeos D (2002) A combination of chain and neurophilic migration involving the adhesion molecule TAG-1 in the caudal medulla. *Development (Cambridge, England)* 129(2):287–296
- Lein ES, Hawrylycz MJ, Ao N, Ayres M, Bensinger A, Bernard A, Boe AF, Boguski MS, Brockway KS, Byrnes EJ, Chen L, Chen L, Chen TM, Chin MC, Chong J, Crook BE, Czaplinska A, Dang CN, Datta S, Dee NR, Desaki AL, Desta T, Diep E, Dolbeare TA, Donelan MJ, Dong HW, Dougherty JG, Duncan BJ, Ebbert AJ, Eichele G, Estin LK, Faber C, Facer BA, Fields R, Fischer SR, Fliss TP, Frensley C, Gates SN, Glattfelder KJ, Halverson KR, Hart MR, Hohmann JG, Howell MP, Jeung DP, Johnson RA, Karr PT, Kawal R, Kidney JM, Knapik RH, Kuan CL, Lake JH, Laramee AR, Larsen KD, Lau C, Lemon TA, Liang AJ, Liu Y, Luong LT, Michaels J, Morgan JJ, Morgan RJ, Mortrud MT, Mosqueda NF, Ng LL, Ng R, Orta GJ, Overly CC, Pak TH, Parry SE, Pathak SD, Pearson OC, Puchalski RB, Riley ZL, Rockett HR, Rowland SA, Royall JJ, Ruiz MJ, Sarno NR, Schaffnit K, Shapovalova NV, Sivisay T, Slaughterbeck CR, Smith SC, Smith KA, Smith BI, Sodt AJ, Stewart NN, Stumpf KR, Sunkin SM, Sutram M, Tam A, Teemer CD, Thaller C, Thompson CL, Varnam LR, Visel A, Whitlock RM, Wohnoutka PE, Wolkey CK, Wong VY, Wood M, Yaylaoglu MB, Young RC, Youngstrom BL, Yuan XF, Zhang B, Zwingman TA, Jones AR (2007) Genome-wide atlas of gene expression in the adult mouse brain. *Nat J Biol Chem* 268(14):10573–10581
- Levy JB, Canoll PD, Silvennoinen O, Barnea G, Morse B, Honegger AM, Huang JT, Cannizzaro LA, Park SH, Druck T et al (1993) The cloning of a receptor-type protein tyrosine phosphatase expressed in the central nervous system. *J Biol Chem* 268(14):10573–10581
- Lieberoth A, Splittstoesser F, Katagihallimath N, Jakovcevski I, Loers G, Ranscht B, Karagogeos D, Schachner M, Kleene R (2009) Lewis(x) and alpha2,3-sialyl glycans and their receptors TAG-1, Contactin, and L1 mediate CD24-dependent neurite outgrowth. *J Neurosci* 29(20):6677–6690. <https://doi.org/10.1523/JNEUROSCI.4361-08.2009>
- Ma QH, Futagawa T, Yang WL, Jiang XD, Zeng L, Takeda Y, Xu RX, Bagnard D, Schachner M, Furley AJ, Karagogeos D, Watanabe K, Dawe GS, Xiao ZC (2008) A TAG1-APP signalling pathway through Fe65 negatively modulates neurogenesis. *Nat Cell Biol* 10(3):283–294. <https://doi.org/10.1038/ncb1690>
- Masuda T (2017) Contactin-2/TAG-1, active on the front line for three decades. *Cell Adh Migr* 11(5–6):524–531. <https://doi.org/10.1080/19336918.2016.1269998>
- Masuda T, Okado N, Shiga T (2000) The involvement of axo-nin-1/SC2 in mediating notochord-derived chemorepulsive activities for dorsal root ganglion neurites. *Dev Biol* 224:112–121. <https://doi.org/10.1006/dbio.2000.9813>
- Milev P, Maurel P, Häring M, Margolis RK, Margolis RU (1996) TAG-1/axonin-1 is a high-affinity ligand of neurocan, phosphacan/protein-tyrosine phosphatase-zeta/beta, and N-CAM. *J Biol Chem* 271(26):15716–15723
- Namba T, Kibe Y, Funahashi Y, Nakamuta S, Takano T, Ueno T, Shimada A, Kozawa S, Okamoto M, Shimoda Y, Oda K, Wada Y, Masuda T, Sakakibara A, Igarashi M, Miyata T, Faivre-Sarrailh C, Takeuchi K, Kaibuchi K (2014) Pioneering axons regulate neuronal polarization in the developing cerebral cortex. *Neuron* 81:814–829. <https://doi.org/10.1016/j.neuron.2013.12.015>

- Ng L, Bernard A, Lau C, Overly CC, Dong HW, Kuan C, Pathak S, Sunkin SM, Dang C, Bohland JW, Bokil H, Mitra PP, Puelles L, Hohmann J, Anderson DJ, Lein ES, Jones AR, Hawrylycz M (2009) An anatomic gene expression atlas of the adult mouse brain. *Nat Neurosci* 12(3):356–362. <https://doi.org/10.1038/nn.2281>
- Okamoto M, Namba T, Shinoda T, Kondo T, Watanabe T, Inoue Y, Takeuchi K, Enomoto Y, Ota K, Oda K, Wada Y, Sagou K, Saito K, Sakakibara A, Kawaguchi A, Nakajima K, Adachi T, Fujimori T, Ueda M, Hayashi S, Kaibuchi K, Miyata T (2013) TAG-1-assisted progenitor elongation streamlines nuclear migration to optimize subapical crowding. *Nat Neurosci* 16:1556–1566. <https://doi.org/10.1038/nn.3525>
- Paz Soldán MM, Pirkó I (2012) Biogenesis and significance of central nervous system myelin. *Semin Neurol* 32(1):9–14. <https://doi.org/10.1055/s-0032-1306381>
- Pinatel D, Hivert B, Saint-Martin M, Noraz N, Savvaki M, Karageorgos D, Faivre-Sarrailh C (2017) The Kv1-associated molecules TAG-1 and Caspr2 are selectively targeted to the axon initial segment in hippocampal neurons. *J Cell Sci* 130(13):2209–2220. <https://doi.org/10.1242/jcs.202267>
- Poliak S, Salomon D, Elhanany H, Sabanay H, Kiernan B, Pevny L, Stewart CL, Xu X, Chiu SY, Shrager P, Furley AJ, Peles E (2003) Juxtaparanodal clustering of Shaker-like K<sup>+</sup> channels in myelinated axons depends on Caspr2 and TAG-1. *J Cell Biol* 162(6):1149–1160
- Savvaki M, Panagiotaropoulos T, Stamatakis A, Sargiannidou I, Karatzioula P, Watanabe K, Stylianopoulou F, Karageorgos D, Kleopa KA (2008) Impairment of learning and memory in TAG-1 deficient mice associated with shorter CNS internodes and disrupted juxtaparanodes. *Mol Cell Neurosci* 39(3):478–490. <https://doi.org/10.1016/j.mcn.2008.07.025>
- Savvaki M, Theodorakis K, Zoupi L, Stamatakis A, Tivodar S, Kyriacou K, Stylianopoulou F, Karageorgos D (2010) The expression of TAG-1 in glial cells is sufficient for the formation of the juxtaparanodal complex and the phenotypic rescue of tag-1 homozygous mutants in the CNS. *J Neurosci: Off J Soc Neurosci* 30(42):13943–13954. <https://doi.org/10.1523/JNEUROSCI.2574-10.2010>
- Stoeckli ET, Kuhn TB, Duc CO, Ruegg MA, Sonderegger P (1991) The axonally secreted protein axonin-1 is a potent substratum for neurite growth. *J Cell Biol* 112:449–455. <https://doi.org/10.1083/jcb.112.3.449>
- Stogmann E, Reinthaler E, Eltawil S, El Etribi MA, Hemeda M, El Nahhas N, Gaber AM, Fouad A, Edris S, Benet-Pages A, Eck SH, Pataraja E, Mei D, Brice A, Lesage S, Guerrini R, Zimprich F, Strom TM, Zimprich A (2013) Autosomal recessive cortical myoclonic tremor and epilepsy: association with a mutation in the potassium channel associated gene CNTN2. *Brain* 136(Pt 4):1155–1160. <https://doi.org/10.1093/brain/awt068>
- Tabula Muris Consortium, Overall Coordination, Logistical Coordination, Organ Collection and Processing, Library Preparation and Sequencing, Computational Data Analysis, Cell Type Annotation, Writing group, Supplemental Text Writing Group, Principal investigators (2018) Single-cell transcriptomics of 20 mouse organs creates a Tabula Muris. *Nature* 562(7727):367–372. <https://doi.org/10.1038/s41586-018-0590-4>
- Tachi N, Hashimoto Y, Nawa M, Matsuoka M (2010) TAG-1 is an inhibitor of TGFβ2-induced neuronal death via amyloid beta precursor protein. *Biochem Biophys Res Commun* 394(1):119–125. <https://doi.org/10.1016/j.bbrc.2010.02.127>
- Theodosiou T, Papanikolaou N, Savvaki M, Bonetto G, Maxouri S, Fakourelis E, Eliouopoulos AG, Tavernarakis N, Amoutzias GD, Pavlopoulos GA, Aivaliotis M, Nikolettou V, Tzamaris D, Karageorgos D, Iliopoulos I (2020) UniProt-Related Documents (UniReD): assisting wet lab biologists in their quest on finding novel counterparts in a protein network. *NAR Genom Bioinform*. <https://doi.org/10.1093/nargab/lqaa005>
- Traka M, Dupree JL, Popko B, Karageorgos D (2002) The neuronal adhesion protein TAG-1 is expressed by Schwann cells and oligodendrocytes and is localized to the juxtaparanodal region of myelinated fibers. *J Neurosci* 22(8):3016–3024
- Traka M, Goutebroze L, Denisenko N, Bessa M, Nifli A, Havaki S, Iwakura Y, Fukamauchi F, Watanabe K, Soliven B, Girault JA, Karageorgos D (2003) Association of TAG-1 with Caspr2 is essential for the molecular organization of juxtaparanodal regions of myelinated fibers. *J Cell Biol* 162(6):1161–1172
- Wang W, Karageorgos D, Kilpatrick DL (2011) The effects of Tag-1 on the maturation of mouse cerebellar granule neurons. *Cell Mol Neurobiol* 31(3):351–356. <https://doi.org/10.1007/s10571-010-9641-6>
- Xenaki D, Martin IB, Yoshida L, Ohyama K, Gennarini G, Grumet M, Sakurai T, Furley AJ (2011) F3/contactin and TAG1 play antagonistic roles in the regulation of sonic hedgehog-induced cerebellar granule neuron progenitor proliferation. *Development* 138:519–529. <https://doi.org/10.1242/dev.051912>
- Yamamoto M, Boyer AM, Crandall JE, Edwards M, Tanaka H (1986) Distribution of stage-specific neurite-associated proteins in the developing murine nervous system recognized by a monoclonal antibody. *J Neurosci* 6(12):3576–3594
- Yan Y, Jiang Y (2016) RACK1 affects glioma cell growth and differentiation through the CNTN2-mediated RTK/Ras/MAPK pathway. *Int J Mol Med* 37(1):251–257. <https://doi.org/10.3892/ijmm.2015.2421>
- Zaldivar A, Krichmar JL (2014) Allen Brain Atlas-Driven visualizations: a web-based gene expression energy visualization tool. *Front Neuroinform* 8:51. <https://doi.org/10.3389/fninf.2014.00051>
- Zhou L, Barão S, Laga M, Bockstael K, Borgers M, Gijzen H, Annaert W, Moechars D, Mercken M, Gevaert K, De Strooper B (2012) The neural cell adhesion molecules L1 and CHL1 are cleaved by BACE1 protease in vivo. *J Biol Chem* 287(31):25927–25940. <https://doi.org/10.1074/jbc.M112.377465>
- Zoupi L, Savvaki M, Karageorgos D (2011) Axons and myelinating glia: an intimate contact. *IUBMB Life* 63(9):730–735. <https://doi.org/10.1002/iub.513>
- Zoupi L, Savvaki M, Kalemaki K, Kalafatakis I, Sidiropoulou K, Karageorgos D (2018) The function of contactin-2/TAG-1 in oligodendrocytes in health and demyelinating pathology. *Glia* 66(3):576–591. <https://doi.org/10.1002/glia.23266>

**Publisher's Note** Springer Nature remains neutral with regard to jurisdictional claims in published maps and institutional affiliations.